https://ntrs.nasa.gov/search.jsp?R=19740024819 2020-03-23T05:19:43+00:00Z

NASA CR-134649
Boeing D180-18189-1

DEEP FLAWS IN WELDMENTS OF ALUMINUM AND TITANIUM

By

J. N. Masters
W. L. Engstrom
W. D. Bixler

THE BOEING AEROSPACE COMPANY

Prepared For:

NATIONAL AERONAUTICS
AND
SPACE ADMINISTRATION

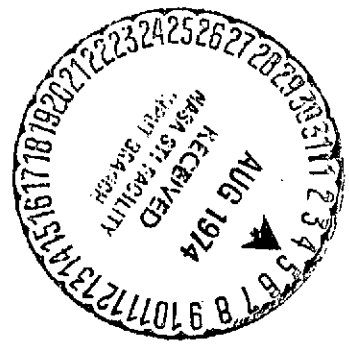

NASA- LEWIS RESEARCH CENTER
Contract NAS 3-14386
John A. Misencik - Project Manager

(NASA-CR-134649) DEEP FLAWS IN WELDMENTS OF ALUMINUM AND TITANIUM Contractor Report, Jun. 1971 - Oct. 1972 (Boeing Aerospace Co., Seattle, Wash.) 221 p HC $14.25 CSCL 13H G3/15

N74-32932

Unclas
54444

1. Report No. NASA CR-134649	2. Government Accession No.	3. Recipient's Catalog No.
4. Title and Subtitle DEEP FLAWS IN WELDMENTS OF ALUMINUM AND TITANIUM		5. Report Date APRIL 1974 6. Performing Organization Code
7. Author(s) J. N. Masters, W. L. Engstrom and W. D. Bixler		8. Performing Organization Report No. D180-18189-1 10. Work Unit No.
9. Performing Organization Name and Address BOEING AEROSPACE COMPANY RESEARCH AND ENGINEERING DIVISION SEATTLE, WASHINGTON 98124		11. Contract or Grant No. NAS 3-14386 13. Type of Report and Period Covered Contract Report June 1971 through October 1972
12. Sponsoring Agency Name and Address NATIONAL AERONAUTICS AND SPACE ADMINISTRATION LEWIS RESEARCH CENTER 21000 BROOKPARK ROAD CLEVELAND, OHIO 44135		14. Sponsoring Agency Code

15. Supplementary Notes

PROJECT MANAGER, John A. Misencik
MATERIALS AND STRUCTURES DIVISION
NASA Lewis Research Center
Cleveland, Ohio 44135

16. Abstract

Surface flawed specimens of 2219-T87 and 6Al-4V STA titanium weldments were tested to determine static failure mode, failure strength, and fatigue flaw growth characteristics. Thicknesses selected for this study were purposely set at values where, for most test conditions, abrupt instability of the flaw at fracture would not be expected. Static tests for the aluminum weldments were performed at room, LN_2 and LH_2 temperatures. Titanium static tests were performed at room and LH_2 temperatures. Results of the static tests were used to plot curves relating initial flaw size to leakage- or failure-stresses (i.e., "failure" locus curves). Cyclic tests, for both materials, were then performed at room temperature, using initial flaws only slightly below the previously established failure locus for typical proof stress levels. Cyclic testing was performed on pairs of specimens, one with and one without a simulated proof test cycle. Comparisons were made then to determine the value and effect of proof testing as affected by the various variables of proof and operating stress, flaw shape, material thickness, and alloy.

17. Key Words (Suggested by Author(s))		18. Distribution Statement
2219-T87 Aluminum 6Al-4V Titanium Fracture Characteristics Weldments Pressure Vessel	Cryogenic Cyclic Crack Growth Rates Surface Flaws Proof Testing	Unclassified, Unlimited.

19. Security Classif. (of this report)	20. Security Classif. (of this page)	21. No. of Pages	22. Price*
Unclassified.	Unclassified.	235	$3.00

* For sale by the National Technical Information Service, Springfield, Virginia 22151

NASA-C-168 (Rev. 6-71)

FOREWORD

This report describes an investigation of fracture characteristics and cyclic flaw growth in weldments of 2219 aluminum and 6Al-4V titanium performed by The Boeing Aerospace Company from June 1971 through October 1972 under Contract NAS 3-14386. The work was administered by Mr. John A. Misencik of the NASA Lewis Research Center.

Boeing personnel who participated in this investigation included J. N. Masters, Program Manager, and W. L. Engstrom, Principal Investigator. W. D. Bixler assisted in analyzing the cyclic test results. Test support was provided by A. A. Ottlyk on non-hazardous testing and by G. E. Vermillion on hazardous testing. Welding support was provided by C. W. Bosworth (aluminum) and J. Mallas (titanium). Metallurgical support was provided by E. C. Roberts. Don Good and G. Buehler prepared the art work.

The information contained in this report is also released as Boeing Document D180-18189-1.

TABLE OF CONTENTS

PRECEDING PAGE BLANK NOT FILMED

TABLE OF CONTENTS (Continued)

SYMBOLS AND ACRONYMS

a	Crack depth of semi-elliptical surface flaw.
a_{cr}	Critical crack depth at which breakthrough or failure occurs during a proof test.
a_o	Initial crack depth at Operating stress level.
BT	Breakthrough of surface flaw to the backside of the specimen.
$2c$	Flaw length of semi-elliptical surface flaw and through-the-thickness flaw.
C	Crack opening displacement constant.
COD	Crack opening displacement.
E	Youngs Modulus.
EDM	Electrical discharge machine
GOL	Growth on loading.
K_I	Irwin Stress Intensity.
K_{IE}	Surface Flaw Stress Intensity.
$K_{I_{MAX}}$	Maximum Cyclic Surface Flaw Stress Intensity
K_{CN}	Through-the-thickness Center Notch Stress Intensity.
KR	Stress Intensity ratio relating operating stress intensity to proof stress intensity in evaluation of cyclic test results.
M_K	Deep flaw magnification factor.
N	Number of fatigue cycles.
NA	Not available.
Q	Flaw shape parameter = $\Phi^2 - 0.212(\sigma/\sigma_y)^2$.
R	Cyclic stress ratio.
t	Thickness of specimen at flaw plane.
t_n	Ligament size (=t-a).
W	Width of specimen at flaw plane.
δ	Crack opening displacement.
σ, σ_A, σ_G	Applied gross stress.
σ_B	Stress level at which flaw breakthrough occurs.
σ_D	Stress level at which backside dimpling takes place.
σ_{MAX}	Maximum Cyclic Stress Level.
σ_N	Net section stress.
σ_o	Operating Stress Level.
σ_p	Proof Stress Level.

σ_{ys}, σ_y	Yield strength.
σ_u	Ultimate strength.
μ	Poisson's ratio.
Φ	Complete elliptical integral of the second kind corresponding to modulus $k = [(c^2 - a^2)/c^2]^{1/2}$.
~~N~~	Cycle(s).

SUBSCRIPTS

f	final condition.
i	initial condition.

LIST OF FIGURES

LIST OF FIGURES (Continued)

LIST OF FIGURES (Continued)

LIST OF FIGURES (Continued)

LIST OF FIGURES (Continued)

LIST OF FIGURES (Continued)

LIST OF FIGURES (Continued)

LIST OF TABLES

LIST OF TABLES (Continued)

LIST OF TABLES (Continued)

LIST OF TABLES (Continued)

LIST OF TABLES (Continued)

LIST OF TABLES (Continued)

SUMMARY

This experimental program was undertaken to determine static failure mode and failure strength and to determine the effects of proof testing on subsequent cyclic life in weldments of 2219-T87 aluminum alloy and 6Al-4V STA titanium alloy. The ultimate use of the data generated herein is application to thin walled tankage such as employed in Space Shuttle systems. Gages tested included 1.60 mm (0.063 inch), 2.67 mm (0.105 inch) and 7.62 mm (0.300 inch) for the aluminum and 0.51 mm (0.020 inch), 1.78 mm (0.070 inch) and 5.33 mm (0.210 inch) for the titanium. Families of maximum flaw size curves surviving room temperature proof tests were determined and specimens containing flaws only slightly smaller than these maximum flaw sizes were tested under cyclic fatigue loading, both with and without prior proof. In addition, failure stresses and associated flaw sizes were determined at LN_2 and LH_2 temperatures for the aluminum and LH_2 temperature for the titanium.

Results of aluminum weldment static tests indicate leak before break mode is assured at the following stress levels:

THICKNESS mm(inch)	TEMPERATURE °K (°F)		
	RT, 295(72)	LN_2 78 (-320)	LH_2 20 (-423)
1.60 (0.063)	$0.7 < \sigma/\sigma_{ys} < 1.0$	$0.7 < \sigma/\sigma_{ys} < 1.0$	$0.7 < \sigma/\sigma_{ys} < 0.85$
2.67 (0.105)	$0.7 < \sigma/\sigma_{ys} < 1.0$	$0.7 < \sigma/\sigma_{ys} < 1.0$	$0.7 = \sigma/\sigma_{ys}$
7.62 (0.300)	$0.7 < \sigma/\sigma_{ys} < 1.0$	$0.7 < \sigma/\sigma_{ys} < 0.91$	$0.7 = \sigma/\sigma_{ys}$

Results of titanium weldment static tests show that leak before break mode is assured only for the 0.51 mm (0.020 inch) material at 0.70 σ_{ys} at room and LH_2 temperatures.

The stress level at which leakage occurs can not presently be predicted, however, it appears to be strongly dependent upon flaw depth-to-thickness ratio, flaw shape and yield strength.

A successful proof test of materials in which leak-before-break mode prevails can provide assurance of subsequent safe life operation. While significant flaw growth can occur during a proof test of these materials, subsequent retardation in cyclic growth more than compensates for the proof test "damage".

1.0 INTRODUCTION

The semi-elliptical surface flaw is an excellent model of common failure origins in aerospace structure and so has been the object of considerable study. This type of defect is especially prevalent in failure analysis reports of welded aerospace pressure vessels and to a lesser degree, percentagewise, in aircraft primary structures.

Pressure vessel design methods have been developed (1)* for assuring that crack-like defects will not grow sufficiently to initiate failure during the required operational life. Similar efforts are now underway to develop more effective guidelines for assuring structural integrity of military aircraft[2]. A large part of the data used in the formulation of the procedures of the reference 1 monograph resulted from testing and analysis of surface flaws in relatively brittle materials. Flaw and plastic zone sizes usually were relatively small with respect to other specimen or structure dimensions. The most significant structural failures of high performance aircraft, those prompting accelerated Air Force research efforts, also involved surface defects in high strength (brittle) materials.

With the above situations the defect becomes critical before it can grow through the thickness and become detectable. Catastrophic failure can and has occurred. Exact stress intensity solutions for these conditions are not available, however, the solution due to Irwin[3] for shallow surface flaws when combined with Kobayashi's original deep flaw magnification values has proven to be quite useful in solving practical engineering problems.

Recognition of the factors causing these past failure problems has resulted in gradual but marked changes in new designs and structures. Improved materials and material processing, and reduced strength and stress levels have combined to result in conditions in which critical flaw sizes approach or exceed the wall thickness of the structure. While this improves structural

---

* numbers in parenthesis refer to references at end of report

safety and durability, it complicates the failure mode and life prediction efforts. The previously developed analytical procedures based upon modified linear elastic fracture theory become increasingly ineffective as flaw and plastic zone size become large with respect to other dimensions, and one must rely heavily on experimental results.

Initial experimental work devoted strictly to the deep flaw problem was initiated in 1967 and is published in Reference 4. This work involved static and cyclic testing of 2219-T87 aluminum and 5Al-2.5Sn titanium base metal and weldments. Very thick and very thin gages of material were tested to bracket the problem. Values of a/t and a/2c were systematically varied to cover a complete range of flaw sizes and shapes. The resulting data were analyzed to determine deep flaw magnification factors, M_K, which could be applied to the Irwin stress intensity solution. It was concluded that these values of M_K applied for net failure stresses up to 0.90 σ_{ys} and ligament thicknesses ($t_n = t - a$) greater than 0.20 $(K_{IE}/\sigma_{ys})^2$. Instrumentation was not available during the Reference 4 program to detect stable flaw growth preceding fracture, however, it was suspected that such behavior did affect both static and cyclic behavior.

A subsequent experimental program[5] was undertaken to further explore the static and cyclic behavior of flaw depth, flaw shapes and thicknesses thru that range where failure mode changed from "catastrophic failure" to leak-before-failure. Base metal tests of 2219-T87 and 7075-T651 aluminum and 6Al-4V titanium were tested in a manner similar to that of the Reference 4 program and several intermediate thicknesses were added to expand applicability of the results. Instrumentation was added to detect flaw breakthrough (leakage). Cyclic and sustained load tests were run with and without a simulated proof overload. Results indicated that K_{IE} values obtained from any of three available deep flaw solutions[4,6,7] can be used to describe failing stress/flaw size locii for a wide range of thicknesses, flaw shapes, alloys, and stress loads. These ranges were

a) for maximum failing stresses of about 0.90 σ_{ys}

b) for minimum thickness of about 0.25 $(\frac{K_{IE}}{\sigma_{ys}})^2$; and

c) for ligament size greater than about 0.10 $(\frac{K_{IE}}{\sigma_{ys}})^2$. For ligaments less than this value, leakage prior to failure would be expected.

It was concluded that cyclic flaw growth rate data can also be adequately described as a function of applied K_{IE} levels (using deep flaw magnification factors) within the same limits set for static testing noted above. Additionally, it was observed that proof overloads generally resulted in subsequent retardation in cyclic flaw growth rates.

While the two programs of References 4 and 5 generated much useful data on base metal materials, there was still a lack of data relating to weldments. Thus the present work on weldments is a necessary and natural addition to the two earlier programs. At the beginning of this test program preliminary design studies had shown that primary Space Shuttle propellant tanks would very probably be fabricated from 2219-T87 aluminum alloy with weld land thicknesses varying between 1.02 mm (0.040 inch) and 7.62 mm (0.300 inch). Maximum proof stress levels on the order of 0.9 to 1.0 σ_{ys} would be used. A wide range of auxilliary tankage is required, and some undoubtedly would be fabricated of 6Al-4V STA titanium in several gages ranging possibly from 0.51 mm (0.020 inch) through 6.35 mm (0.250 inch). For tankage having the foregoing characteristics, it was anticipated that in many cases, embedded or surface crack defects would not become unstable at typical proof pressure levels. Thus, it was not clear whether proof testing could be used as an effective tool in assuring safety of the planned tankage. Since inception of this program, major Shuttle configuration changes have occurred, however, the gages and alloys selected are still applicable to the majority of tankage planned for use on the Shuttle system.

Primary objectives of this program thus were to evaluate the flaw growth and failure characteristics of weldments of alloys applicable to planned aerospace hardware and to reduce the resulting data in a manner required for design usage.

Static fracture tests of weldments were performed using surface flawed 2219-T87 aluminum specimens of 1.60 mm (0.063 inch), 2.67 mm (0.105 inch) and 7.62 mm (0.300 inch) at room temperature, 78°K (-320°F) and 20°K (-423°F). Titanium weldment (6Al-4V) specimens were tested in thicknesses of 0.51 mm (0.020 inch), 1.78 mm (0.070 inch) and 5.33 mm (0.210 inch) at room temperature and at 20°K (-423°F). Specimens were tested using a wide range of a/t and a/2c values in order to fully characterize the effects of these variables. Results of these tests are analyzed to determine combinations of maximum flaw depths as affected by flaw shape which can survive a vessel proof test (i.e., no leak-no fail). Subsequent testing consisted of conducting cyclic tests to determine crack growth rates and cyclic life. These test specimens were run in pairs; one specimen was cycled to failure or leakage; the other received a simulated proof overload and then was cycled. The data were then analyzed to determine the effects of the proof overload for the several combinations of shapes and depths which would barely survive the overload cycle.

The following sections of this report describe materials and procedures, and include a presentation and discussion of results. Applicable data from prior programs are compared with results of this program in the discussion section.

2.0 MATERIALS AND WELDING

2.1 Aluminum

The aluminum specimens were fabricated from both 3.18 mm (0.125 inch) sheet or 12.70 mm (0.50 inch) plate. The alloy was 2219-T87. The 3.18 mm (0.125 inch) sheet was ordered per Boeing specification BMS 7-105C and the 12.70 mm (0.50 inch) material was ordered per the equivalent Military Specification MIL-A-8920-A. Each thickness of material was from a single heat. As determined by Boeing tests, both thicknesses had cleanliness ratings better than Classification "A" per ASTM E45-63. Chemical composition of the aluminum as determined at Boeing is shown in Table 1.

The welding of the aluminum panels was accomplished using a Welduction mechanized gas tungsten arc (GTA) welder. 2319 alloy weld wire was used in the welding of the 3.18 mm (0.125 inch) sheet. The cleanliness rating of the weld wire as determined by Boeing was Classification "A" per ASTM E45-63. The chemical composition of the 2319 weld wire as determined at Boeing is shown in Table 2. No weld wire was used to weld the 12.70 mm (0.50 inch) plate. A square butt edge preparation was used on all panels.

Just prior to welding, the machined joint edges were cleaned with MEK and scraped to remove surface oxides. Welding was performed in the downhand position using direct current straight polarity (DCSP) gas tungsten arc procedures. A single pass on one side was used for the 3.18 mm (0.125 inch) sheet and a single pass on both sides was used for the 12.70 mm (0.50 inch) plate. The weld was parallel to the major rolling direction of the material. Other weld parameters are listed below:

3.18 mm (0.125 inch) weldments	
Travel:	180 mm/min (7 inch/min)
Voltage:	14.0 V
Amperage:	145 A
Torch gas:	Helium @ 2.5 m^3/hour (90 ft^3/hour)

3.18 mm (0.125 inch) weldments, cont'd.

Backup gas:	Helium @ 0.6 m^3/hour (20 ft^3/hour)
Electrode:	3.18 mm (0.125 inch) diameter, 2% thoria
Wire travel:	500 mm/min (20 inch/min)
Backup bar:	Copper, 4.3 mm (0.17 inch) wide, 1.3 mm (0.05 inch) deep
Hold down bars:	Copper, spaced 6.4 mm (0.25 inch) each side of weld centerline.

12.70 mm (0.50 inch) weldments

Travel:	100 mm/min (4 inch/min)
Voltage:	13.5 V
Amperage:	265 A on first pass, 260 A on second pass
Torch gas:	Helium @ 2.5 m^3/hour (90 ft^3/hour)
Backup gas:	Helium @ 0.6 m^3/hour (20 ft^3/hour)
Electrode:	3.18 mm (0.125 inch) diameter 2% thoria
Backup bar:	Copper, 4.3 mm (0.17 inch) wide, 1.3 mm (0.05 inch) deep
Hold down bars:	Copper, spaced 6.4 mm (0.25 inch) each side of weld centerline.

No heat treatment was conducted after welding and all weldments were X-rayed to Boeing BAC 5935 Class A acceptance criteria. Macrographs of typical aluminum weldments are shown in Figure 1.

2.2 Titanium

The titanium specimens were fabricated from both 2.03 mm (0.080 inch) 6Al-4V sheet or 6.35 mm (0.250 inch) 6Al-4V plate purchased per Boeing specification XBMS 7-174B. This specifies upper limits on aluminum and oxygen contents of 6.3% and 0.13% respectively. The heat treat condition of the 2.03 mm (0.080 inch) sheet was Condition III, STA 811°K (1000°F). The 6.35 mm (0.250 inch) plate was ordered in Condition I, Mill-Annealed; it was subsequently heat treated at The Boeing Company to Condition III, STA 811°K (1000°F). As determined by Boeing tests, both thicknesses had cleanliness ratings of Classification "A" or better per ASTM E45-63. Chemical composition of the titanium as determined at Boeing is shown in Table 3.

The welding of the titanium panels was accomplished using a Vickers "400" welder in a Wolff Inert Atmosphere chamber. The welding was performed in the down hand position using DCSP. A square butt edge preparation was used for the 2.03 mm (0.080 inch) sheet material. Filler wire was not used in welding the sheet material. The edge preparation for the 6.35 mm (0.25 inch) plate material was a double "U" edge containing two 2.54 mm (0.10 inch) radii cut so that they culminated in a 1.25 mm (0.050 inch) nose thickness. Titanium 6Al-4V filler wire was used in welding of the plate material. The cleanliness rating of the weld wire as determined by Boeing was Classification "A" per ASTM E45-63. The chemical composition of the filler wire as determined at Boeing is reported in Table 4.

Just prior to welding, the materials were cleaned using a nitro-hydrofluorine acid cleaning, descaling and etching process. A single fusion weld pass on each side was used for the 2.03 mm (0.080 inch) material. A single fusion weld pass on one side was followed by a single weld filler pass on each side for the 6.35 mm (0.25 inch) plate. The weld was parallel to the major rolling direction in both thicknesses. Other weld parameters are listed below:

2.03 mm (0.080 inch) weldments

Travel:	203 mm/min (8 inch/min)
Voltage:	11 V
Amperage:	90 A
Torch gas:	Argon
Electrode:	2.38 mm (0.094 inch) diameter, 2% thoria
Backup bar:	Copper
Hold down bars:	Copper, spaced 12.7 mm (0.50 inch) each side of weld centerline

6.35 mm (0.250 inch) weldments

Travel:	152 mm/min (6 inch/min) on all passes
Voltage:	12 V on fusion pass, 13 V on filler passes
Amperage:	150 A on fusion pass, 160 A on filler passes
Torch gas:	Argon

6.35 mm (0.250 inch) weldments, cont'd.

Electrode:	3.18 mm (0.125 inch) diameter, 2% thoria
Wire Travel:	737 mm/min (29 inches/min) on filler passes only
Backup bar:	Copper
Hold down bar:	Copper, spaced 12.7 mm (0.50 inch) each side of weld centerline.

After welding, the titanium was stress relieved in a vacuum furnace at 811°K (1000°F) for 4 hours. The weldments were X-rayed to Boeing BAC 5935 Class A acceptance criteria. Macrographs of typical titanium weldments are shown in Figure 2.

3.0 PROCEDURES

3.1 Specimen Fabrication

3.1.1 Tensile Specimens

Tensile specimens for base metal 6Al-4V titanium alloy and the 2219-T87 aluminum base metal and weldment were fabricated per Figure 3. Titanium base metal specimens in the 0.51 mm (0.020 inch) and 2.03 mm (0.080 inch) thickness were cut from 2.03 mm (0.080 inch) sheet meterial. The 6.35 mm (0.25 inch) titanium base metal specimens were cut from 6.35 mm (0.25 inch) plate material. Base metal aluminum specimens in the 1.60 mm (0.063 inch) and 3.18 mm (0.125 inch) thicknesses were cut from 3.18 mm (0.125 inch) sheet material, while those in the 7.62 mm (0.30 inch) thickness were cut from 12.70 mm (0.50 inch) plate. Tests were conducted on specimens with the loading axis oriented parallel (longitudinal) to the major rolling direction and on specimens with the loading axis oriented perpendicular (transverse) to the major rolling direction.

The 1.60 mm (0.063 inch) and 2.67 mm (0.105 inch) aluminum weldment specimens were cut from 3.18 mm (0.125 inch) welded sheet. Aluminum weldment specimens in the 7.62 mm (0.30 inch) thickness were cut from 12.70 mm (0.50 inch) welded plate. The specimens were cut so that the weld extended across the reduced section of the specimen.

The tensile strengths of the titanium weldment specimens were anticipated to be approximately the same as the tensile strengths of the base metal. Therefore, a modified version of the specimen shown in Figure 3 was used for titanium weldment tests. In order to insure a failure at the weld, this specimen was prepared with an additional neckdown as shown in Figure 4.

Weldment specimens of titanium in the 0.51 mm (0.020 inch) and 1.78 mm (0.070 inch) thicknesses were cut from 2.03 mm (0.080 inch) welded sheet. The 5.33 mm (0.21 inch) specimens were cut from 6.35 mm (0.25 inch) welded plate.

3.1.2 Surface Flawed Fracture and Cyclic Crack Growth Specimens

Aluminum base metal fracture test specimen configurations are shown in Figures 5, 6, and 7. Base metal titanium static fracture specimens are shown in Figures 8, 9, 10, and 11. Aluminum weldment specimen configurations are shown in Figures 12 through 16. The titanium weldment specimens are shown in Figures 17 through 23 and in Figure 8. The specimen configurations used were such that the specimen width was at least 4 times the flaw length.

Base metal specimens were fabricated so that the loading axis was perpendicular (transverse) to the major rolling direction (WT loading/propagation orientation). Weldment specimens were fabricated so that the weld extended across the reduced section of the weld, perpendicular to the loading axis. Loading holes were drilled and reamed either by a numerically controlled milling machine or by a standard drill press using drill jigs. Surface flaws in the weldment specimens were located in the centerline of the weld. The reasons for this flaw location are presented in Section 3.4.

All initial flaws were prepared by using an electric discharge machine (EDM) to introduce an initial flaw. The EDM flaw was then extended using low stress fatigue. Maximum cyclic stress levels used for aluminum base metal specimens varied from 69 to 103 MN/m^2 (10 to 15 ksi). The number of cycles varied from 5 to 35 thousand depending on initial flaw size and cyclic stress. Titanium base metal specimens were precracked at 207 to 310 MN/m^2 (30 to 45 ksi) in 2 to 12 thousand cycles. The majority of the aluminum weldment specimens were precracked at 55 to 83 MN/m^2 (8 to 12 ksi); the maximum precrack stress used was 138 MN/m^2 (20 ksi). The number of cycles required for precracking ranged from 2- to 30-thousand. Titanium weldment specimens were precracked at 138 to 310 MN/m^2 (20 to 45 ksi) in 1 to 22 thousand cycles. A microscope was used to visually observe the flaw periphery in order to determine that precracking was complete.

3.2 Test Setups

All non-hazardous tests were conducted in an environmentally controlled laboratory at the Boeing Space Center in Kent, Washington. Tests conducted at 78°K (-320°F) utilized an environment chamber such as shown in Figure 24. This chamber was installed around the specimen and it was then filled with enough

liquid nitrogen (LN_2) to completely cover the specimen. Specimens were soaked at temperature for at least ten minutes before each test. All non-hazardous static tests were conducted in a 534 kN (120 kip) Baldwin universal testing machine, a 1110 kN cyclic/1330 kN static (250 kip cyclic/300 static) MTS machine, or a 267 kN (60 kip) hydraulic test machine fabricated by Boeing. All cyclic tests were conducted in the aforementioned MTS machine or the 267 kN (60 kip) Boeing machine.

Hazardous tests involving liquid hydrogen (LH_2) at 20°K (-423°F) were conducted at Boeing's remote Tulalip test site. Specimens were installed in a cryostat and pulled to failure in a 1779 kN (400 kip) Riehle hydraulic test machine.

During static fracture tests, flaw growth through-the-thickness (breakthrough) prior to ultimate failure was determined with the use of pressure cups and/or examination of back surface strain gage data. In some cases it was found that the strain gages located on the back side of the specimen interfered with the pressure cup breakthrough determination. In addition, pressure cup utilization was sometimes unsuccessful in testing aluminum weldments because the plastic deformations in the weld during loading made it difficult to maintain a good seal between the pressure cup and the specimen. However, because there was an abrupt relaxation in the strain field surrounding the flaw when breakthrough occurred, the strain gage records generally provided a reliable indication of breakthrough as shown in Figure 25. Where strain gage and/or pressure cup data records did not clearly show breakthrough, replicate specimens instrumented only with pressure cups were tested to confirm breakthrough determinations.

The pressure cups were clamped to the specimens and a pressure differential of approximately 3.5 to 7 kN/m^2 (5 to 10 psi) was used. Helium gas was used as the pressurizing medium. Pressure transducers were employed on the front and/or backside to sense the pressure change associated with flaw breakthrough. Pressure cups were utilized on all cyclic tests to assist in determining breakthrough. Examples of pressure cups are shown in Figure 26.

3.3 Experimental Approach

3.3.1 Tensile Tests

Extensometers were used on all tensile specimens. Tensile specimens of the weldments were also instrumented with 3.18 mm (0.125 inch) gage length strain gages placed on the weld bead. For the aluminum base metal and weldment specimens and the titanium base metal specimens, the engineering yield strength based on 0.2% offset yield in 50.8 mm (2.0 inches) was used. The yield strength based on the strain gage measurements was used for the titanium weldment specimens. During loading of the specimens a strain rate of 0.005 in/in/minute was used until the material yield strength was reached. A strain rate of 0.10 in/in/minute was then used for the remaining portion of the loading sequence until failure.

3.3.2 Fracture and Cyclic Crack Growth Tests

All static fracture surface flawed specimens were tested with targeted flaw shapes $(a/2c)_i$ of 0.05, 0.15, 0.225, 0.30 or 0.45. Aluminum specimens were tested in room temperature air, LN_2 at 78°K (-320°F), or LH_2 at 20°K (-423°F). Titanium specimens were tested in room temperature air or in LH_2 at 20°K (-423°F). Each specimen was loaded to failure in one to two minutes. The static specimens were instrumented with pressure cups and/or back side strain gages described above to determine if and when breakthrough occurred prior to failure. The strain gages were also used to determine strain distributions on the backside of the specimens in the area of the flaw, and to determine dimpling.

Dimpling in this report is defined as the point at which the back side plastic strain reaches 0.2% offset yield. While dimpling has been described elsewhere (Reference 8) as an elongated surface depression visibly observed, direct observation was not possible in this study. Strain gage and pressure cup instrumentation made visual observation of the backside of the specimen virtually impossible. In addition, the environment chambers used in the cryogenic tests further complicate the problem. Therefore, in order to determine dimpling on all the tests in a consistent manner, the 0.2% offset yield

criterion described in Reference 5 was used and strain gages were judiciously placed to ascertain when this dimpling occurred. In addition to the strain gage used for dimpling determination, most static fracture specimens were instrumented with at least two other strain gages.

In order to determine crack opening displacements (COD), specimens were instrumented with a clip gage as shown in Figure 27. The clip gage was spring loaded against knife edges spot welded to the specimen. An expression for the opening displacements of a completely embedded flaw has been provided by Green and Sneddon (Reference 9). Their study examined a flaw embedded in an elastic solid which was subjected to a uniform load normal to the crack surface at infinity. The maximum opening displacement occurs at the diametrical center of the crack and is expressed by the equation,

$$COD = \delta = \frac{4(1 - \mu^2)}{E} \cdot \frac{\sigma a}{\Phi}$$

Although a rigorous solution is not available for flaw opening displacements for a semi-elliptical surface flaw, such displacements should also be proportional to σ and a/Φ for elastic materials. By following Irwin's procedure (Reference 3) to account for the effect of plastic yielding, the COD for a surface flaw can be approximated by

$$\delta = C\frac{\sigma a}{\sqrt{Q}}$$

where C is a constant.

At the completion of static fracture testing, flaw sizes were determined which would just barely pass proof tests to σ_{ys} or 0.91 σ_{ys}. Cyclic tests were then run on specimens which had these flaw sizes. Maximum cyclic test stresses were 0.85 σ_{ys} or 0.70 σ_{ys}. A stress ratio of zero was used for all tests. Cycling was conducted both with and without prior proof testing to the above mentioned proof loads. All cyclic tests employed sinusoidal loading.

During proof testing, strain gage and COD records were monitored and whenever failure appeared imminent, the proof test was terminated. Although this procedure necessitated proof testing in some cases to loads slightly different than the target loads, it assured that critical conditions were approached as closely as possible while minimizing the number of specimens which failed during the proof cycle.

Cyclic specimens were instrumented with the clip gages described above to determine COD during cycling tests. The COD measurements were used to calculate instantaneous growth rates by using the following approach.

The crack opening displacement constant, C, can be determined at test initiation and termination from knowledge of the stress level, initial and final flaw sizes, and the corresponding flaw opening displacements as indicated below:

$$C_i = \frac{\delta i}{\sigma} \left(\frac{\sqrt{Q}}{a} \right)_i$$

$$C_f = \frac{\delta f}{\sigma} \left(\frac{\sqrt{Q}}{a} \right)_f$$

where the subscripts i and f refer to initial and final conditions, respectively.

Tests have shown for relatively deep flaws in the tougher materials that the value of C tends to increase with increasing crack size, rather than remain constant. Crack growth rate calculations in this report were based on an assumed linear variation in C between the known initial and final values.

In order to relate the flaw parameter $(a/\sqrt{Q})$ to δ for values of $a/\sqrt{Q})$ between the initial and final values an assumption must be made as to the manner in which the flaw shape changes from

$$\frac{a - a_i}{a_f - a_i} = \frac{2c - (2c)_i}{(2c)_f - (2c)_i}$$

i.e., both flaw depth and width growth simultaneously reach the same percentage of their respective total growth from initial to final values. The flaw shape parameter, Q, can now be determined as a function of flaw depth and,

in turn, can be related to crack depth. The number of cycles, N, corresponding to each selected flaw depth value can be determined from the test record and, consequently, the change in N for each increment of flaw depth is known. The crack growth rate da/dN can then be calculated.

In addition to the clip gage, each cyclic specimen was instrumented with a strain gage to determine dimpling and a pressure cup to determine breakthrough. As mentioned earlier in the description of the static tests, the strain gages sometimes interfered with the pressure cups. However, it was generally found that if the pressure cup system failed to determine breakthrough, the breakthrough could still be determined by examining strain gage and COD records for any sharp changes.

Cyclic specimens which did not fail during testing were subsequently pulled to failure.

3.4 Flaw Location in Weldment Specimens

All flaws in the weldment specimens were located in the weld centerline because that is the most probable location of a weld defect. Additional reasons for testing at this location are presented below.

Witzell and Kropp[10] evaluated fracture and flaw growth characteristics of welded 2219-T81 aluminum. Included in their study were tests to evaluate cryogenic and room temperature fracture toughness and cyclic flaw growth rates in the various metallurgically different areas of the weld (i.e., weld nugget, fusion line, heat affected zone). They concluded that weld centerline toughness was lower for most test conditions, and fatigue growth rates were faster at all temperatures than in any other area tested. Data in References 11 thru 13 further substantiate these results.

Comparable data concerning flaw locations in titanium weldments were limited. That of References 14 and 15 indicated that weld centerlines might be the most critical location. Tests were performed in order to determine which area is the most critical part of the weld. Flaws were cut in the base metal (BM), heat affected zone (HAZ), fusion line (FL) and centerline (CL) of 1.78 mm

(0.070 inch) weldment specimens which were pulled to failure in room temperature air. Test results are tabulated in Table 5 and plotted as a function of location in Figure 28. The test results indicate no major differences in Irwin fracture toughness for static failures. However they do indicate that the CL flaw location is more susceptible to a leakage prior to failure.

Placement of the flaws in the aluminum specimens was relatively easy because the machined surfaces of the specimens displayed a definite contrast between the weldment and the base metal. Determination of the weld location in the titanium specimens was more difficult. It was necessary to etch the edges of the titanium specimens with Kroll's Etchant to locate the weld.

3.5 Stress Intensity Solutions

3.5.1 Surface Flaws

Where stress intensity values are reported, they were based on the following expression from Reference 3:

$$K_I = 1.95\ \sigma(a/Q)^{1/2}$$

where

K_I = Irwin stress intensity
σ = gross stress
a = flaw depth
Q = shape parameter.

Values of Q are shown in Figure 29.

K_{IE} values reported are calculated by multiplying the above expression by appropriate M_K terms developed in Reference 4 and shown in Figure 30.

3.5.2 Through Cracks

Where through crack stress intensity values are reported, they were based on the expression from Reference 16:

$$K_{CN} = \sigma \cdot \sqrt{\pi c} \cdot \sqrt{\sec \frac{\pi c}{W}}$$

where

K_{CN} = through crack stress intensity

c = half flaw length

W = specimen width

4.0 TEST RESULTS AND ANALYSIS

4.1 Mechanical Properties

4.1.1 Base Metal

Tensile properties of the base metal materials used in the program are shown in Tables 6 through 9. Tests of both alloys were performed at room temperature in air and at 20°K (-423°F) in liquid hydrogen.

Measured properties are plotted as a function of test temperature in figures 31 through 33 for the aluminum alloy, and in Figures 34 through 36 for the titanium alloy. It is noted that the yield and ultimate strengths of the 7.62 mm (0.300 inch) aluminum plate are slightly higher than those of the thinner gages. However, all properties are quite similar to those of the 2219-T87 stock tested in both References 4 and 5.

The titanium exhibited approximately the same yield and ultimate strengths at room temperature for the three gages tested. At LH_2 temperature, the 2.03 mm (0.080 inch) specimens showed slightly higher strength levels than the 0.51 mm (0.020) specimens. The 6.35 mm (0.250 inch) material showed LH_2 strength levels substantially lower than those of the thinner material. Properties for the two thinner gages compare favorably with those of similarly processed 6Al-4V STA titanium tested in Reference 5.

4.1.2 Weldments

Tensile properties of the weldments are shown in Tables 10 through 14. Tests of the aluminum weldments were performed at room temperature in air at 78°K (-320°F) in liquid nitrogen and at 20°K (-423°F) in liquid hydrogen. The titanium weldments were tested at room temperature and 20°K (-423°F).

Properties for the aluminum weldments are shown in Figures 37 through 39. Note that yield strengths are shown as measured both by a 50.8 mm (2.00 inches) extensometer (engineering yield) and by strain gages placed directly on the

PRECEDING PAGE BLANK NOT FILMED

on the weld nugget. The engineering yield strength is used in subsequent calculations, however it is recognized that the local (nugget) strength is significantly less than the engineering yield strength. All other properties are typical of 2219-T87 as welded joints[4].

Mechanical properties for the titanium weldments are shown in Figures 40 through 42. The yield strengths noted represent data from strain gages and these values are used in later calculations. The strength values of the two thinner weldments are seen to be slightly less than that of base metal. Unlike the base metal, the thickest weldment exhibits strength similar to that of the thinner weldments.

4.2 Static Fracture Tests

4.2.1 Base Metal Static Fracture Tests

Limited static fracture tests were conducted on both alloys at room temperature in air and at 20K (-423°F) in liquid hydrogen for each of the three thicknesses noted earlier. Results are tabulated in Tables 15 and 16 for the aluminum tests and in Tables 17 and 18 for the titanium tests.

In each of the above noted tables, specimen dimensions, location of back surface strain gage to detect dimpling and test environment are shown in the first several left-hand columns. The next columns show stress levels at failure and as applicable at back side dimpling, and flaw break-through. Subsequent columns show initial flaw dimensions as measured after fracture.

The last three columns show break through stress to yield strength ratios and maximum stress to yield strength ratios, and for reference purposes only, the calculated Irwin stress intensity value at break-through or failure, whichever occurred first.

The dimple gage location noted is the angle formed between the plane of the crack and the gage centerline on the back surface with the angle measured radially from the crack tip. Based on analytical results of References 17

and 18 and experimental work of Reference 5 maximum back surface strain should occur at an angle of about 47° to 50°. Thus, the gages were located at a targeted angle of 48°. Because of the very small dimensions involved in some of the test specimens, there were occasionally relatively large errors in the actual placement angle. This of course would result in an over estimate of the dimpling stress.

2219-T87 Aluminum

The aluminum base metal fracture data are plotted in Figure 43 in terms of applied stress versus initial a/t. Figure 43(a) includes data for a thickness of 1.60 mm (0.063 in.); 43(b) for 3.18 mm (0.125 in.); and 43(c) for 7.62 mm (0.30 in.). Both room and cryogenic temperature test results are shown. Open circles indicate leak-before-fail mode and solid circles denote fail mode.

As can be seen from the tables and figures only four specimens failed before break-through within or near the limits tentatively set for valid K_{IE} results. These were the two liquid hydrogen tests in the thickest gage (specimens AB3-3 and AB3-4) and the deepest flaw tested at room temperature in each of the two thickest gages (specimens AB2-2 and AB3-1). The two liquid hydrogen tests in the 7.62 mm (0.30 in.) material yielded K_{IE} values of 52.4 and 50.9 $MN/m^{3/2}$ (47.7 and 46.3 $ksi\sqrt{in}$). These values are about 6 percent lower than the values reported in Reference 4 for 2219-T87 base metal.

The calculated K_{IE} values for the two room temperature tests are 41.0 and 44.5 $MN/m^{3/2}$, (37.3 and 40.5 $ksi\sqrt{in}$) for specimens AB2-2 and AB3-1, respectively. Both of these values are somewhat low when compared with previous data. This probably results from the relatively high failing stress ratios of around 0.90 σ_{ys}.

With one exception, the failure mode of all specimens shown in Figure 43 agreed with predicted mode based upon initial ligament size. The single exception is specimen AB1-2 which apparently failed before breaking through. The initial ligament dimension for this specimen was about 0.04 $\left(\frac{K_{IE}}{\sigma_{ys}}\right)^2$.

6Al-4V Titanium

The titanium base metal fracture data are plotted in Figure 44 in terms of applied stress versus initial a/t. Figure 44(a) includes data for the 0.51 mm (0.020 in.) thick specimens; 44(b) for the 2.03 mm (0.080 in.) specimens and, 44(c) for the 6.35 mm (0.250 in.) specimens. The format is identical to that of the aluminum data figures. Six of the eleven specimens tested in this series failed before leaking within the limits tentatively set for valid K_{IE} values. The results are shown below:

THICKNESS - mm (Inch)	K_{IE} - $MN/m^{3/2}$ ($ksi\sqrt{in}$) ROOM TEMPERATURE	LH_2 TEMPERATURE
0.51 (0.020)	-	44.9 (40.9)*
2.03 (0.080)	48.5 (53.2)	42.7 (38.9)
6.35 (0.250)	93.3 (84.9)	58.4 (53.1)

* average of 2

It is seen from the above that the toughness of the 6.35 mm (0.250 in.) material (Heat #304623) is significantly higher than the thinner gages (both machined from Heat #304610). The room temperature toughness value shown for the thick stock compares favorably with that obtained in References 15 and 19 for 6Al-4V STA titanium of comparable yield strength. The thinner specimen stock exhibited higher yield strengths and this is probably responsible for the lower toughness for these tests.

Constant K_{IE} curves were calculated for all data except the 0.51 mm (0.020 in.) tests run at room temperature. These curves are plotted through the range of applicability in Figure 44. The 0.51 mm (0.20 in.) specimens tested at room temperature leaked before failing as would be expected for this thickness and toughness.

All other specimens shown on Figure 44 failed in the expected mode except the 6.35 mm (0.250 in.) specimen with the deepest flaw. This specimen leaked and then failed at only a two percent further increase in load.

4.2.2 Weld Metal Static Fracture Tests

Results of the static fracture tests of surface flaw specimens are shown in:

Tables	19	through	21	-	2219-T87	aluminum	weldments	at room temp.
"	22	"	24	-	"	"	"	in liquid nitrogen
"	25	"	27	-	"	"	"	in liquid hydrogen
"	28	"	30	-	6Al-4V	titanium	weldments	at room temperature
"	31	"	33	-	"	"	"	in liquid hydrogen

The makeup of these tables is identical to that of the earlier base metal static test result tables except that an additional row is added. This row includes calculated through-crack K_{CN} values. This value is included for specimens which leaked and then failed at a net section stress less than 0.80 σ_{ys}. The K_{CN} value is based on initial flaw length (2c) and maximum load. In subsequent paragraphs the data of Tables 19 through 33 are analyzed and discussed from the standpoint of (1) stress/flaw size relationship, (2) through-crack analysis, (3) break-through stress analysis and, (4) back side dimpling.

4.2.2.1 Stress/Flaw Size Relationship

2219-T87 Aluminum Weldments

The data of Tables 19 through 27 are plotted in terms of applied stress versus a/t in Figures 45 through 47. Solid circles indicate fracture mode and open circles indicate leak-before-fail mode. Nominal a/2c values are noted in parentheses. The room temperature data for all thicknesses and flaw shapes are shown in Figure 45. Figure 45 (a) shows data for the thinnest gage tested, 1.60 mm (0.063 in.). It is seen that all specimens tested in this gage experienced flaw break-through prior to fracture. Curves were manually faired through constant a/2c data points. It is seen that, for any given a/t value, the required applied stress to cause leakage increases with increasing a/2c value. This is analogous to brittle fracture behavior, but as shown later, this behavior in thin materials is not relatable to applied stress intensity as with the brittle materials.

A similar plot for the intermediate thickness of 2.67 mm (0.105 in.) tested at room temperature is shown in Figure 45(b). Behavior is quite similar to that of the thinner gage data. Again, all specimens leaked before failing.

Figure 45(c) shows the room temperature test data for the 7.62 mm (0.30 inch) thick specimens. Three of these specimens fractured before leaking but at stresses well above engineering yield strength. From all of the room temperature data shown in Figure 45 it is apparent that elastic fracture of weldments in 2219-T87 vessels in thicknesses up to at least 7.62 mm (0.30 in.) should be virtually non existent. This is of course a major reason for the popularity of this alloy in aerospace structures.

Results of the 2219-T87 weldment fracture tests performed at 78°K (-320°F) are shown in Figure 46. For the most part, results for all thicknesses are similar to those of the room temperature tests. Leakage prior to failure is observed in all specimens of the 1.60 mm (0.063 in.) and the 2.67 mm (0.105 in. gages. Failure before leakage can occur in the 7.62 mm (0.30 in.) thickness, but only at stress levels at or above yield strength. Constant a/2c curves for all thicknesses at 78°K (-320°F) are shifted upwards, as compared to the room temperature data. This shift is comparable to the corresponding increase in engineering yield strength with decreasing temperature.

Test data for the 2219-T87 weldment static fracture tests performed at 20K (-423F) are shown in Figure 47. Leakage mode still predominates, however, it is seen that fracture can occur at levels slightly less than yield. One data point plotted in Figure 47(c) exhibited a fracture mode at a stress somewhat less than 0.90 σ_{ys}. This was specimen #SAH 3-3-5 with a thickness of 7.62 mm (0.30 in.). As seen in Table 27, the calculated Irwin K for this specimen is 25.2 MN/m^2 (22.9 $ksi\sqrt{in}$). Back surface magnification would elevate this value by another ten percent. This value is still much lower than apparent K's obtained previously in 16.0 mm (0.625 in.) weldments (e.g., Ref. (4)). As noted earlier, the weld nugget yield strength under these test conditions is significantly less than the engineering yield strength. The stress at fracture for specimen #SAH 3-3-5 is above the nugget yield strength. For this reason the toughness value listed above is not considered valid.

6Al-4V Titanium Weldments

The titanium weldment fracture data reported in Tables 28 through 33 are plotted in Figures 48 (room temperature tests) and 49 (liquid hydrogen temperature tests). The format and nomenclature of these figures are identical to those of the aluminum in the preceding paragraphs.

The fracture data for the room temperature tests of the 0.51 mm (0.020 in.) gage are shown in Figure 48(a). It is seen that leakage prior to fracture occurs for most specimens in the elastic range, and that fracture can occur only at stress levels approaching or exceeding yield strength. General trends are similar to those of the aluminum except that the constant a/2c curves are flatter at high stresses. This is due to the fact that the yield and ultimate strengths are so close together.

The data for the 1.78 mm (0.07 in.) gage room temperature tests are shown in Figure 48(b). The constant a/2c curves are comparable to those of the thinner stock except for one data point. This is specimen #STR 8-1-4, the deepest flaw with nominal a/2c of 0.15 which fractured before leaking. Gross stress at failure was 0.80 σ_{ys}, yielding a presumably valid K_{IE} value of 68.0 $MN/m^{3/2}$ (61.9 $ksi\sqrt{in}$). This is somewhat higher than that obtained for base metal under the same test conditions. With the above noted K_{IE} value and ligament restrictions discussed earlier, one would expect leakage prior to fracture for any flaw depth greater than about 0.75t. This is in good agreement with the experimental findings shown in Figure 48(b).

The 5.33 mm (0.21 in.) weldment fracture data are shown in Figure 48(c). A total of five specimens in this group failed within acceptable limits for valid K_{IE} measurement. Average calculated K_{IE} for this set is 99.0 $MN/m^{3/2}$ (90.1 $ksi\sqrt{in}$) which compares quite well with the value obtained for the thick base metal value of 93.3 $MN/m^{3/2}$ (84.9 $ksi\sqrt{in}$). At this thickness and toughness, leak before failure would be predicted for any flaw depth greater than 0.80t which again agrees well with observations.

The weldment fracture data obtained at 20K (-423F) are shown in Figure 49. Data for the 0.51 mm (0.02 in.) gage are plotted in Figure 49(a). The single

specimen which fractured elastically before leaking yields a K_{IE} value of 41.9 $MN/m^{3/2}$ (38.1 $ksi\sqrt{in}$) which is about seven per cent less than that obtained from comparable base metal tests. In this gage and test temperature, leakage prior to fracture would be expected for flaws deeper than about 0.80t. While all flaws in this range did break-through several shallower flaws also broke-through. Several of these specimens with shallower flaws did fracture at only slightly higher stresses than the respective break-through stress.

Data for the 1.78 mm (0.070 in.) gage weldment fracture tests performed at liquid hydrogen temperature are shown in Figure 49(b). K_{IE} values were obtained from six specimens. These values are summarized below:

SPECIMEN #	a/2c	K_{IE} $MN/m^{3/2}$	($ksi\sqrt{in}$)
STH 8-1-1	0.15	59.8	(54.4)
STH 8-1-5	0.15	60.6	(55.1)
STH 8-3-1	0.29	58.9	(53.6)
STH 8-3-4	0.34	55.3	(50.3)
STH 8-5-1	0.47	54.4	(49.5)
STH 8-5-4	0.48	52.3	(47.6)

As noted in Section 4.2.1 a single base metal specimen for these test conditions resulted in a K_{IE} value of 42.7 $MN/m^{3/2}$ (38.9 $ksi\sqrt{in}$). Leakage occurred in some specimens with ligaments greater than 0.10 $(K_{IE}/\sigma_{ys})^2$, this behavior is similar to that of the 0.51 mm (0.020 in.) gage results.

Static fracture data for the thick gage titanium weldment specimens tested at liquid hydrogen temperature are plotted in Figure 49(c). One specimen leaked before failing. Fracture load for this specimen was about four percent higher than the break-through load. The remaining specimens failed elastically and resultant K_{IE} values can be considered valid. Results were:

SPECIMEN #	a/2c	K_{IE} $MN/m^{3/2}$	K_{IE} ($ksi\sqrt{in}$)
STH 21-1-1	0.14	61.8	(56.2)
STH 21-1-2	0.14	54.5	(49.6)
STH 21-3-1	0.29	53.5	(48.7)
STH 21-3-2	0.28	67.9	(61.8)
STH 21-3-3	0.28	66.8	(60.8)
STH 21-3-1	0.46	59.3	(54.0)
STH 21-3-2	0.47	52.3	(47.6)
STH 21-3-3	0.47	49.9	(45.4)

A single base metal K_{IE} value for these test conditions was reported earlier to be 58.4 $MN/m^{3/2}$ (53.1 $ksi\sqrt{in}$).

4.2.2.2 Thru-Crack Analysis

It was observed in the work of References 4 and 5 that the fracture strength of specimens which leaked prior to fracturing at elastic stresses could be predicted using the initial surface flaw length and the appropriate K_{CN} value for the material. It was believed that this would hold true for net section stresses less than about 0.80 σ_{ys}.

The vast majority of the aluminum weldment specimens discussed in the preceding section leaked before fracturing. Several leaked at stress levels as low as one-half the yield strength. However, in all cases fracture occurred at net section stresses near or above the yield strength. Obviously the K_{CN} values for these aluminum weldments are in excess of that which can be developed in the specimen sizes and crack lengths which were tested.

In the more brittle titanium weldments tested several specimens leaked and subsequently fractured at elastic stresses. K_{CN} values were calculated for these specimens and are included in the test tables 28 through 33. For clarity, the results are summarized below:

THICKNESS mm (inch)	TEST TEMP °K (°F)	APPARENT K_{CN} - $MN/m^{3/2}$ ($ksi\sqrt{in}$)			
		a/2c = 0.05	a/2c = 0.15	a/2c = 0.30	a/2c = 0.50
5.33 (0.21)	Room	-	146.7 (133.5) 137.6 (125.2)	-	-
0.51 (0.02)	20 (-423)	82.6 (75.2) 85.1 (77.4) 90.8 (82.6)	75.8 (89.0) 69.5 (63.2) -	56.2 (51.1) - -	- - -
1.78 (0.07)	20 (-423)	-	82.5 (75.1) 75.1 (68.3)	79.6 (72.4) 71.1 (64.7)	67.6 (61.5) 66.0 (60.1)
5.33 (0.21)	20 (-423)	-	84.5 (76.9)	-	-

There are very little K_{CN} data available for comparison with the above. The reduction in K_{CN} for the thin gage specimens with decreasing temperature and the ratio of K_{CN} to K_{IE} for the thin and intermediate gages appear reasonable. It is noted that the apparent K_{CN} for the 5.33 mm (0.21 inch) gage specimens tested at 20°K (-423°F) is slightly higher than that of the 1.78 (0.07 inch) gage specimens. Recall that the yield strength was lower and the K_{IE} values were higher for the heat of material used for the thicker specimens. Observation of the fracture faces of these specimens indicated full shear lips in the intermediate thickness specimens and about fifty percent shear in the thicker ones. Additionally, it is noted that apparent K_{CN} values exhibit a slight but consistent trend of reduced values with increase in a/2c.

4.2.2.3 Variables Affecting Break-Through Stress

From discussion and data presented in previous sections and the prior work of Reference 5, it appears that fracture stress (in the elastic range) of surface flaw specimens can be predicted using available solutions regardless of failure mode. For specimens which fracture before leaking the prediction is based upon surface flaw stress intensity solutions which incorporate back surface magnification terms and thus failure strength is primarily a function of flaw depth, flaw shape, thickness, and K_{IE}. For specimens which leak before fracturing, the final fracture strength is primarily dependent on original surface flaw length and the K_{CN} value for the material. Additionally use of a ligament requirement of $0.10\ (\frac{K_{IE}}{\sigma_{ys}})^2$ appears to be a useful criterion for predicting whether leakage will precede fracture.

On the other hand, for those cases where leakage does precede fracture, procedures are not available for predicting the stress at which leakage will occur. From discussions of Section 4.2.2 and from observation of the shape of stress/flaw size curves it is apparent that stress at leakage is not primarily dependent upon applied stress intensity. This is also borne out in Figure 50. Here the data for the 2219 weldments are plotted to show the observed relationship of flaw depth-to-thickness and flaw shape required to cause leakage (or fracture) at yield strength for the various test conditions studied in this program. These curves are cross plots of curves of Figures 45 thru 47. Figure 50(a) shows flaw-depth-to-thickness ratios and a/2c combinations which will cause leakage at the engineering yield strength at room temperature. The data are plotted in terms of a/t versus thickness with the family of a/2c values tested. Open circles denote leakage, solid circles denote fracture before leakage. In this instance (i.e., room temperature) only leakage occurs. Of primary significance in Figure 50(a) is the nearly horizontal slope of the curves. A stress intensity controlled process would exhibit curves with a high negative slope. For example, the calculated stress intensity for an a/t value of 0.70 and an a/2c of 0.15 is about 70 percent higher for the 7.62 mm (0.300 inch) thickness than the 2.67 mm (0.105 inch) thickness. A constant K curve would require the a/t value to drop to about 0.40 at a thickness of 7.62 mm (0.300 inch). There is a gross correspondence with stress intensity and the relative locations of the a/2c curves for a given thickness. Calculated stress intensity is somewhat lower for the high a/2c ratios.

Curves for the cryogenic temperatures in Figures 50(b) and (c) are similar. Interestingly the 78K (-320F) data are nearly duplicates of the room temperature curves. Note that the curves are plotted for leakage at engineering yield at 78K (-320F). The curves for liquid hydrogen temperature tests, Figure 50(c) do show a drop in a/t values at all thicknesses and there is a mode change to fracture before leakage in the thickest gage. Recall, however, that both engineering yield and local yield strength increase rapidly below 78K (-320F) with engineering yield increasing faster.

It is concluded that leakage stress is not K controlled. Rather, it appears to be strongly dependent on yield strength, a/t and a/2c.

In Reference (5) a study was made of the amount of flaw growth which took place on increasing load. Crack growth driving and resistance curves were constructed to describe instability for 12.7 mm (0.50 inch) thick base metal specimens which fractured before leakage. A similar attempt was made in this program using data from proof overload specimens described later in Section 4.3. However, data scatter precluded such an exercise. It did appear that stable growth initiated at a relatively constant calculated stress intensity with this level increasing slightly as thickness increases. Data for the 1.60 mm (0.063 inch) gage specimens are shown in Figure 51.

4.2.2.4 Back Surface Dimpling

Recent studies of back surface dimpling have made use of inteferometric techniques to study the surface displacements caused by the formation of plastic zones[8,20]. Such techniques were not feasible on this program because instrumentation used to detect flaw break through made the rear surface inaccessible for direct observation. For this reason, strain gages were affixed to the rear surface to detect plastic zone penetration. Strain gage locations are noted in the data tables as described in Section 4.2.1.

For these tests it was assumed that dimpling had occurred when the maximum strain on the back surface was equal to the yield strain of the material defined by 0.20 percent offset. The gross section stress at which this strain was reached is noted as the dimpling stress for each specimen in Table 19 thru 66. It is recognized that this definition of dimpling threshold is somewhat arbitrary; however it does represent a procedure which is fairly reproducible in view of the fact that we are considering lateral deformations in the realm of a few hundred microinches. The procedure noted above is identical to that used in the Reference 5 program.

Results of the dimpling measurements are shown in Figures 52 thru 55. These are plots of the crack aspect ratio a/2c, versus crack depth ratio, a/t at the dimple stress to engineering yield strength ratio. Figures 52 and 53

show results for the 2219 weldment data at room temperature and 20K (-423F), respectively. Figures 54 and 55 show dimpling theshold for the 6Al-4V titanium weldments at room temperature and 20K (-423F), respectively.

Included in the figures is a comparison of the raw data with threshold curves (solid lines) estimated by the Dugdale model of plastic yielding proposed in Reference 21.

In general, all figures show a definite trend for the data to group together for a given applied stress ratio (σ_D/σ_{ys}) with the perceived dimple threshold for a deeper crack occurring at a lower stress level as expected. The perceived dimple threshold is also relatively insensitive to changes in crack aspect ratio at all applied stress ratios. The agreement between predicted and observed threshold of dimpling is relatively good, with the experimental points having a consistent trend of lying on a slightly lower slope than that of either the predicted curves, or of the curves of the Reference 5 data. Further, it is seen that the test results are not strongly affected by test temperature.

Francis et al measured dimpling thresholds on 6Al-4V[20] and 2219-T87[8] alloys at room temperature by visual methods. His results showed dimpling could be visually observed at lower stress levels than those recorded in this program.

The test results of Figure 54 are replotted in Figure 56 in terms of a non-dimensionalized form of stress intensity versus applied stress. This figure was plotted in this form to determine whether or not the threshold of perceived dimpling could possibly be used to estimate the corresponding stress intensity factor for a given applied stress level and plate thickness. It is seen that the estimate could be quite accurate at relatively high stress ratios, however, if stress ratios decrease, the calculated stress intensity is strongly dependent upon flaw shape.

4.3 Cyclic Tests

The effects of flaw shape, proof overload cycle and stress level on the cyclic life of various thicknesses of "as-welded" 2219-T87 aluminum and 6Al-4V STA titanium were investigated and are presented in this section. All tests were

conducted in laboratory air at 295 K (72 F) using surface flawed specimens. The flaw shapes (a/2c values) for these specimens ranged from about 0.05 to 0.50 and the test cyclic stress level was either 0.70 σ_{ys} or 0.85 σ_{ys}. Specimens that were proof tested were proofed to a stress equal to σ_{ys} or 0.91 σ_{ys}. The thicknesses investigated for the aluminum were 1.60 mm (0.063 inch), 2.67 mm (0.105 inch), and 7.62 mm (0.30 inch) while thicknesses for the titanium were 0.51 mm (0.020 inch), 1.78 mm (0.070 inch), and 5.33 mm (0.21 inch).

4.3.1 Fatigue Crack Growth Rates

The cyclic crack growth rates for the materials investigated were determined in terms of da/dN and are presented as a function of maximum stress intensity, $K_{I_{MAX}}$. The stress intensity values were calculated using the equation:

$$K_{I_{MAX}} = 1.1\ \sigma_{MAX}\ \left(\frac{\pi a}{Q}\right)^{1/2} M_K$$

where the deep flaw magnification factor is defined in Figure 30. For specimens receiving a proof test prior to cyclic testing, the amount of crack growth occurring during the proof test was not included in calculating the crack growth rates. This growth-on-loading was clearly defined by the adjacent precrack band and subsequent cyclic test band. For specimens that were not proof tested, the amount of growth-on-loading that occurred on the first cycle was not clearly defined and therefore was included in the growth rate calculations. This procedure would result in somewhat higher initial apparent cyclic crack growth rates than would actually exist.

For each thickness of material investigated, proof and non-proofed specimens were tested. The stress conditions for the specimens which were proof tested are presented below:

PROOF STRESS	CYCLIC STRESS
1.0 σ_{ys}	0.85 σ_{ys}
1.0 σ_{ys}	0.70 σ_{ys}
0.91 σ_{ys}	0.70 σ_{ys}

The non-proofed specimens were cycled at the same cyclic stress levels as the proofed specimens. The initial flaw sizes for these cyclic tests (proofed and non-proofed specimens) were selected based on the flaw size that would just pass the specified proof stress for a given flaw shape, as determined from the prior static tests (ref. Section 4.2).

2219-T87 Aluminum

The cyclic crack growth rates developed for the "as-welded" 2219-T87 aluminum are shown in Figures 57 through 65 as a function of stress intensity. The crack growth rates obtained were very orderly when presented as a function of stress intensity which incorporated a deep flaw magnification factor. The specimens that were proof tested exhibited slightly retarded growth rates compared to the non-proofed specimens as illustrated in Figure 66. The amount of retardation also appears to increase for the proofed specimens having low a/2c values (long flaws), as observed in Figure 61 through 65. In general, these cyclic crack growth rate curves do not show a dependency on flaw shape for the majority of tests conducted. The variation in flaw shape is accounted for in the calculation of stress intensity in terms of the flaw shape parameter, Q. The specimen and test details for these tests are presented in Tables 34 through 51.

A summary of the cyclic crack growth rates obtained for the "as-welded" 2219-T87 aluminum material tested is presented in Figure 67. All of the data presented in Figures 57 through 65 are incorporated into Figure 67. There appears to be a slight increase in cyclic growth rates at a constant stress intensity value as material thickness decreases. This same phenomena was observed for 2219-T87 aluminum as presented in Reference 4 and 5. As Figure 67 illustrates, the cyclic crack growth rates are grouped within fairly narrow scatterbands for each material thickness, even though a wide range of flaw shapes, proof stress levels and cyclic stress levels were tested.

6Al-4V STA Titanium

The cyclic crack growth rates developed for the "as-welded" 6Al-4V STA titanium are shown in Figures 68 through 76 as a function of stress intensity. The data presentation for the titanium cyclic crack growth rates is the same as that

used for the aluminum, and the results obtained are similar. The crack growth rates obtained were very orderly and within the limits of the data generated, no dependency of crack growth rates on flaw shape was observed. The specimens that were proof tested exhibited moderately retarded growth rates compared to the non-proofed specimens. The amount of retardation is summarized in Figure 77 for the material thicknesses tested. The specimen and test details for these tests are presented in Tables 52 through 69.

A summary of the cyclic crack growth rates obtained for the "as-welded" 6Al-4V STA titanium is presented in Figure 78. All of the data presented in Figure 68 through 76 are incorporated into Figure 78. Although the scatterbands for the titanium results are somewhat larger than those reported for the aluminum, there still appears to be a dependency of cyclic crack growth rates on material thickness. In general, the growth rates increase for decreasing material thickness at a constant stress intensity level.

4.3.2 Influence of Flaw Shape on Cyclic Life

One fundamental question which requires answering is what influence does the flaw shape have on the cyclic life of a pressure vessel that has been proof tested? As illustrated by the static fracture data presented in Section 4.2, a given proof stress level can screen both a long shallow and a deeper round flaw. A typical example is illustrated in Figure 79 for the 1.60 mm (0.063 inch) "as-welded" 2219-T87 aluminum. Under cyclic operation, which flaw will break-through the back surface first; the shallow long flaw or the round deep flaw? To answer this question, the cyclic life data generated in this investigation were analyzed and presented in terms of the operating stress to proof stress ratio for the particular test under consideration. The procedure used parallels that which is employed when dealing with modified linear elastic fracture mechanics procedures. A brief explanation is presented below.

If the cyclic crack growth rates are a stress intensity controlled phenomena, then the ratio of initial to critical stress intensity (K_{1i}/K_{IE}) would be a measure of the cyclic life of a structure. If a structure is operated at a cyclic stress of σ_o after being subjected to a proof stress of σ_p, then the ratio of σ_o/σ_p is equal to K_{1i}/K_{IE} as illustrated in Figure 80. Specimens that were subjected to cyclic profiles in this investigation contained flaw

sizes that were targeted at the size that would cause break-through at the proof stress level. The instant of proof test termination was based on information obtained from the crack opening displacement (COD) instrumentation. When the COD instrumentation indicated imminent flaw break-through or fracture, the proof test was terminated. In general, this would mean that the actual proof stress level would either be slightly higher or lower than desired. The difference between actual flaw size present in a specimen and the critical flaw size, a_{cr}, predicted from stress-flaw size loci would increase or decrease the cyclic life of a test specimen. In essence, if the flaw size was less than the critical amount, the cyclic test would start at a lower initial stress intensity value (K_{1i}) as illustrated in Figure 80; the converse is also true. The ratio K_{1i}/K_{IE} is then a better measure of cyclic life of the actual test specimens. As presented in Figure 80, the ratio K_{1i}/K_{IE} is numerically equal to $\left(\frac{\sigma_o}{\sigma_p}\right)\cdot\left(\frac{a_o}{a_{cr}}\right)^{1/2}$ for a given flaw shape parameter. All of the cyclic life data generated in this report was analyzed and presented as a function of this stress-flaw depth parameter. (This parameter will hereafter be referred to as KR).

Cycles to break-through versus the KR parameter for the "as-welded" aluminum and titanium are presented in Figures 81 and 82. All of the results indicate a dependency of cyclic life on flaw shape with the shallow long flaw yielding significantly less life than the round deep flaw. The conclusion being that the long flaw barely passing a proof test will have substantially less cyclic life than a round (deeper) flaw barely passing the same proof test.

The curves presented in Figure 81 and 82 could be used to select an operating stress level for a specific mission cyclic life requirement if the structure was proof tested at or near the weld yield strength and operated in an inert environment (i.e., air, helium, argon, etc.). If the structures successfully passed a proof test, a_o would be assumed to be equal to a_{cr} and the plots presented in Figure 81 and 82 would be reduced to operating-to-proof stress ratio versus cycles to leak or fracture. Since the flaw shape would be an unknown quantity, an analysis of this type would have to assume that a long flaw ($a/2c \sim 0.05$) existed. This would be conservative, yielding the shortest cyclic life.

It is interesting to see how the flaw shape affects cyclic life at a given operating stress level. This is most clearly illustrated by a specific example; in this case the 1.60 mm (0.063 inch) "as-welded" 2219-T87 aluminum. A cross-plot of the data from Figure 81 for that thickness of material yields the results presented in Figure 83 by the solid line. For comparison purposes, an analysis was conducted to determine the number of cycles necessary to grow flaws (of various flaw shapes which successfully passed a proof test) to the point of break-through. The initial flaw sizes screened by the proof test were used as the starting point and no flaw growth was assumed to occur during proof. The cyclic crack growth rate data used was based on the non-proofed rates presented in Section 4.3.1 for a given material thickness. The specific initial flaw depths for various initial flaw shapes are indicated in Figure 79 for the example being presented. The initial stress intensity levels at the operating stress for each of the three flaw shapes investigated are also indicated in Figure 79. The initial stress intensity values (calculated using the deep flaw magnification factor of Figure 30) are essentially the same for the 0.05 and 0.15 a/2c values and then decrease for the 0.30 flaw shape. The final stress intensity values at break-through were higher than the initial values and also decreased as the a/2c value increased. The net result is that the average stress intensity ($\frac{K_{Ii} + K_{If}}{2}$) for a given flaw shape decreased as the a/2c value increased. Since the cyclic crack growth rate (da/dN) has been shown to be essentially independent of flaw shape when presented as a function of stress intensity (see Section 4.3.1), the higher average stress intensity for the long flaw would yield a higher crack growth rate than that for the round flaw. Even though the long flaw screened by the proof test had a larger amount of flaw growth potential before break-through than the round flaw, the higher crack growth rates for the long flaw results in the least cyclic life of any flaw shape. The results of this stress intensity/rate analysis are presented in Figure 83, as the dashed line, for the thin aluminum tested. The results compared very favorably with those obtained from the cyclic life versus operating-to-proof stress ratio analysis.

4.3.3 Influence of Proof Test on Cyclic Life

It has been observed for the weldments investigated herein that a proof test to about the yield strength of the weldment will yield information as to the initial flaw size that could have existed in the proofed structure. It is also

observed that a certain amount of flaw growth will occur during that proof test if the flaw size present in the structure approaches the critical initial size that would cause break-through. Since flaw growth can occur during the proof test, the question arises does the proof test actually reduce the available cyclic life of the structure compared to a non-proofed structure having the same initial flaw present prior to any testing? The data presented in Figures 81 and 82 do not suggest this. These figures present the cyclic life of specimens that were proofed and non-proofed as a function of KR. For a given initial flaw shape, the cyclic life results for proofed specimens are essentially the same as the non-proofed specimens within the scatter of the data obtained. These figures also do not show any dependency on proof stress level (i.e., σ_p=0.91 $\sigma_{ys} \rightarrow \sigma_{ys}$).

An even clearer demonstration of what effect the proof test has on the cyclic life of a welded structure can be observed in Figures 84 and 85. These figures illustrate that proofed and non-proofed specimens of approximately the same initial flaw size yield essentially the same cyclic life even though a considerable amount of proof test flaw growth takes place for the proofed specimens.

Specimens that are cycled after a proof test exhibit reduced cyclic crack growth rates (see Section 4.3.1) compared to non-proofed specimens. The results presented above appear to indicate that any detrimental effect caused by proof test flaw growth is compensated for in the subsequent reduced cyclic crack growth rates for these materials. This is most clearly expressed in terms of an example as presented in Figure 86. Two titanium specimens having essentially the same initial flaw size are cycled to break-through; one specimen is proof tested while the other one is not. A considerable amount of flaw growth occurs for the proofed specimen as shown in Figure 86. The manner in which the flaws grow during the cyclic test for these two specimens is also shown in Figure 86. The proofed specimen grows considerably slower initially than the non-proofed specimen with the net result being almost identical cyclic lives for the two specimens.

In conclusion, there appears to be no detrimental effect of a proof test on the cyclic life of the "as-welded" material investigated.

Another interesting point concerning proof tests of the "as-welded" materials investigated is that a room temperature proof test could be used to guarantee the operation at cryogenic temperatures as shown in Figure 87. In this example, a room temperature proof test to σ_{ys} would screen the same size flaw as σ_p at 20K (-423F). Thus the cryogenic cyclic life of a structure which passes a room temperature proof test could be estimated by use of the type of plot as shown in Figure 81 and 82. In this case the data required would be obtained by cyclically testing specimens at 20K (-423F) after being subjected to a room temperature proof test.

5.0 CONCLUSIONS

The following conclusions are based upon test results of surface flawed 2219-T87 aluminum and 6Al-4V titanium weldments in thicknesses which would result in a leak-before-fracture mode. However, these conclusions may also be generally applicable to other alloys:

Static Fracture Behavior

(1) Leak-before-fracture mode can normally be expected if the initial flaw ligament dimension is less than about 0.10 $\left(\frac{K_{IE}}{\sigma_{ys}} \right)^2$.

(2) Fracture strength of specimens which leak-before-break can be estimated by considering the initial flaw length (2c) and the appropriate thru-crack toughness value of the material.

(3) The stress level at which crack break-through occurs can not presently be predicted, however, it appears to be strongly dependent upon flaw depth-to-thickness ratio, flaw shape and yield strength.

(4) Flaw sizes in a proof tested structure may be estimated by observing back surface dimpling and this technique may eventually prove useful as a nondestructive inspection tool.

Cyclic Behavior

(1) The cyclic crack growth rates for "as-welded" 2219-T87 aluminum and 6Al-4V STA titanium can be adequately described as a function of applied K_I levels (incorporating deep flaw magnification factors). The crack growth rates presented in this manner appear to be independent of flaw shape and cyclic stress level. The crack growth rates increase with decreasing thickness.

(2) A successful proof test of materials in which leak-before-break mode prevails can provide assurance of subsequent safe life operation.

(3) When equally critical shallow long flaws and deep round flaws, (i.e., both flaws would barely survive a given proof stress), are cyclically tested the shallow long flaws yield the shortest cyclic lives.

(4) While significant flaw growth can occur during a proof test of thin and/or high toughness materials, subsequent cyclic life is not impaired when compared to a non proof tested condition. The growth which occurs during proof testing is compensated for by retarded cyclic crack growth rates.

REFERENCES

1. C. F. Tiffany, "Fracture Control of Metallic Pressure Vessels," NASA SP-8040, 1970.

2. Current Efforts at Updating MIL-STD 1530 (USAF), September 1972.

3. G. R. Irwin, "Crack Extension Force for a Part-Through Crack in a Plate", Journal of Applied Mechanics, Vol. 29, Trans. ASME, Vol. 84, Series E, December 1962.

4. J. N. Masters, W. P. Haese and R. W. Finger, "Investigation of Deep Flaws in Thin Walled Tanks," NASA CR-72606, December 1969.

5. J. N. Masters, W. D. Bixler and R. W. Finger, "Fracture Characteristics of Aerospace Alloys Containing Deep Surface Flaws", NASA CR 134587 December 1973.

6. R. C. Shah and A. S. Kobayashi, "On the Surface Flaw Problem", The Surface Crack: Physical Problems and Computational Solutions, edited by J. L. Swedlow, ASME, November 1972.

7. F. W. Smith, "Stress Intensity Factors for a Surface Flawed Fracture Specimen," Tech. Report No. 1, NASA Grant NGR--6-007-063, Colorado State University, 1971.

8. P. H. Francis and D. L. Davidson, "Experimental Characterization of Yield Induced by Surface Flaws", The Surface Crack: Physical Problems and Computational Solutions, ASME, November 1972.

9. A. E. Green and I. N. Sneddon, "The Distribution of Stress in the Neighborhood of a Flat Elliptical Crack in an Elastic Solid", Proc. Cambridge Phil. Soc., Vol. 46 (1950).

10. E. E. Witzell and C. J. Kropp, "Weldment Flaw Growth Characteristics of 2219-T81 Aluminum Alloy", NASA CR-72288, September 1967.

11. P. M. Lorenz, "Fracture Toughness and Subcritical Flaw Growth Characteristics of Saturn S1-C Tankage Materials", Boeing Document D2-22802, July 1964.

12. L. R. Hall and C. F. Tiffany, "Fracture and Flaw Growth Investigation for 2014-T6 Aluminum Weldments Used in Saturn S-11 LH_2 Tanks", Boeing Document D5-15737, November 1967.

13. D. E. Pettit and D. W. Hoeppner, "Fatigue Flaw Growth and NDI Evaluation for Preventing Through Cracks in Spacecraft Tankage Structures", NASA CR-1285600, September 25, 1972.

14. C. F. Tiffany, J. N. Masters and W. D. Bixler, "Flaw Growth of 6Al-4V Titanium in a Freon TF Environment", NASA CR-99632, April 1969.

15. C. F. Tiffany and J. N. Masters, "Investigation of the Flaw Growth Characteristics of 6Al-4V Titanium Used in Apollo Spacecraft Pressure Vessels", NASA CR-65586, March 1967.

16. C. E. Fedderson, "Discussion to Plane Strain Crack Toughness Testing of High Strength Metallic Materials", ASTM STP 410, pp. 77-79, 1966.

17. D. J. Ayres, "A Numerical Procedure for Calculating Stress and Deformation Near a Slit in a Three-Dimensional Elastic-Plastic Solid", Engineering Fracture Mechanics, Vol. 2, No. 2, November 1970.

18. A. S. Kobayashi, B. G. Wade and D. E. Maiden, "An Investigation of the Crack Arrest Capability of a Hole", Tech. Rep. No. 11, ONR Contract N 00014-67-A-0103-0018, NR 064 478, University of Washington, January 1971.

19. L. R. Hall and W. D. Bixler, "Subcritical Crack Growth of Selected Aerospace Pressure Vessel Materials", NASA CR-120834, December 1972.

20. P. H. Francis, D. L. Davidson and R. G. Forman, "An Experimental Investigation into the Mechanics of Deep Semi-elliptical Surface Cracks in Mode I Loading", Engineering Fracture Mechanics, (to be published).

21. A. S. Kobayashi and W. L. Moss, "Stress Intensity Magnification Factors to Surface-Flawed Tension Plate and Round Notched Tension Bar", Frac. Proc. 2nd International Conference on Fracture (Brighton), Chapman and Krell, London, 1969.

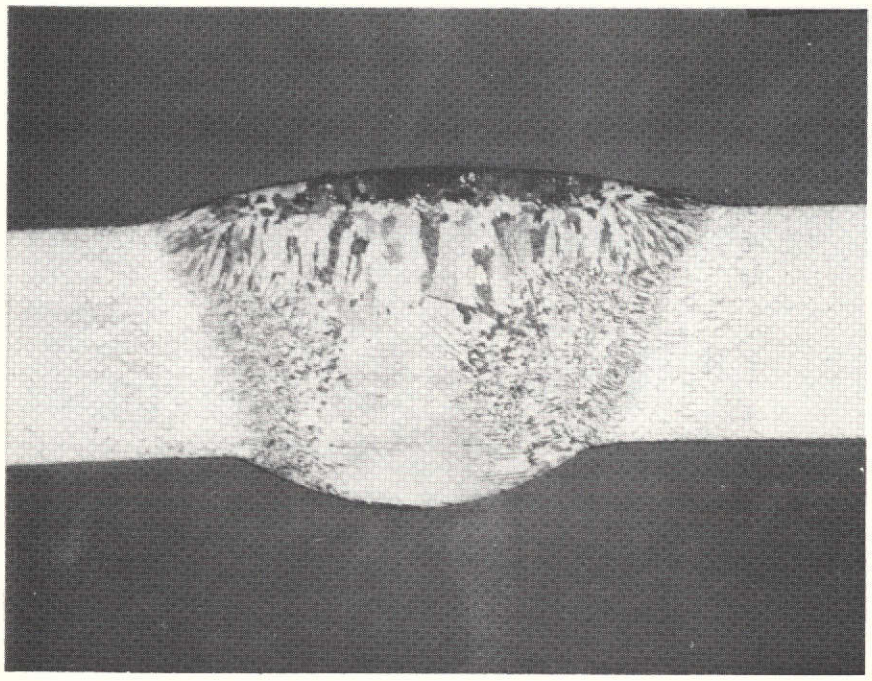

a) 3.18 mm (0.125 INCH) MATERIAL *10X*

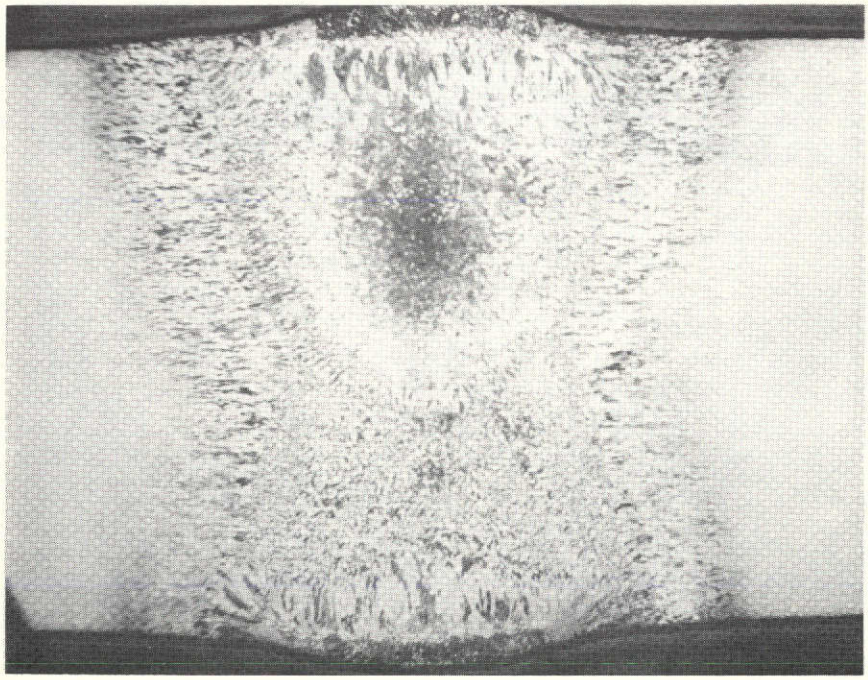

6X

b) 12.70 mm (0.500 INCH) MATERIAL

ETCHANT USED: KELLER'S ETCH

Figure 1 : 2219-T87 ALUMINUM WELDS

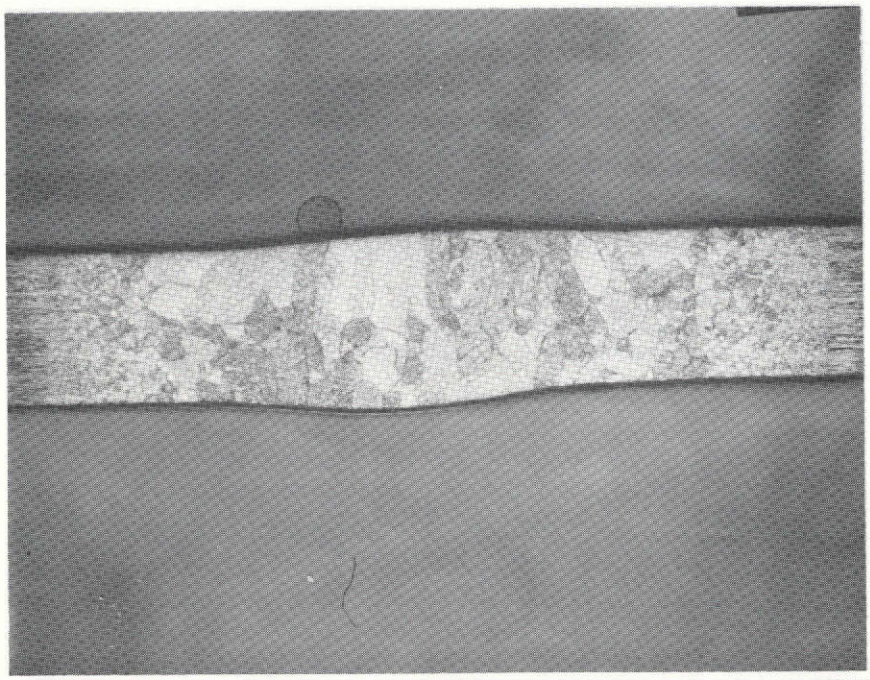

10X

a) 2.03 mm (0.080 INCH) MATERIAL

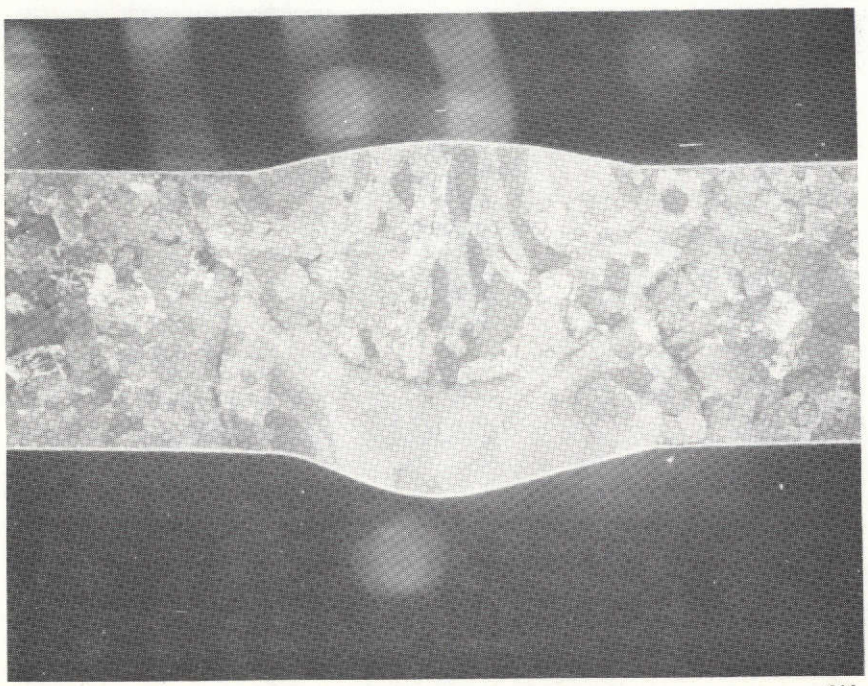

6X

b) 6.35 mm (0.250 INCH) MATERIAL

ETCHANT USED: KROLL'S ETCH

Figure 2 : 6Al-4V TITANIUM WELDS

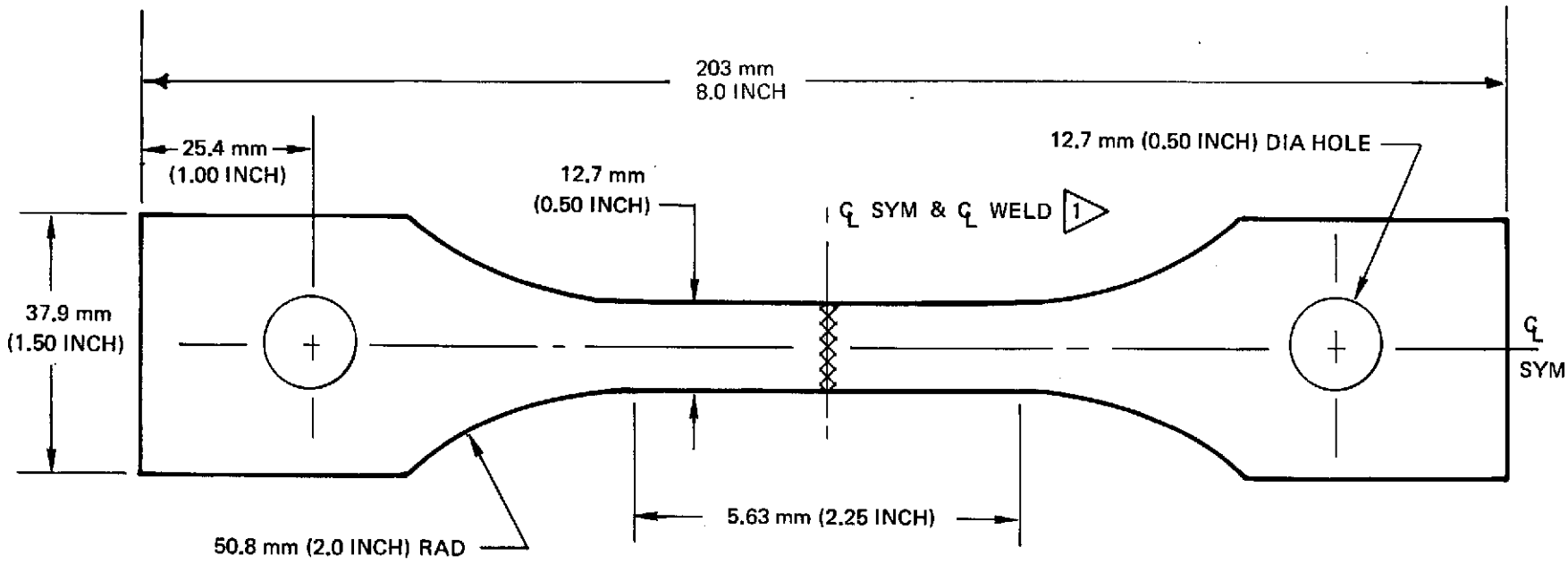

MATERIAL	THICKNESS
2219-T87 BASE METAL	1.60, 3.18, 7.62 mm (0.063, 0.125, 0.300 INCH)
2219-T87 WELDMENT	1.60, 2.67, 7.62 mm (0.063, 0.105, 0.300 INCH)
6AL-4V BASE METAL	0.51, 2.03, 6.35 mm (0.020, 0.080, 0.25 INCH)

1 WELDMENT SPECIMENS ONLY

Figure 3: 2219-T87 ALUMINUM ALLOY BASE METAL AND WELDMENT, AND 6AL–4V TITANIUM ALLOY BASE METAL TENSILE SPECIMEN

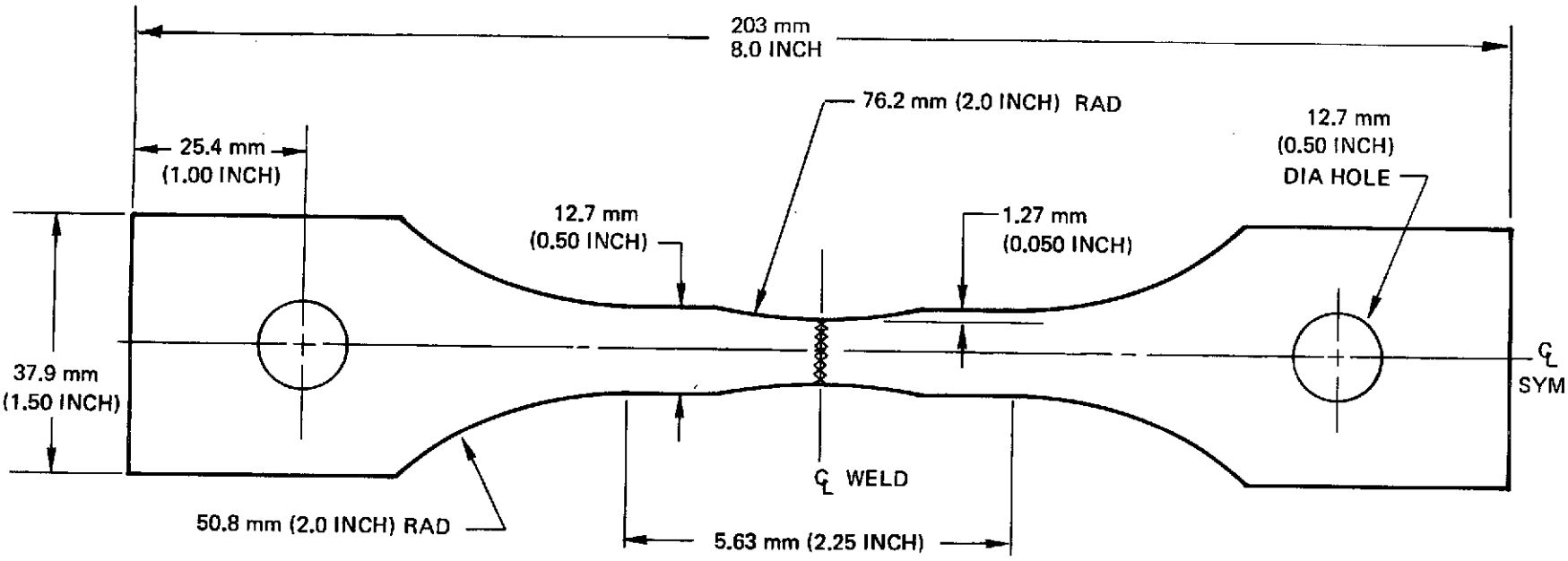

THICKNESS: 0.51, 1.78, 5.33 mm
(0.020, 0.070, 0.210 INCH)

Figure 4: 6AL–4V TITANIUM ALLOY WELDMENT TENSILE SPECIMEN

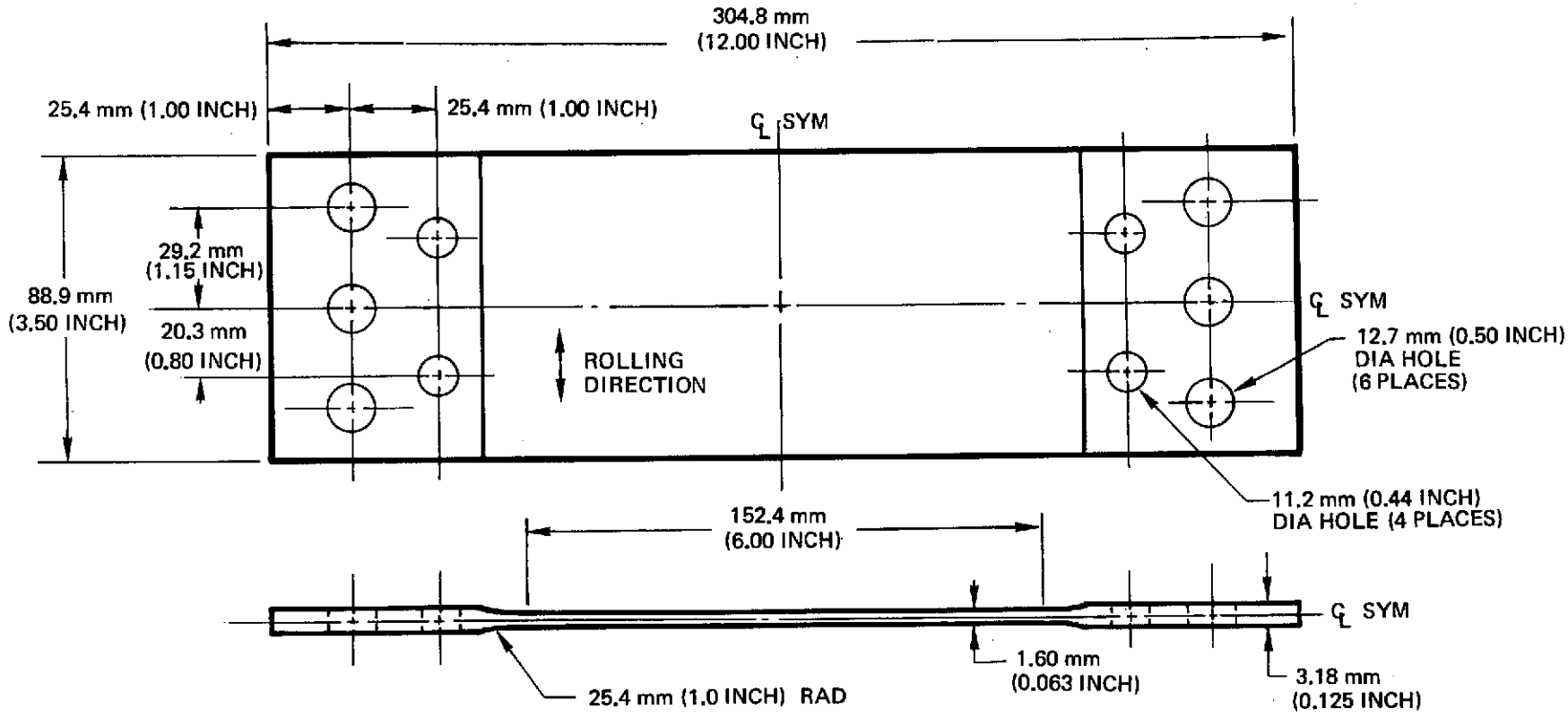

Figure 5: 1.60 mm (0.063 INCH) THICK 2219-T87 ALUMINUM ALLOY BASE METAL SPECIMEN

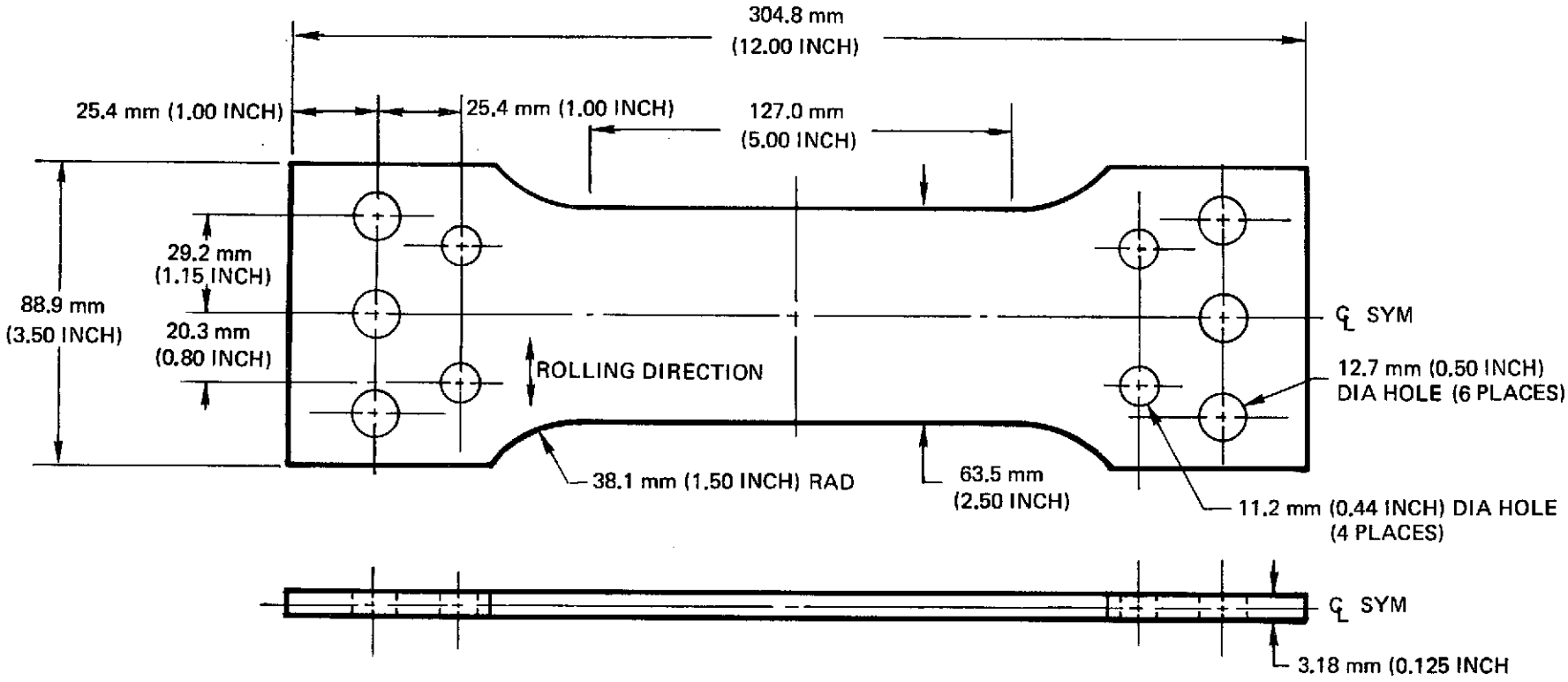

Figure 6: 3.18 mm (0.125 INCH) THICK 2219-T87 ALUMINUM ALLOY BASE METAL SPECIMEN

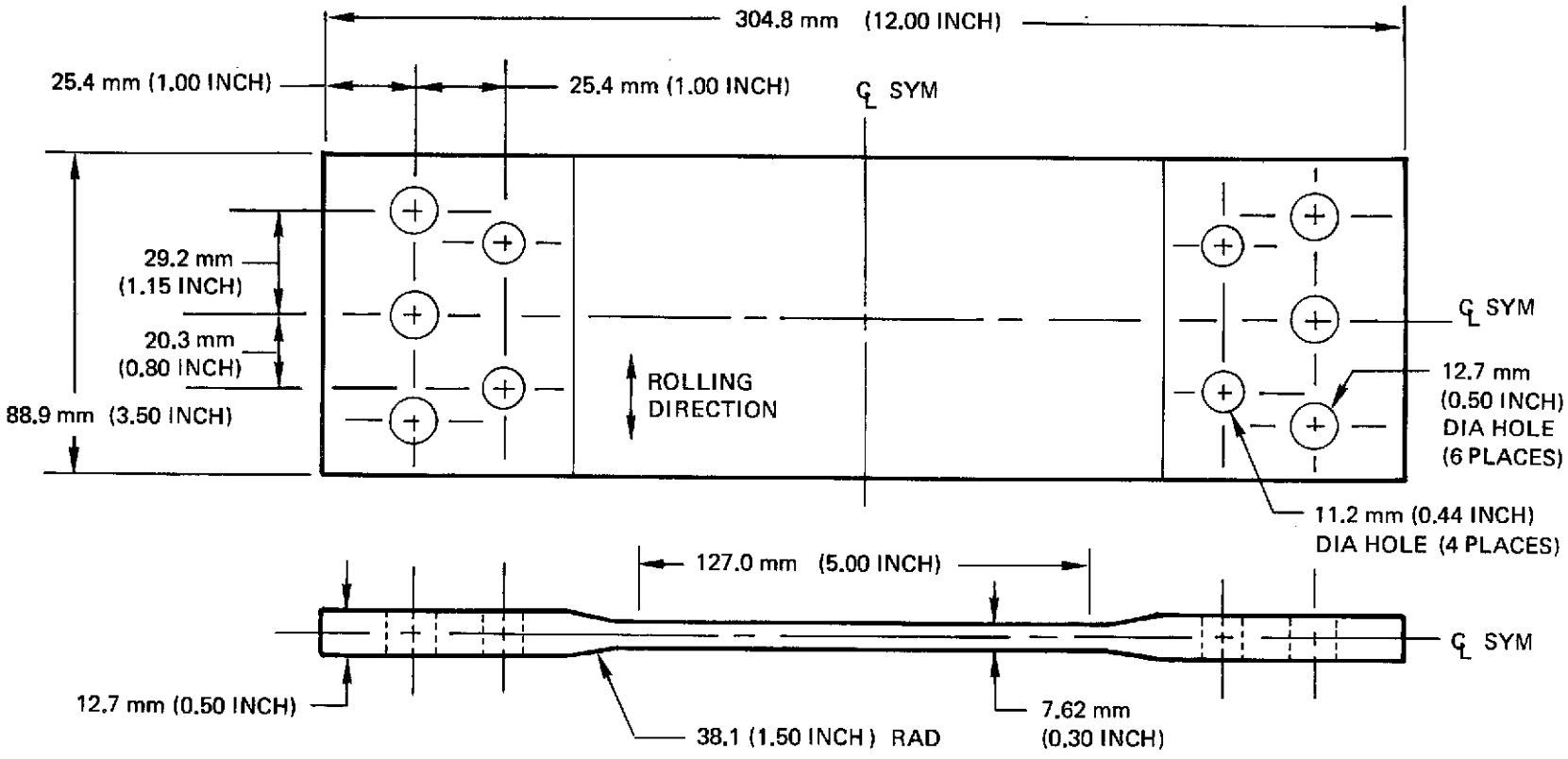

Figure 7: 7.62 mm (0.300 INCH) THICK 2219-T87 ALUMINUM ALLOY BASE METAL SPECIMEN

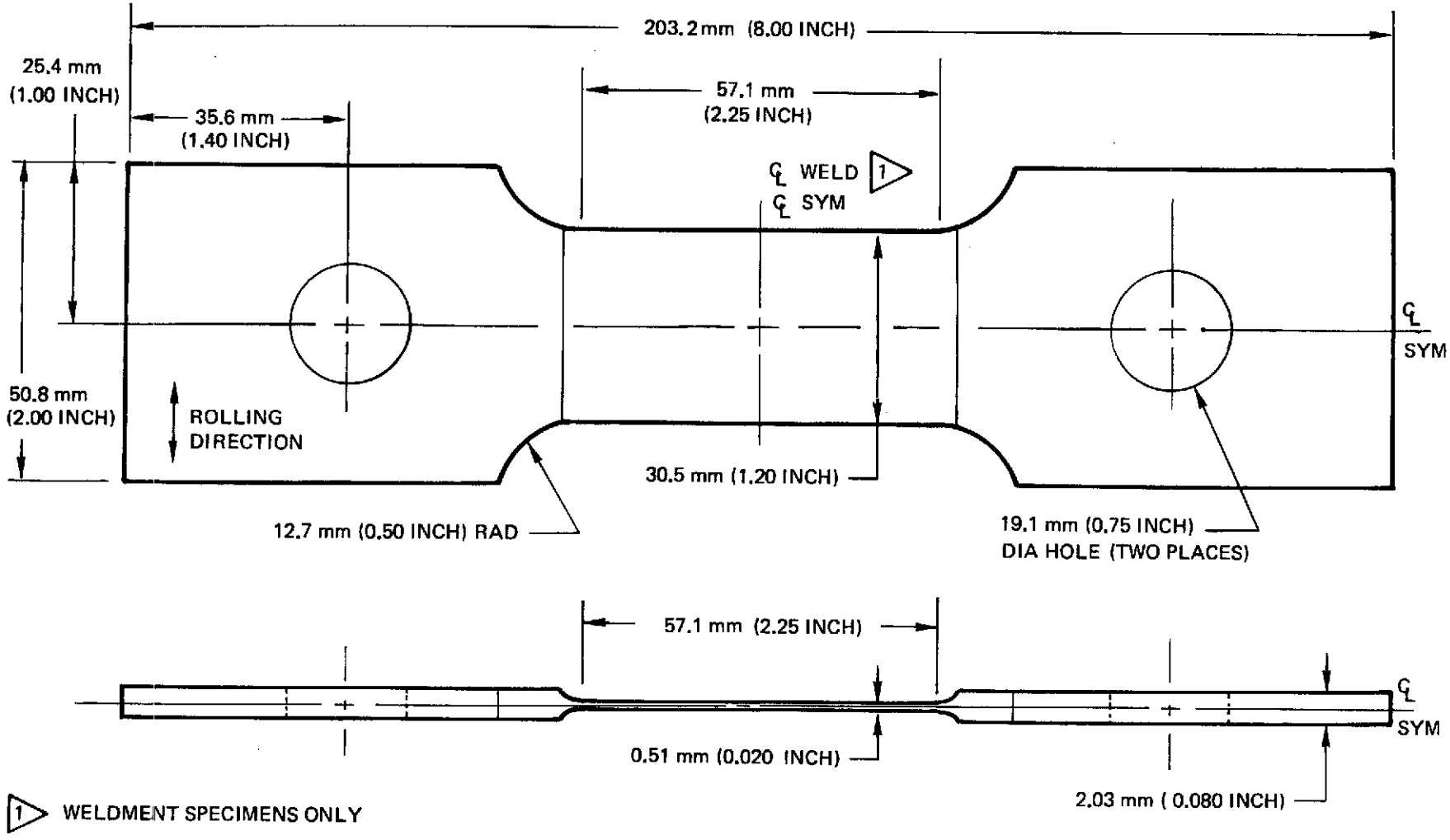

Figure 8: 0.51 mm (0.020 INCH) THICK 6AL-4V TITANIUM ALLOY BASE METAL AND WELDMENT SPECIMEN

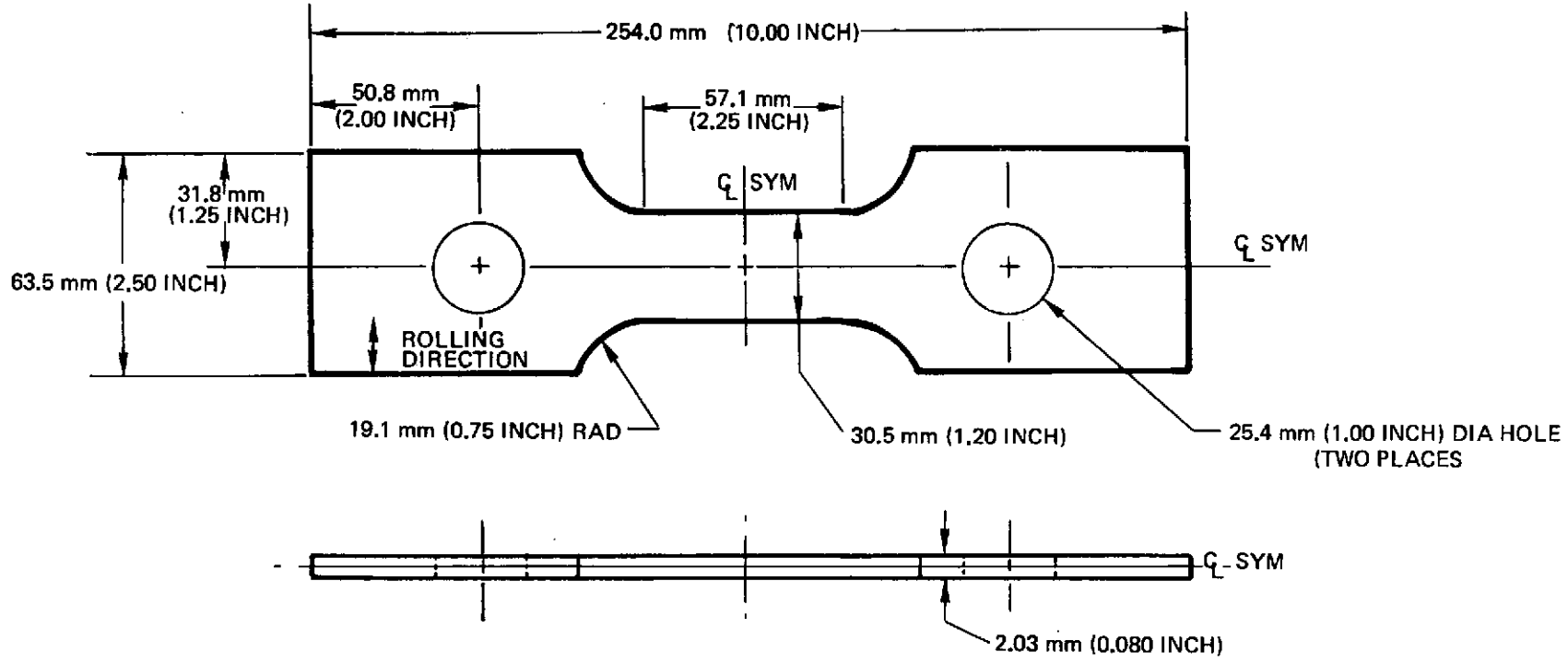

Figure 9: ***2.03 mm (0.080 INCH) THICK 6 AL–4V TITANIUM ALLOY BASE METAL SPECIMEN***

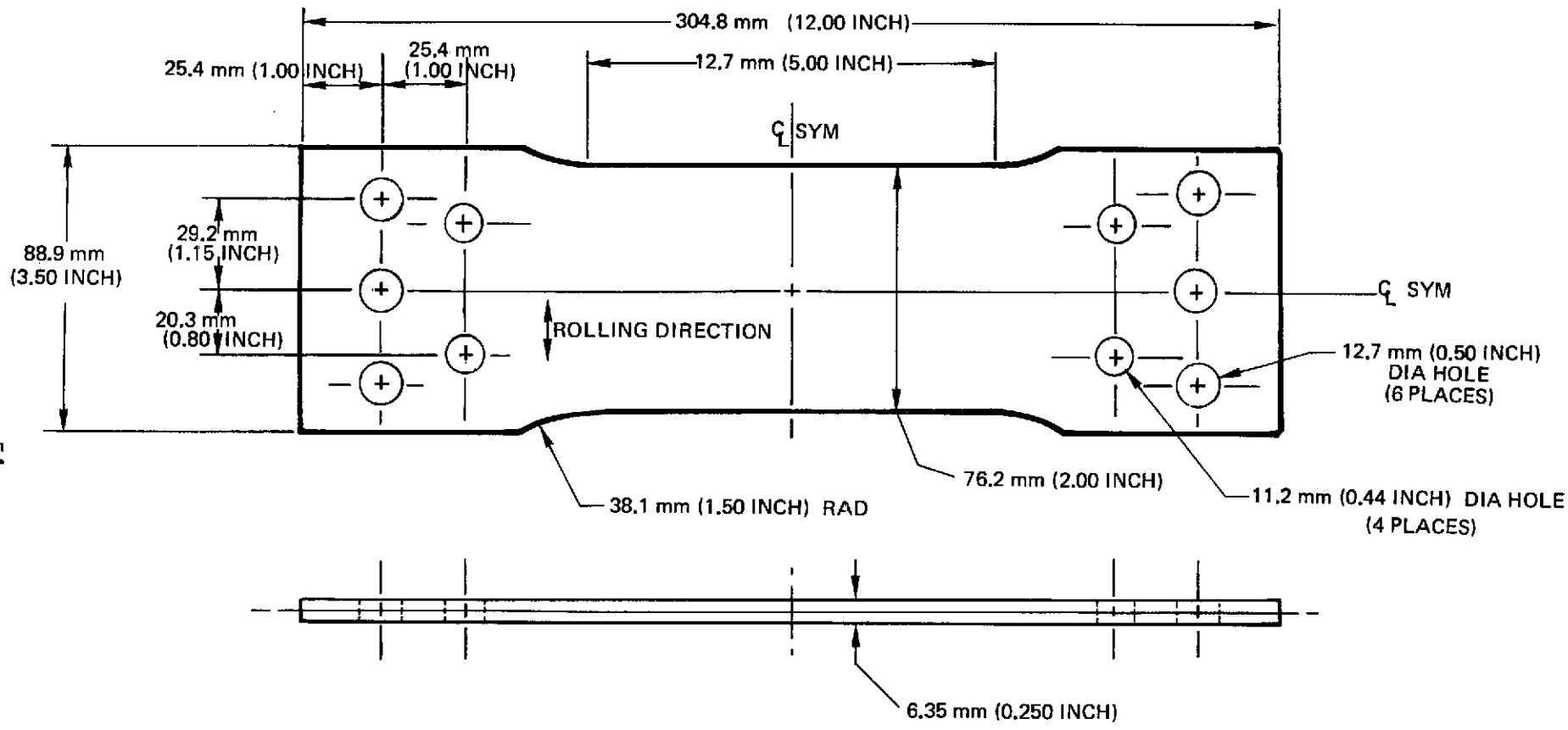

Figure 10: 6.35 mm (0.250 INCH) THICK 6AL–4V TITANIUM ALLOY BASE METAL SPECIMEN

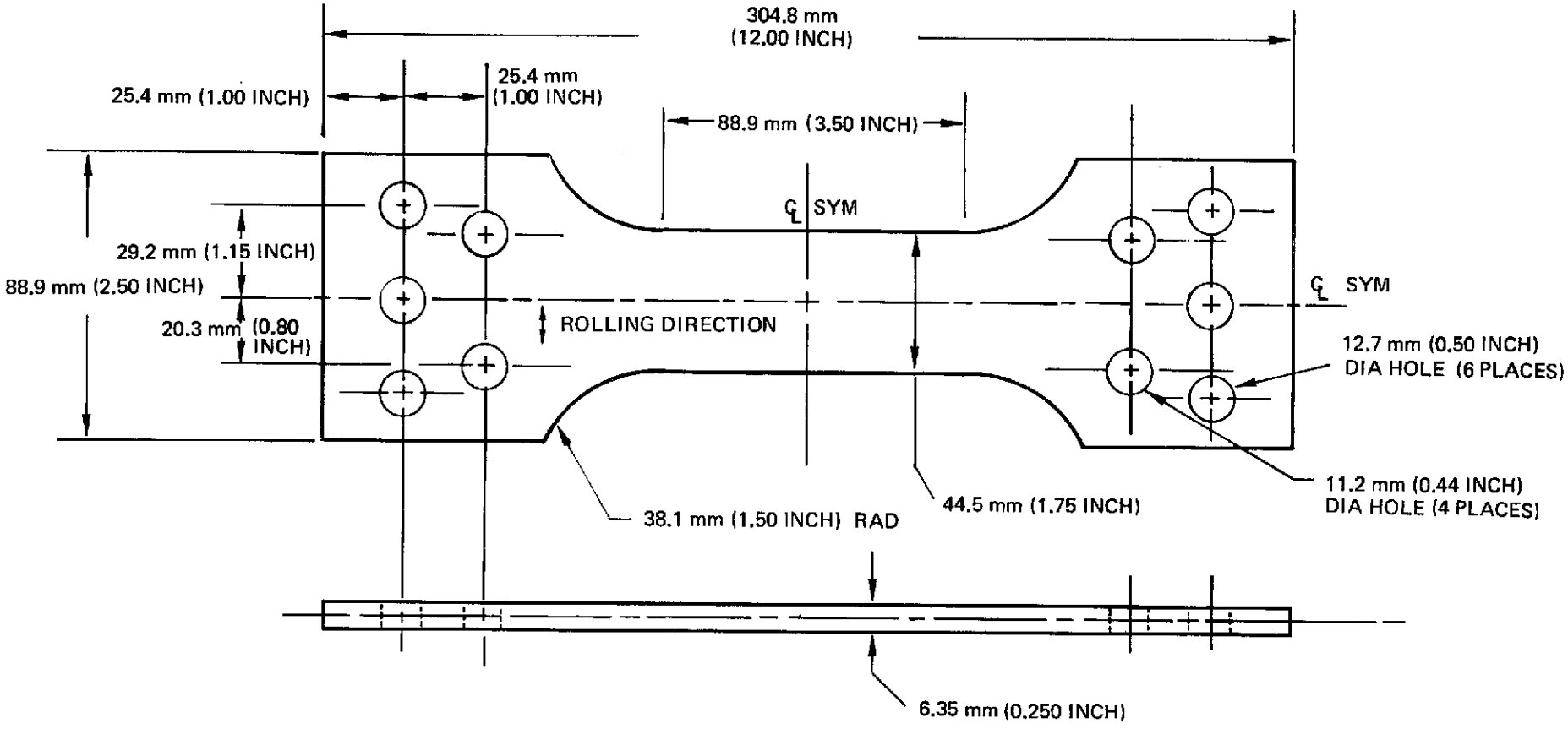

Figure 11. 6.35 mm (0.250 INCH) THICK 6 AL–4V TITANIUM ALLOY BASE METAL SPECIMEN (TB-3-4)

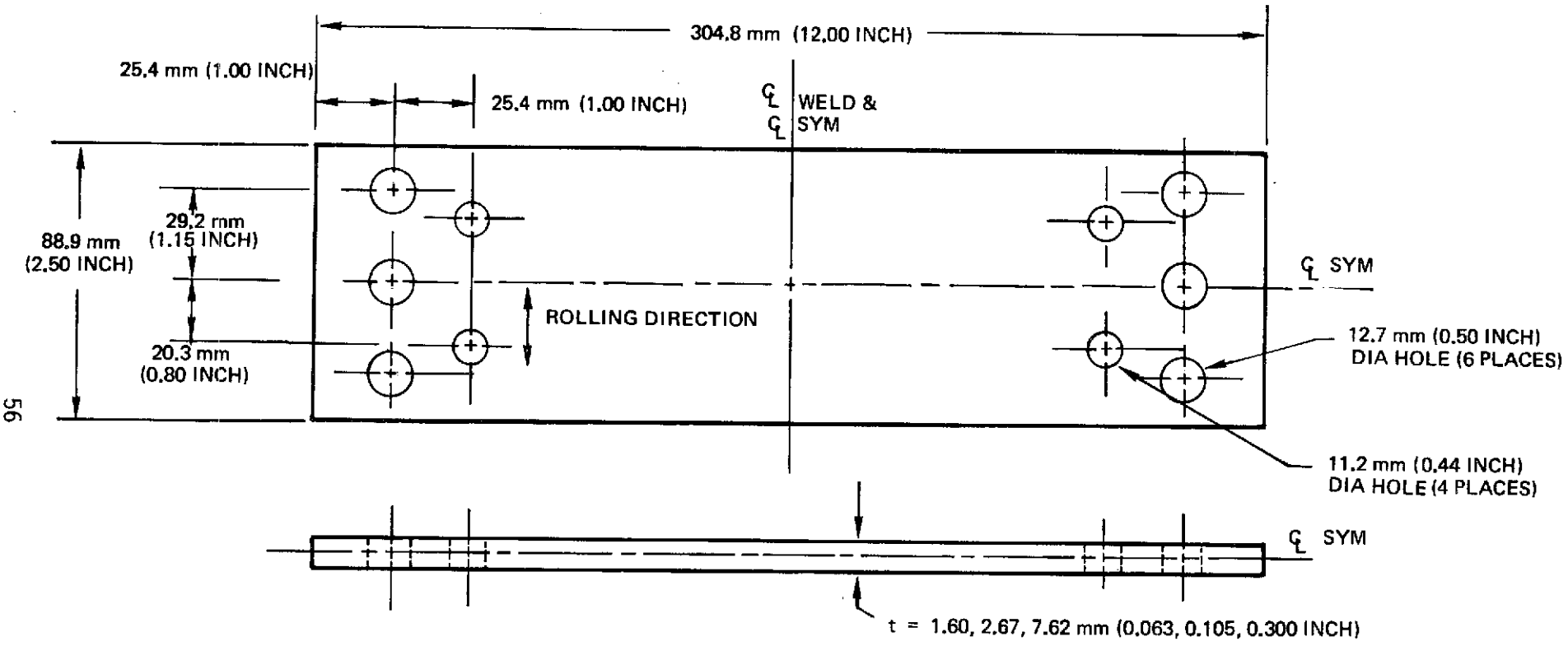

Figure 12: 88.9 mm (3.50 INCH) WIDE 2219-T87 ALUMINUM ALLOY WELDMENT SPECIMEN

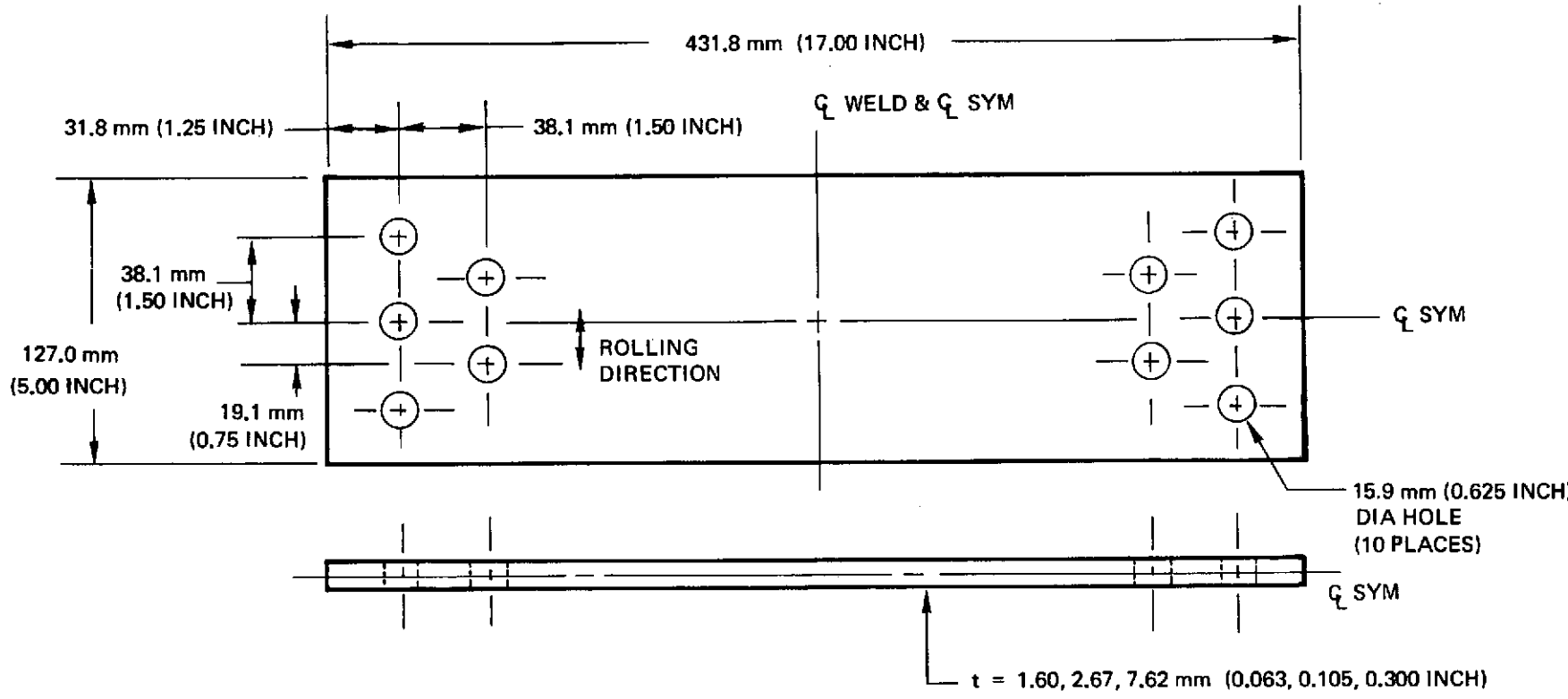

Figure 13: 127.0 mm (5.00 INCH) WIDE 2219-T87 ALUMINUM ALLOY WELDMENT SPECIMEN

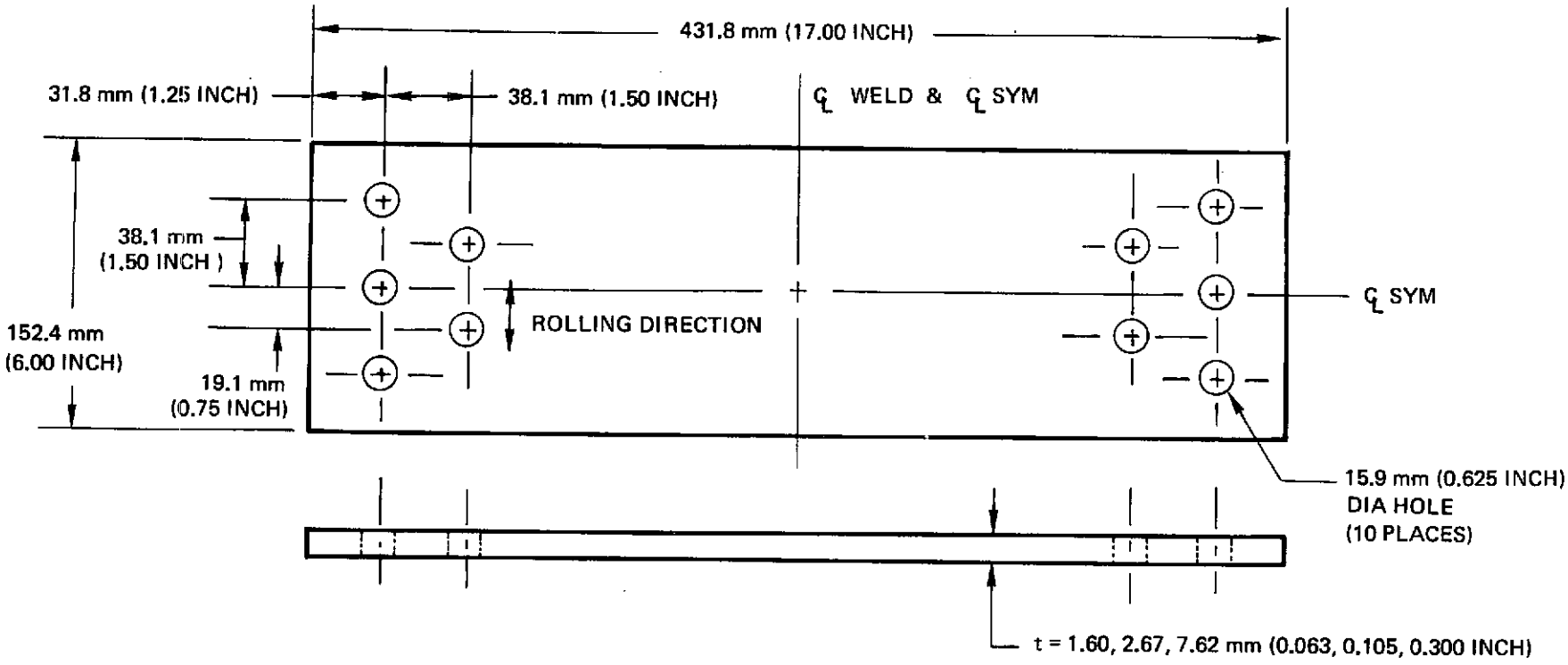

Figure 14: 152.4 mm (6.00 INCH) WIDE 2219 – T87 ALUMINUM ALLOY WELDMENT SPECIMEN

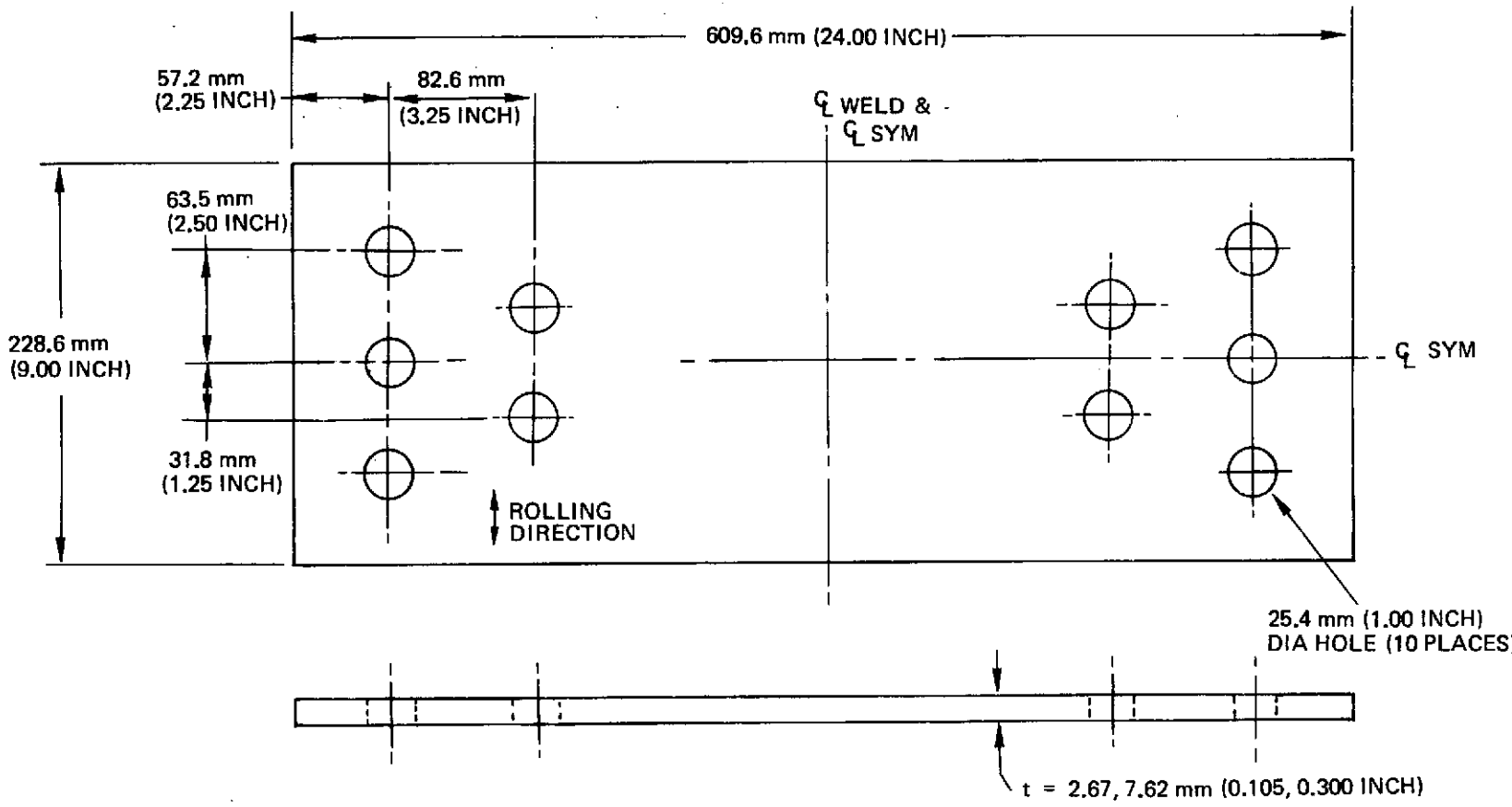

Figure 15: 228.6 mm (9.00 INCH) WIDE 2219-T87 ALUMINUM ALLOY WELDMENT SPECIMEN

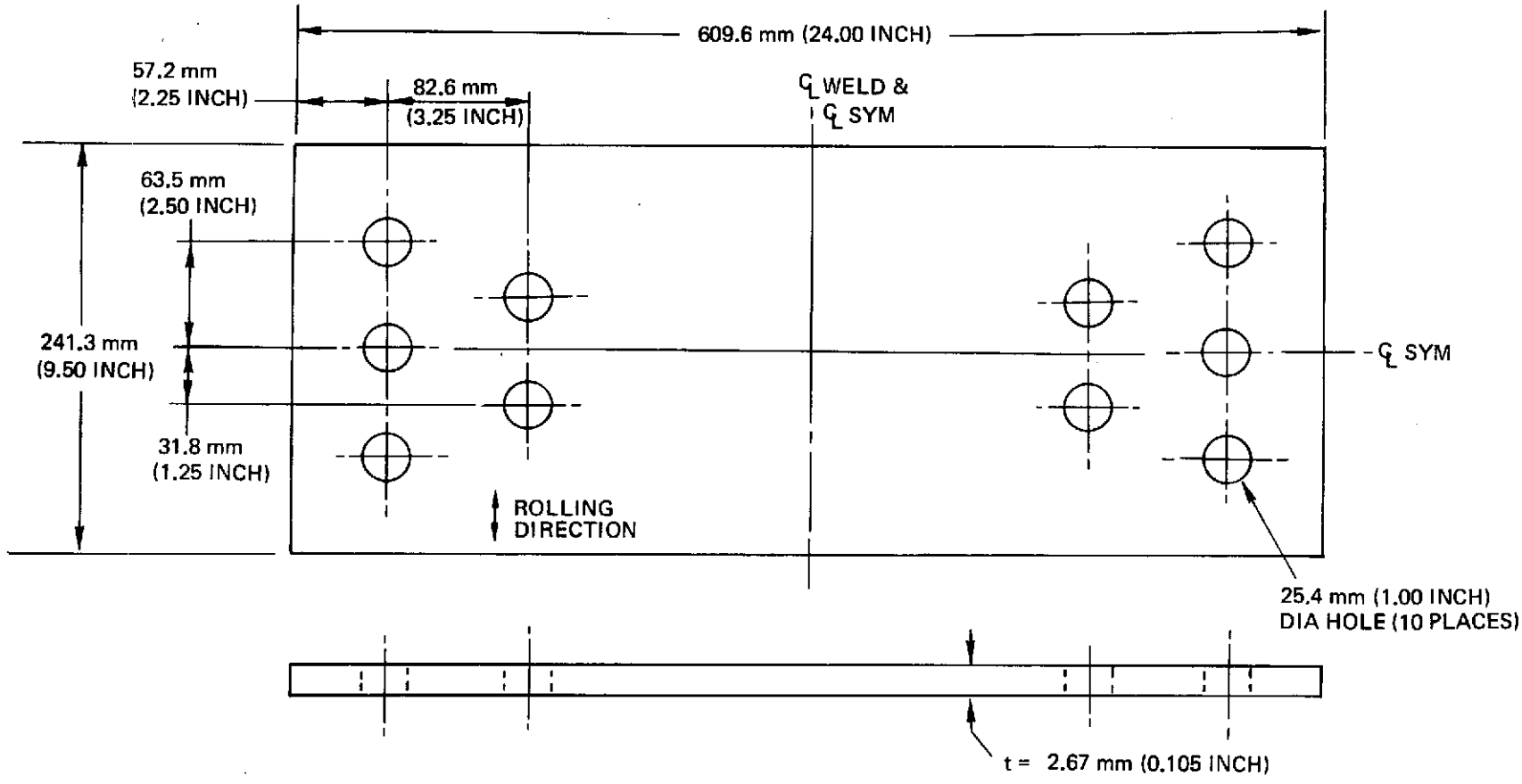

Figure 16. 241.3 mm (9.50 INCH) WIDE 2219-T87 ALUMINUM ALLOY WELDMENT SPECIMEN

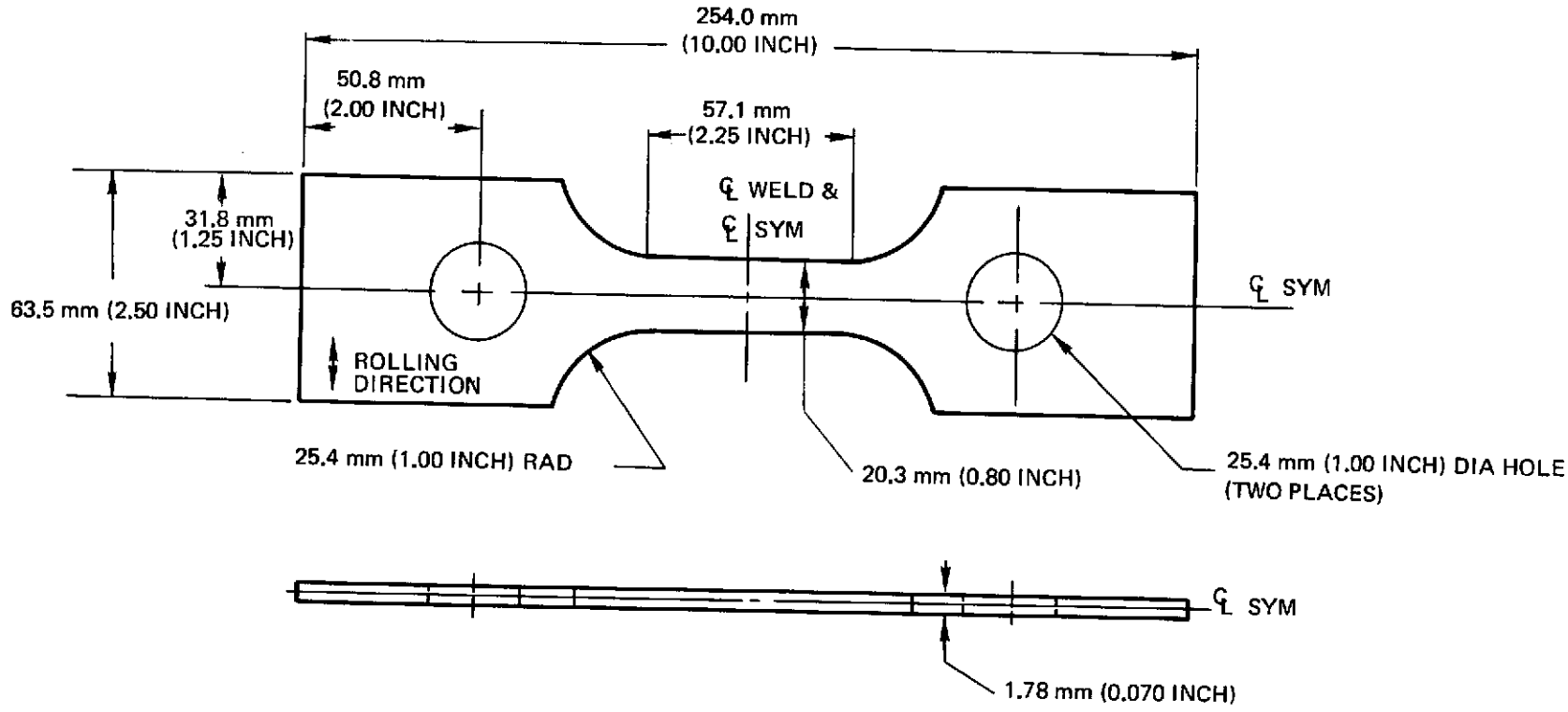

Figure 17: *1.78 mm (0.070 INCH) X 20.3 mm (0.80 INCH) 6 AL–4V TITANIUM ALLOY WELDMENT SPECIMEN*

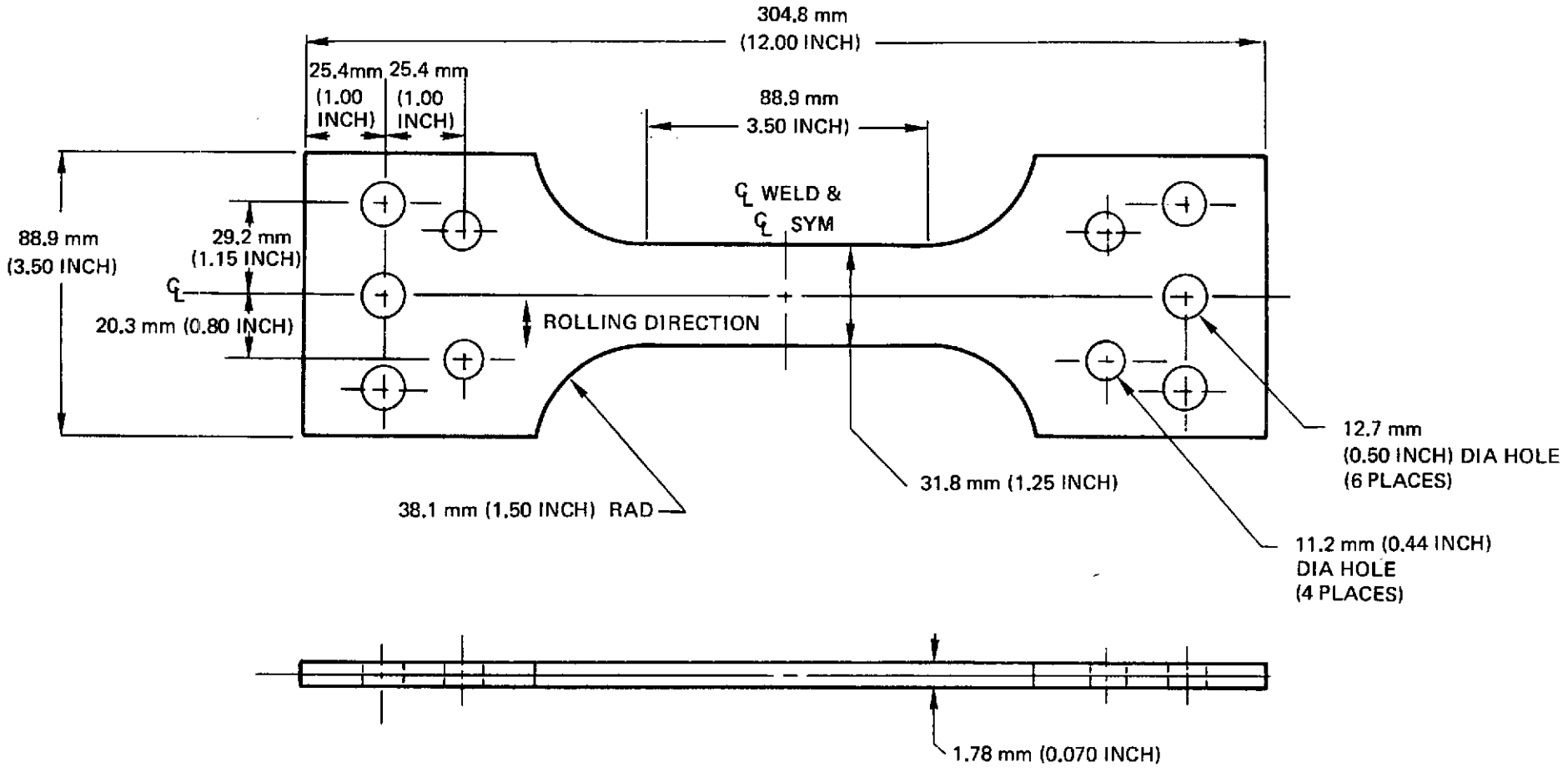

Figure 18: 1.78 mm (0.070 INCH) X 31.8 mm (1.25 INCH) 6 AL–4V TITANIUM ALLOY WELDMENT SPECIMEN

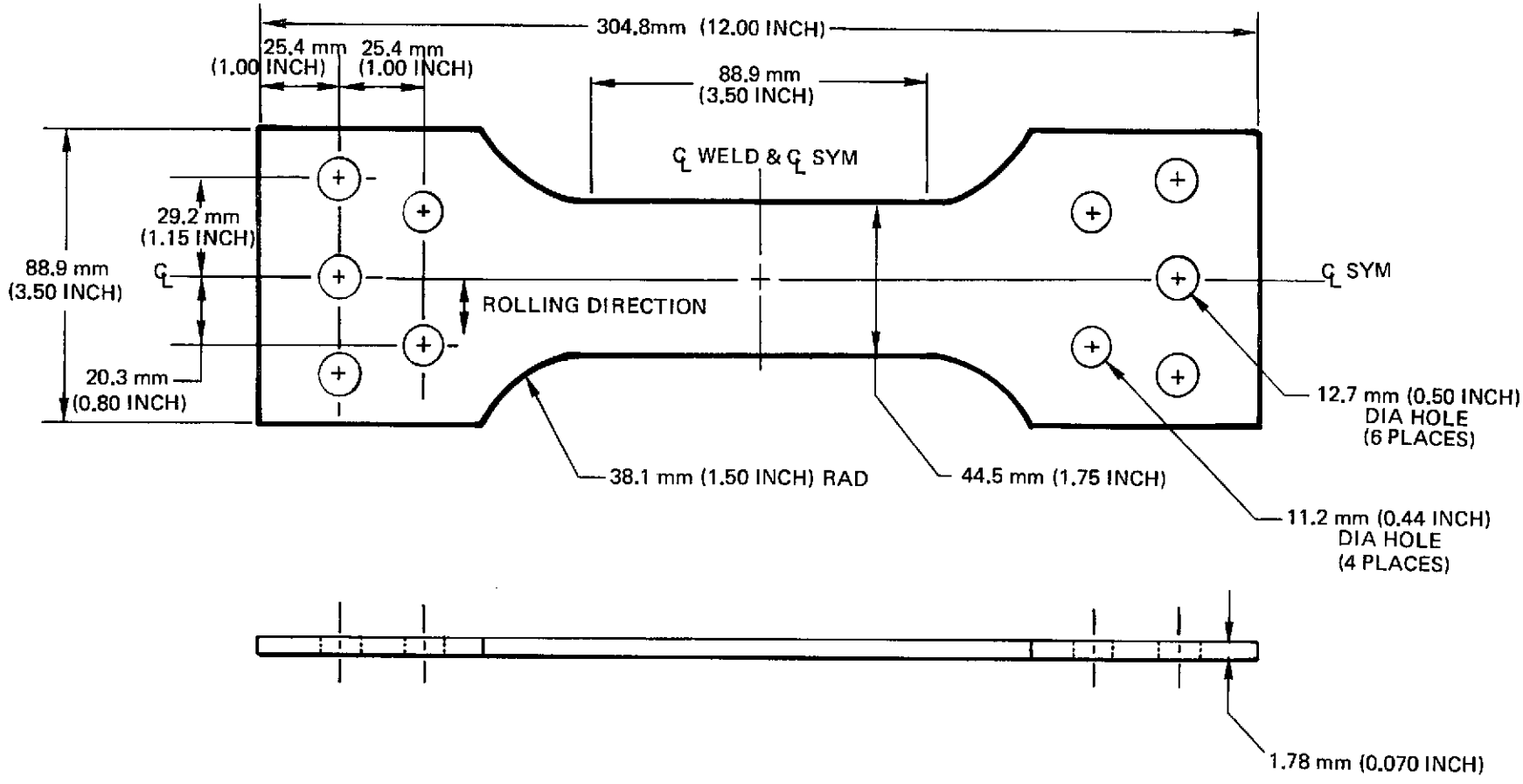

Figure 19: *1.78 mm (0.070 INCH) X 44.5 mm (1.75 INCH) 6AL–4V TITANIUM ALLOY WELDMENT SPECIMEN*

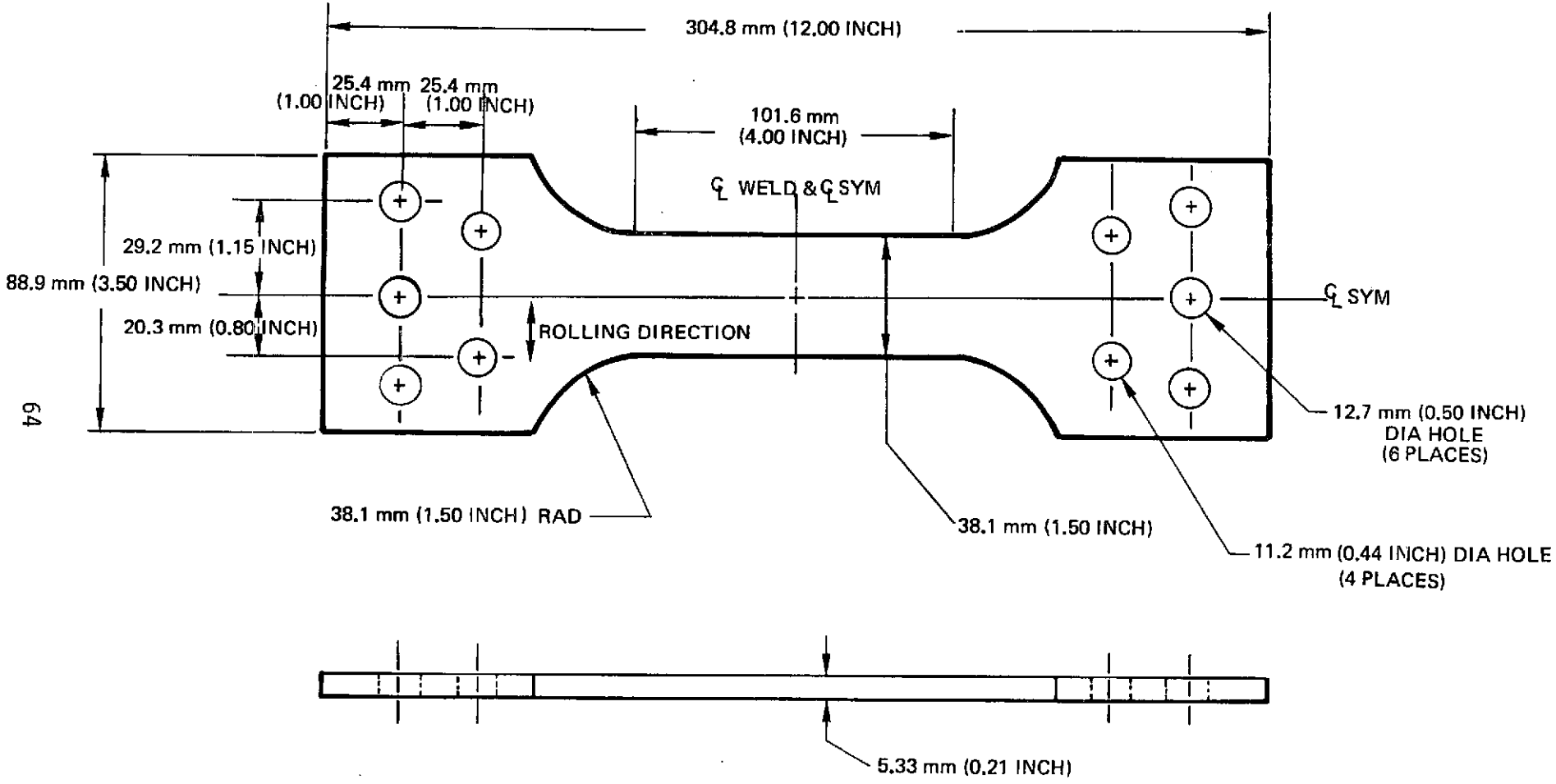

Figure 20: *5.33 mm (0.21 INCH) X 38.1 mm (1.50 INCH) 6AL-4V TITANIUM ALLOY WELDMENT SPECIMEN*

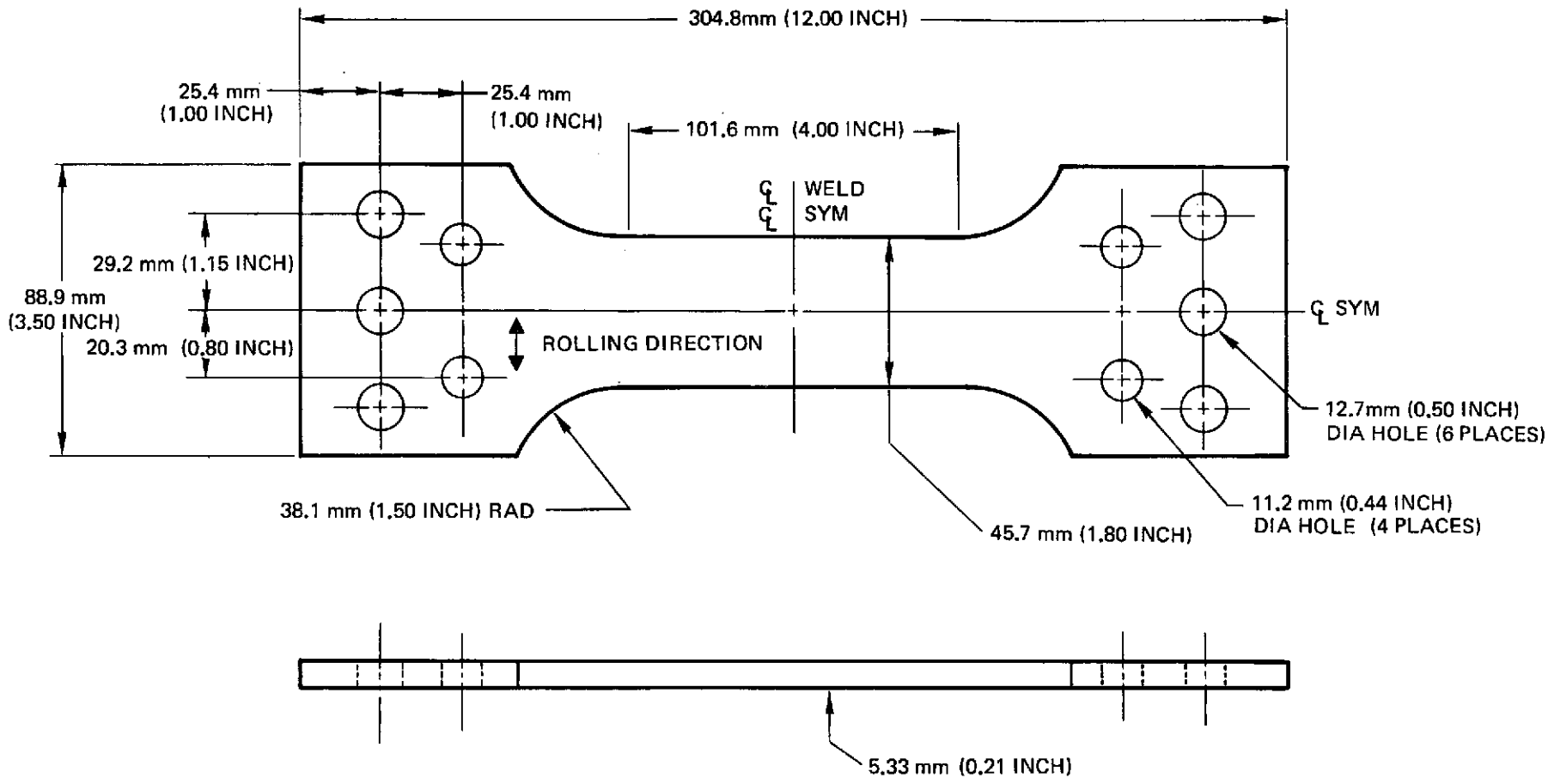

Figure 21: 5.33 mm (0.21 INCH) X 45.7 mm (1.80 INCH) 6 AL–4V TITANIUM ALLOY WELDMENT SPECIMEN

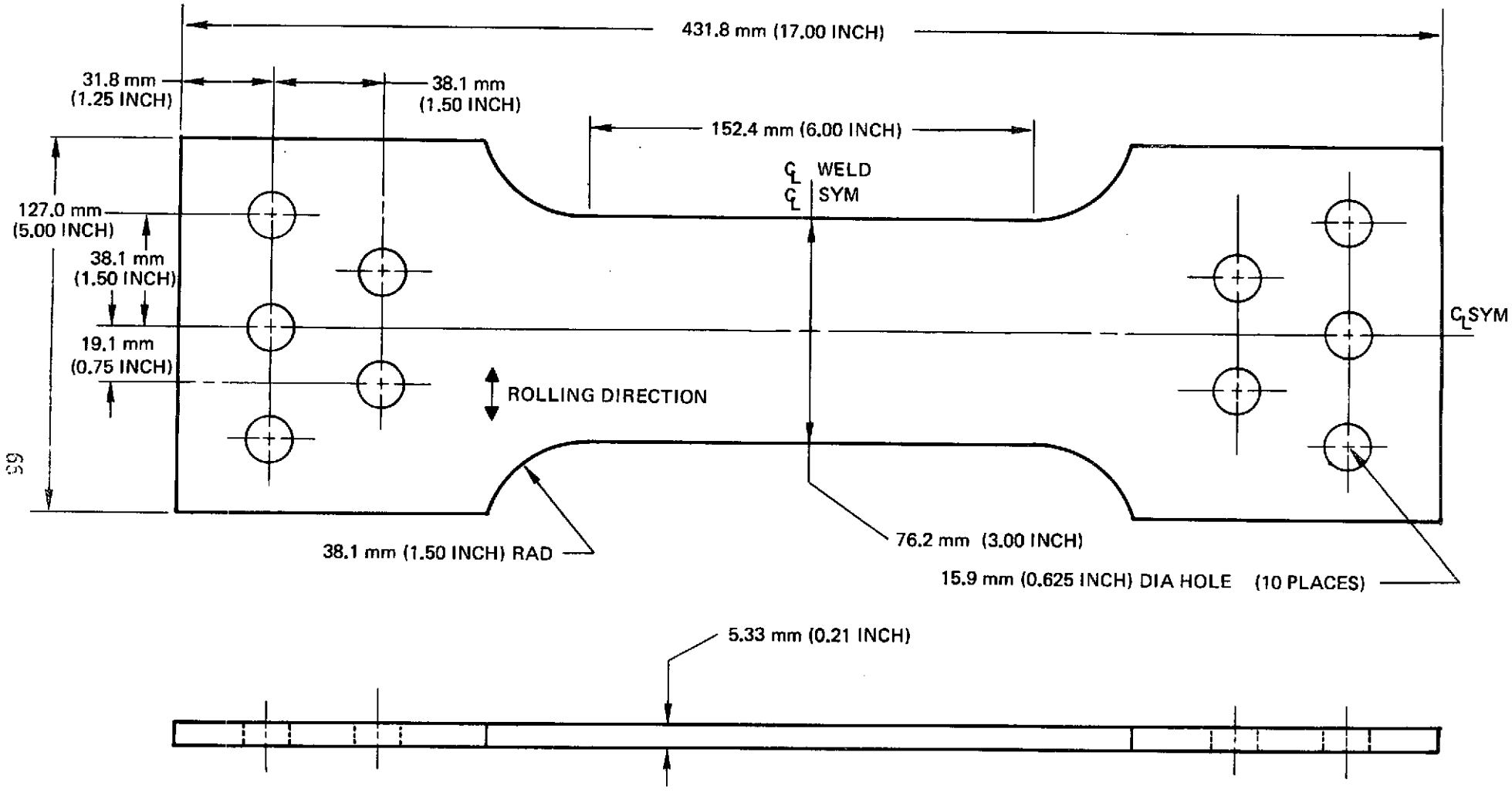

Figure 22: *5.33 mm (0.21 INCH) X 76.2 mm (3.00 INCH)*
6 AL–4V TITANIUM ALLOY WELDMENT SPECIMEN

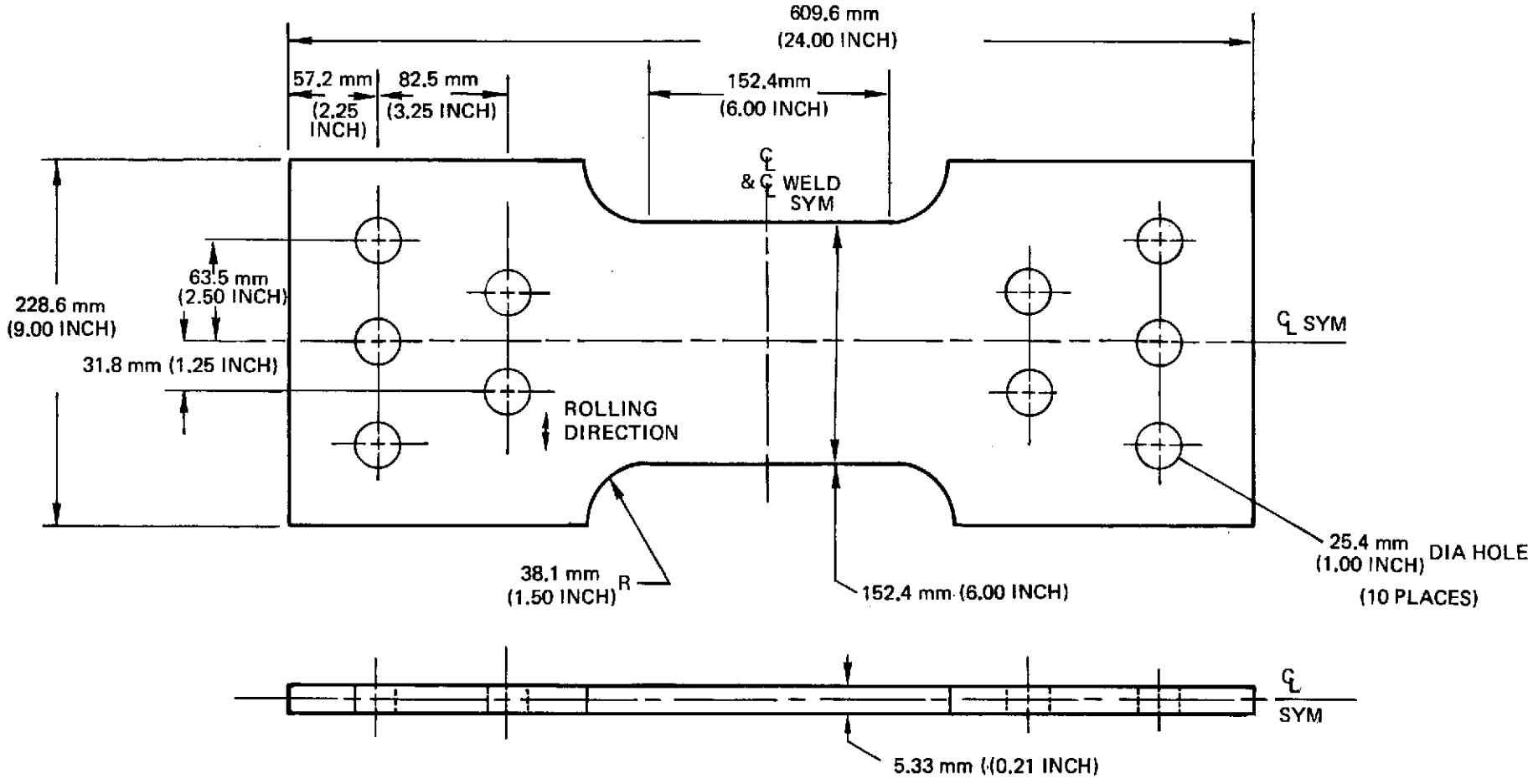

Figure 23: *5.33mm (0.21INCH) X 152.4 mm (6.00 INCH) 6 AL-4V TITANIUM ALLOY WELDMENT SPECIMEN*

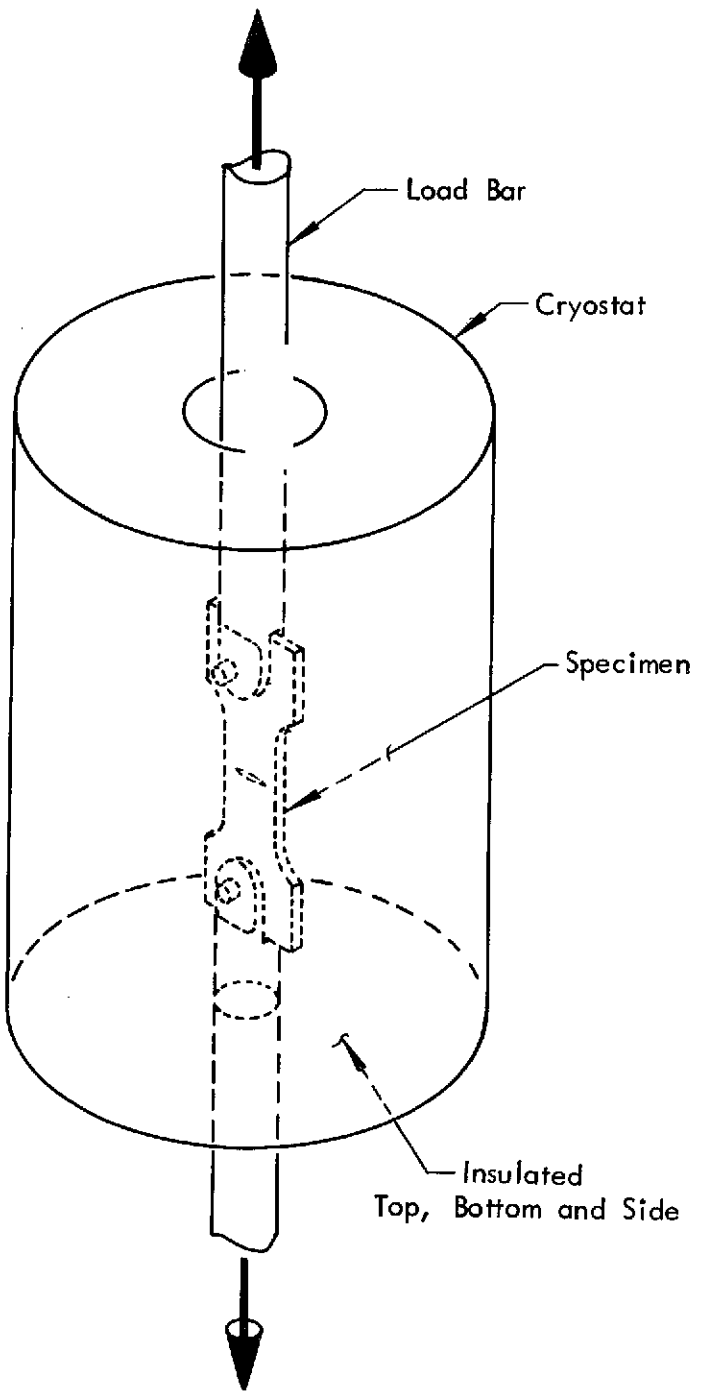

Figure 24: CRYOSTAT USED FOR LN_2 & LH_2 TESTS

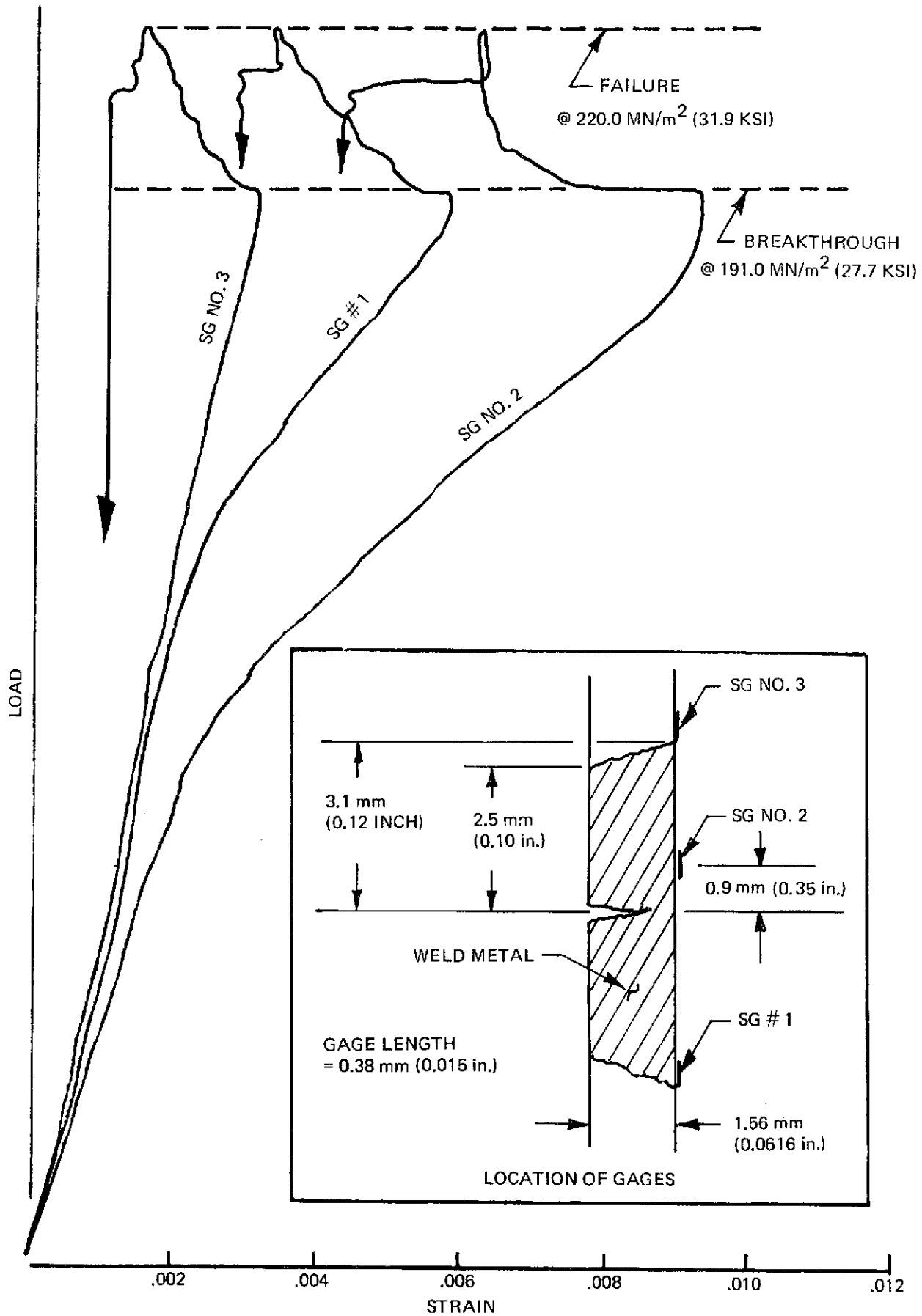

Figure 25: BREAKTHROUGH INDICATED BY STRAIN GAGES (SPECIMEN SAR 6-1-2)

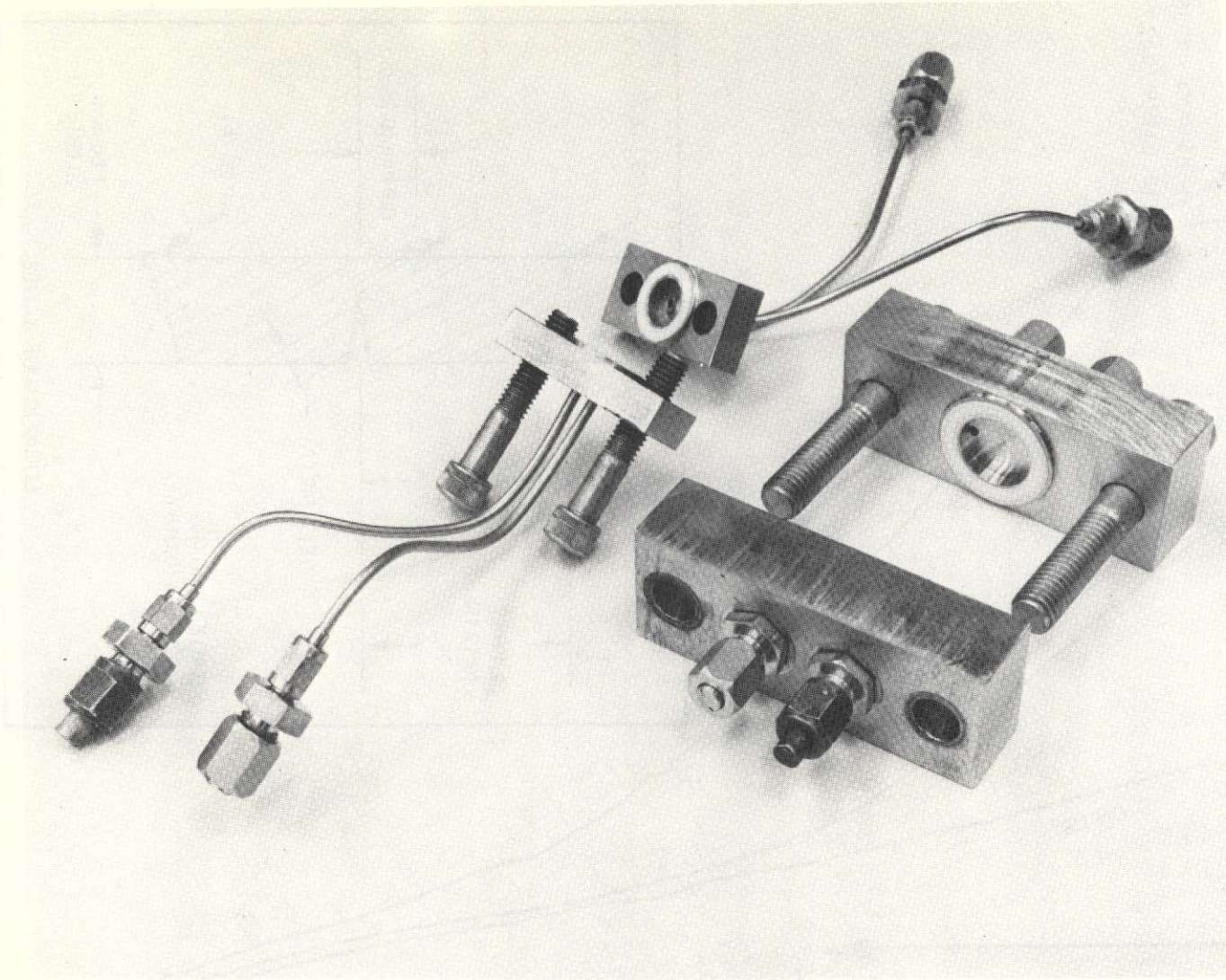

Figure 26: PRESSURE CUPS

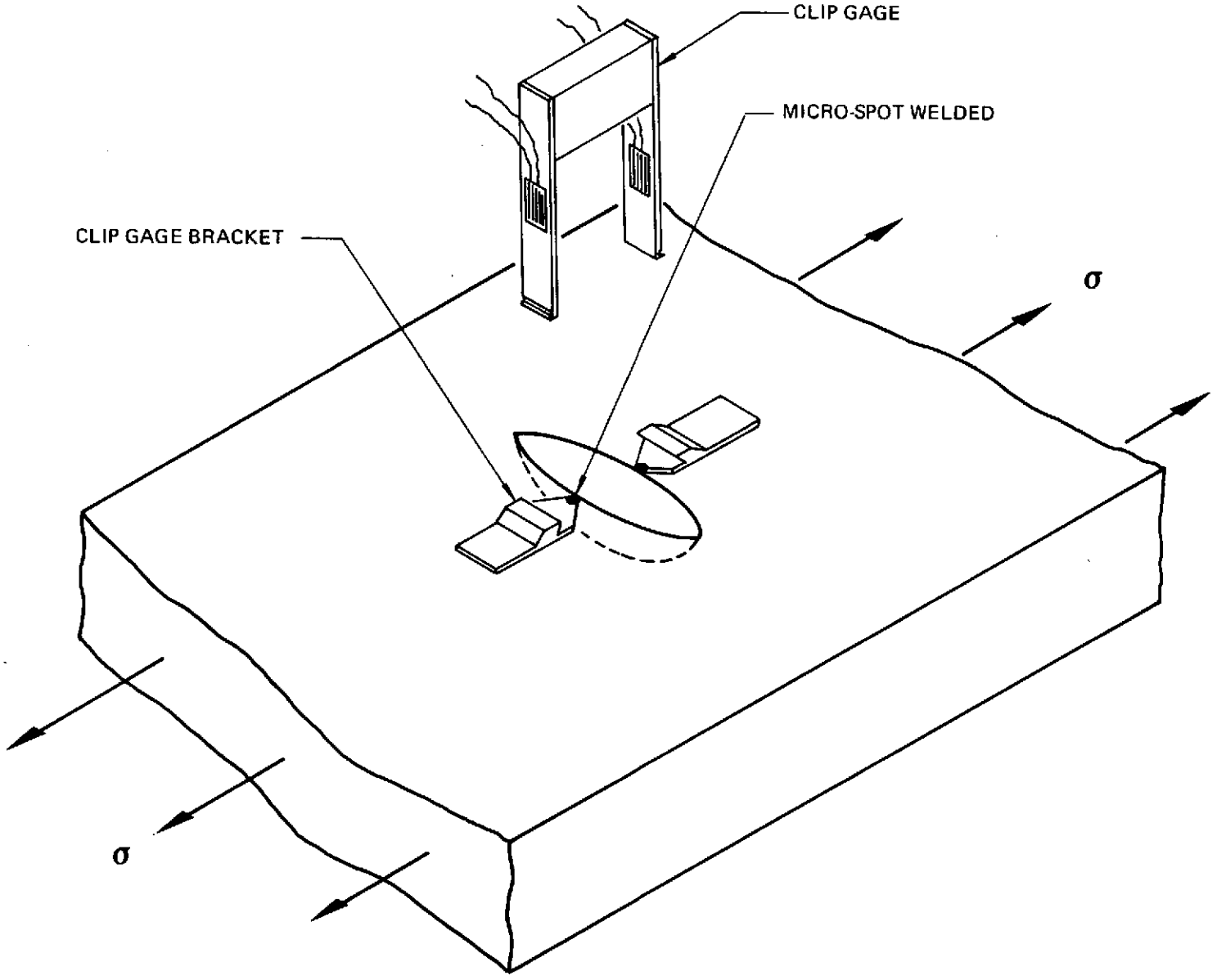

Figure 27: FLAW OPENING MEASUREMENT OF SURFACE FLAWED SPECIMENS

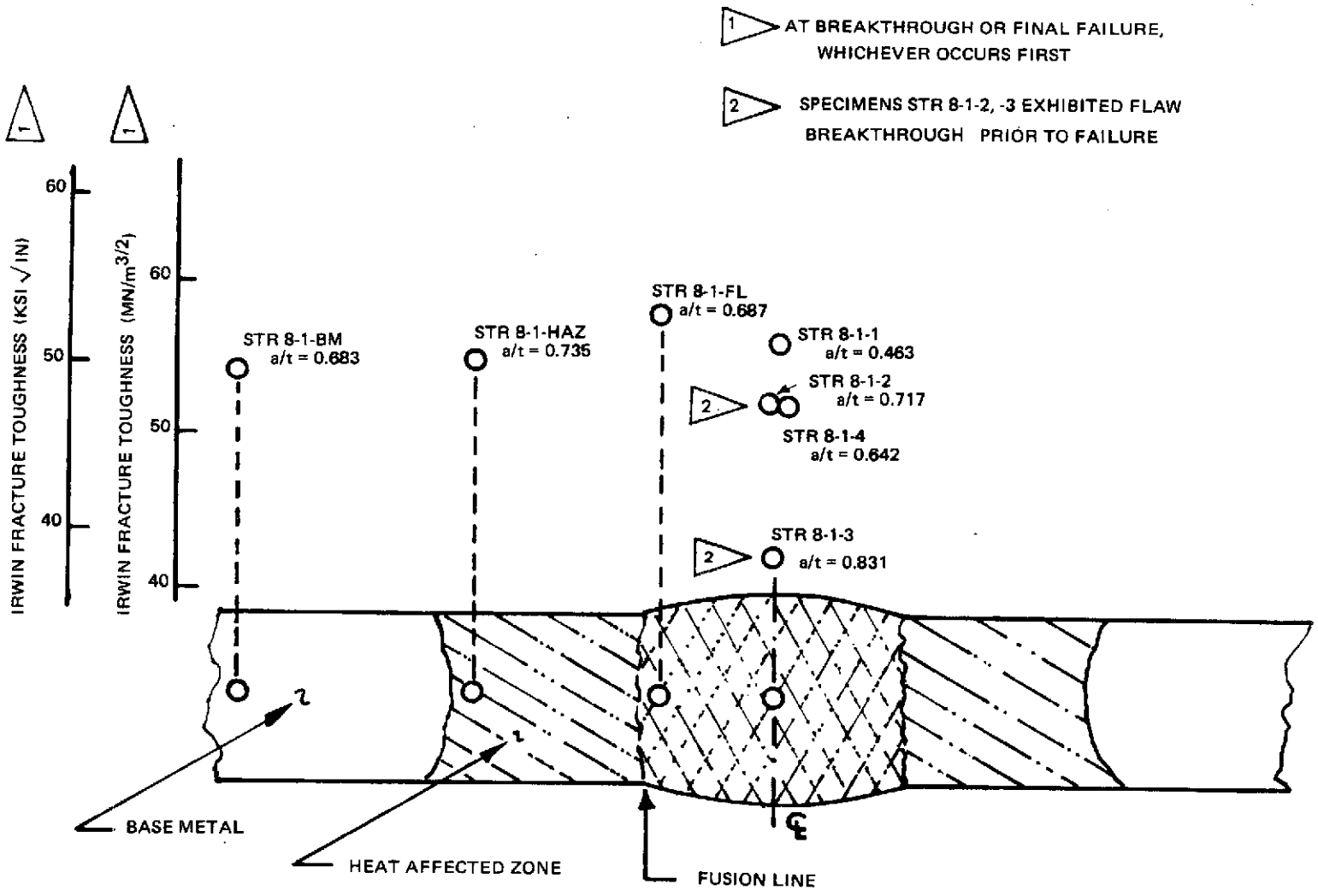

Figure 28: VARIATION IN IRWIN FRACTURE TOUGHNESS WITH RESPECT TO FLAW LOCATION IN WELDED TI 6AI-4V. TESTS CONDUCTED IN ROOM TEMPERATURE AIR.

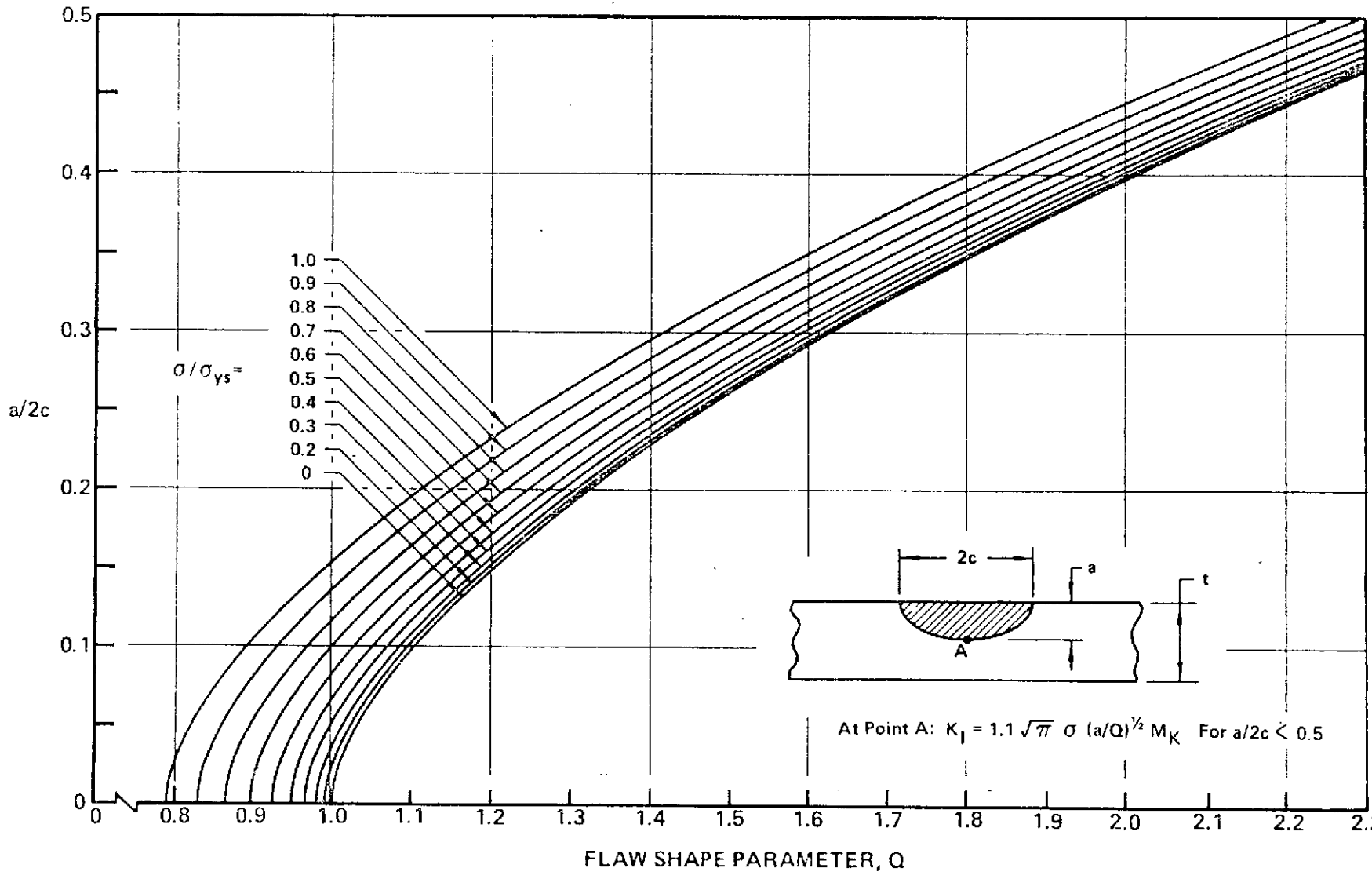

Figure 29: SHAPE PARAMETER CURVES FOR SURFACE AND INTERNAL FLAWS

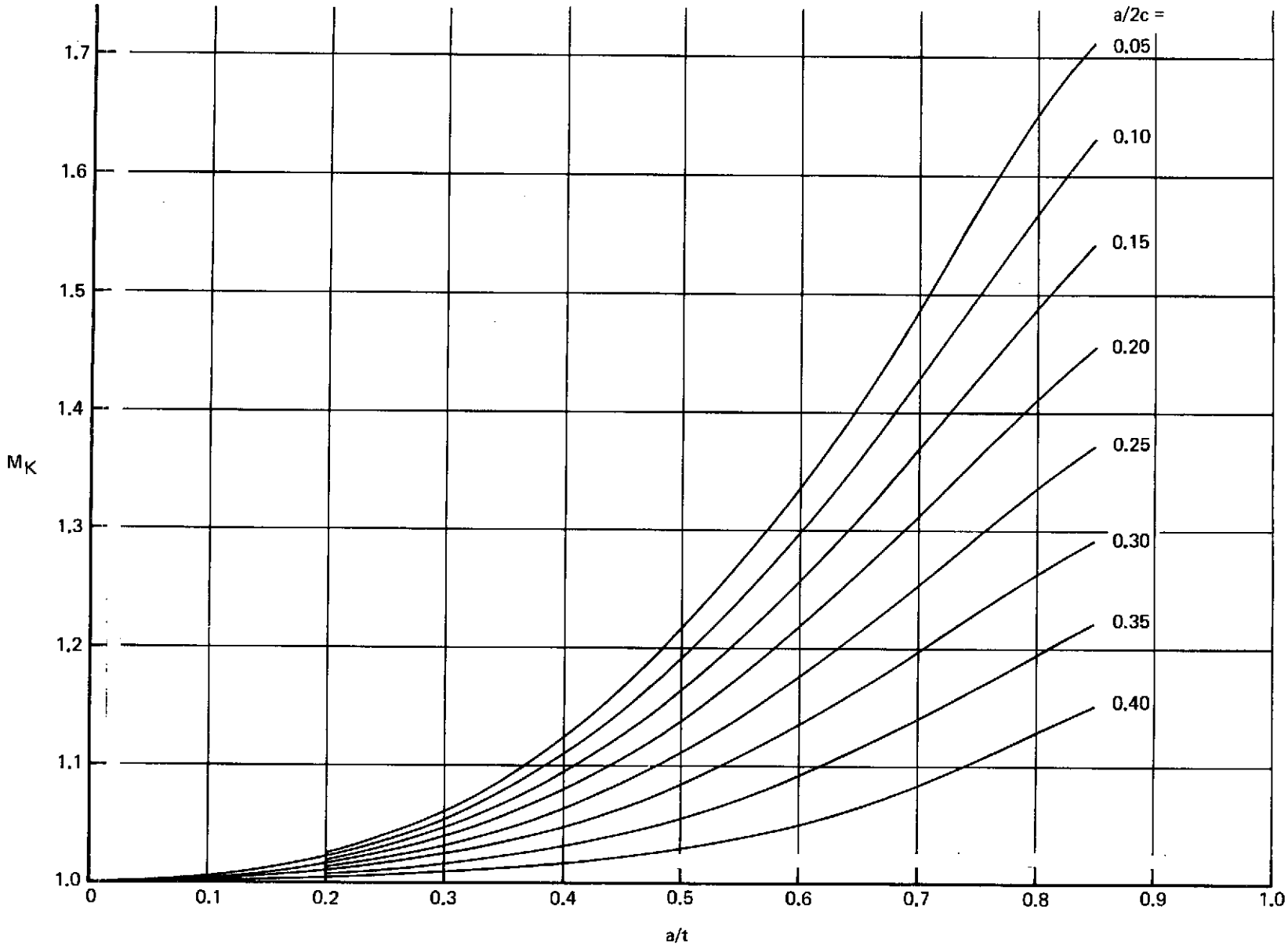

Figure 30: DEEP FLAW MAGNIFICATION CURVES (Reference 4)

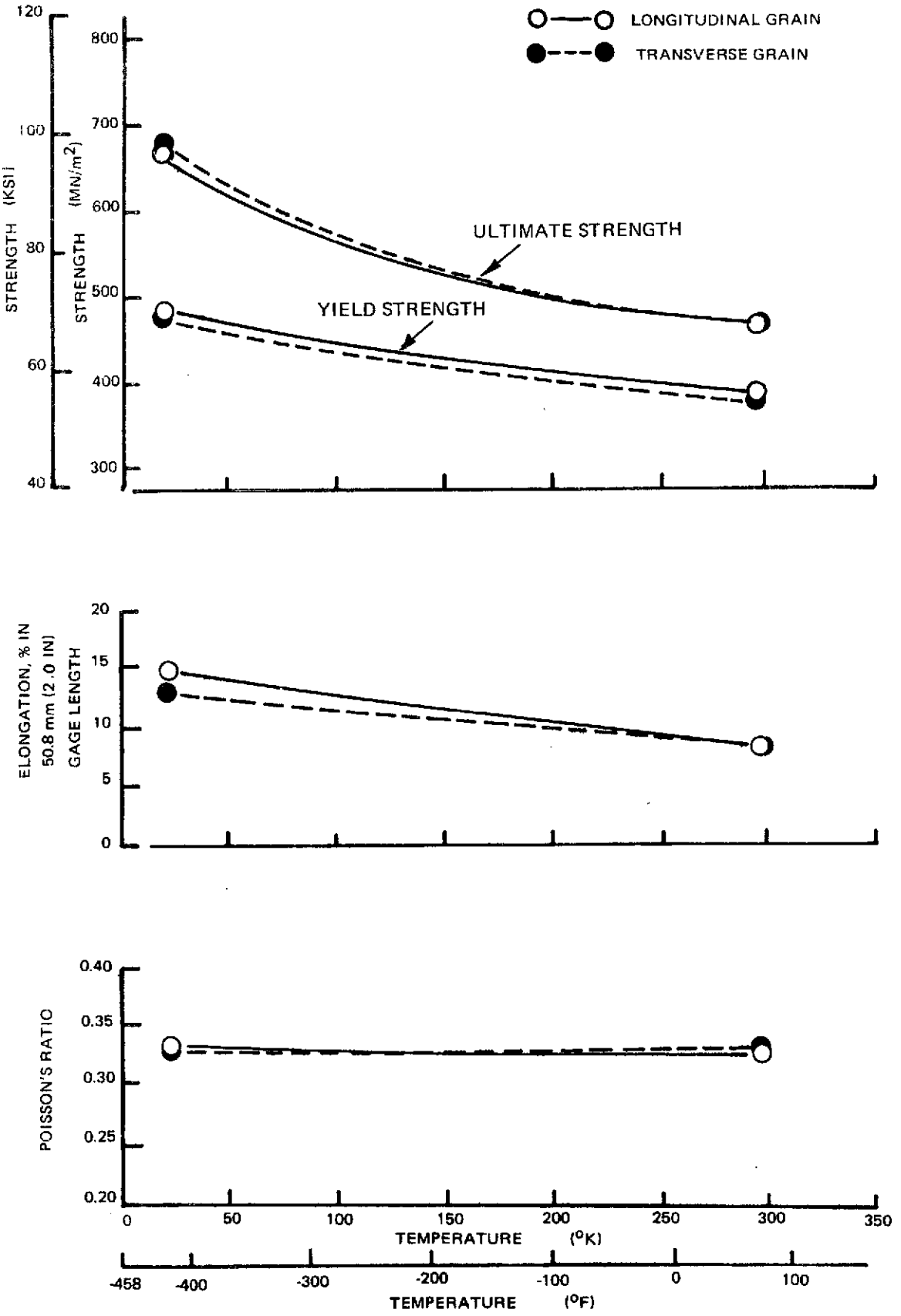

Figure 31: TENSILE PROPERTIES OF 2219-T87 ALUMINUM ALLOY BASE METAL, THICKNESS = 1.60mm (0.063 INCH)

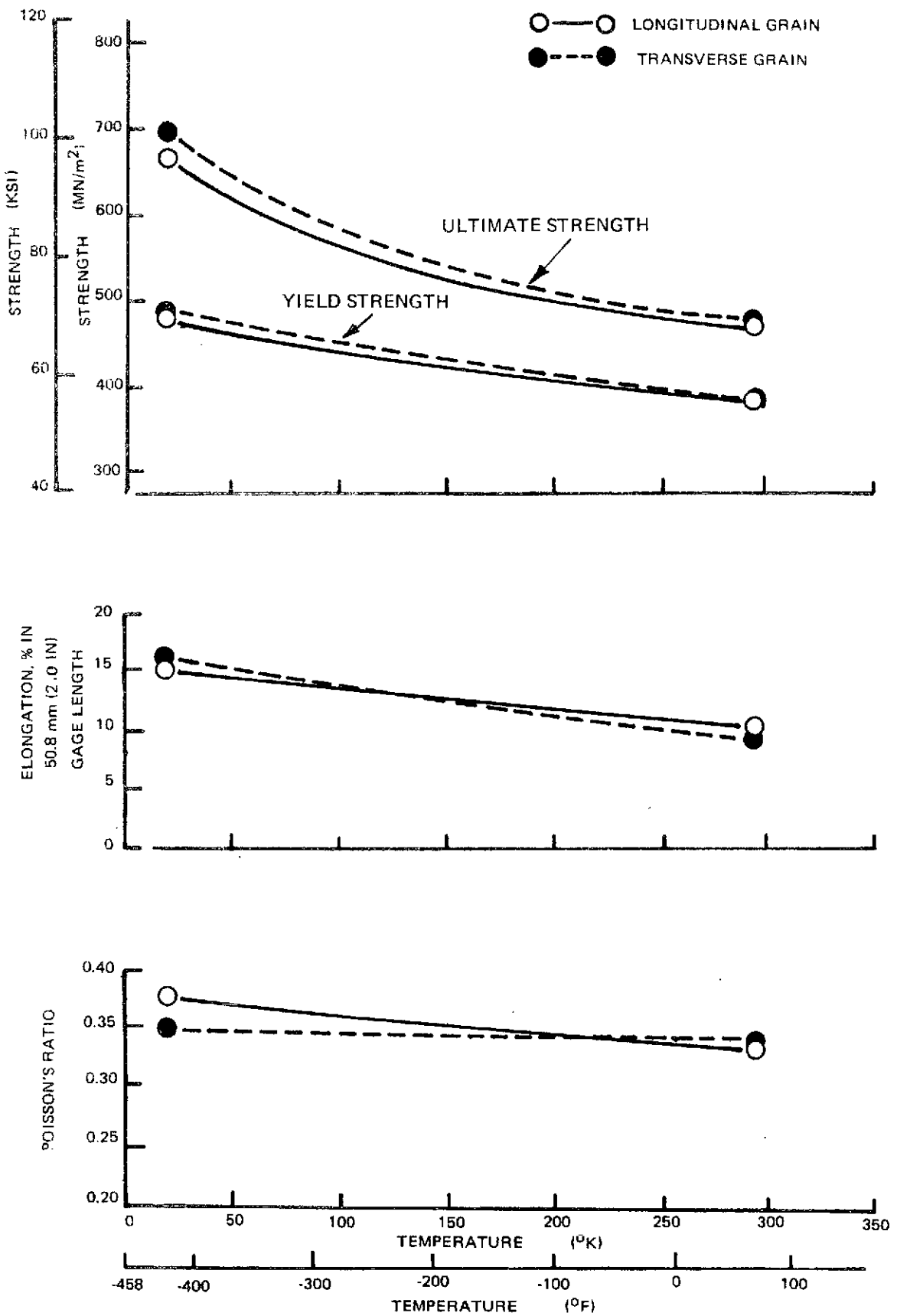

Figure 32: TENSILE PROPERTIES OF 2219-T87 ALUMINUM ALLOY BASE METAL, THICKNESS = 2.67mm (0.105 INCH)

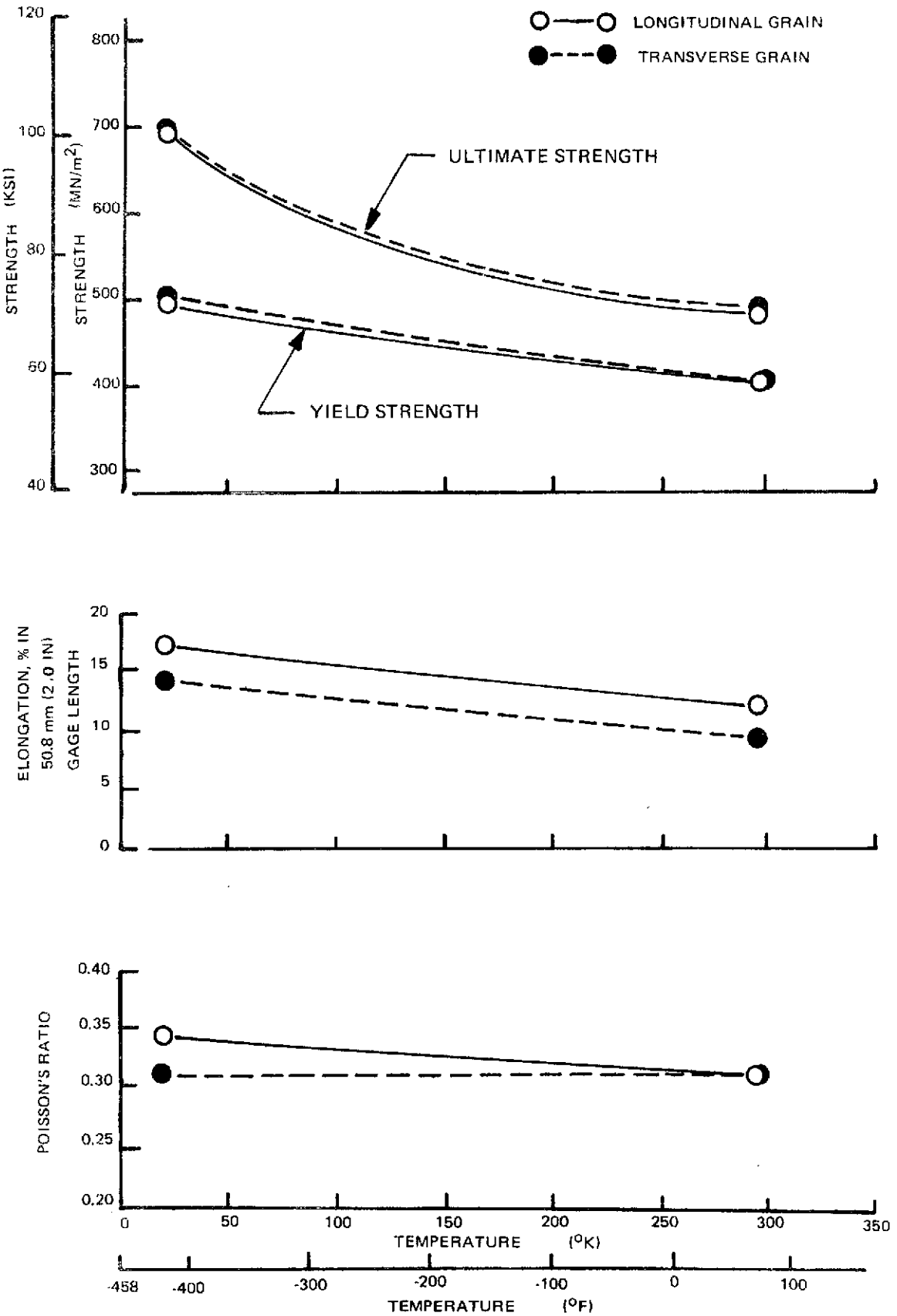

Figure 33: TENSILE PROPERTIES OF 2219-T87 ALUMINUM ALLOY BASE METAL, THICKNESS = 7.62 mm (0.30 INCH)

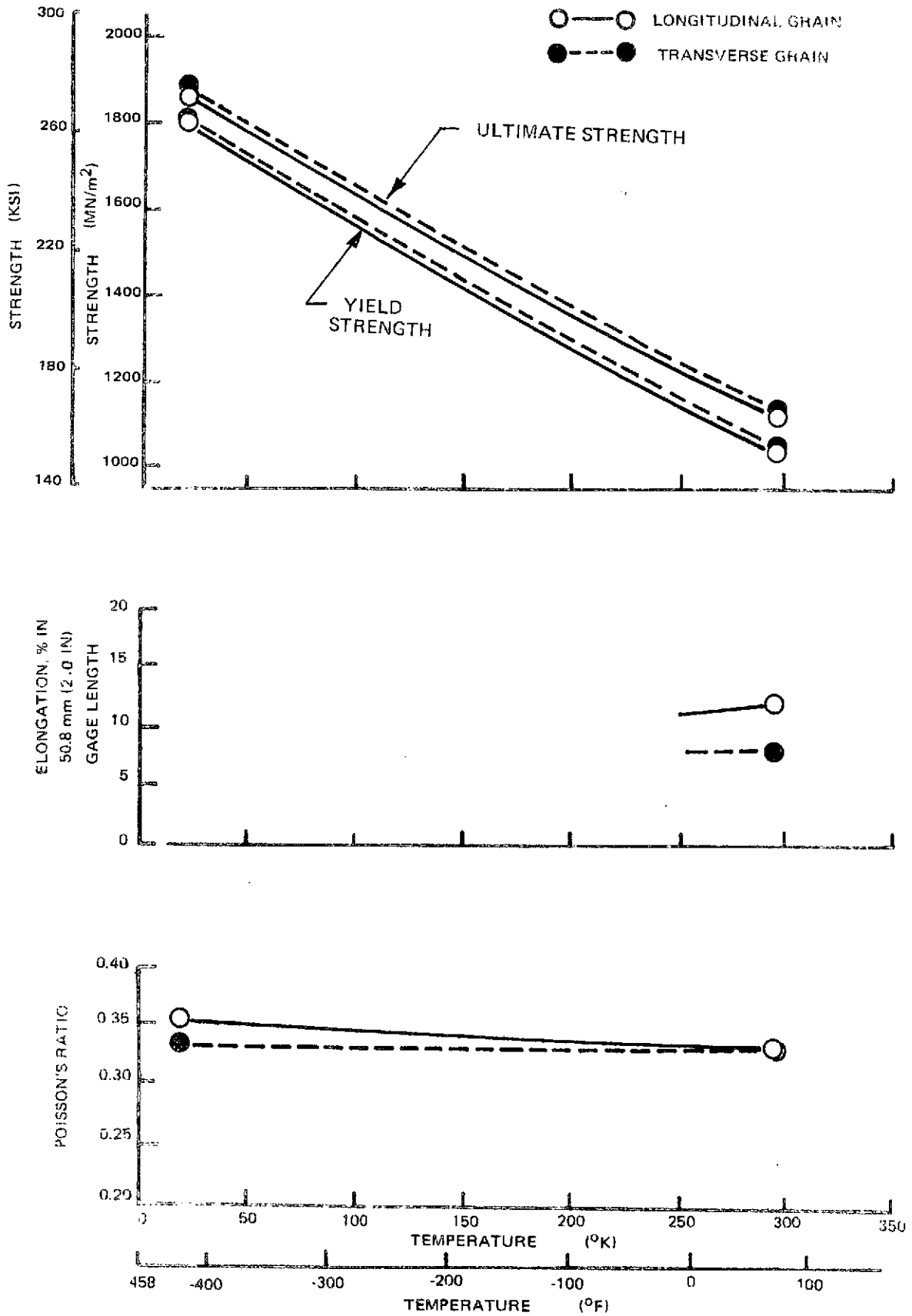

Figure 34: TENSILE PROPERTIES OF Ti 6Al-4V STA 811°K (STA 1000°F) BASE METAL, THICKNESS = 0.51 mm (0.020 in.)

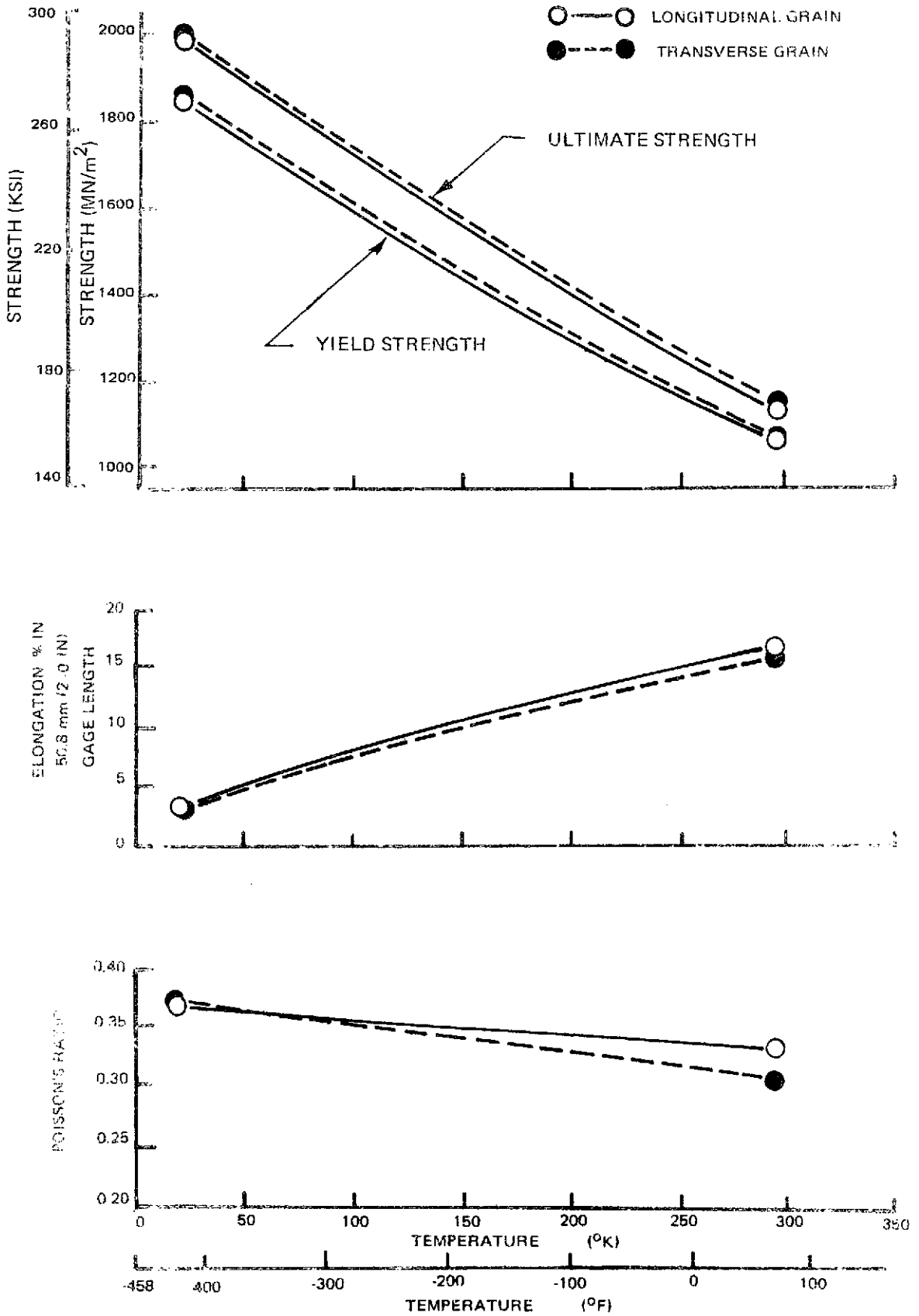

Figure 35: TENSILE PROPERTIES OF Ti 6Al-4V STA 811°K (STA 1000°F) BASE METAL, THICKNESS = 2.03 mm (0.080 in.)

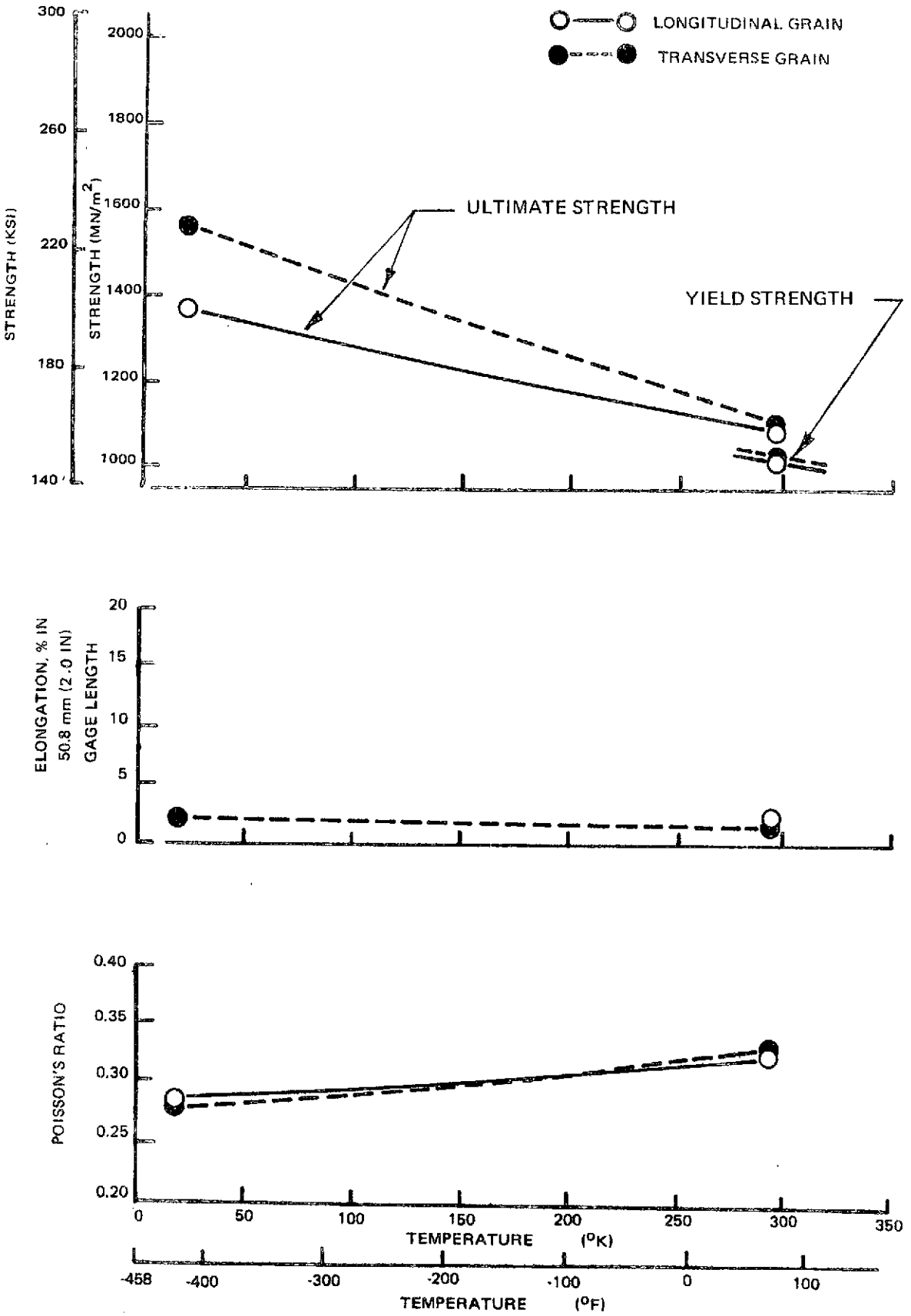

Figure 36: TENSILE PROPERTIES OF Ti 6Al-4V STA 811°K (STA 1000°F) BASE METAL, THICKNESS = 6.35 mm (0.250 in.)

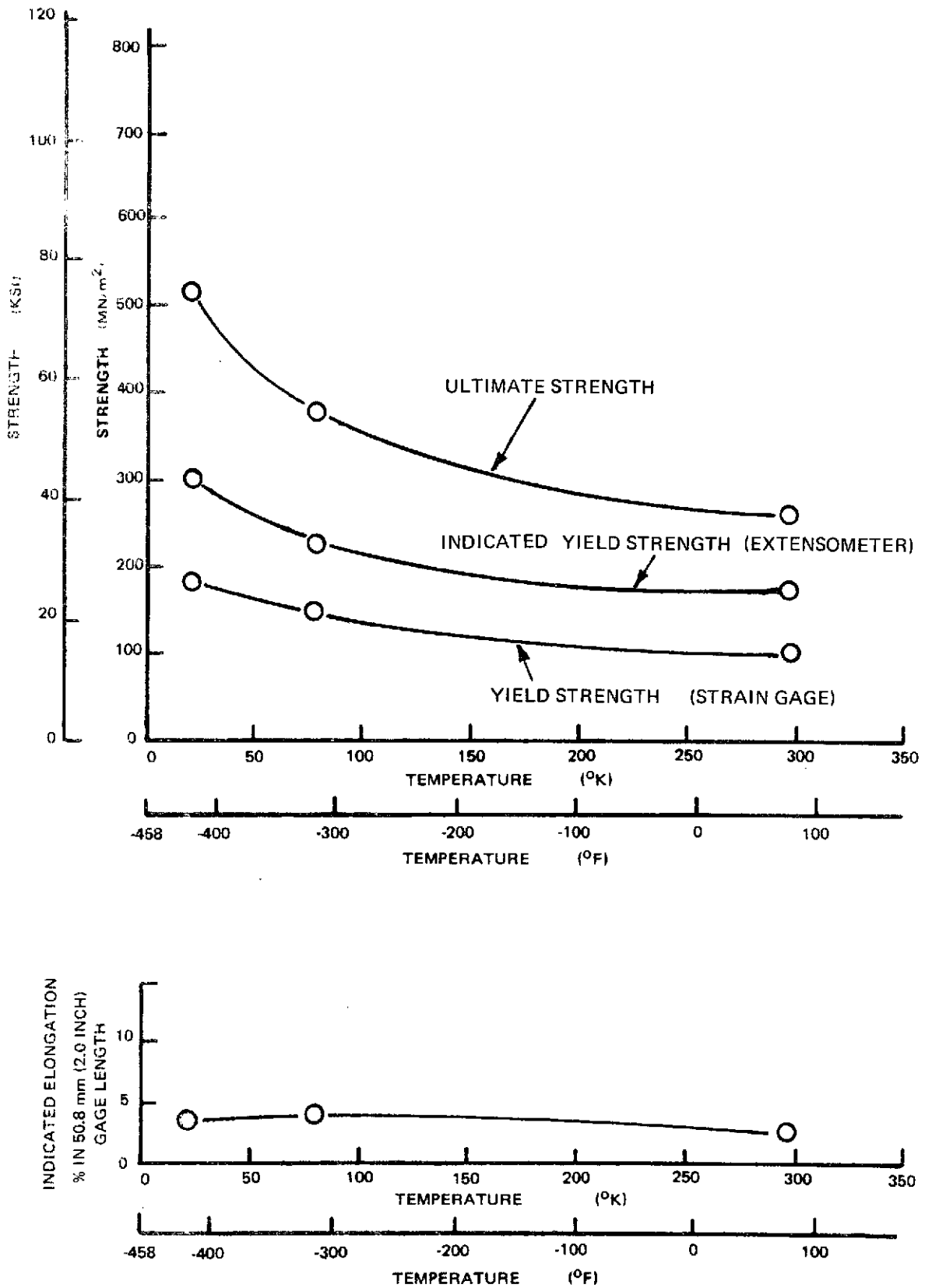

Figure 37: TENSILE PROPERTIES OF 2219-T87 ALUMINUM ALLOY WELDMENTS, NO POST WELD HEAT TREATMENT, THICKNESS = 1.60mm (0.063 INCH)

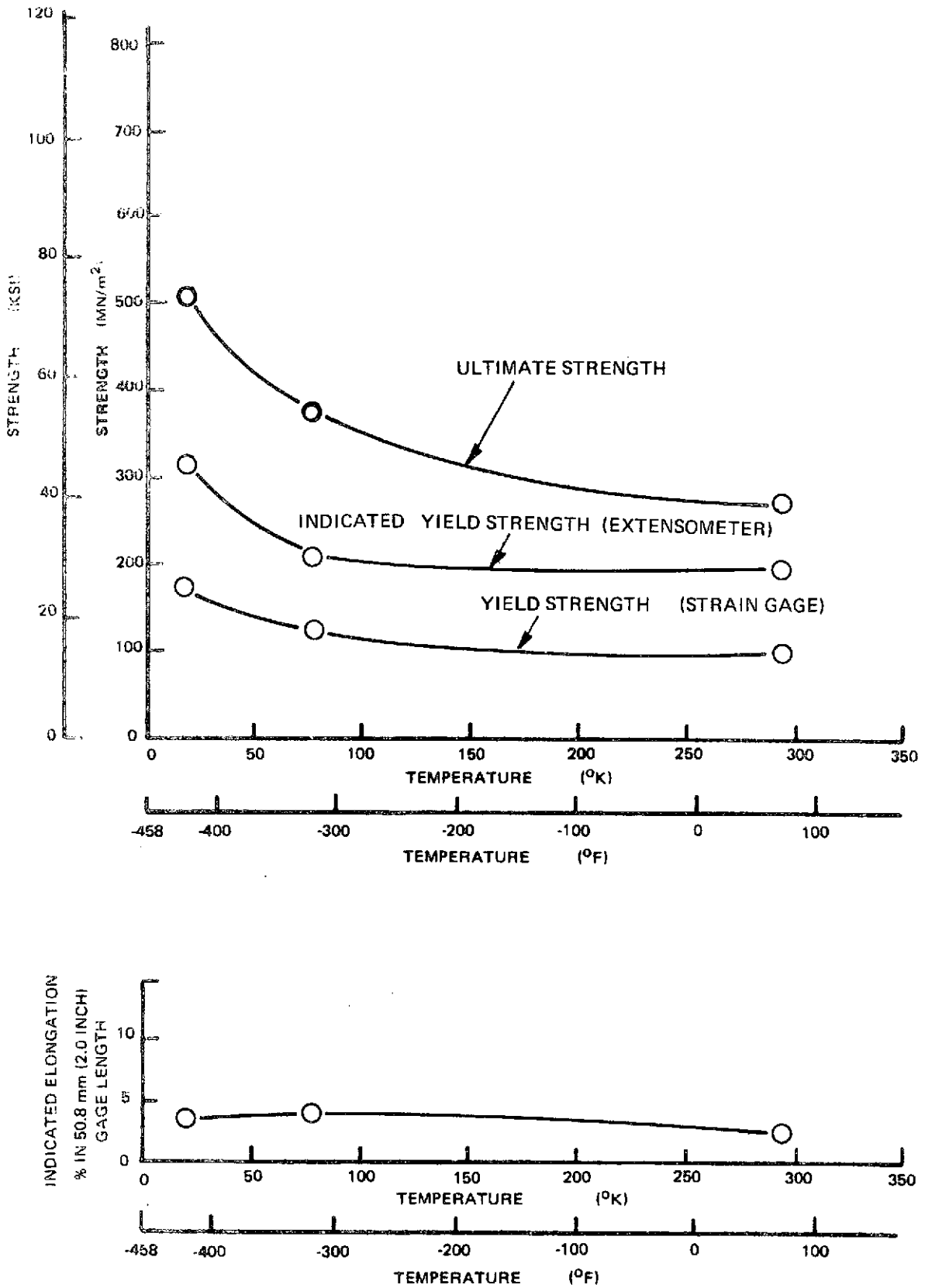

Figure 38: TENSILE PROPERTIES OF 2219-T87 ALUMINUM ALLOY WELDMENTS, NO POST WELD HEAT TREATMENT, THICKNESS = 2.67mm (0.105 INCH)

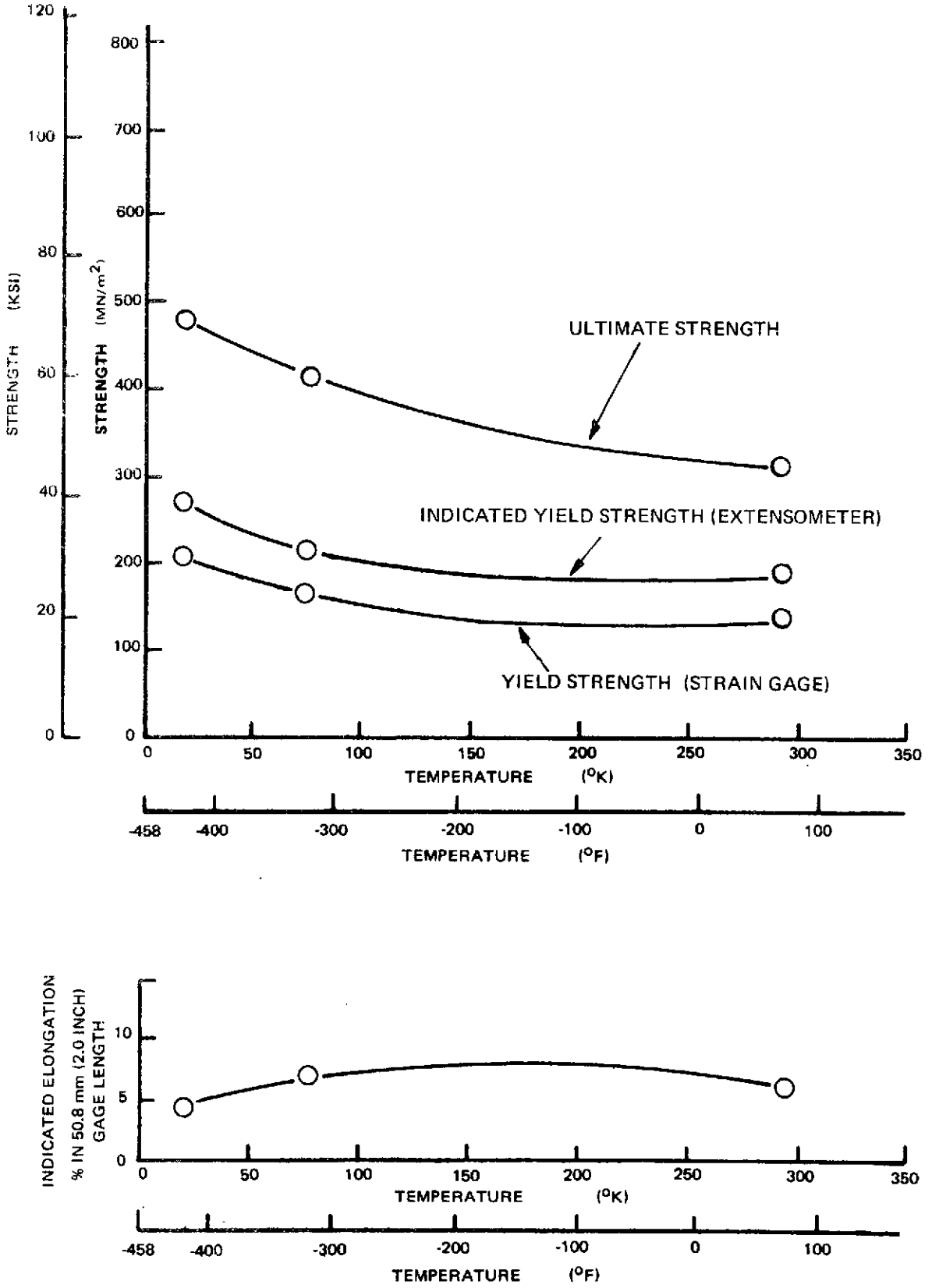

Figure 39: TENSILE PROPERTIES OF 2219-T87 ALUMINUM ALLOY WELDMENTS, NO POST WELD HEAT TREATMENT, THICKNESS = 7.62mm (0.30 INCH)

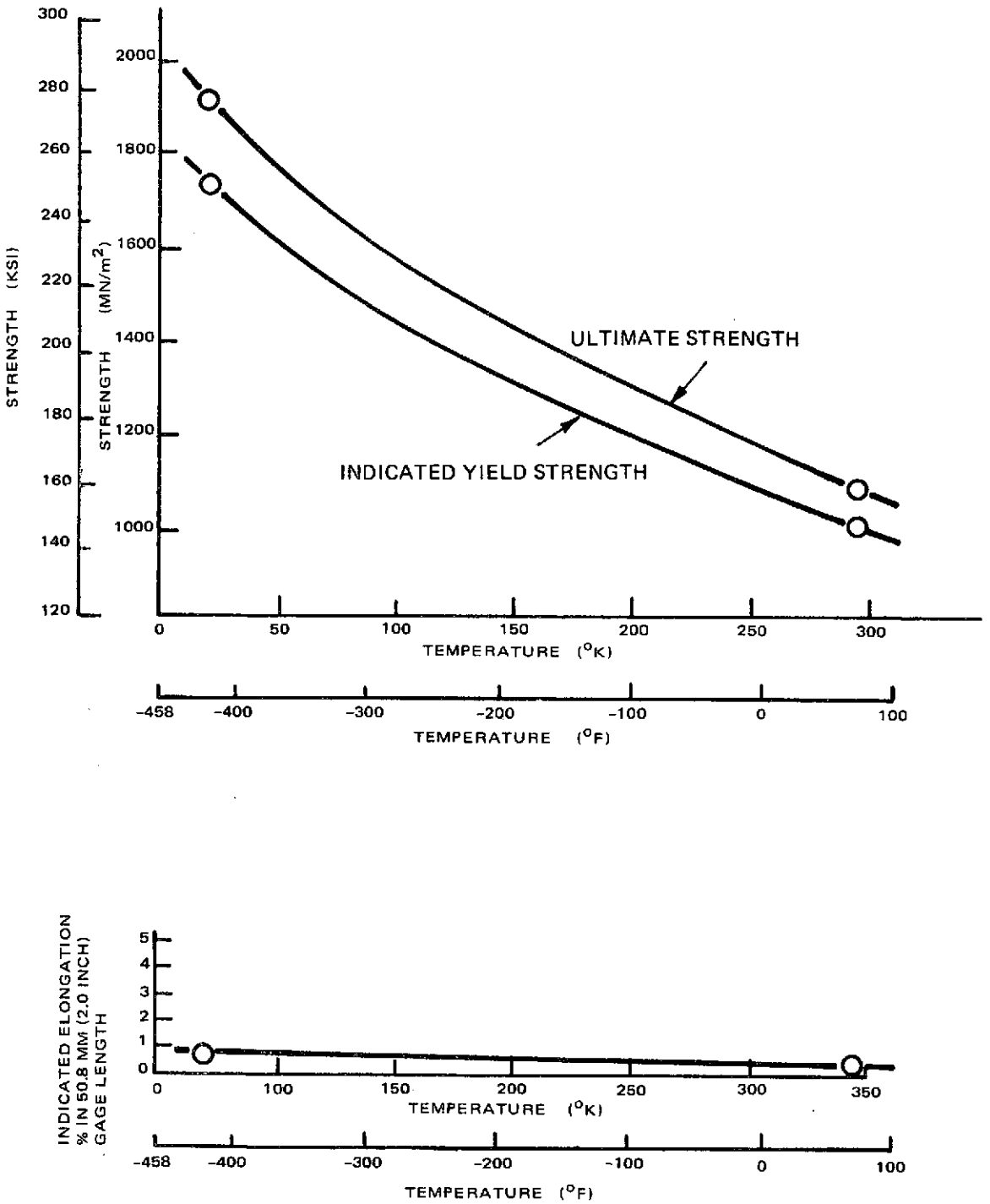

Figure 40: TENSILE PROPERTIES OF 6Al-4V STA 811°K (1000°F) TITANIUM ALLOY WELDMENTS, THICKNESS = 0.51 mm (0.020 in.)

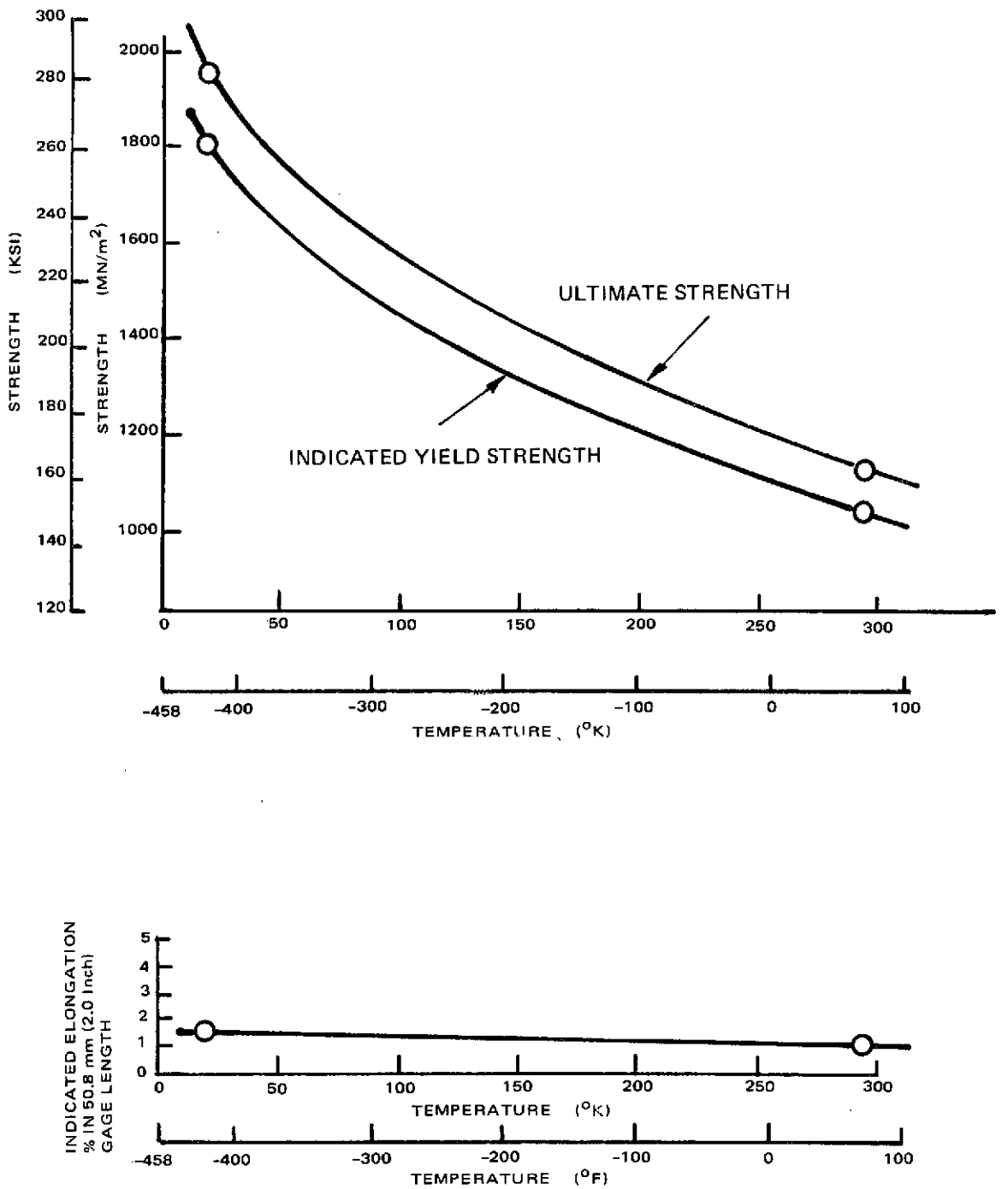

Figure 41: TENSILE PROPERTIES OF 6Al-4V STA 811°K (1000°F) TITANIUM ALLOY WELDMENTS, THICKNESS = 1.78 mm (0.070 in.)

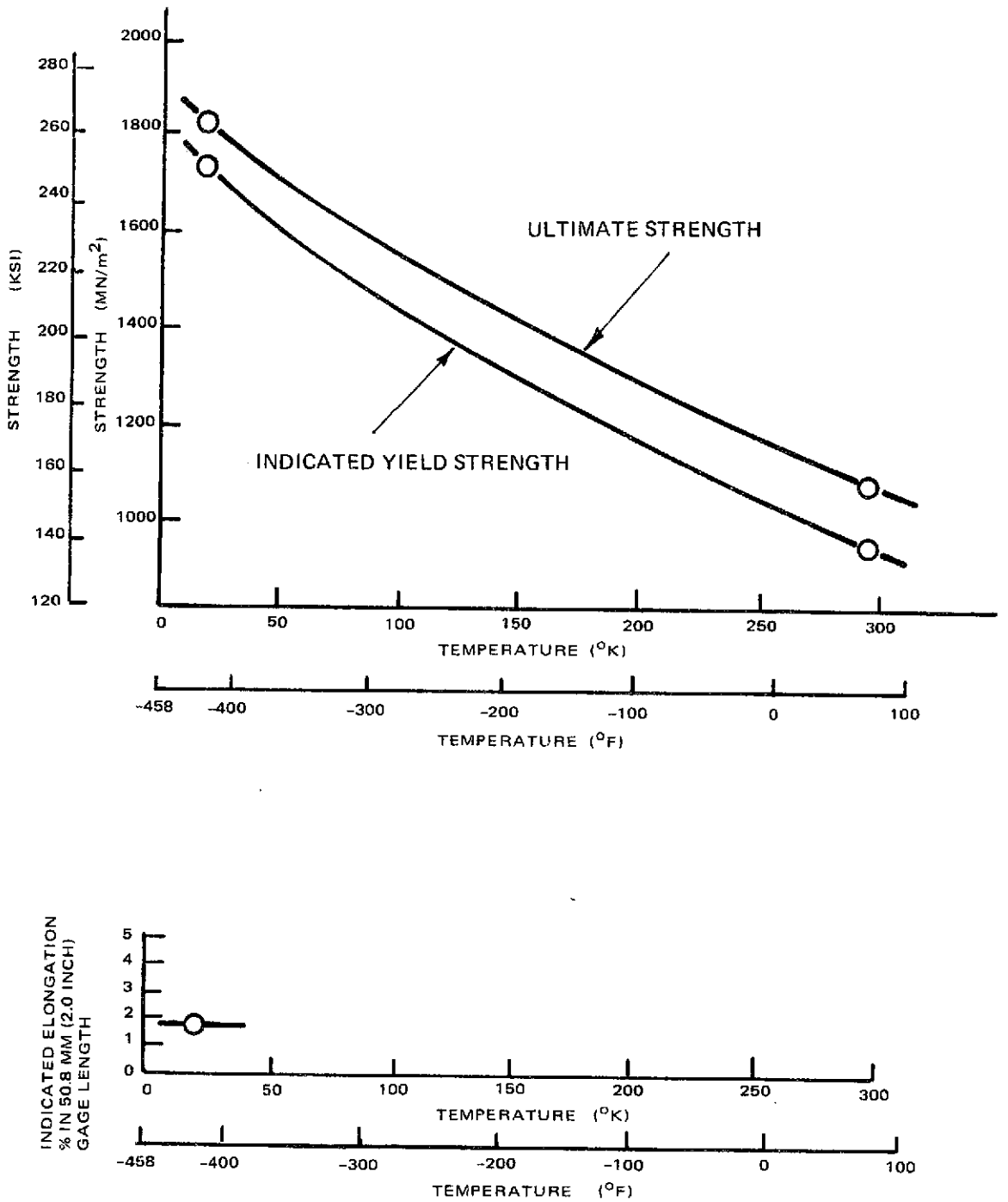

Figure 42: TENSILE PROPERTIES OF 6Al-4V STA 811°K (1000°F) TITANIUM ALLOY WELDMENTS, THICKNESS = 5.33 mm (0.210 in.)

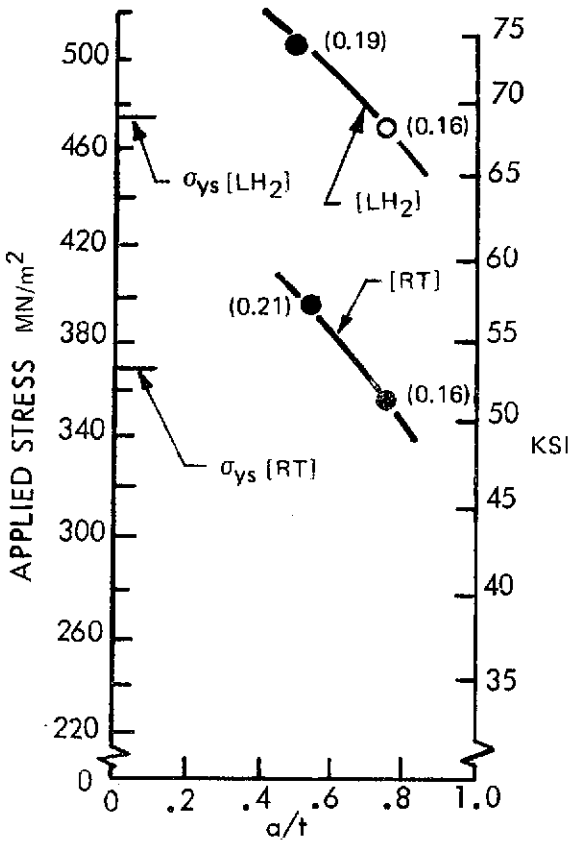

Figure 43(a) t = 1.60 mm (0.063 in)

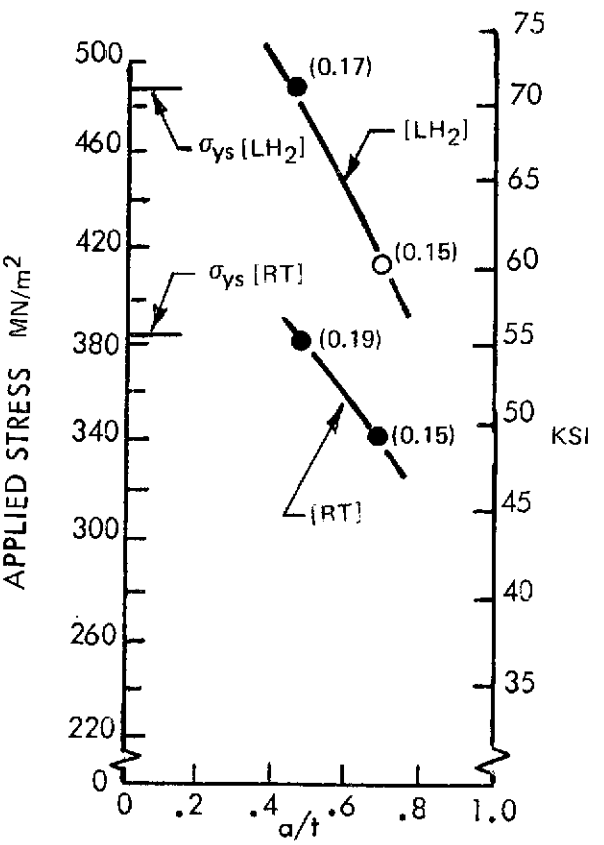

Figure 43(b) t = 3.18 mm (0.125 in)

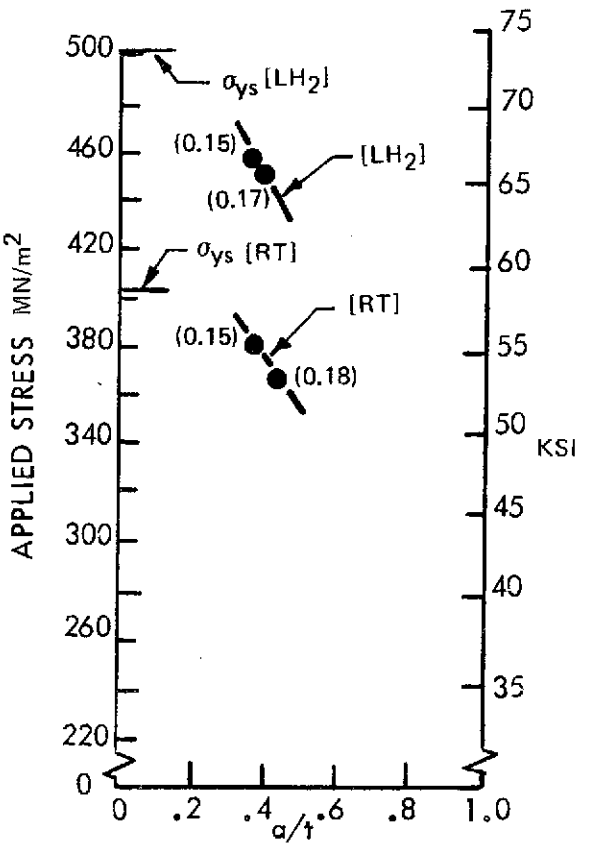

Figure 43(c) t = 7.62 mm (0.30 in)

LEGEND

WT DIRECTION

O LEAK BEFORE FAIL

● FRACTURE

( ) ~ a/2c VALUE

[ ] TEST TEMPERATURE

Figure 43: STRESS VS. a/t CURVES 2219-T87 ALUMINUM BASE METAL

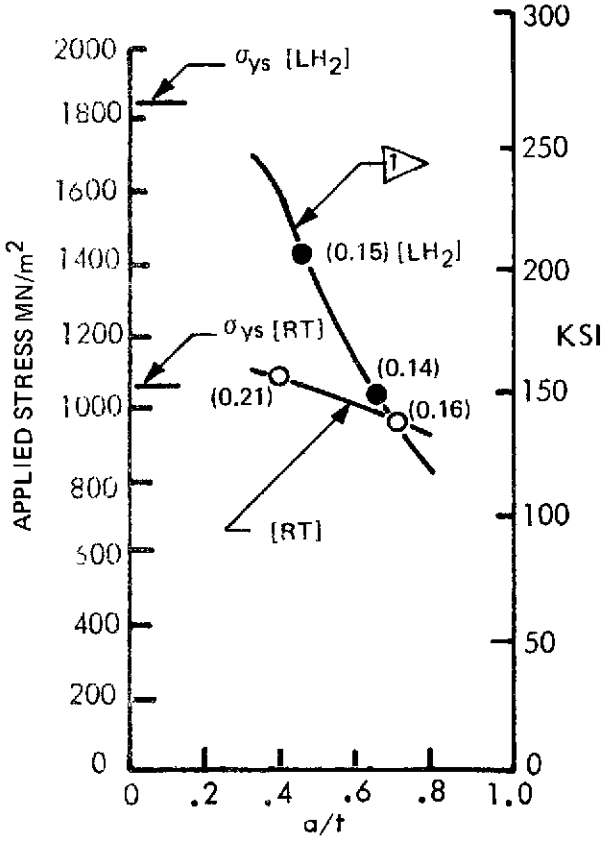

Figure 44 (a) t = 0.51 mm (0.020 in)

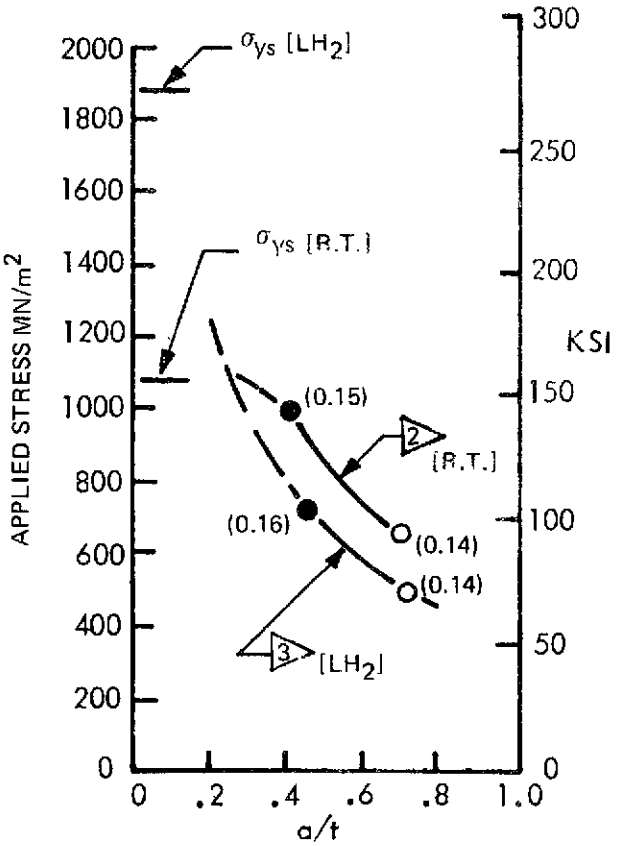

Figure 44 (b) t = 2.03 mm (0.080 in)

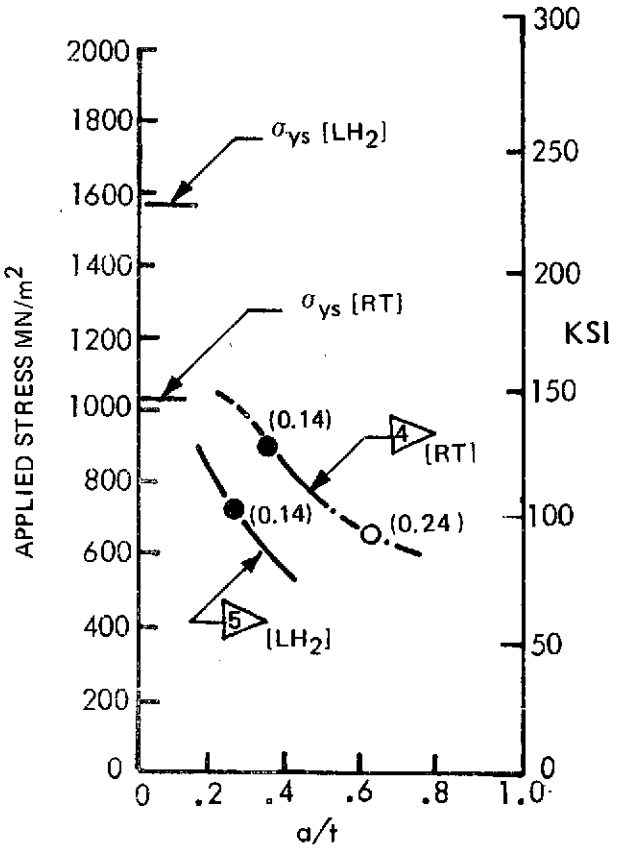

Figure 44 (c) t = 6.35 mm (0.250 in)

LEGEND:
WT DIRECTION
○ LEAK BEFORE FAIL
● FRACTURE
( ) ~a/2c VALUE
[ ] TEST TEMPERATURE

1 KIE = 44.9 MN/m$^{3/2}$ (40.9 KSI $\sqrt{IN.}$)
2 KIE = 58.5 MN/m$^{3/2}$ (53.2 KSI $\sqrt{IN.}$)
3 KIE = 42.7 MN/m$^{3/2}$ (38.9 KSI $\sqrt{IN.}$)
4 KIE = 93.3 MN/m$^{3/2}$ (84.9 KSI $\sqrt{IN.}$)
5 KIE = 58.3 MN/m$^{3/2}$ (53.1 KSI $\sqrt{IN.}$)

Figure 44: STRESS VS. a/t CURVES 6AI-4V TITANIUM BASE METAL

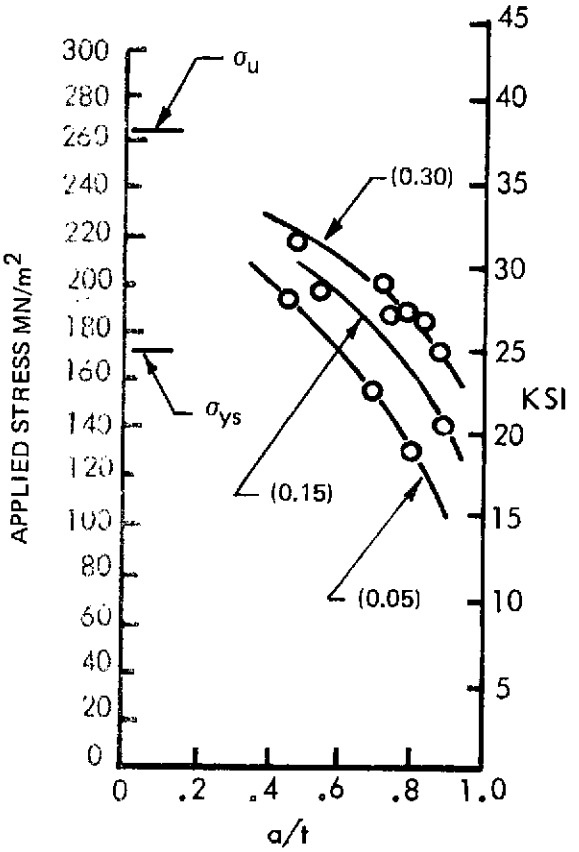

Figure 45 (a) t = 1.60 mm (0.063 in)

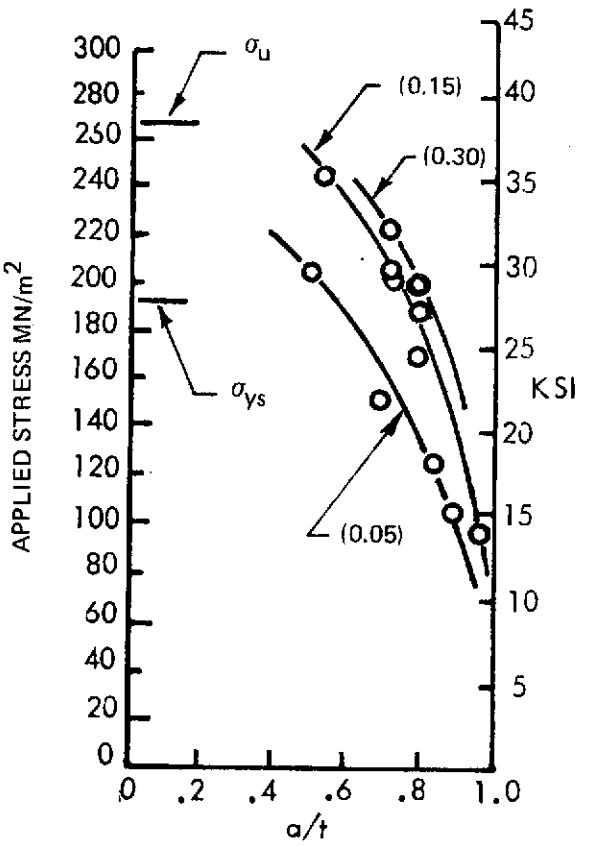

Figure 45 (b) t = 2.67 mm (0.105 in)

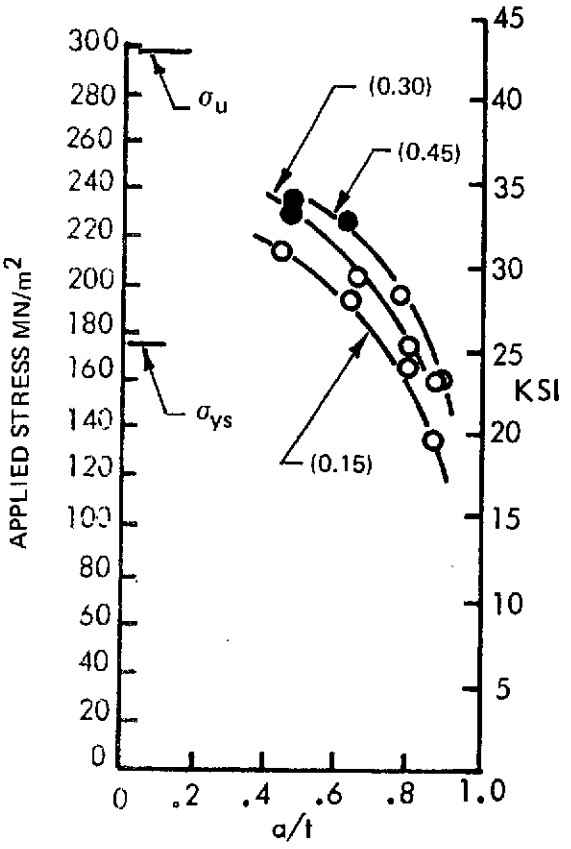

Figure 45 (c) t = 7.62 mm (0.30 in)

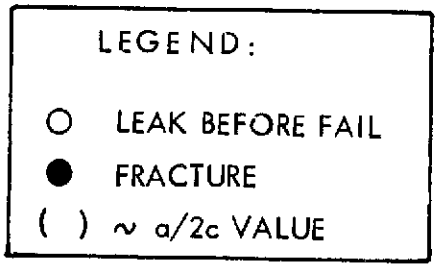

Figure 45: STRESS VS. a/t CURVES 2219-T87 ALUMINUM WELDMENTS @ ROOM TEMPERATURE

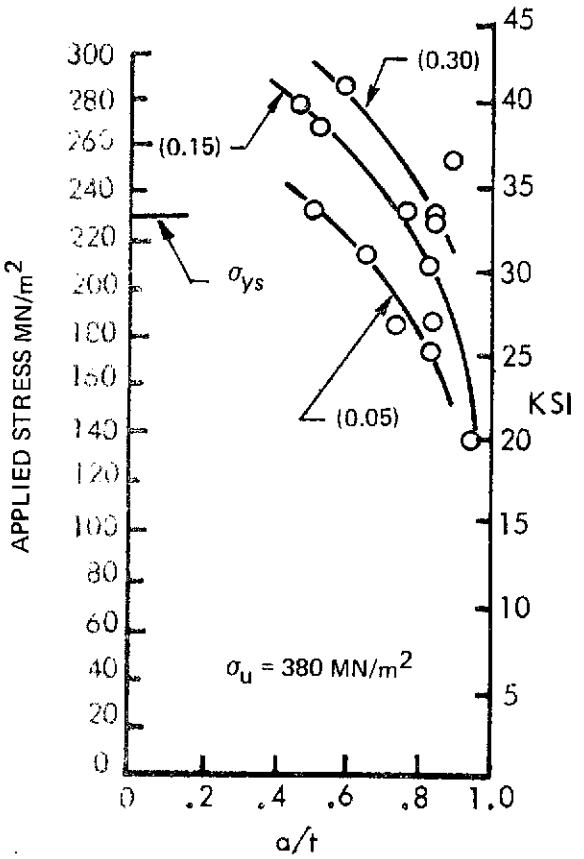

Figure 46 (a) t = 1.60 mm (0.063 in)

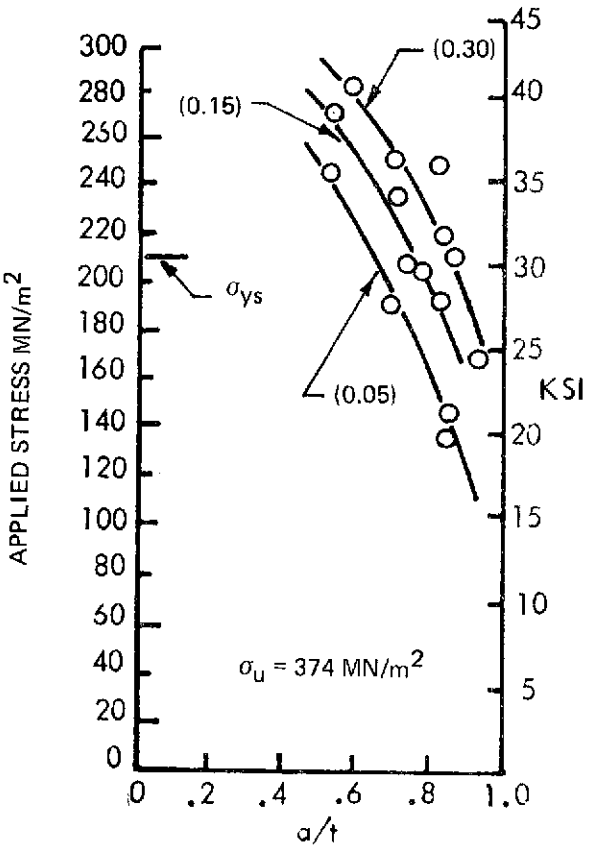

Figure 46 (b) t = 2.67 mm (0.105 in)

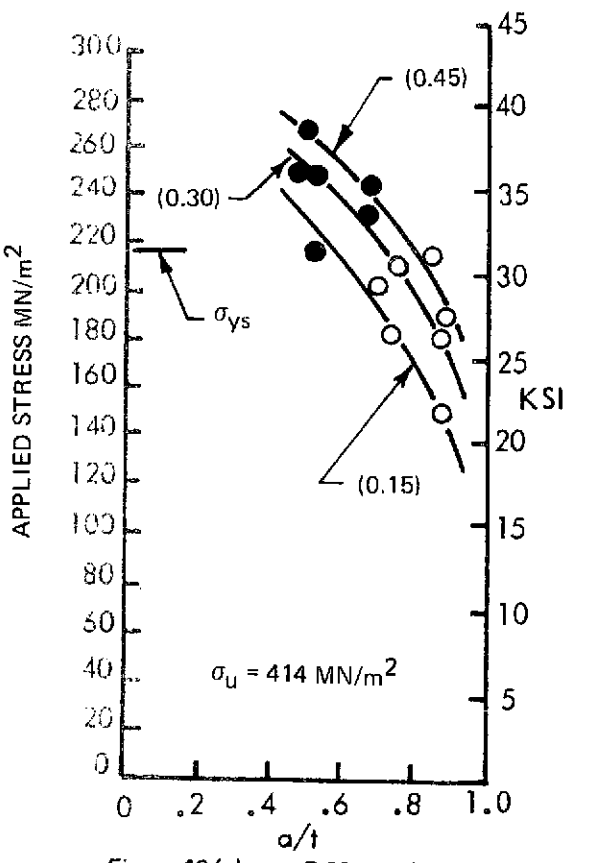

Figure 46 (c) t = 7.62 mm (0.30 in)

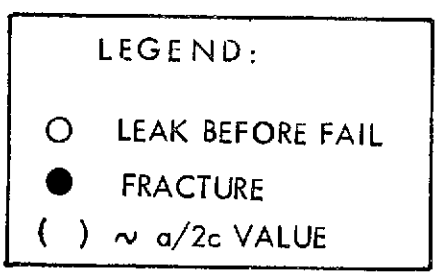

Figure 46: STRESS VS. a/t CURVES 2219-T87 ALUMINUM WELDMENTS @ 78K (-320F)

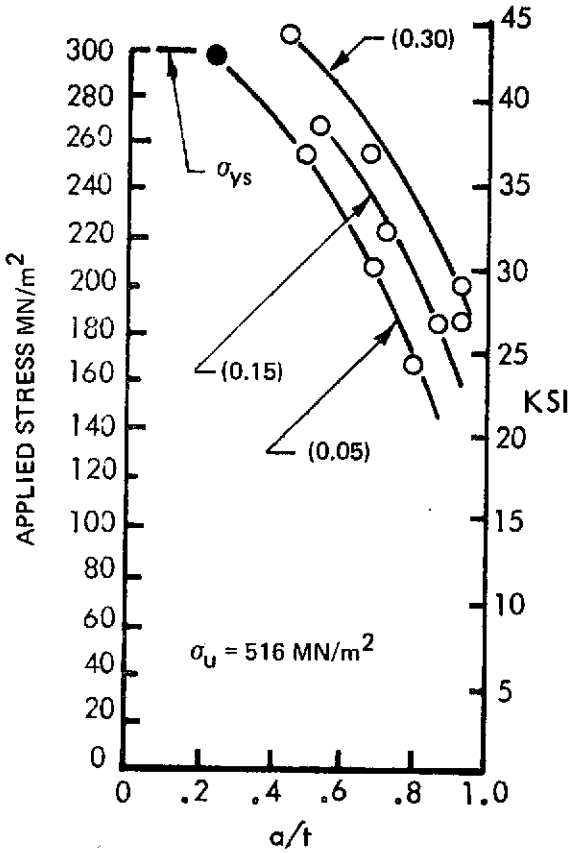

Figure 47(a) t = 1.60 mm (0.063 in)

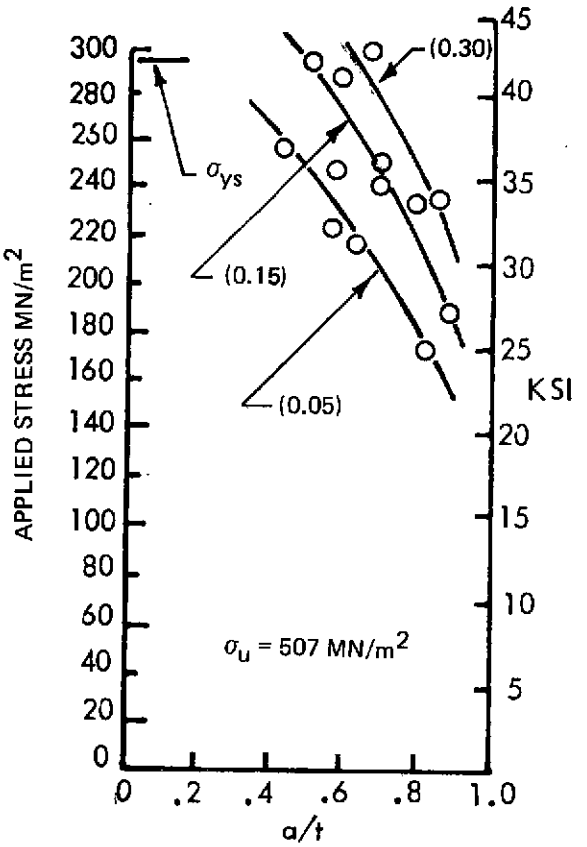

Figure 47(b) t = 2.67 mm (0.105 in)

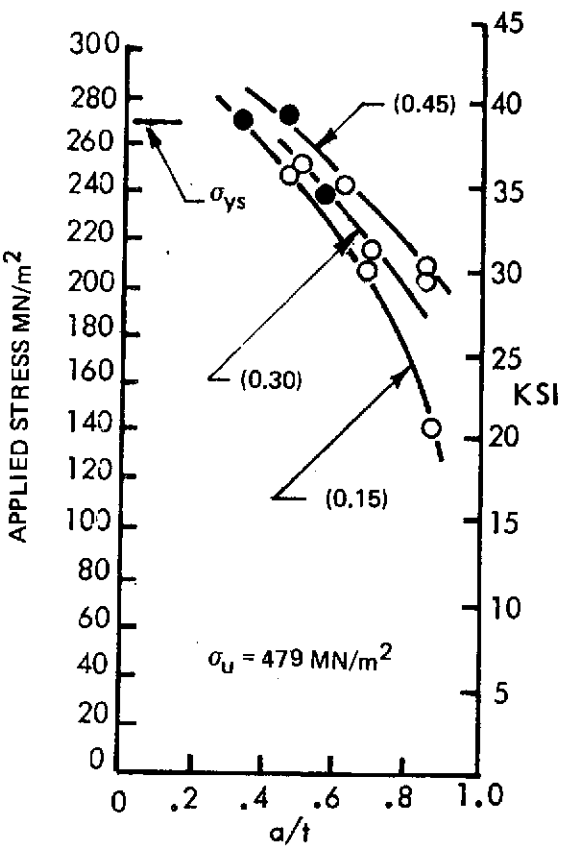

Figure 47(c) t = 7.62 mm (0.30 in)

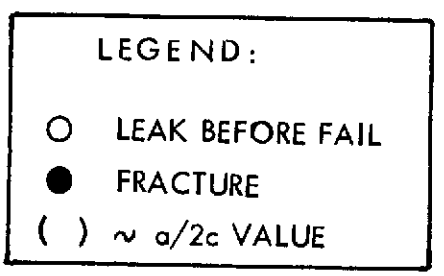

Figure 47: STRESS VS. a/t CURVES 2219-T87 ALUMINUM WELDMENTS @ 20K (-423F)

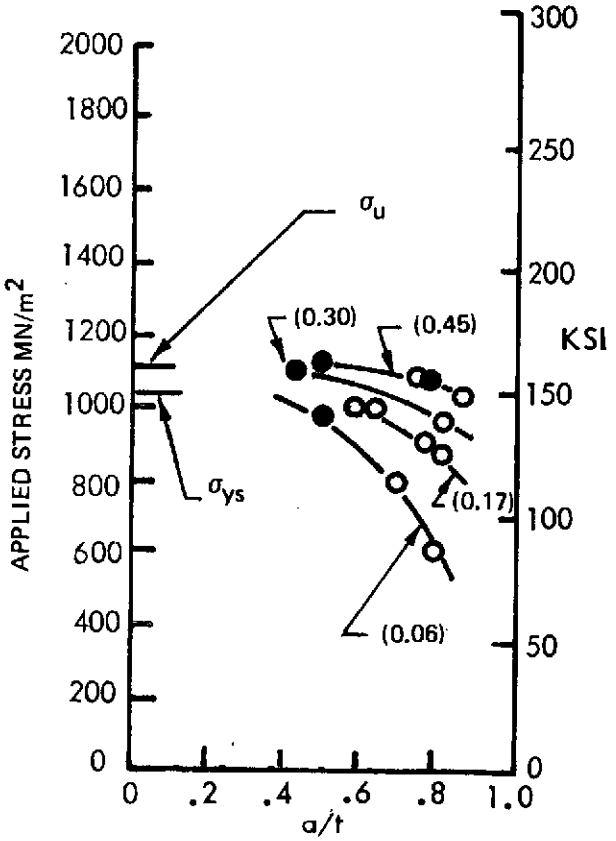

Figure 48 (a) t = 0.51 mm (0.02 in)

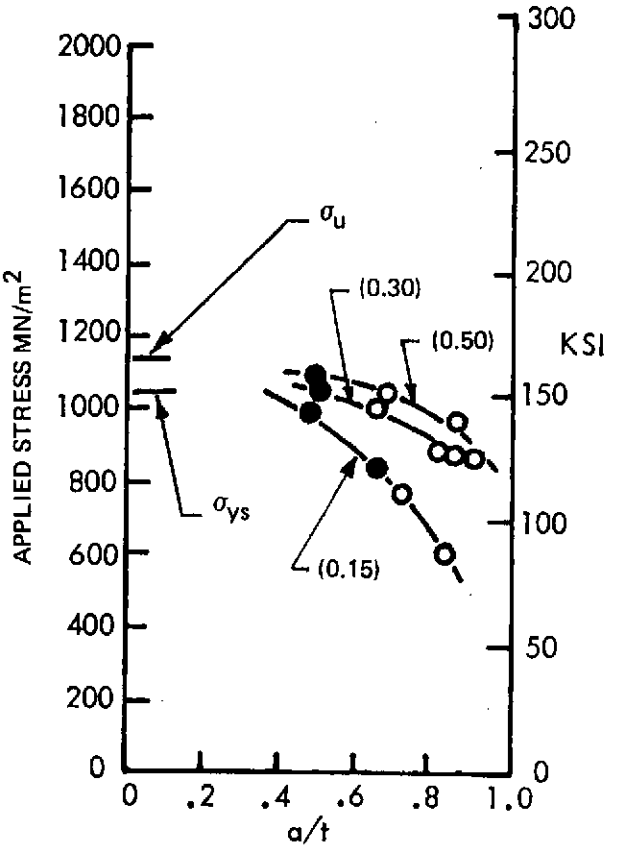

Figure 48 (b) t = 1.78 mm (0.07 in)

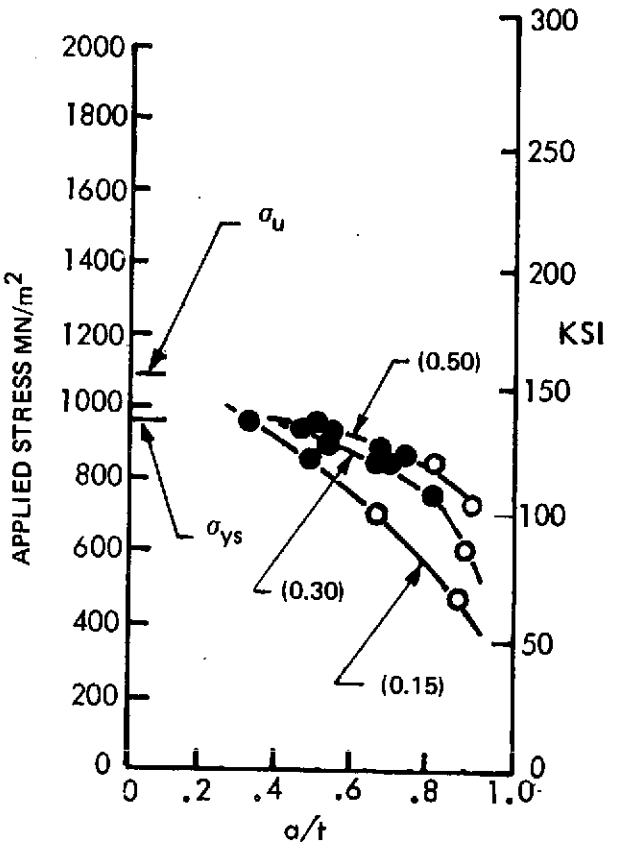

Figure 48 (c) t = 5.33 mm (0.21 in)

LEGEND:

- ○ LEAK BEFORE FAIL
- ● FRACTURE
- ( )~ a/2c VALUE

Figure 48: STRESS VS. a/t CURVES 6AI-4V TITANIUM WELDMENTS @ ROOM TEMPERATURE

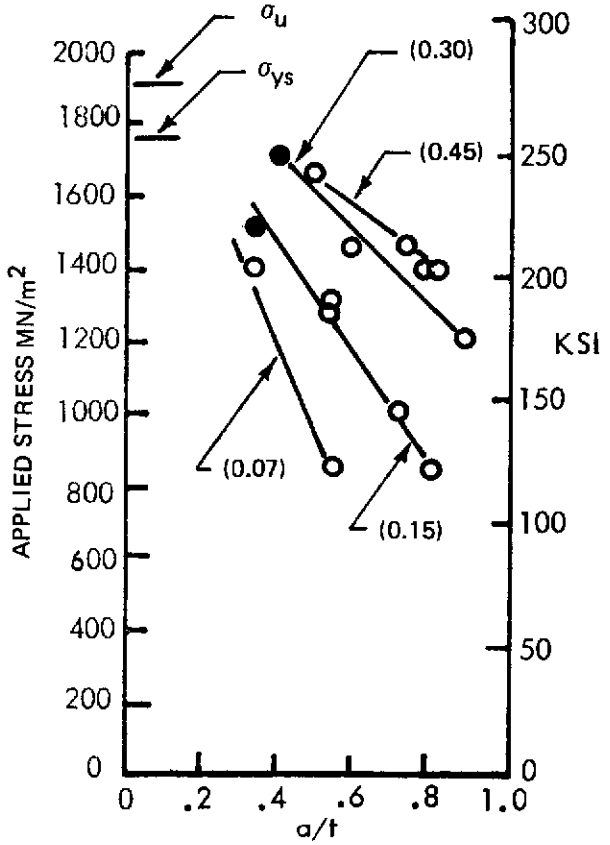

Figure 49 (a) t = 0.51 mm (0.02 in)

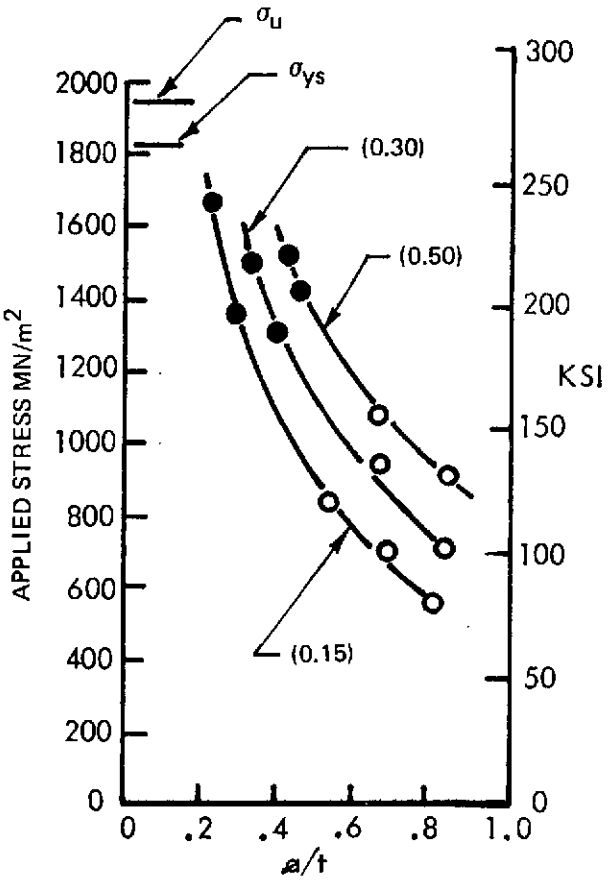

Figure 49 (b) t = 1.78 mm (0.07 in)

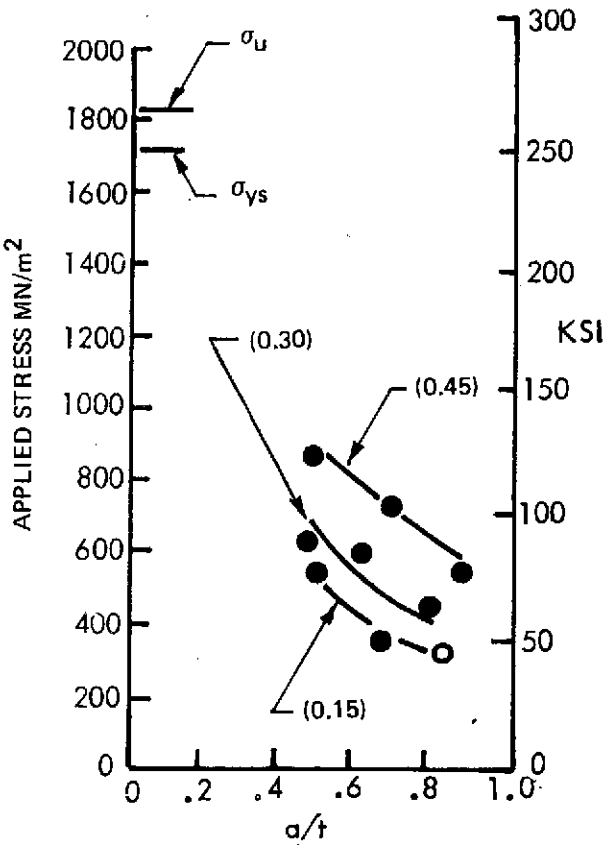

Figure 49(c) t = 5.33 mm (0.21 in)

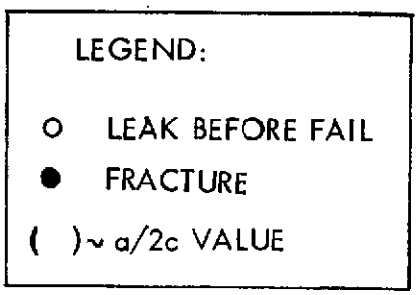

Figure 49: STRESS VS. a/t CURVES 6Al-4V TITANIUM WELDMENTS @ 20K (-423F)

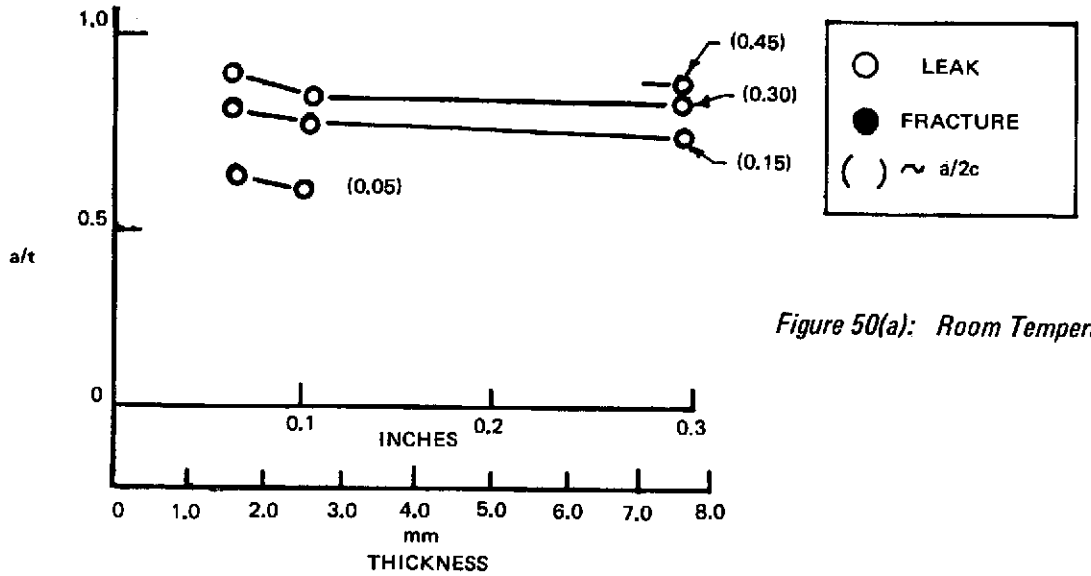

Figure 50(a): Room Temperature

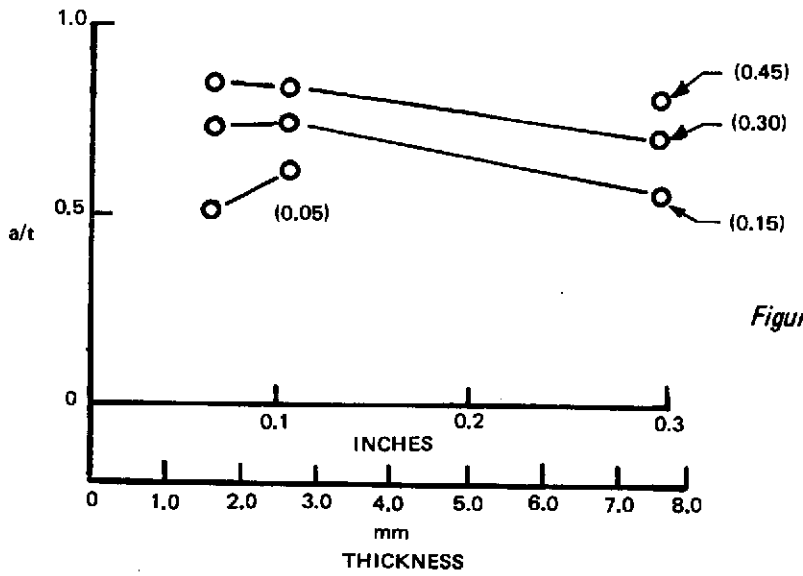

Figure 50(b): 78K (-320F)

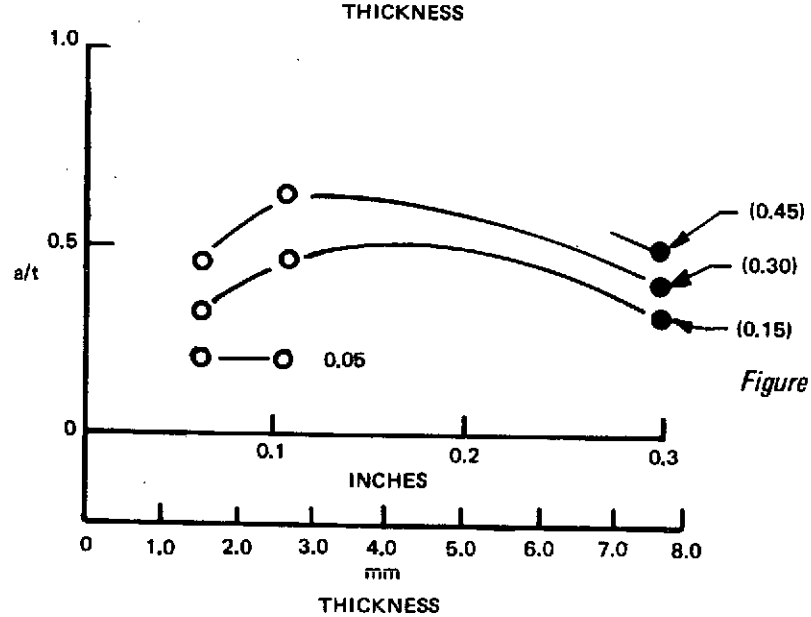

Figure 50(c): 20K (-423)

Figure 50: COMBINATIONS OF FLAW GEOMETRIES AND SIZES CAUSING LEAKAGE AT YIELD STRESS, 2219-T87 ALUMINUM WELDMENTS

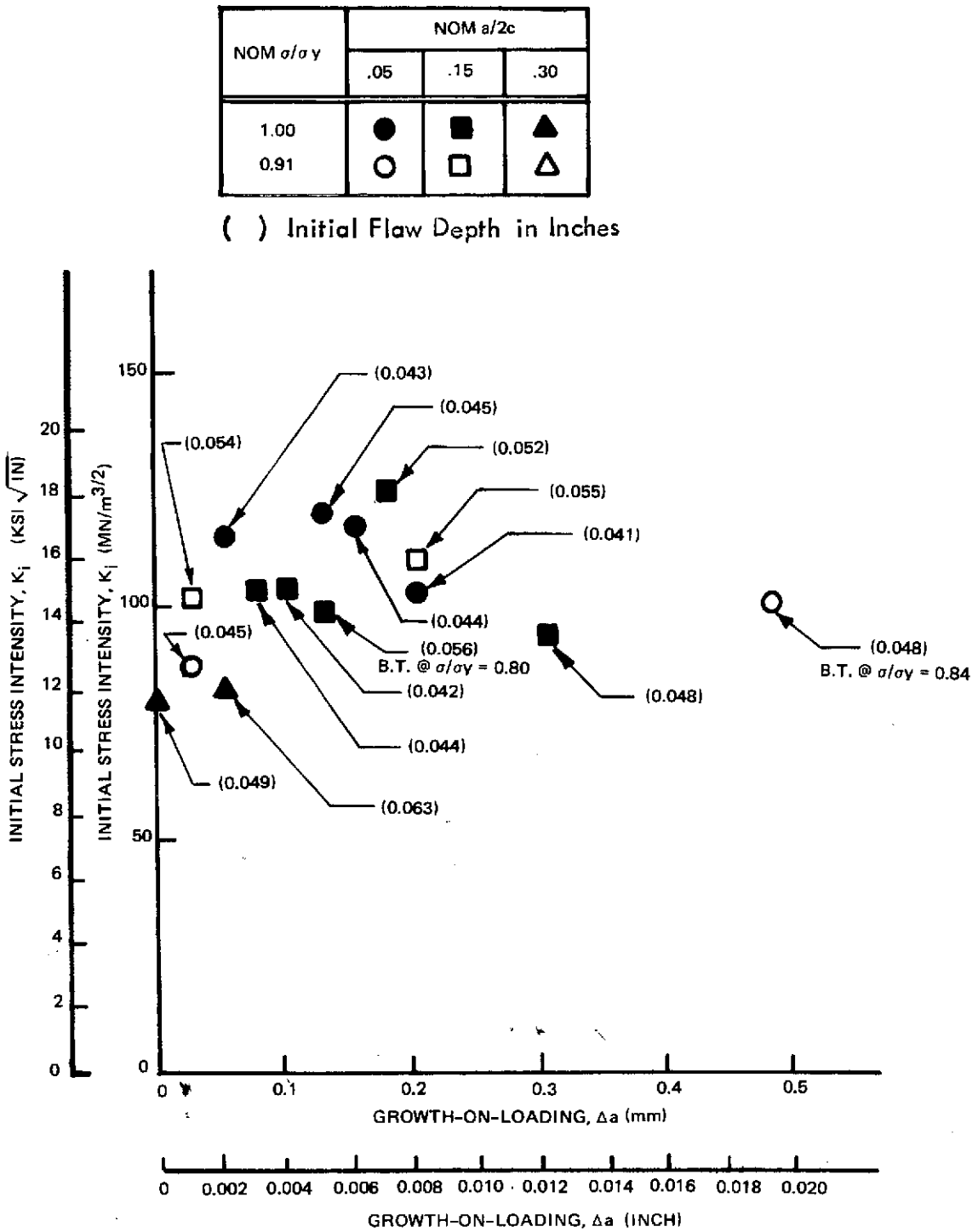

Figure 51: INITIAL STRESS INTENSITY VS. GROWTH-ON-LOADING, 1.60mm (0.063 INCH) 2219-T87 ALUMINUM ALLOY WELDMENTS PROOF TESTED AT ROOM TEMPERATURE

σ/σ_{ys}				THICKNESS mm (Inch)
0.40	0.60	0.80	0.90	
○	●	◑	◐	1.60 (0.063)
△	▲	▲	▲	2.67 (0.105)
□	■	◨	◧	7.62 (0.30)

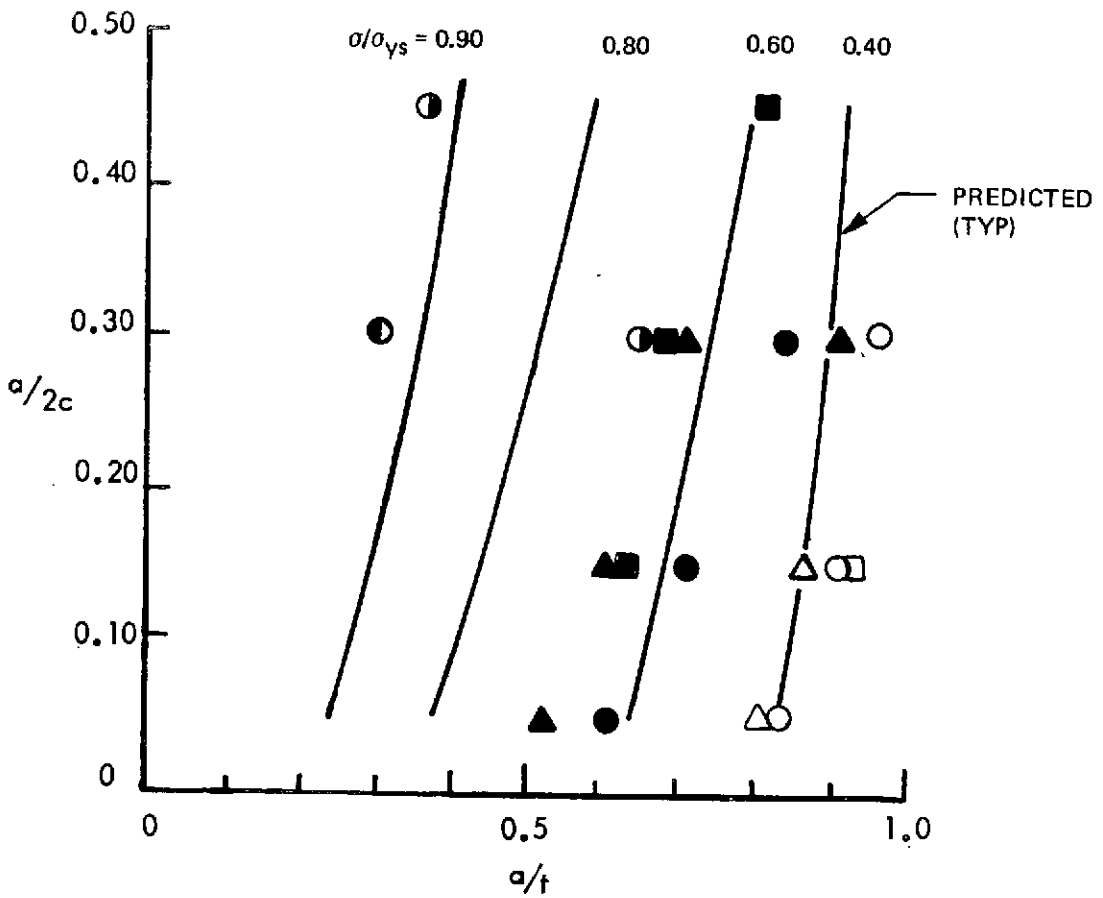

Figure 52: *DIMPLING THRESHOLD FOR 2219-T87 ALUMINUM WELDMENTS AT ROOM TEMPERATURE*

σ/σ_{ys}				THICKNESS mm (Inch)
0.40	0.60	0.80	0.90	
○	●	◑	◐	1.60 (0.063)
△	▲	▲	▲	2.67 (0.105)
□	■	◨	◧	7.62 (0.30)

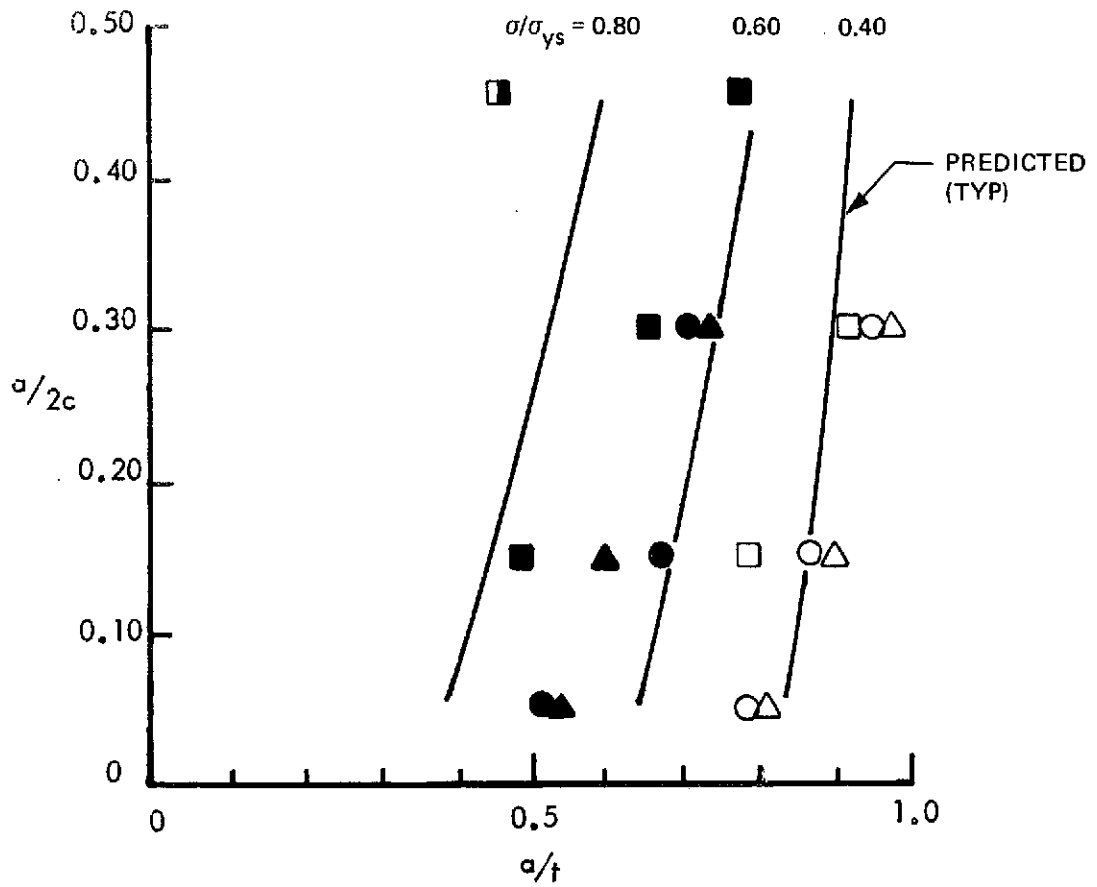

Figure 53: DIMPLING THRESHOLD FOR 2219-T87 ALUMINUM WELDMENTS AT 20K (-423F)

σ/σ_{ys}				THICKNESS mm (Inch)
0.40	0.60	0.80	0.90	
○	●	◑	◐	0.51 (0.02)
△	▲	◭	◮	1.78 (0.07)
□	■	◨	◧	5.33 (0.21)

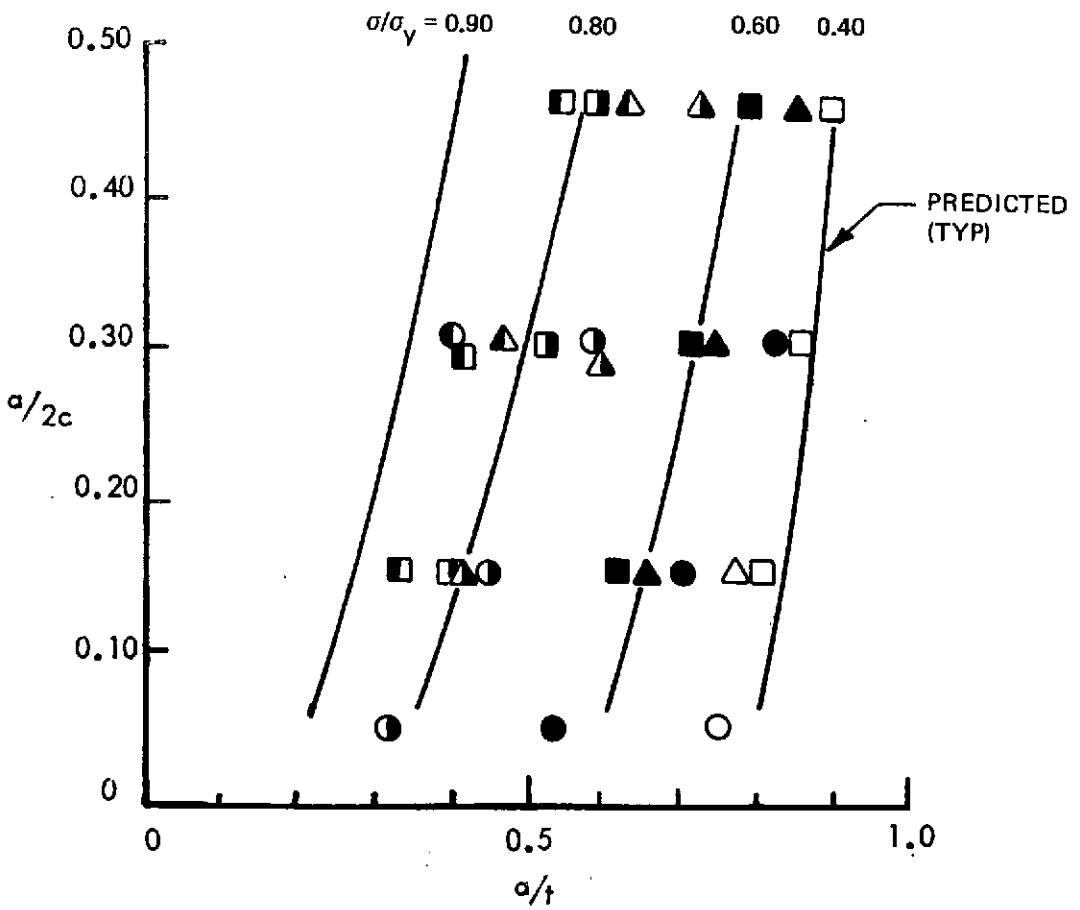

Figure 54: DIMPLING THRESHOLD FOR 6AI-4V TITANIUM WELDMENTS AT ROOM TEMPERATURE

σ/σ_{ys}				THICKNESS mm (Inch)
0.40	0.60	0.80	0.90	
○	●	◑	◐	0.51 (0.02)
△	▲	◭	◮	1.78 (0.07)
□	■	◨	◧	5.33 (0.21)

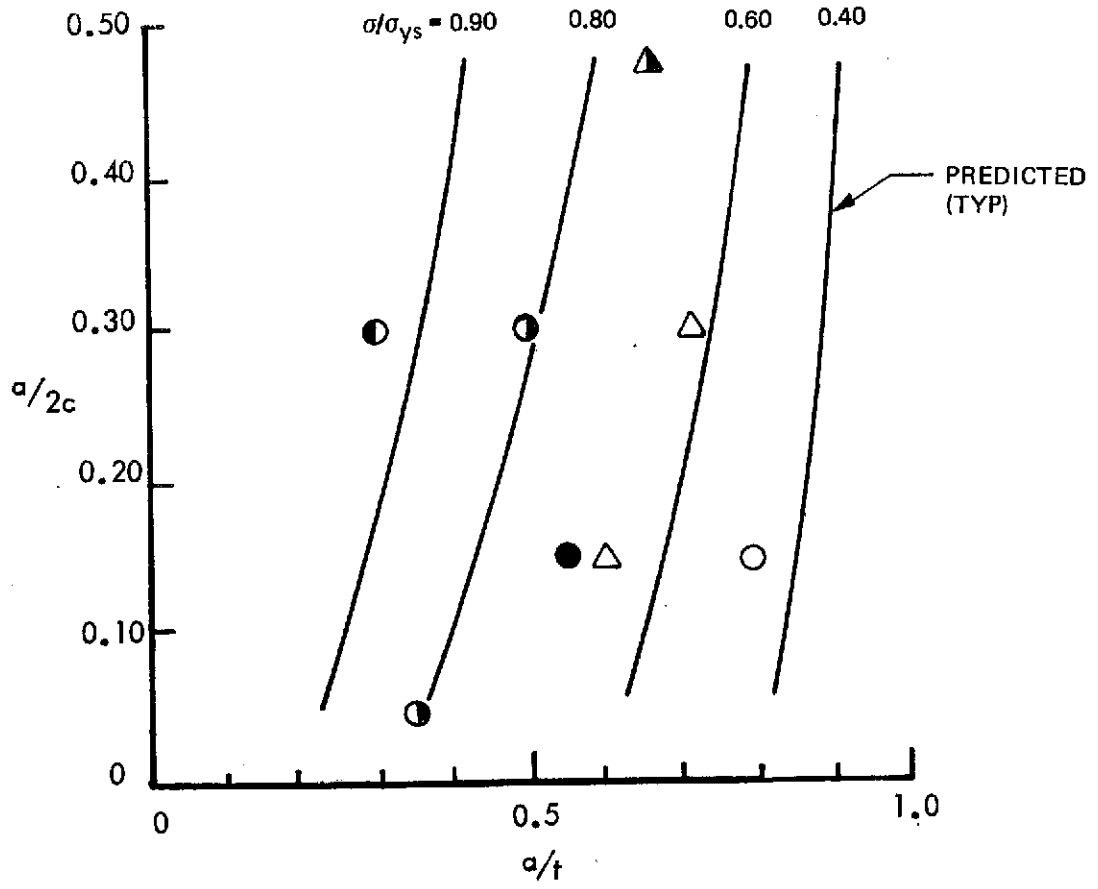

Figure 55: DIMPLING THRESHOLD FOR 6Al-4V TITANIUM WELDMENTS AT 20K (-423F)

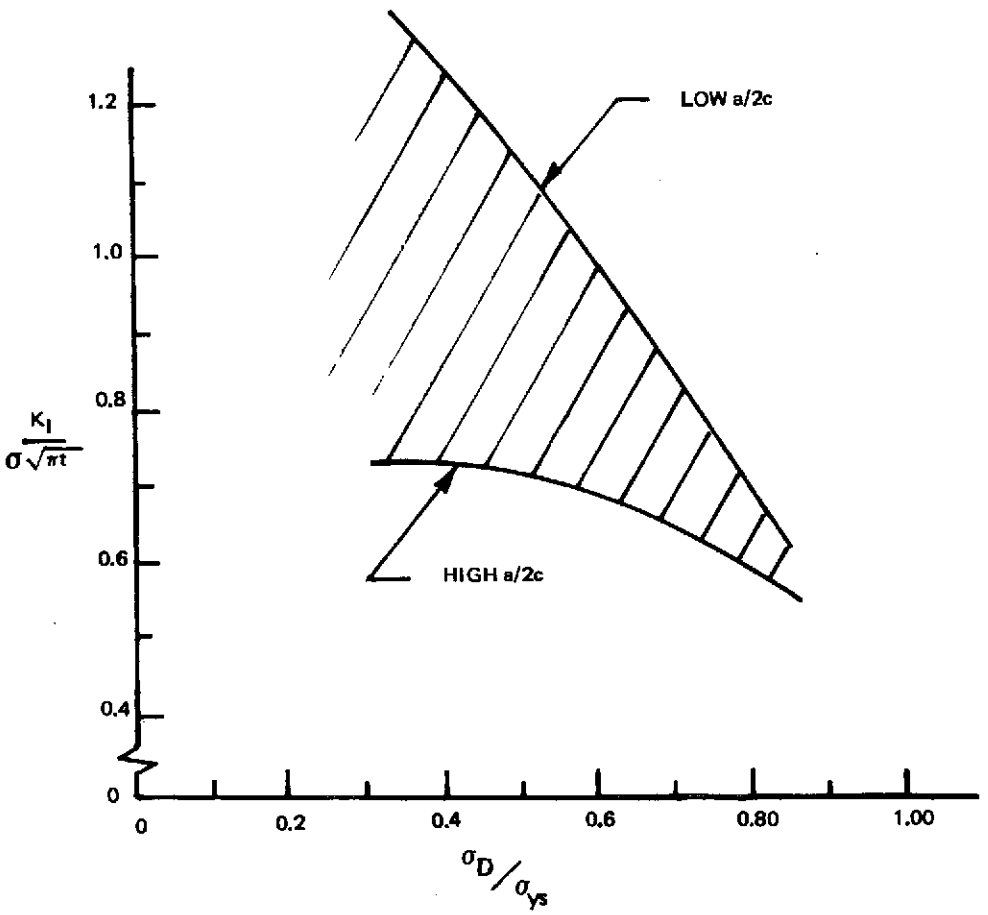

Figure 56: COMPARISON OF APPLIED STRESS INTENSITY AND PERCEIVED DIMPLING 6AI-4V TITANIUM WELDMENTS @ ROOM TEMPERATURE

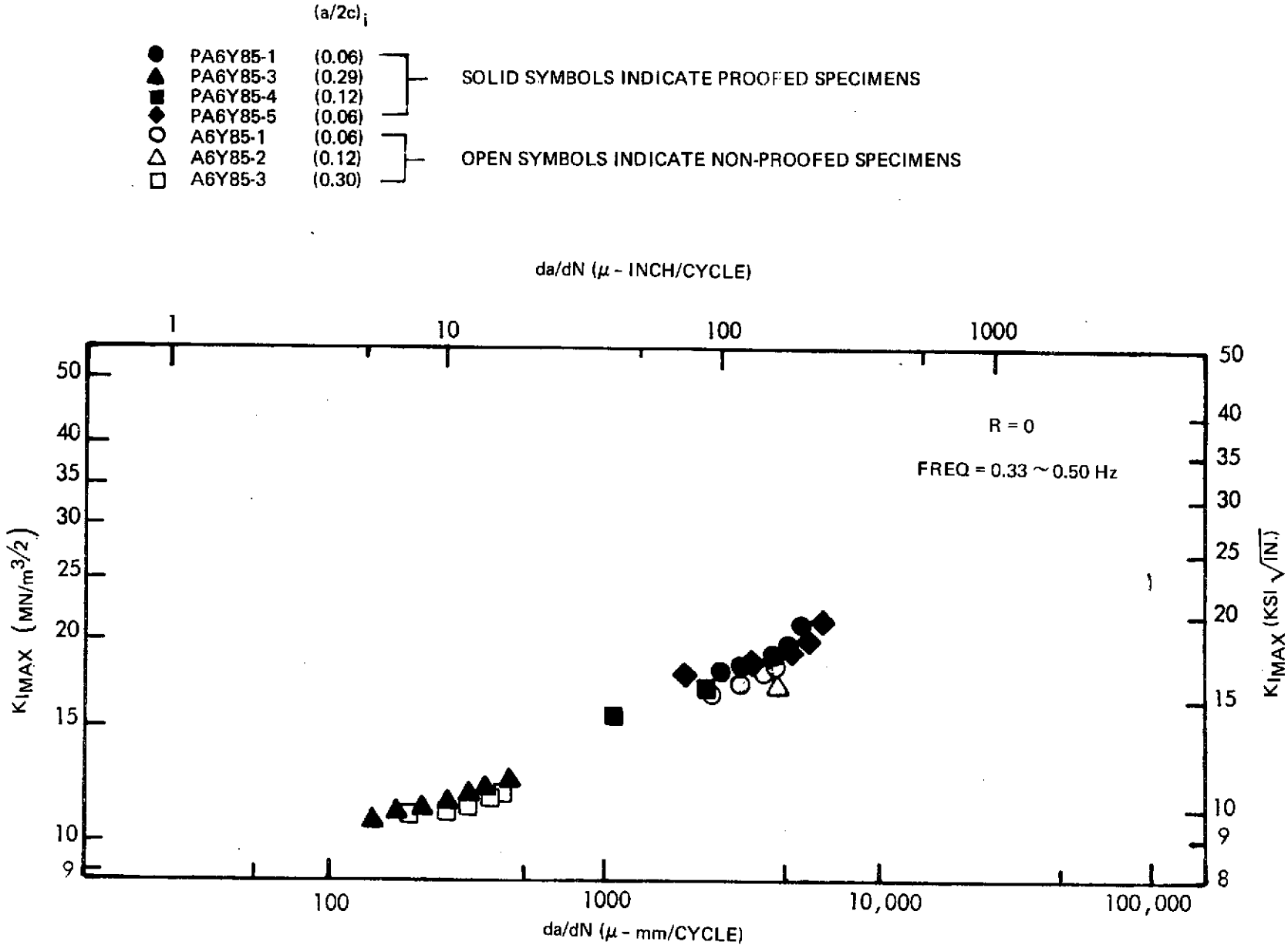

Figure 57: PLOT OF CYCLIC CRACK GROWTH RATES VS. K_I MAX FOR 1.60 mm (0.063 INCH) "AS-WELDED" 2219-T87 ALUMINUM CAPABLE OF PASSING σ_Y PROOF AND CYCLED AT 0.85 σ_Y IN RT AIR

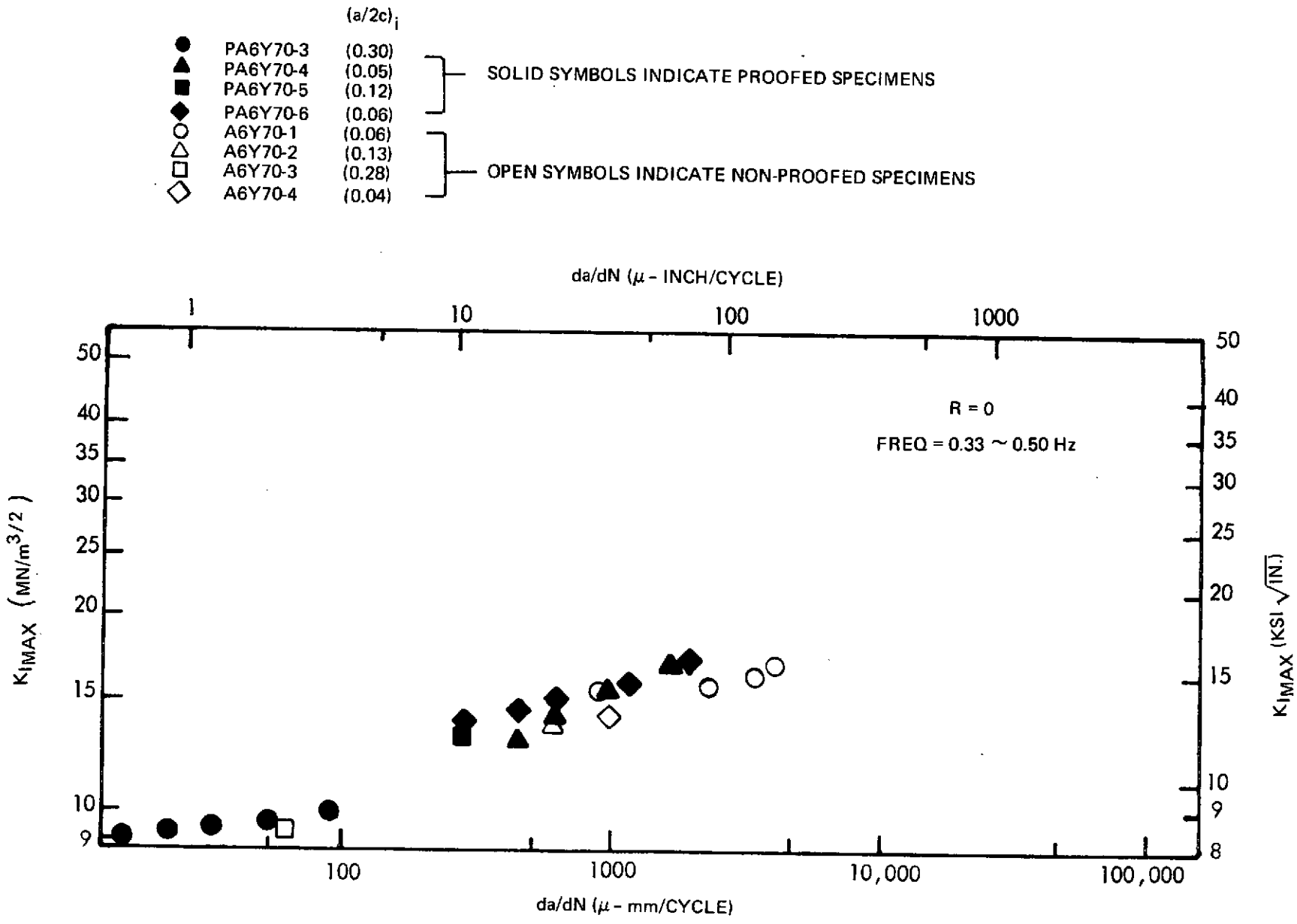

Figure 58: PLOT OF CYCLIC CRACK GROWTH RATES VS. $K_{I_{MAX}}$ FOR 1.60 mm (0.063 INCH) "AS-WELDED" 2219-T87 ALUMINUM CAPABLE OF PASSING σ_Y PROOF AND CYCLED AT 0.70 σ_Y IN RT AIR

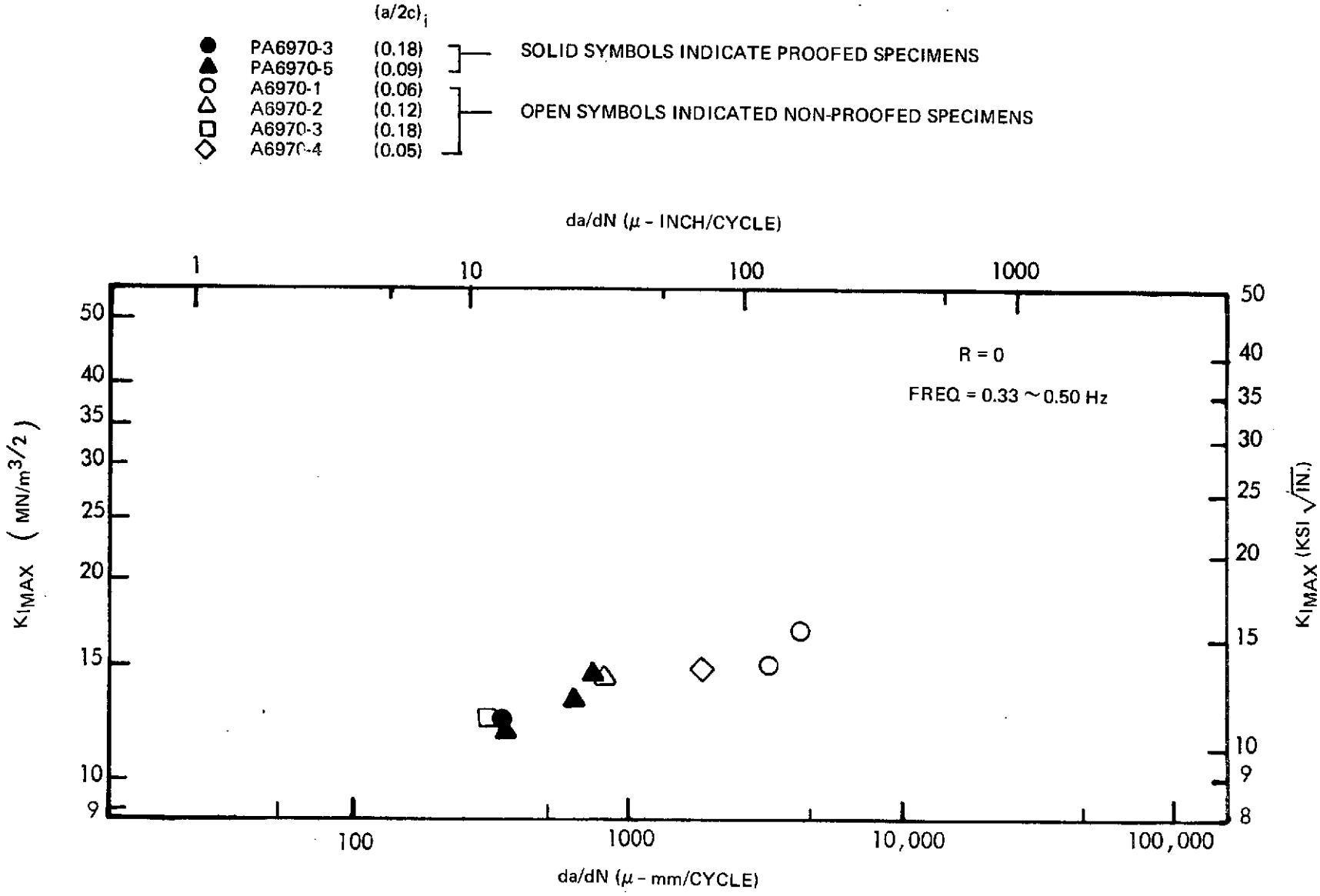

Figure 59: PLOT OF CYCLIC CRACK GROWTH RATES VS. $K_{I_{MAX}}$ FOR 1.60 mm (0.063 INCH) "AS-WELDED" 2219-T87 ALUMINUM CAPABLE OF PASSING 0.91 σ_Y PROOF AND CYCLED AT 0.70 σ_Y IN RT AIR

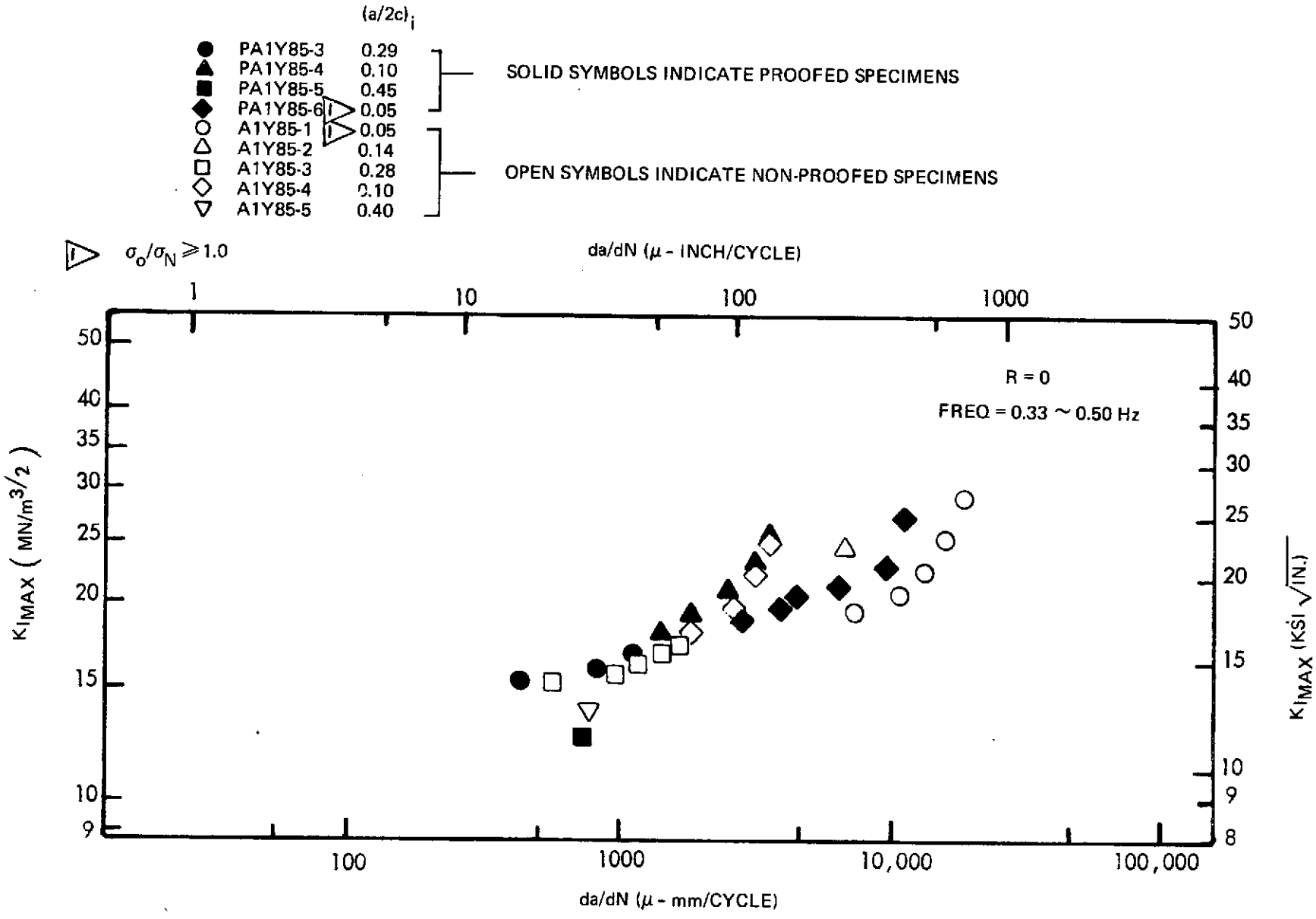

Figure 60: PLOT OF CYCLIC CRACK GROWTH RATES VS. $K_{I_{MAX}}$ FOR 2.67 mm (0.105 INCH) "AS-WELDED" 2219-T87 ALUMINUM CAPABLE OF PASSING σ_Y PROOF AND CYCLED AT 0.85 σ_Y IN RT AIR

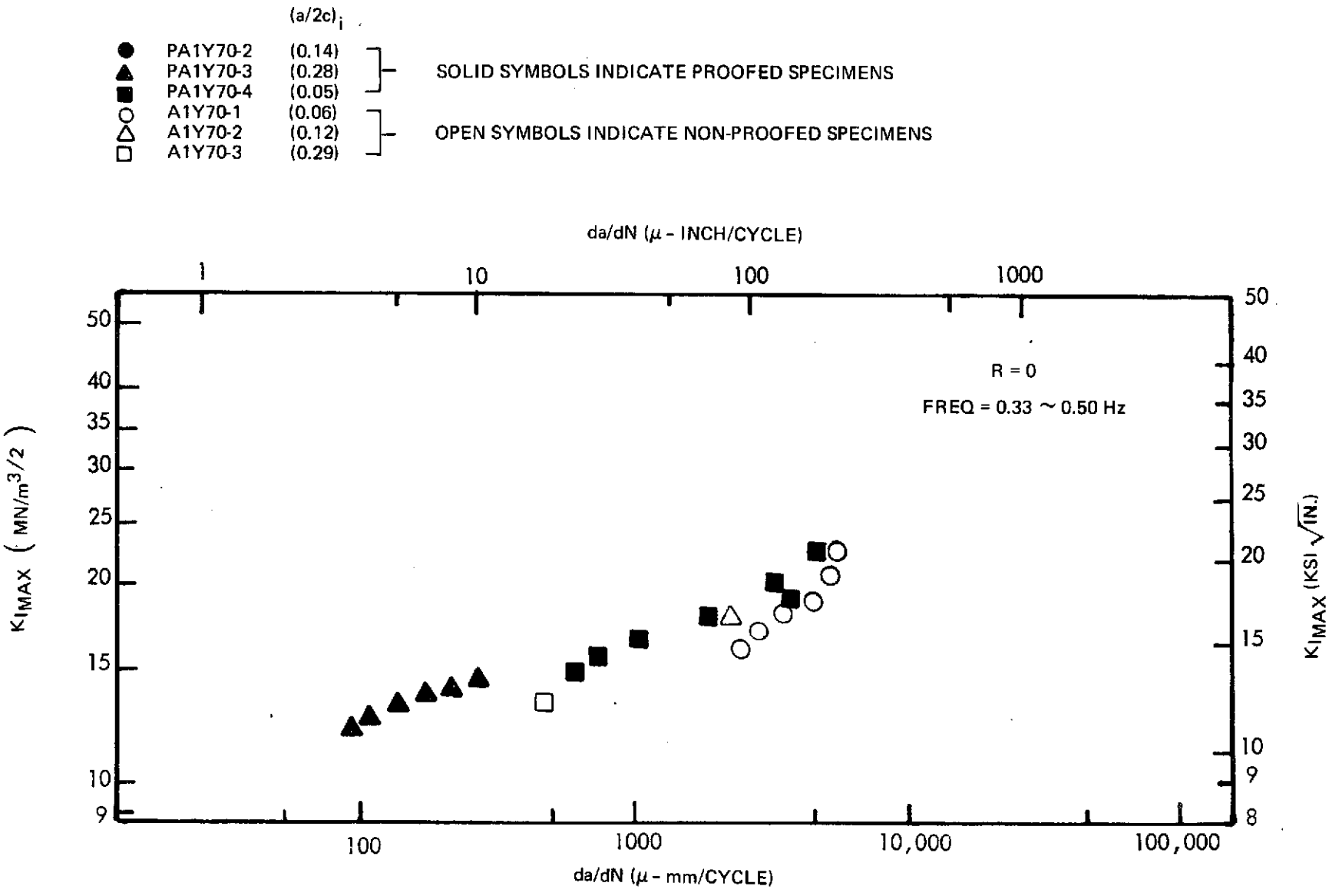

Figure 61: PLOT OF CYCLIC CRACK GROWTH RATES VS. $K_{I_{MAX}}$ for 2.67 mm (0.105 INCH) "AS-WELDED" 2219-T87 ALUMINUM CAPABLE OF PASSING σ_Y PROOF AND CYCLED AT 0.70 σ_Y IN RT AIR

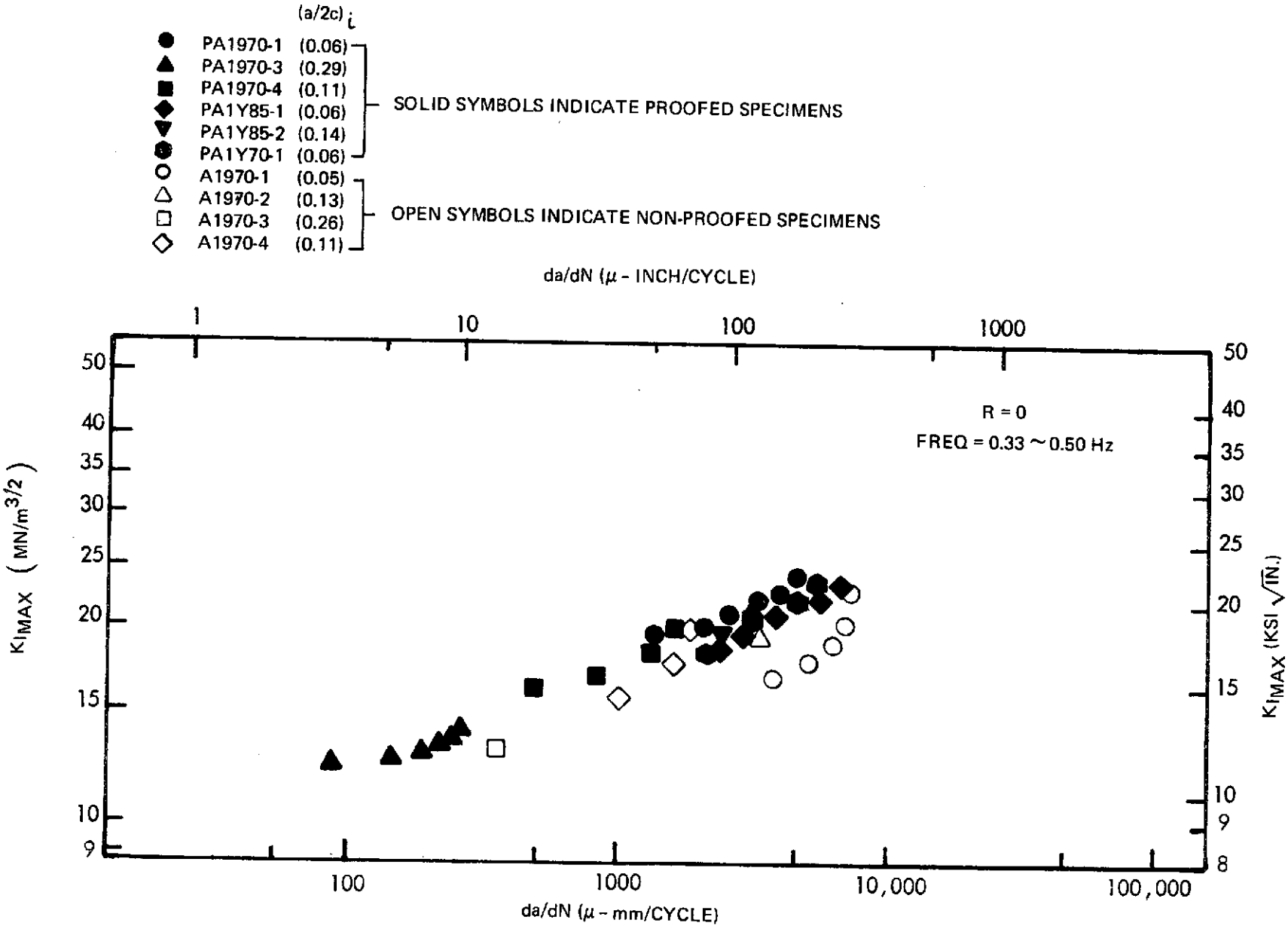

Figure 62: PLOT OF CYCLIC CRACK GROWTH RATES VS. $K_{I_{MAX}}$ FOR 2.67 mm (0.105 INCH) "AS-WELDED" 2219-T87 ALUMINUM CAPABLE OF PASSING 0.91 σ_Y PROOF AND CYCLED AT 0.70 σ_Y IN RT AIR

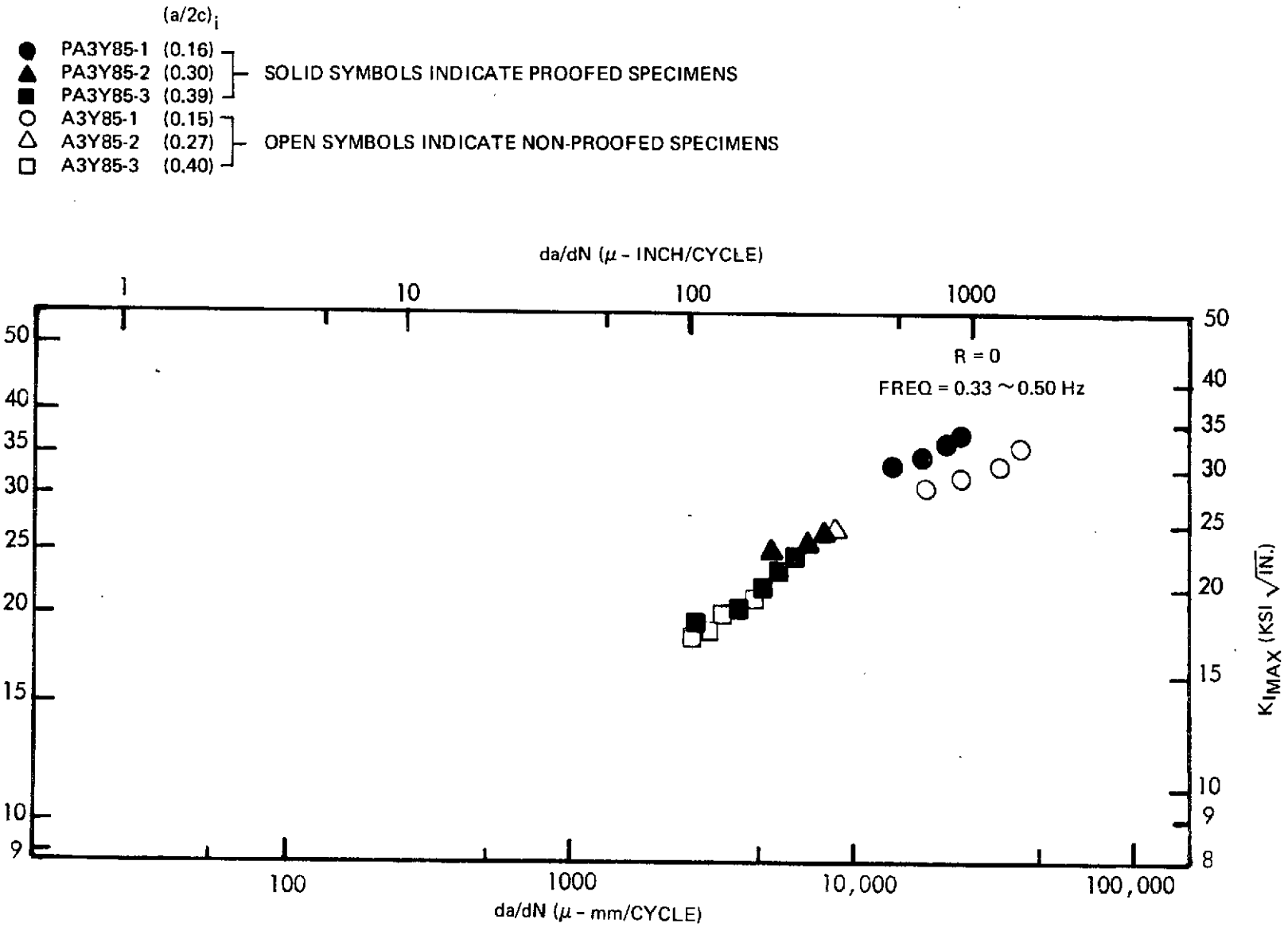

Figure 63: PLOT OF CYCLIC CRACK GROWTH RATES VS. $K_{I_{MAX}}$ FOR 7.62 mm (0.30 INCH) "AS-WELDED" 2219-T87 ALUMINUM CAPABLE OF PASSING σ_Y PROOF AND CYCLED AT 0.85 σ_Y IN RT AIR

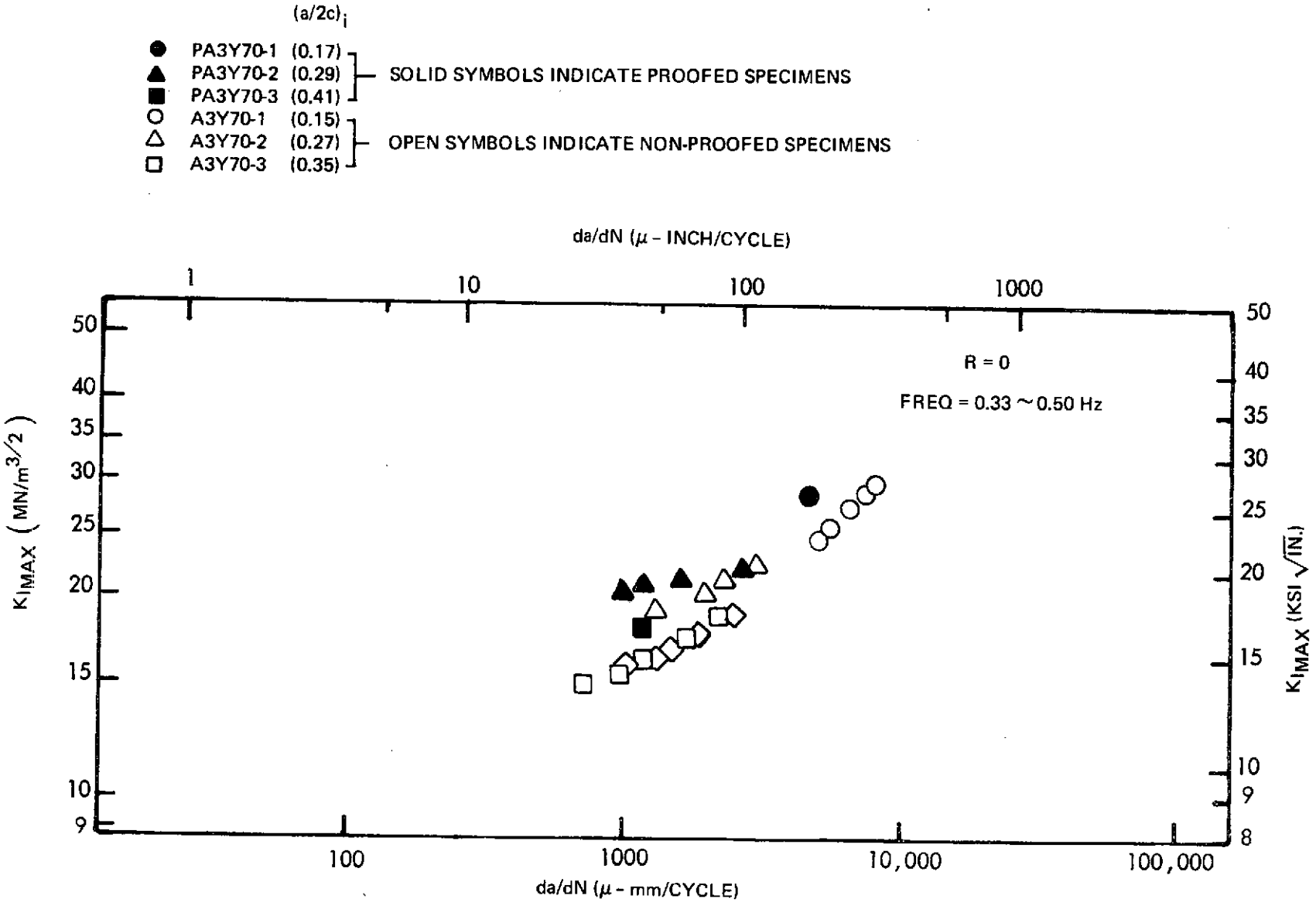

Figure 64: PLOT OF CYCLIC CRACK GROWTH RATES VS. $K_{I_{MAX}}$ FOR 7.62 mm (0.30 INCH) "AS-WELDED" 2219-T87 ALUMINUM CAPABLE OF PASSING σ_Y PROOF AND CYCLED AT 0.70 σ_Y IN RT AIR

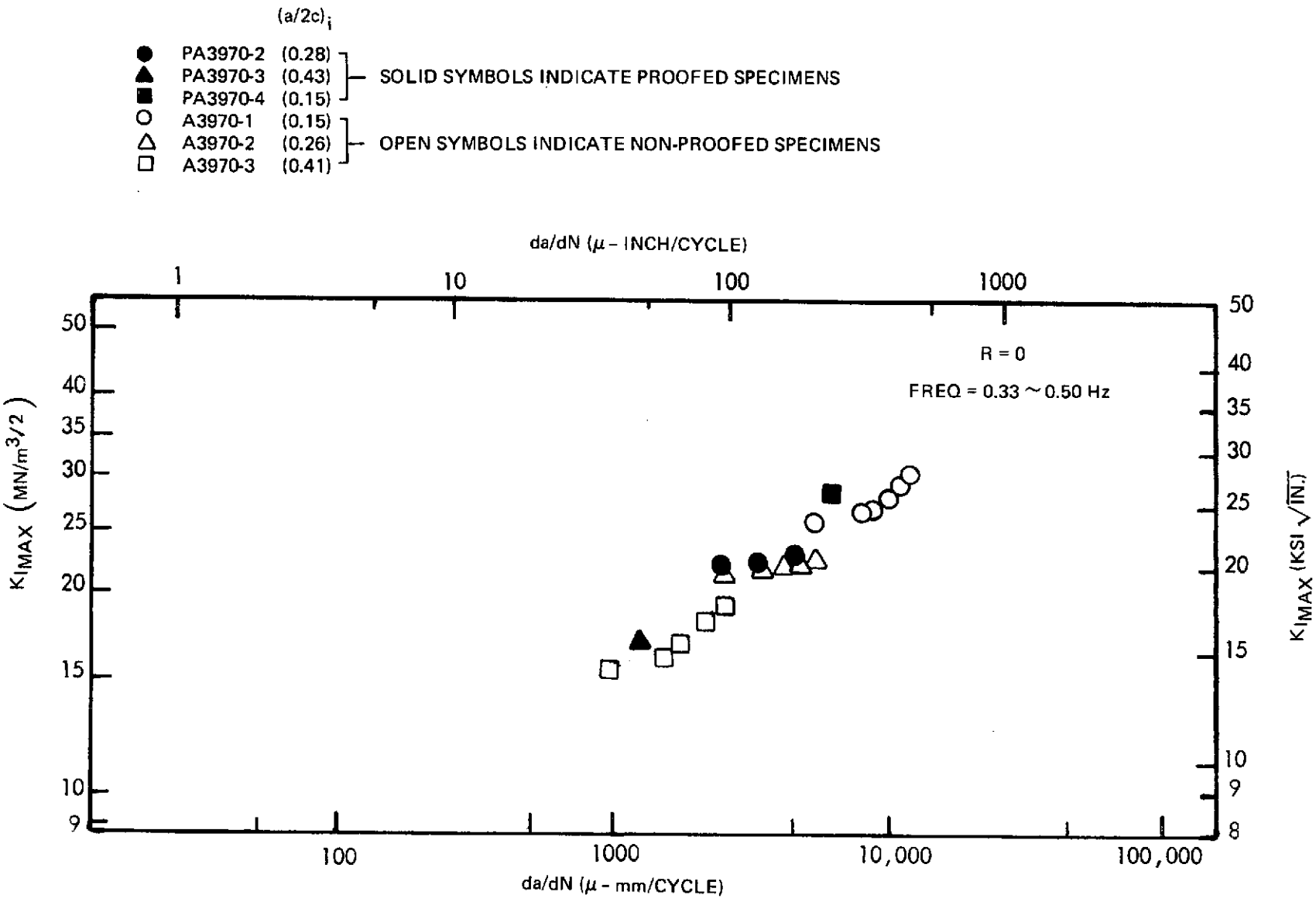

Figure 65: PLOT OF CYCLIC CRACK GROWTH RATES VS. $K_{I_{MAX}}$ FOR 7.62 mm (0.30 INCH) "AS-WELDED" 2219-T87 ALUMINUM CAPABLE OF PASSING 0.9σ_Y PROOF AND CYCLED AT 0.70 σ_Y IN RT AIR

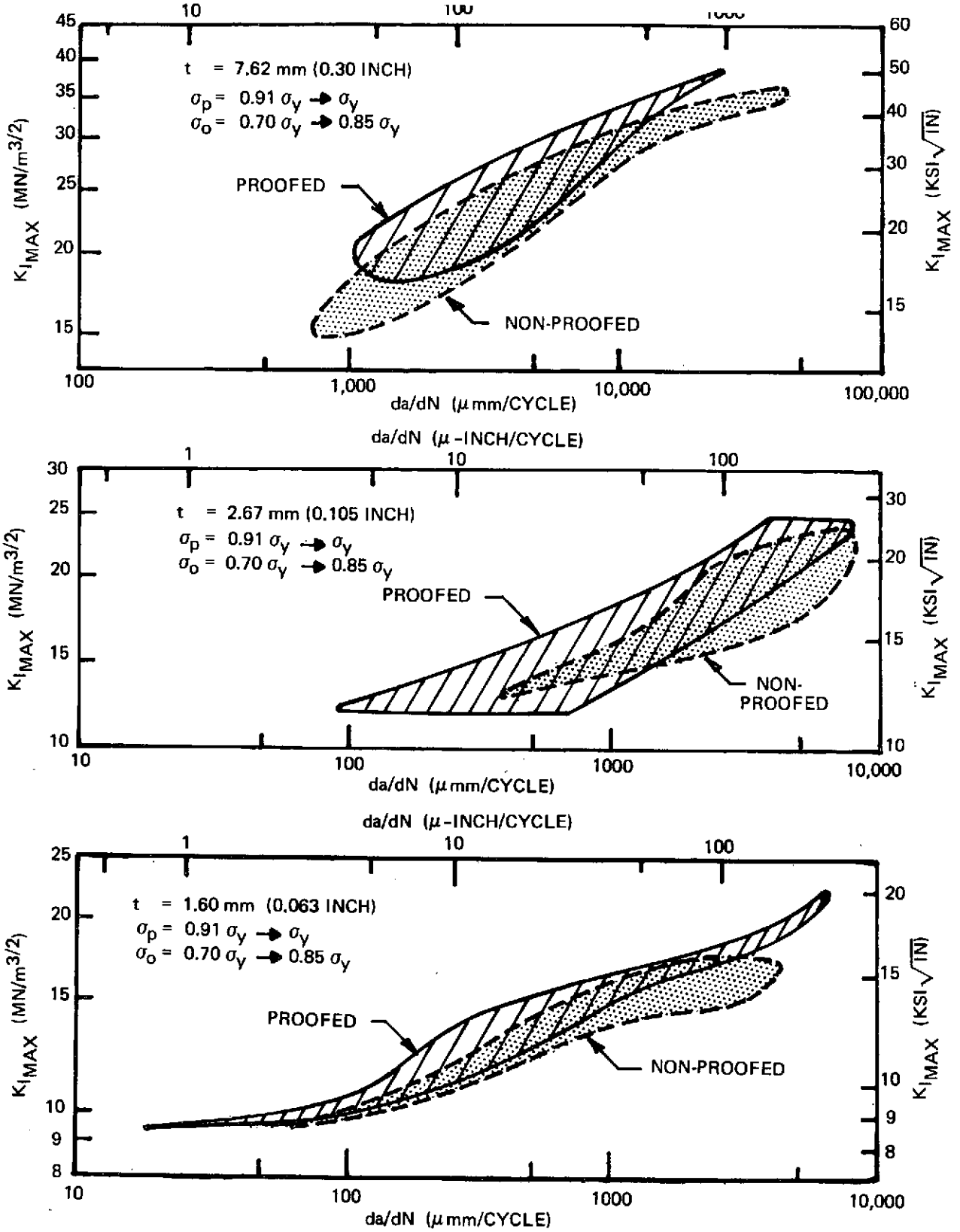

Figure 66: *da/dN VS. $K_{I_{MAX}}$ SHOWING EFFECT OF PROOF TEST ON CYCLIC CRACK GROWTH RATES FOR "AS-WELDED" 2219-T87 ALUMINUM IN RT AIR*

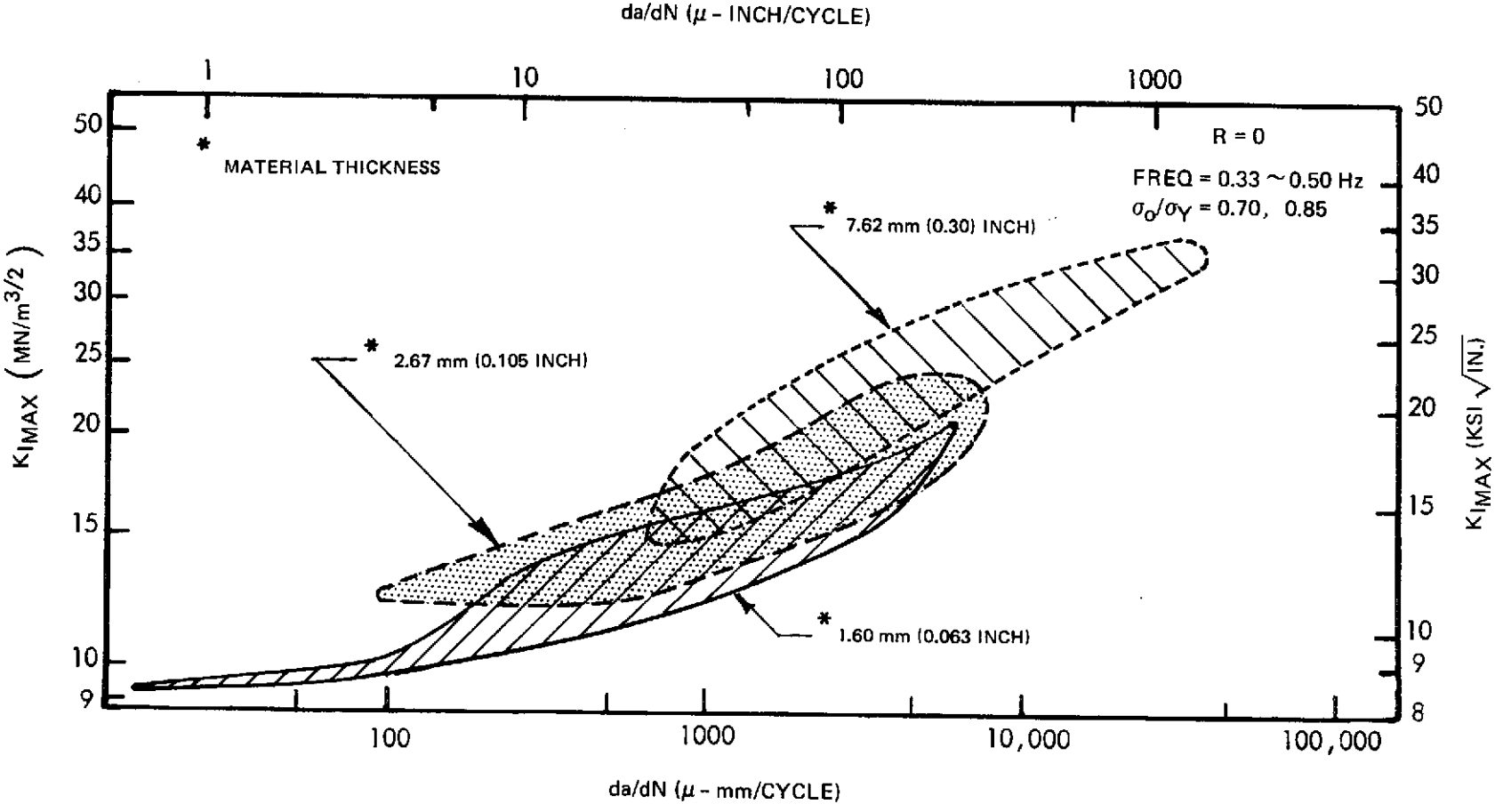

Figure 67: *da/dN VS. K_{IMAX} SHOWING COMPARISON OF CYCLIC CRACK RATES FOR "AS-WELDED" 2219-T87 ALUMINUM IN RT AIR*

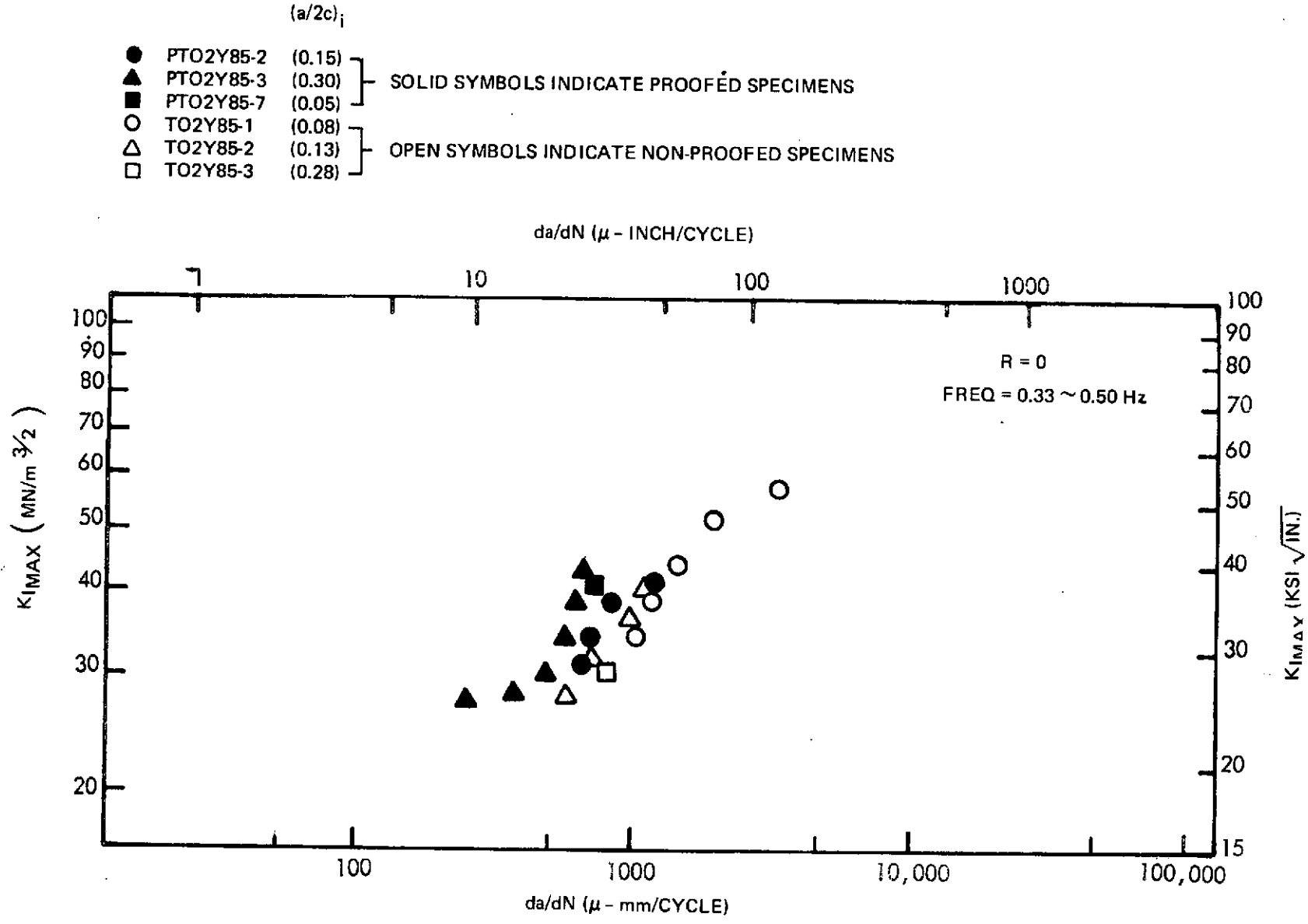

Figure 68: PLOT OF CYCLIC CRACK GROWTH RATES VS. $K_{I_{MAX}}$ FOR 0.51 mm (0.020 INCH) "AS-WELDED" 6AL-4V STA TITANIUM CAPABLE OF PASSING σ_Y PROOF AND CYCLED AT 0.85 σ_Y IN RT AIR

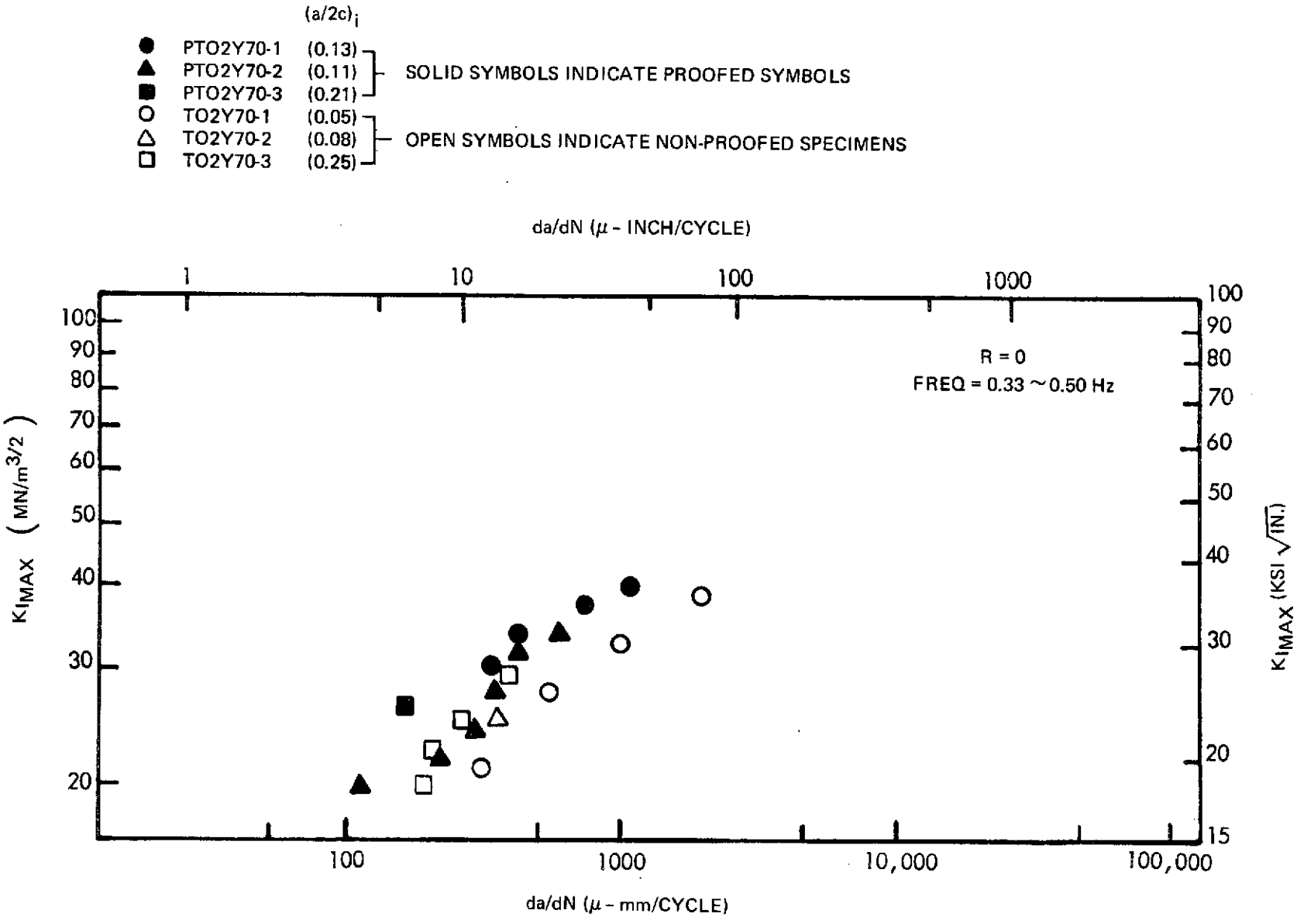

Figure 69: PLOTS OF CYCLIC CRACK GROWTH RATES FOR VS. $K_{I_{MAX}}$ FOR 0.51 mm (0.020 INCH) "AS-WELDED" 6AL-4V STA TITANIUM CAPABLE OF PASSING σ_Y PROOF AND CYCLED AT 0.70 σ_Y IN RT AIR

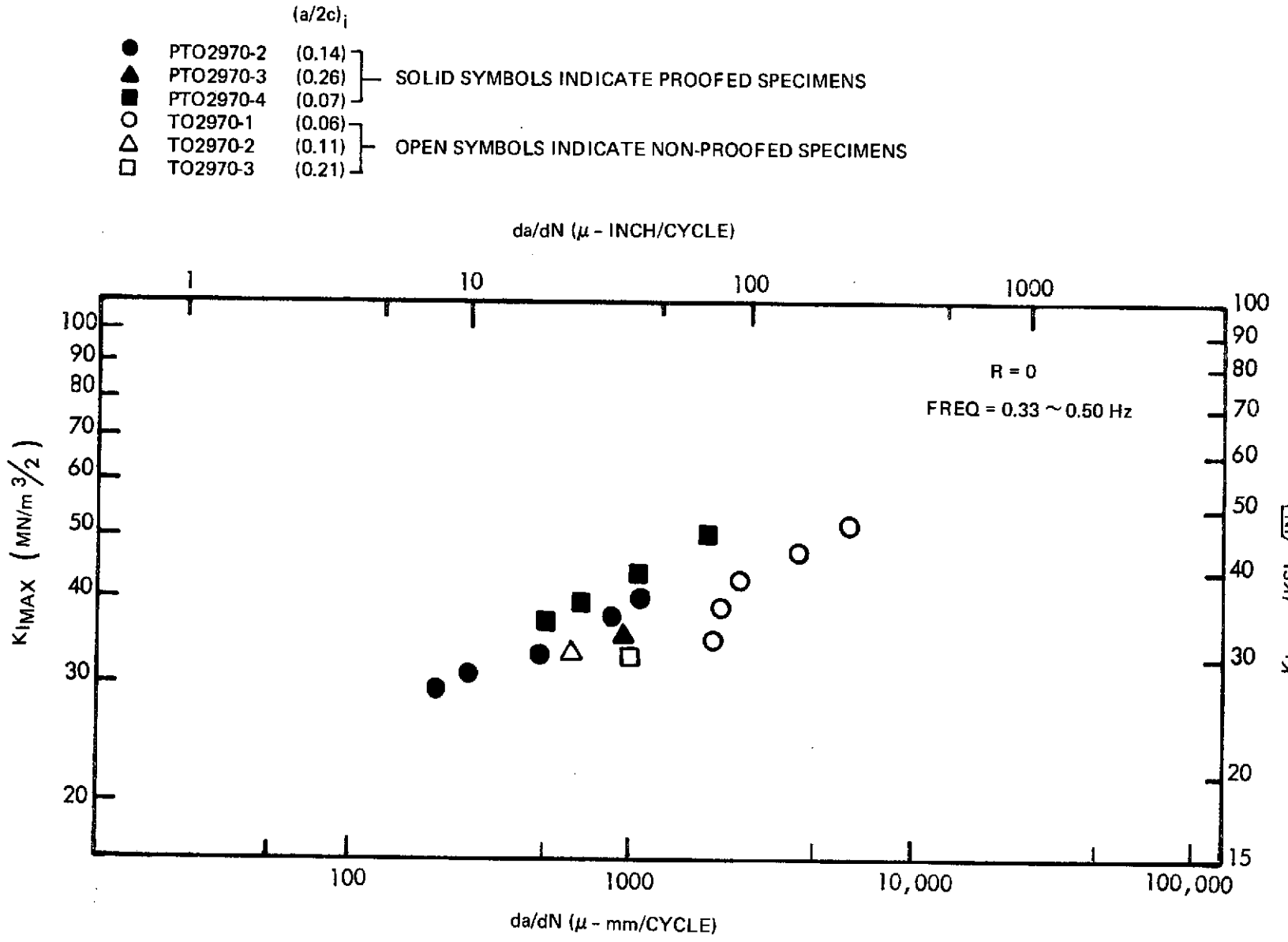

Figure 70: PLOT OF CYCLIC CRACK GROWTH RATES VS. $K_{I\,MAX}$ FOR 0.51 mm (0.020 INCH) "AS-WELDED" 6AL-4V STA TITANIUM CAPABLE OF PASSING 0.91 σ_Y PROOF AND CYCLED AT 0.70 σ_Y IN RT AIR

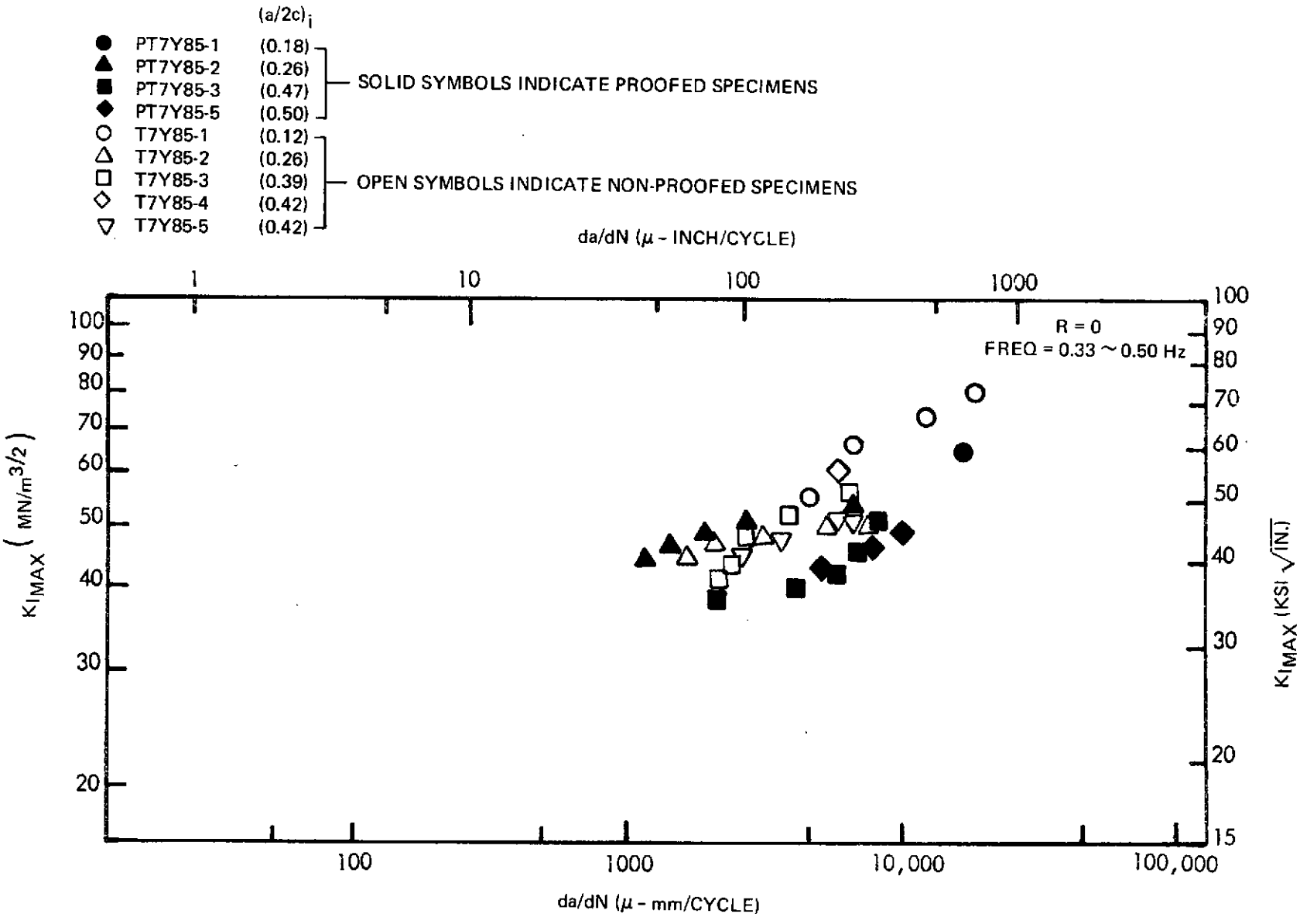

Figure 71: PLOT OF CYCLIC CRACK GROWTH RATES VS. $K_{I_{MAX}}$ FOR 1.78 mm (0.070 INCH) "AS-WELDED" 6AL-4V STA TITANIUM CAPABLE OF PASSING σ_Y PROOF AND CYCLED AT 0.85 σ_Y IN RT AIR

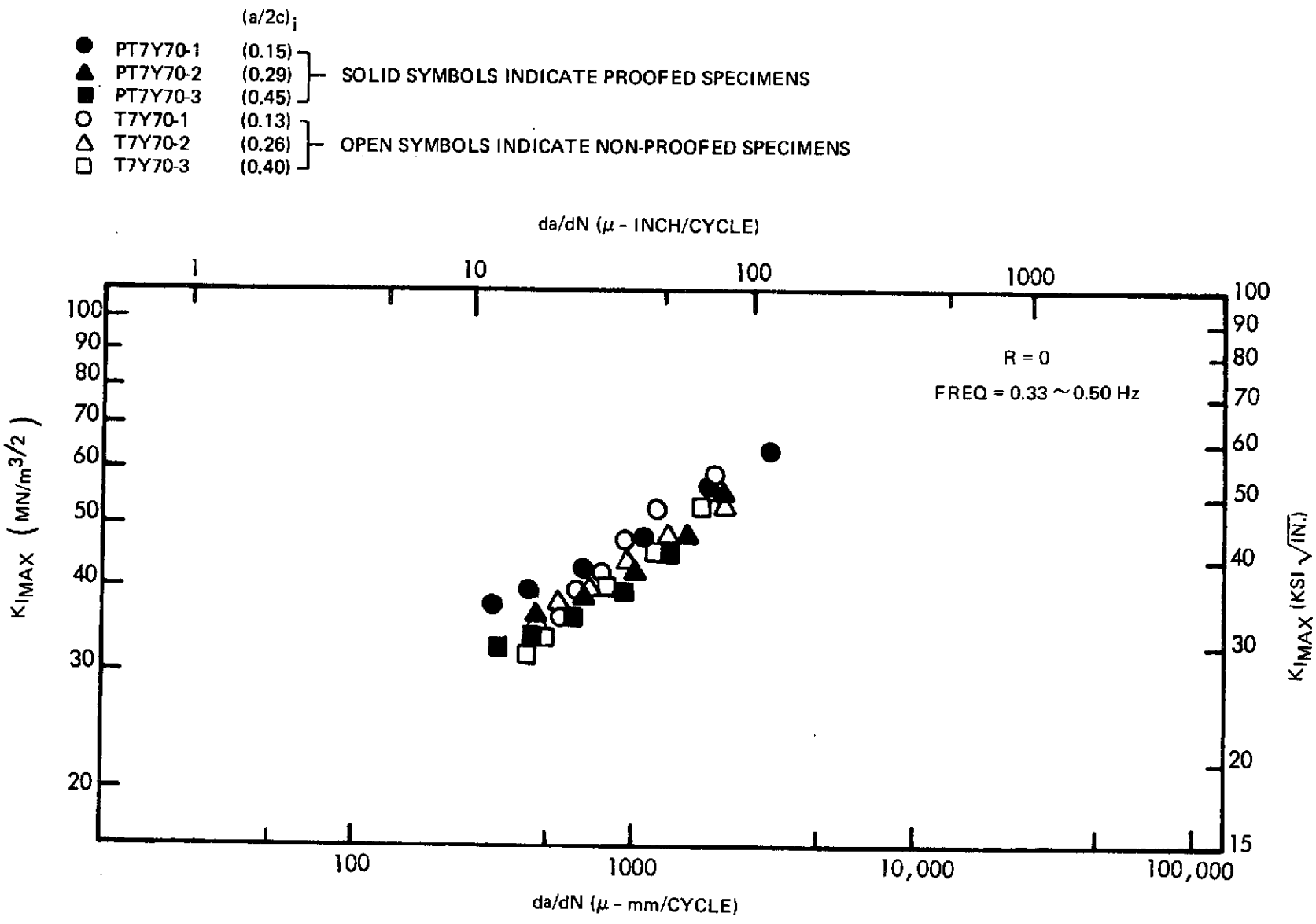

Figure 72: PLOT OF CYCLIC CRACK GROWTH RATES VS. $K_{I_{MAX}}$ FOR 1.78 mm (0.070 INCH) "AS-WELDED" 6AL-4V STA TITANIUM CAPABLE OF PASSING σ_Y PROOF AND CYCLED AT 0.70 σ_Y IN RT AIR

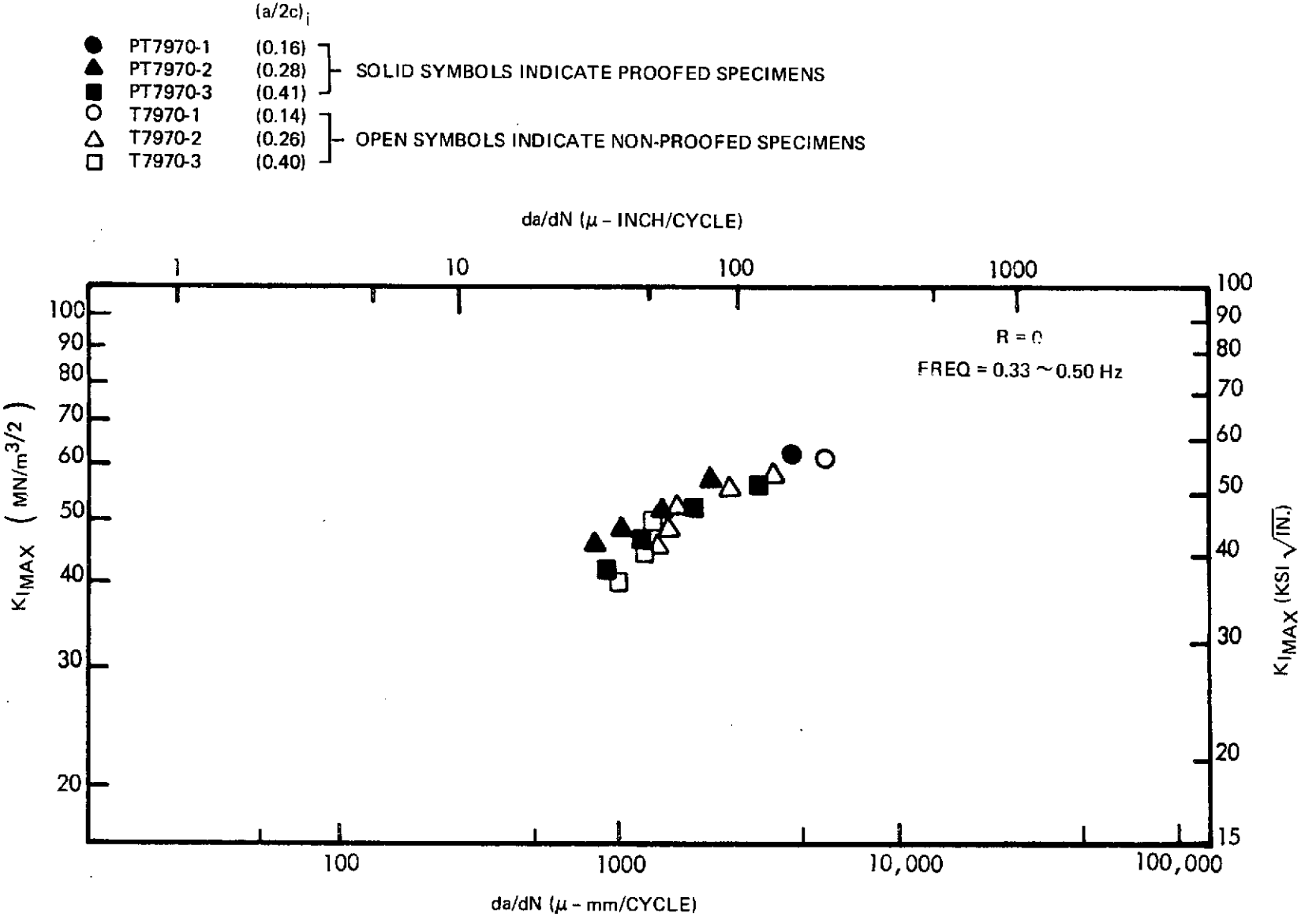

Figure 73: PLOT OF CYCLIC CRACK GROWTH RATES VS. $K_{I_{MAX}}$ FOR 1.78 mm (0.070 INCH) "AS-WELDED" 6AL-4V STA TITANIUM CAPABLE OF PASSING 0.91 σ_Y PROOF AND CYCLED AT 0.70 σ_Y IN RT AIR

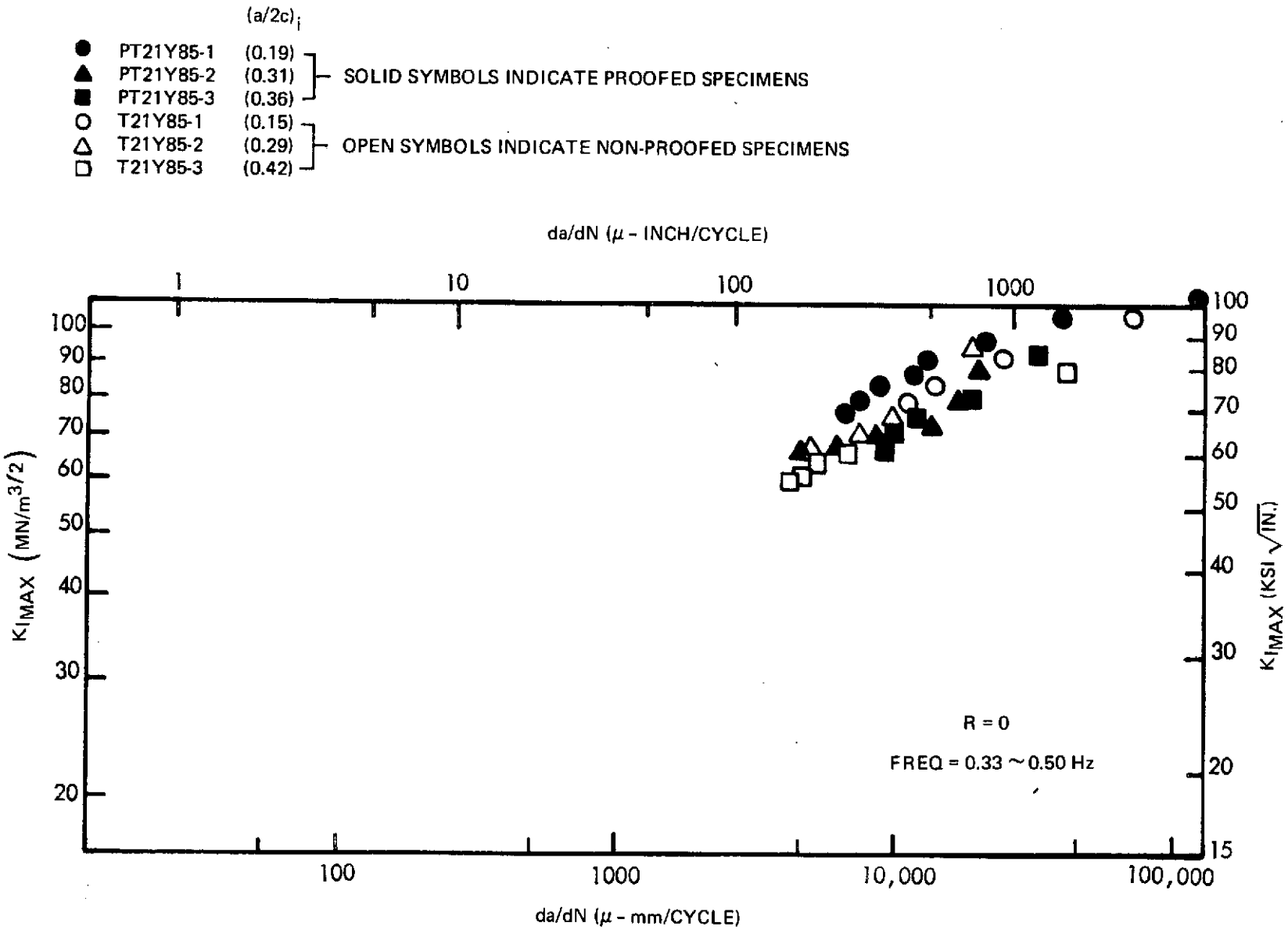

Figure 74: PLOT OF CYCLIC CRACK GROWTH RATES VS. $K_{I_{MAX}}$ FOR 5.33 mm (0.21 INCH) "AS-WELDED" 6AL-4V STA TITANIUM CAPABLE OF PASSING σ_Y PROOF AND CYCLED AT 0.85 σ_Y IN RT AIR

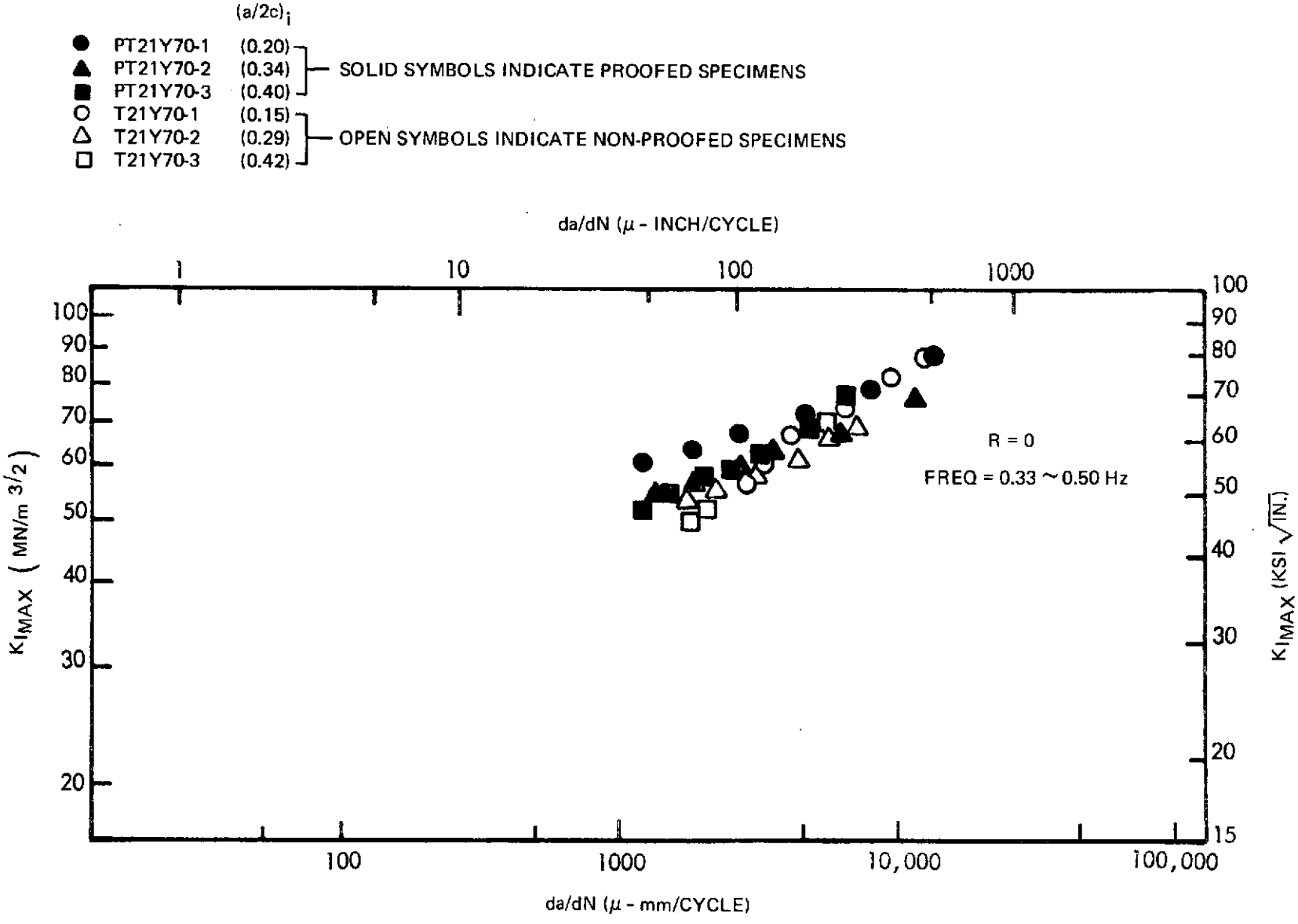

Figure 75: PLOT OF CYCLIC CRACK GROWTH RATES VS. $K_{I_{MAX}}$ FOR 5.33 mm (0.21 INCH) "AS-WELDED" 6AL-4V STA TITANIUM CAPABLE OF PASSING σ_Y PROOF AND CYCLED AT 0.70 σ_Y IN RT AIR

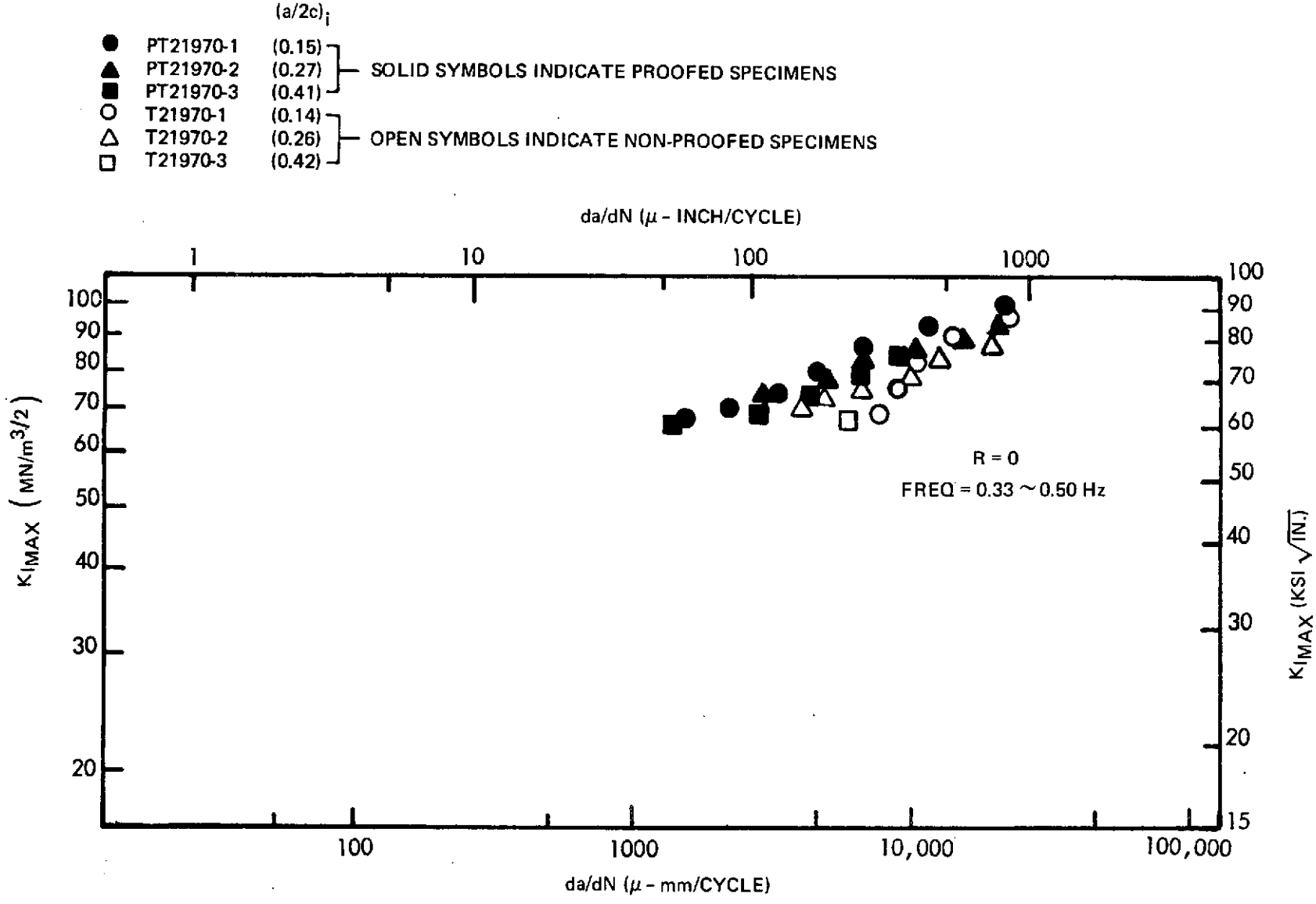

Figure 76: PLOT OF CYCLIC CRACK GROWTH RATES VS. $K_{I_{MAX}}$ FOR 5.33 mm (0.21 INCH) "AS-WELDED" 6AL-4V STA TITANIUM CAPABLE OF PASSING 0.91 σ_Y PROOF AND CYCLED AT 0.70 σ_Y IN RT AIR

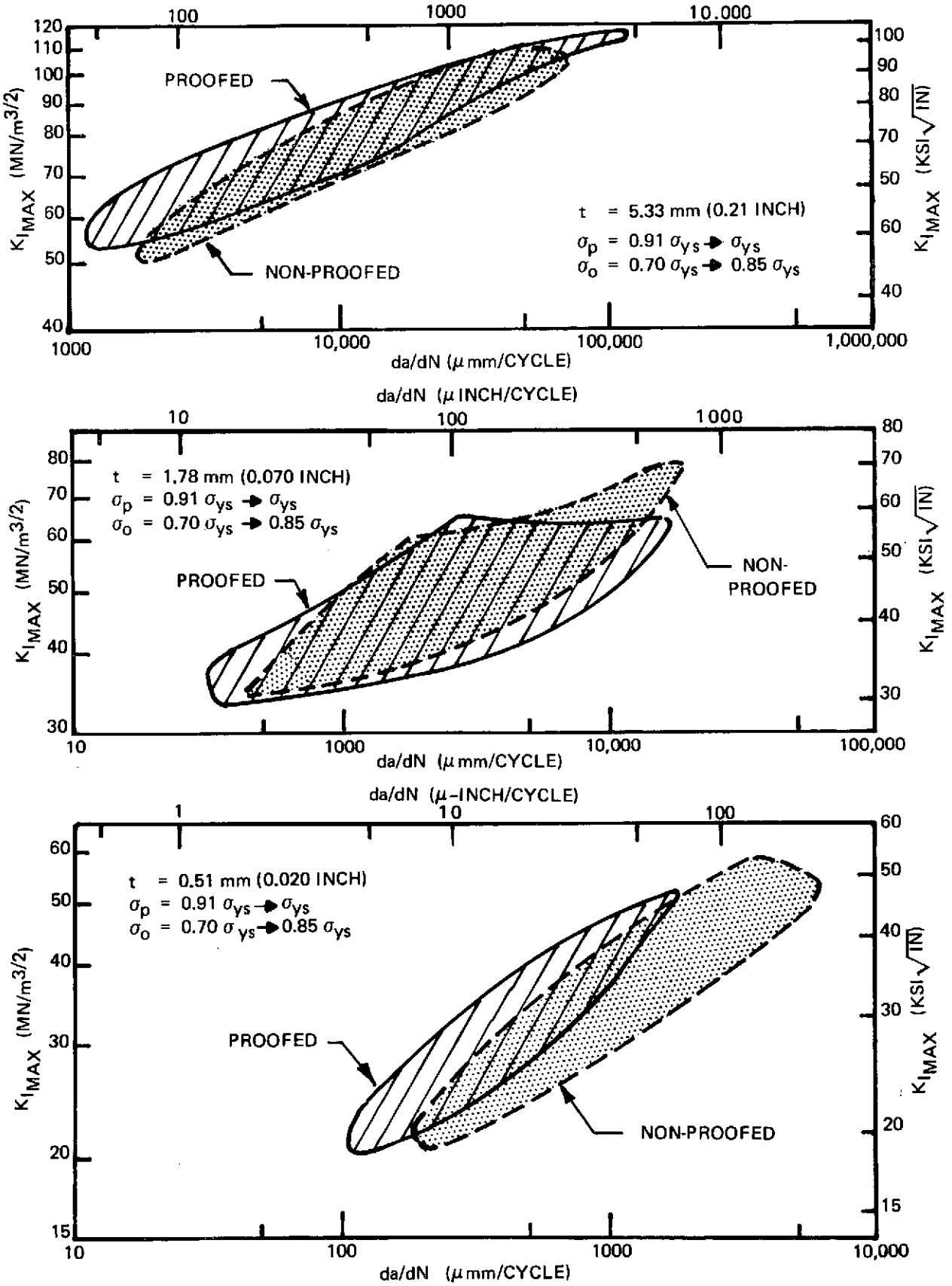

Figure 77: da/dN VS. $K_{I_{MAX}}$ SHOWING EFFECT OF PROOF TEST ON CYCLIC CRACK GROWTH RATES FOR "AS-WELDED" 6AI-4V STA TITANIUM IN RT AIR

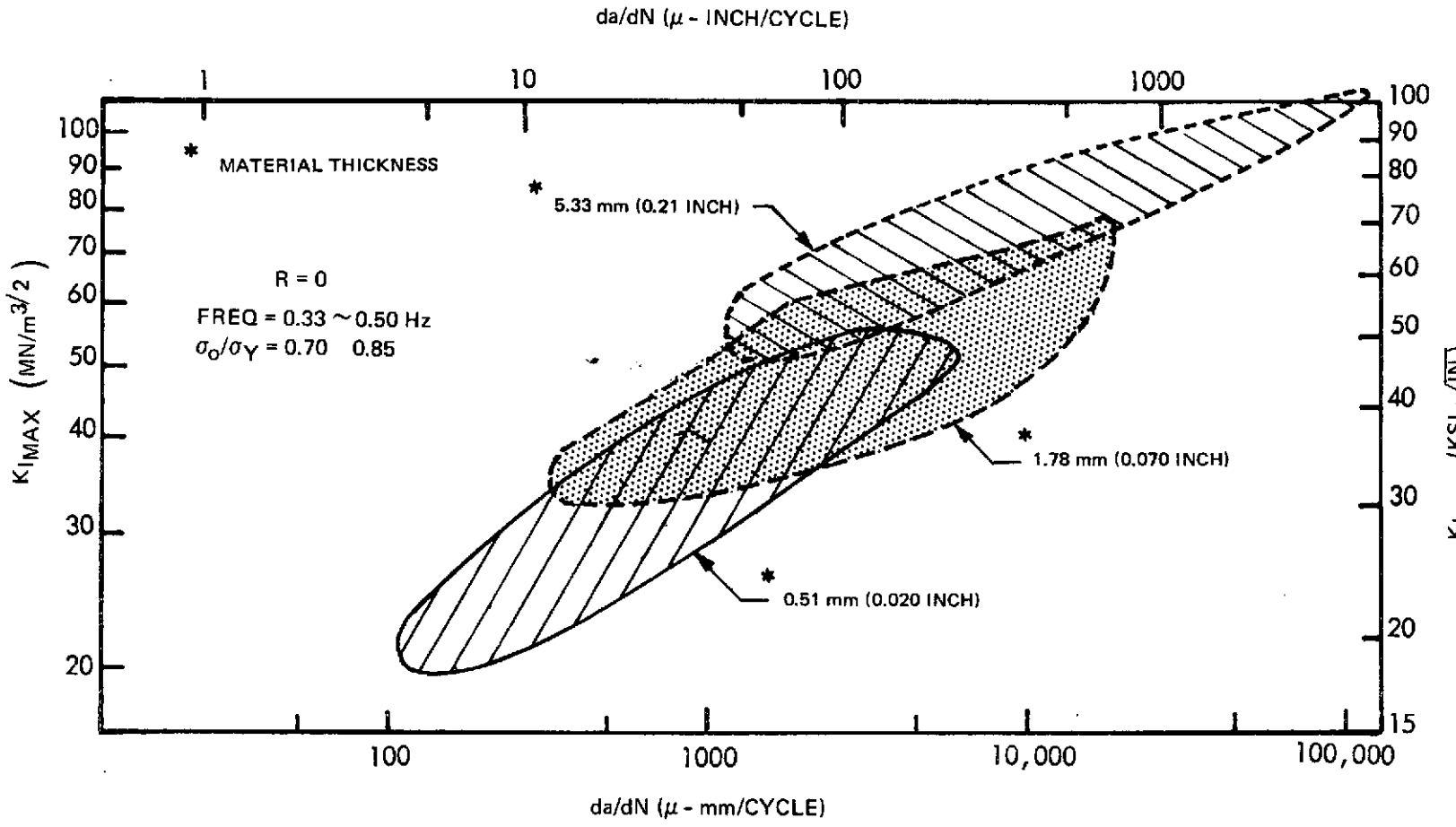

Figure 78: *da/dN VS. $K_{I_{MAX}}$ SHOWING COMPARISON OF CYCLIC CRACK RATES FOR "AS-WELDED" 6AI-4V STA TITANIUM IN RT AIR*

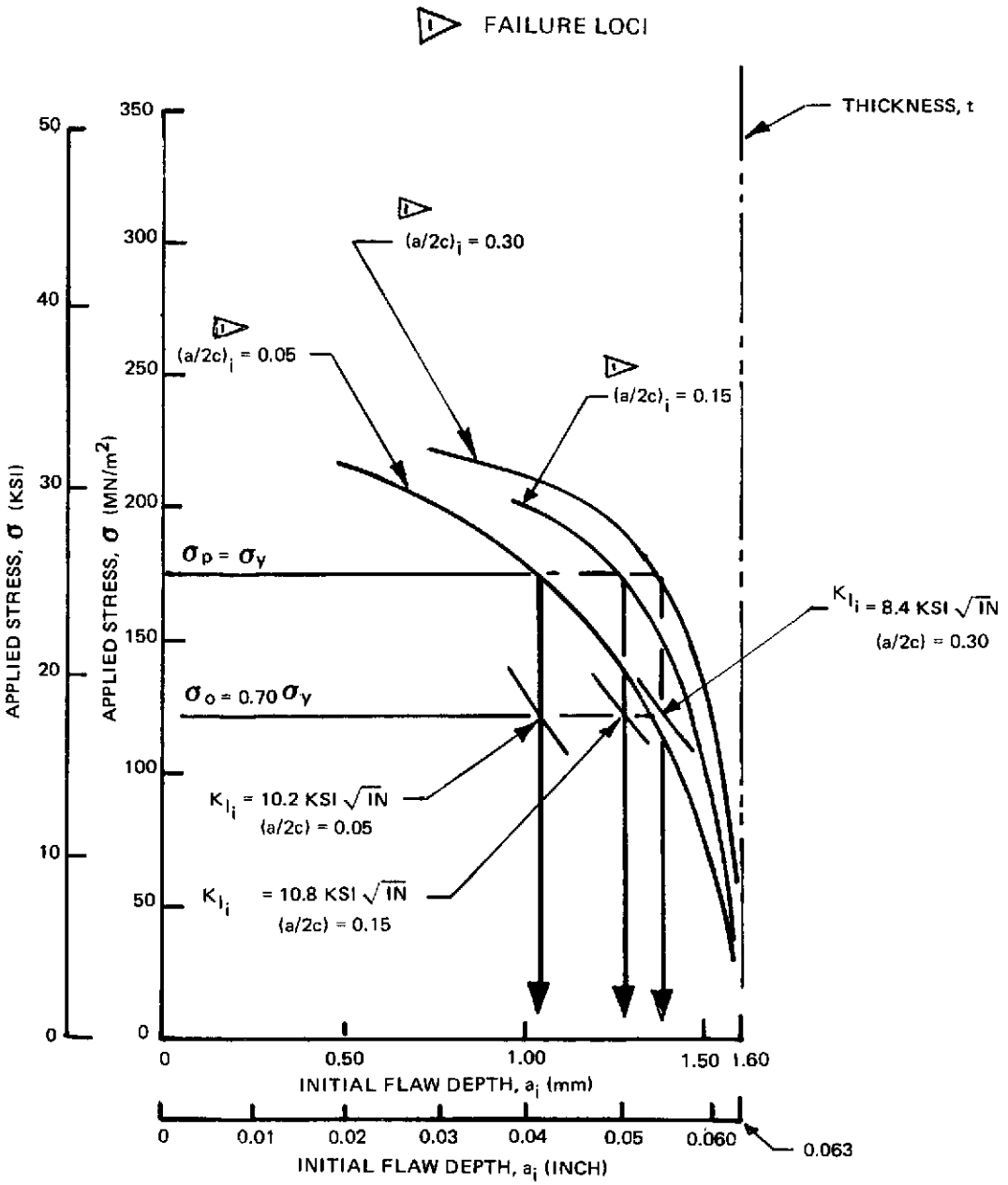

Figure 79: PLOT OF APPLIED STRESS VS. INITIAL FLAW DEPTH FOR 1.60 mm (0.063 INCH) "AS-WELDED" 2219-T87 ALUMINUM AT RT

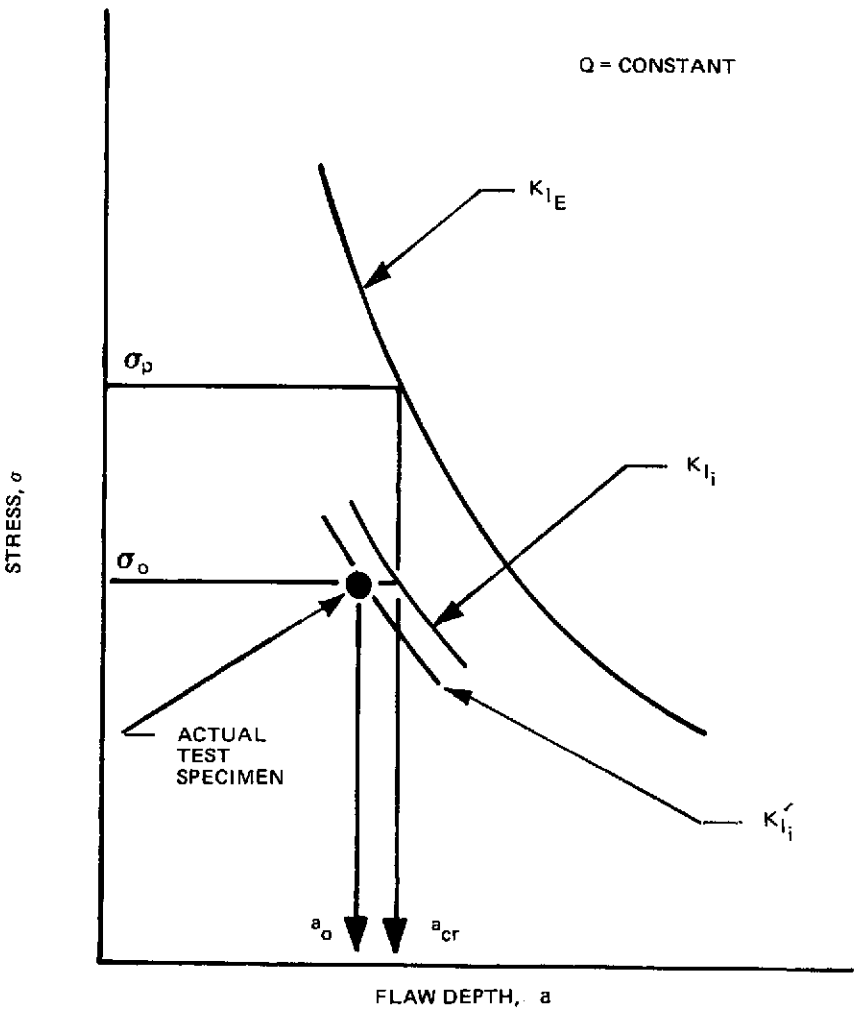

$$\frac{K_{I_i}}{K_{I_E}} = \frac{1.1\ \sigma_o\ (\pi\ a_{cr})^{1/2}}{1.1\ \sigma_p\ (\pi\ a_{cr})^{1/2}} = \frac{\sigma_o}{\sigma_p}$$

$$\frac{K_{I_i}'}{K_{I_E}} = \frac{1.1\ \sigma_o\ (\pi\ a_o)^{1/2}}{1.1\ \sigma_p\ (\pi\ a_{cr})^{1/2}} = \left(\frac{\sigma_o}{\sigma_p}\right)\left(\frac{a_o}{a_{cr}}\right)^{1/2} = KR$$

Figure 80: STRESS INTENSITY RATIO RELATIONSHIPS

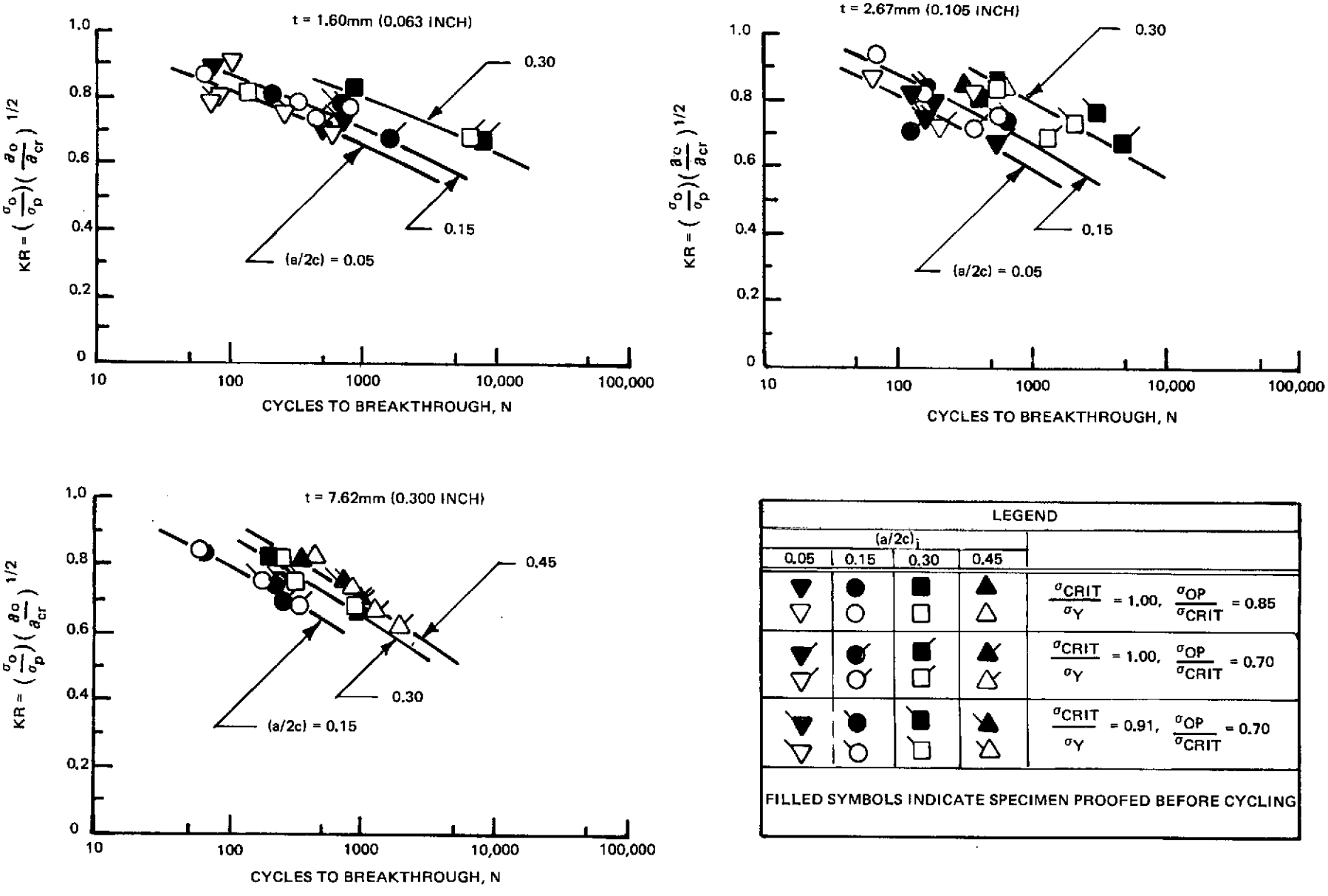

Figure 81: PLOT OF CYCLIC LIFE VS. KR OF "AS-WELDED" 2219-T87 ALUMINUM AT RT

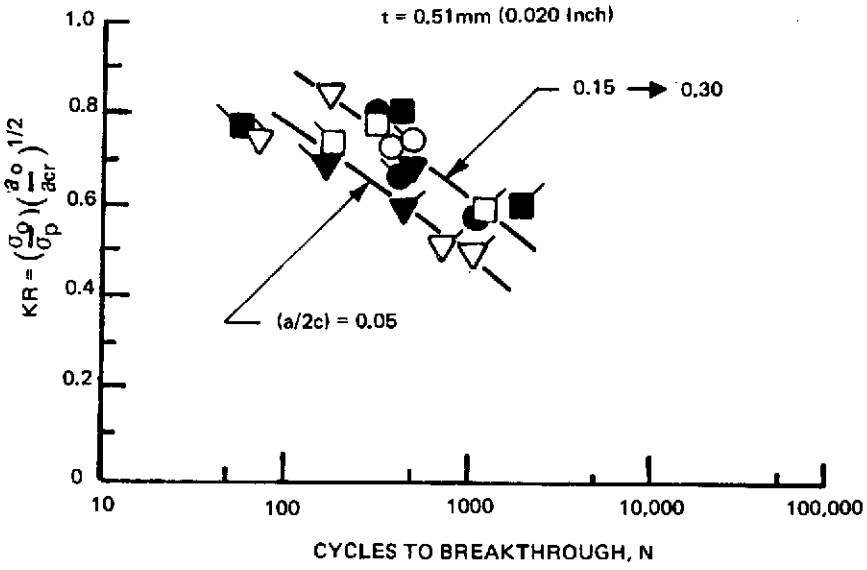

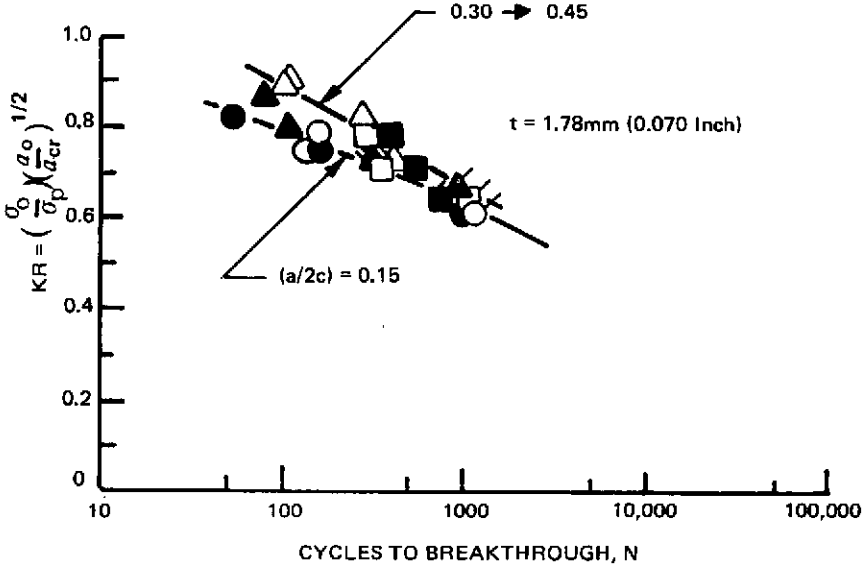

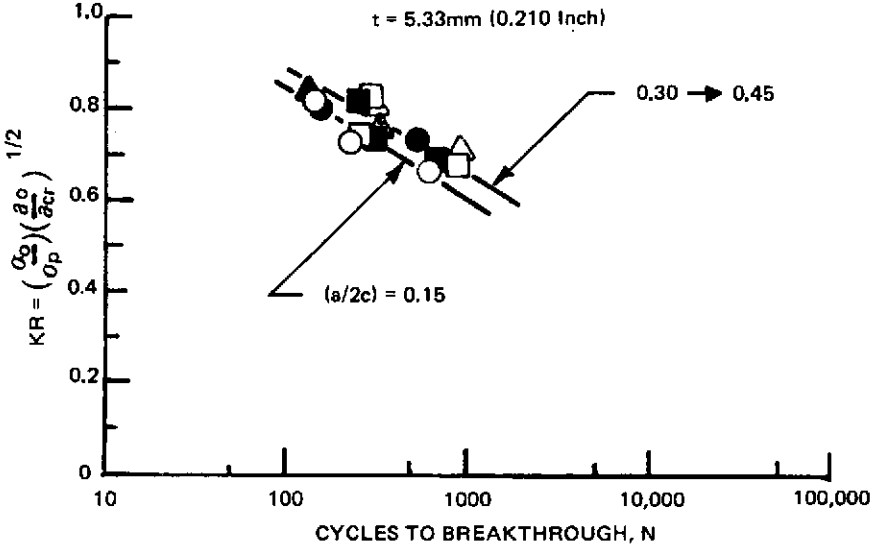

LEGEND				
$(a/2c)_i$				
0.07	0.15	0.30	0.45	
▼ ▽	● ○	■ □	▲ △	$\frac{\sigma_{CRIT}}{\sigma_Y} = 1.00$, $\frac{\sigma_{OP}}{\sigma_{CRIT}} = 0.85$
▼ ▽	● ○	■ □	▲ △	$\frac{\sigma_{CRIT}}{\sigma_Y} = 1.00$, $\frac{\sigma_{OP}}{\sigma_{CRIT}} = 0.70$
▼ ▽	● ○	■ □	▲ △	$\frac{\sigma_{CRIT}}{\sigma_Y} = 0.91$, $\frac{\sigma_{OP}}{\sigma_{CRIT}} = 0.70$
FILLED SYMBOLS INDICATE SPECIMEN PROOFED BEFORE CYCLING				

Figure 82: PLOT OF CYCLIC LIFE VS. KR OF "AS-WELDED" 6AI-4V STA TITANIUM AT RT

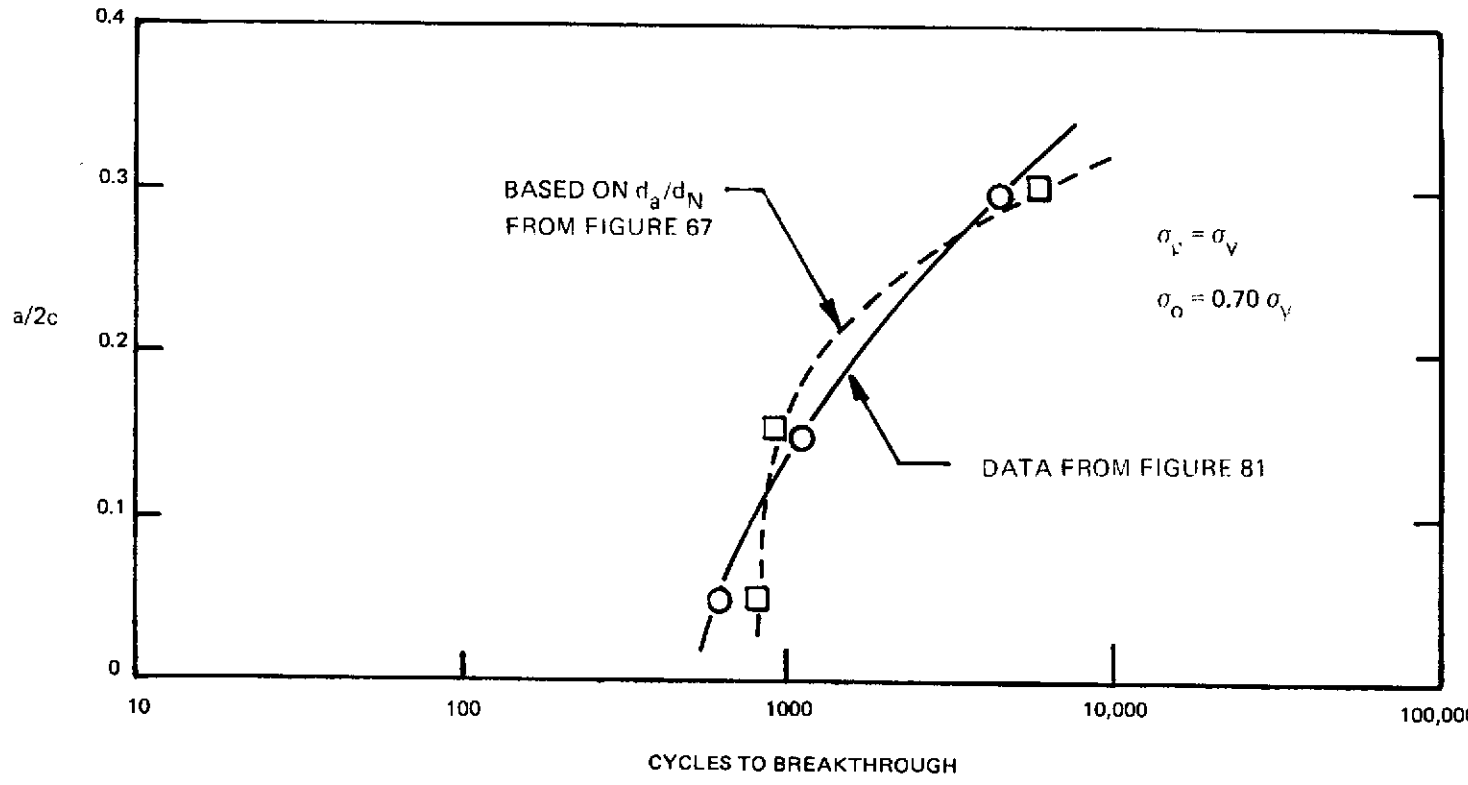

Figure 83: EFFECT OF FLAW SHAPE ON CYCLIC LIFE FOR 1.60 mm (0.063 INCH) "AS-WELDED" 2219-T87 ALUMINUM AT RT

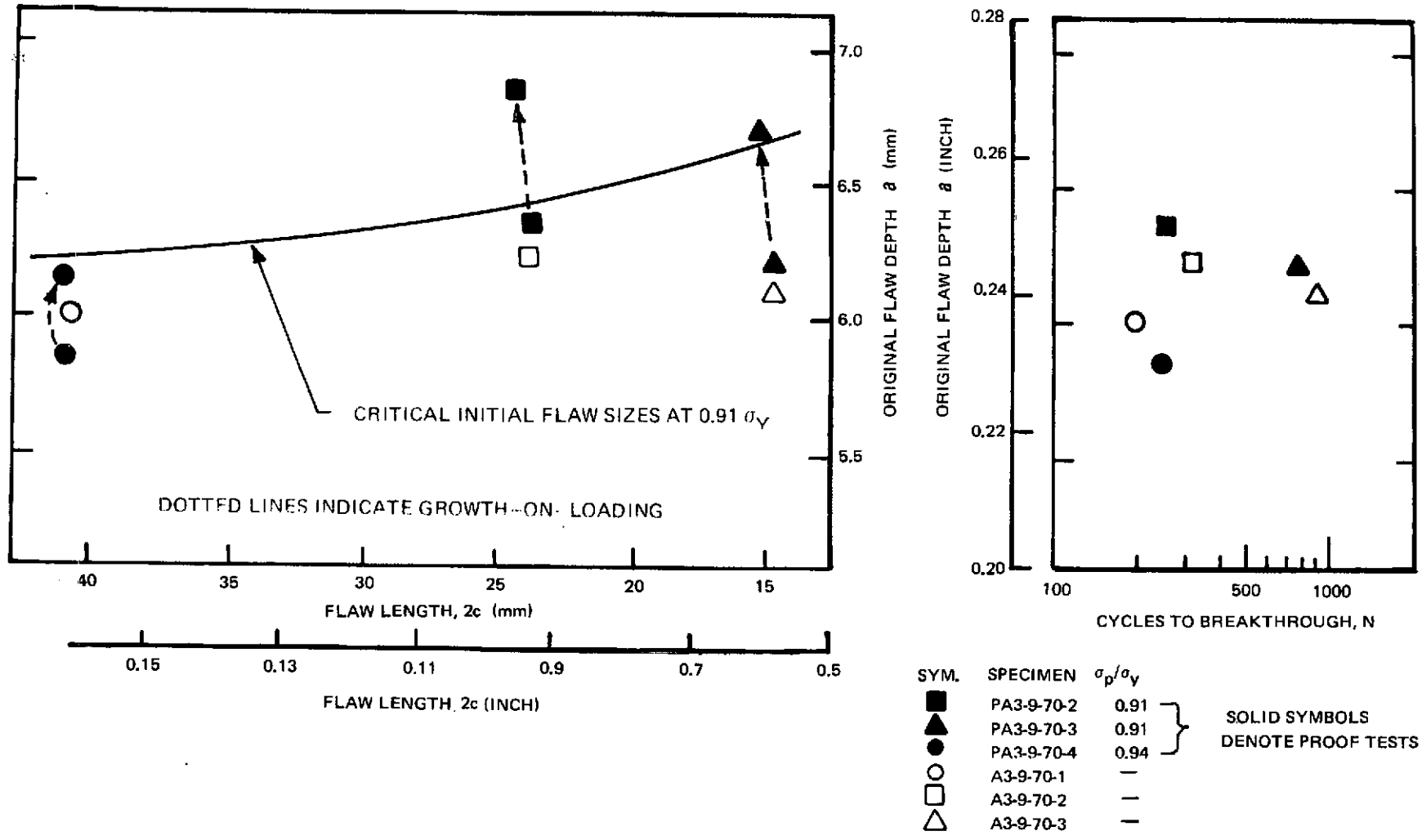

Figure 84: EFFECT OF FLAW SHAPE ON CYCLES TO BREAKTHROUGH, 7.62 mm (0.300 INCH) 2219 ALUMINUM WELDS PASSING 0.91 σ_Y PROOF AND CYCLED AT 0.70 σ_Y, R = 0 IN ROOM TEMPERATURE AIR

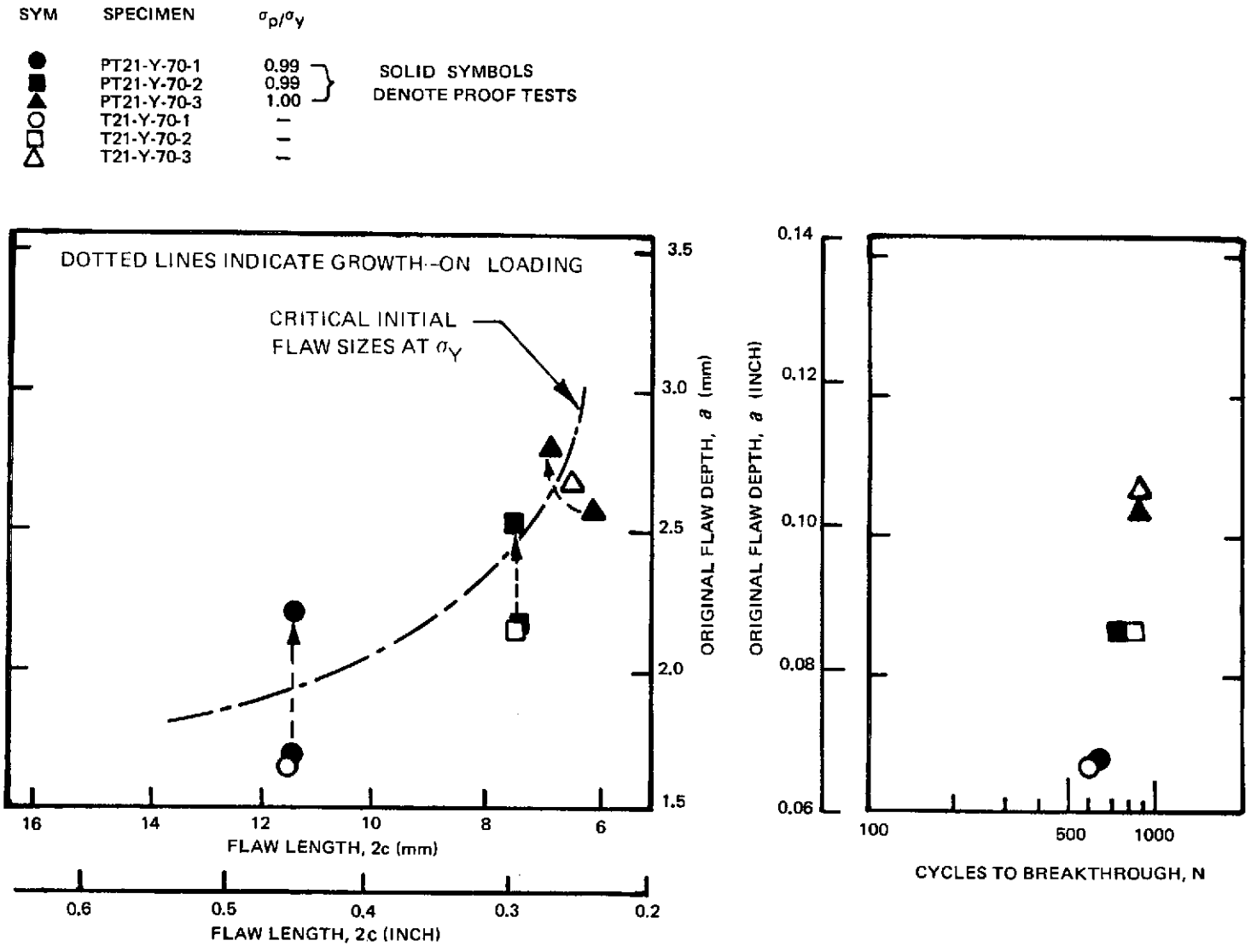

Figure 85: EFFECT OF FLAW SHAPE ON CYCLES TO BREAKTHROUGH 5.33 mm (0.21 INCH) 6AL-4V STA TITANIUM WELDS PASSING σ_Y PROOF AND CYCLED AT 0.70 σ_Y, R = 0 IN ROOM TEMPERATURE AIR

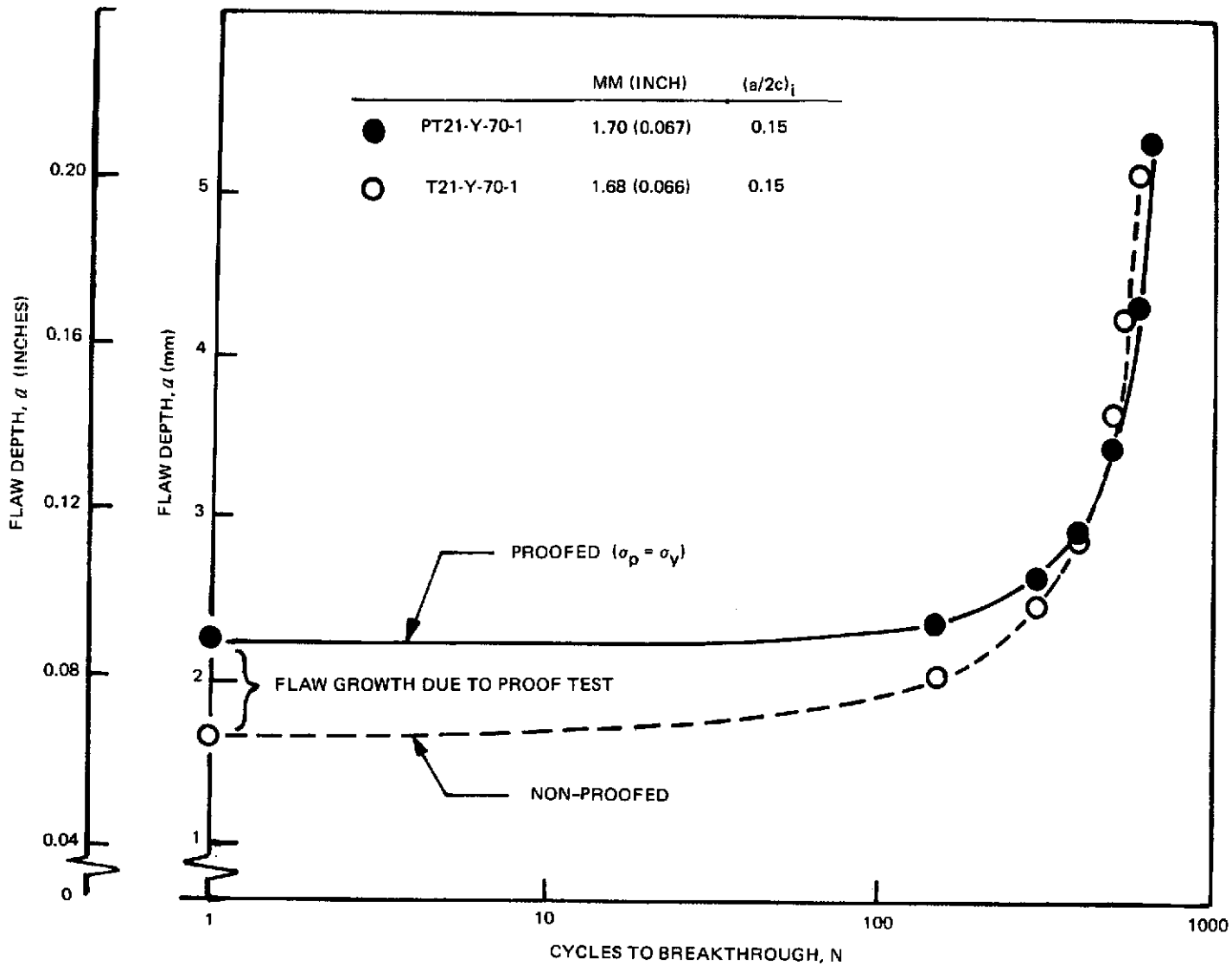

Figure 86: FLAW DEPTH VERSUS CYCLES FOR PROOFED AND NON-PROOFED 5.33 mm (0.21 INCH) "AS-WELDED" 6AL-4V STA TITANIUM CYCLED AT $\sigma_0 = 0.7\,\sigma_Y$ IN RT AIR

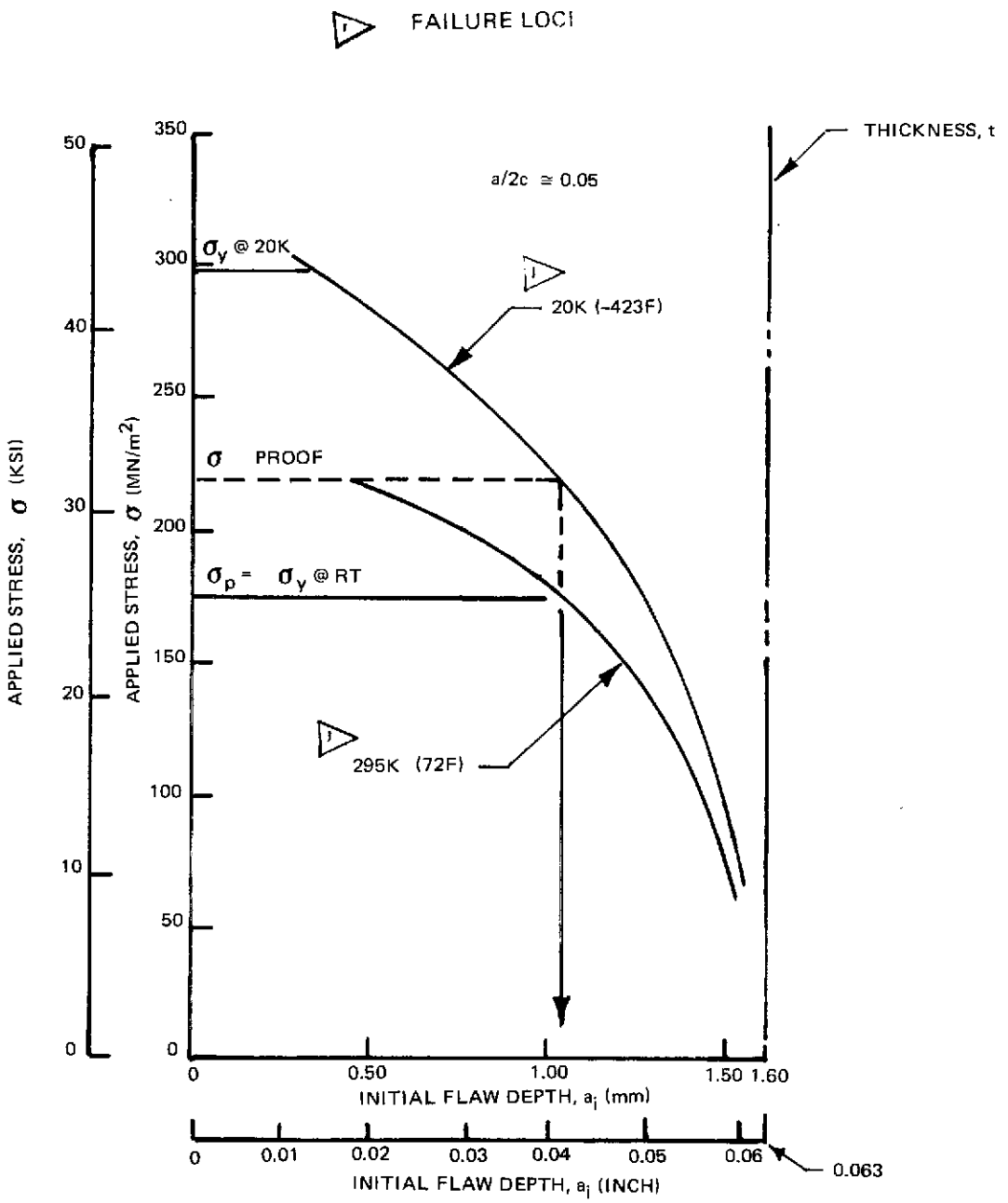

Figure 87. PLOT OF APPLIED STRESS VERSUS INITIAL FLAW DEPTH FOR 1.60 mm (0.063 INCH) "AS-WELDED" 2219-T87 ALUMINUM AT RT AND 20K (-423 ^{0}F)

Table 1: ***CHEMICAL COMPOSITION OF 2219-T87 ALUMINUM (% by WT.)***
AS DETERMINED BY BOEING AEROSPACE COMPANY TESTS

ELEMENT	3.18 mm (0.125 INCH) SHEET ALCOA HEAT 720471	12.7 mm (0.50 INCH) PLATE ALCOA HEAT 613941
MANGANESE	0.28	0.30
VANADIUM	0.09	0.09
SILICON	0.11	0.12
COPPER	6.09	5.95
ZINC	0.09	0.09
TITANIUM	0.08	0.05
IRON	0.22	0.25
MAGNESIUM	0.014	0.005
ZIRCONIUM	0.16	0.12
ALUMINUM	BALANCE	BALANCE

Table 2: ***CHEMICAL COMPOSITION OF 2319 ALUMINUM WELD WIRE***
AS DETERMINED BY BOEING AEROSPACE COMPANY TESTS

ELEMENT	% BY WT.
MANGANESE	0.25
VANADIUM	0.07
SILICON	0.15
COPPER	6.00
ZINC	0.05
TITANIUM	0.14
IRON	0.18
MAGNESIUM	0.02
ZIRCONIUM	0.17
ALUMINUM	BALANCE

MFGR: LINDE, HEAT NO. 354031A, 1.57 mm (0.062 IN.) DIA.

PRECEDING PAGE BLANK NOT FILMED

Table 3: ***CHEMICAL COMPOSITION OF TITANIUM 6AI –4V (% BY WT.) AS DETERMINED BY BOEING AEROSPACE COMPANY TESTS***

ELEMENT	2.03 mm (0.080 INCH) SHEET RMI HEAT 304610	6.35 mm (0.250 INCH) PLATE RMI HEAT 304623
ALUMINUM	6.1	6.1
VANADIUM	3.9	3.9
IRON	0.2	0.17
CARBON	0.01	0.02
NICKEL	0.009	0.010
OXYGEN	0.109	0.109
HYDROGEN	37 ppm	38 ppm
TITANIUM	BALANCE	BALANCE

Table 4. ***CHEMICAL COMPOSITION OF 6AI -4V TITANIUM WELD WIRE AS DETERMINED BY BOEING AEROSPACE COMPANY TESTS***

ELEMENT	% BY WT.
ALUMINUM	6.05
VANADIUM	3.61
IRON	0.01
TITANIUM	BALANCE

MFGR; TMCA, HEAT NO. G8080, 1.57 mm (0.062 IN.) DIA.

Table 5: STATIC FRACTURE TESTS – ROOM TEMPERATURE 6Al-4V TITANIUM, COMPARISON OF FLAW LOCATIONS, t = 1.78 mm (0.070 INCH) a/2c = 0.15

SPECIMEN				TEST		FRACTURE DATA										
FLAW LOCATION	NUMBER	GAGE THICKNESS, t mm (INCH)	GAGE WIDTH, w mm (INCH)	DIMPLING GAGE LOCATION FROM CRACK TIP	ENVIRONMENT	FAILURE STRESS, σ_G MN/m^2 (KSI)	DIMPLING STRESS, σ_D MN/m^2 (KSI)	BREAKTHROUGH STRESS, σ_B MN/m^2 (KSI)	INITIAL FLAW DEPTH, a_i mm (INCH)	INITIAL FLAW LENGTH, $(2c)_i$ mm (INCH)	$\frac{\text{INITIAL FLAW DEPTH}}{\text{GAGE THICKNESS}}$, (a/t)	$\frac{\text{INITIAL FLAW DEPTH}}{\text{INITIAL FLAW LENGTH}}$, $(a/2c)_i$	σ_B/σ_Y [1]	σ_G/σ_Y [1]	IRWIN'S APPARENT K AT BREAKTHROUGH MN/m$^{3/2}$ (KSI$\sqrt{\text{IN}}$)
BASE METAL	STR-8-1-BM	1.79 (0.0703)	4.44 (1.7477)	—	AIR @ 295°K (72°F)	820.5 (119.0)	[2]	—	1.22 (0.048)	8.38 (0.330)	0.683	0.145	—	0.79	54.3 (49.4)
HAZ	STR-8-1-HAZ	1.66 (0.0653)	4.43 (1.7428)	—		834.3 (121.0)	[2]	—	1.22 (0.048)	8.31 (0.327)	0.735	0.147	—	0.81	55.3 (50.3)
FUSION LINE	STR-8-1-FL	1.78 (0.0699)	4.45 (1.7503)	—		871.5 (126.4)	[2]	—	1.22 (0.048)	8.20 (0.323)	0.687	0.149	—	0.84	58.0 (52.8)
℄ (REF.)	STR-8-1-1	1.81 (0.0712)	63.41 (2.4965)	37°		991.5 (143.8)	785.3 (113.9)	—	0.84 (0.033)	5.92 (0.233)	0.463	0.142	—	0.96	56.4 (51.3)
℄ (REF.)	STR-8-1-2	1.84 (0.0725)	44.63 (1.7570)	43°		795.7 (115.4)	503.3 (73.0)	773.6 (112.2)	1.32 (0.052)	8.38 (0.330)	0.717	0.158	0.75	0.77	52.3 (47.6)
℄ (REF.)	STR-8-1-3	1.74 (0.0686)	44.67 (1.7588)	48°		737.1 (106.9)	319.9 (46.4)	599.9 (87.0)	1.45 (0.057)	10.54 (0.415)	0.831	0.137	0.58	0.71	42.4 (38.6)
℄ (REF.)	STR-8-1-4	1.70 (0.0670)	44.44 (1.7496)	27°		829.5 (120.3)	639.9 (92.8)	—	1.09 (0.043)	7.75 (0.305)	0.642	0.141	—	0.80	52.3 (47.6)

[1] σ_Y = 1035 MN/m^2 (150.1 KSI)

[2] NOT INSTRUMENTED FOR DIMPLING

Table 6: ROOM TEMPERATURE TENSILE PROPERTIES OF 2219-T87 ALUMINUM ALLOY BASE METAL

SPECIMEN NUMBER	NOMINAL THICKNESS, mm (INCH)	MEASURED THICKNESS, mm (INCH)	TEST ATMOSPHERE	GRAIN DIRECTION L = LONGITUDINAL T = TRANSVERSE	ULTIMATE STRENGTH, MN/m^2 (KSI)	YIELD STRENGTH, MN/m^2 (KSI)	ELONGATION, % IN 50.8 mm (% IN 2.0 INCHES)	REDUCTION IN AREA, %	MODULUS OF ELASTICITY $Ex10^3 MN/m^2$ ($Ex10^6$PSI)	POISSON'S RATIO
TAL-1	1.60 (0.063)	1.575 (0.0620)	AIR @ 295°K (72°F)	L	464.0 (67.3)	384.1 (55.7)	8	35	—	—
TAL-2		1.582 (0.0623)		L	458.5 (66.5)	378.5 (54.9)	8	34	74.5 (10.8)	0.322
AVG.					461.2 (66.9)	381.3 (55.3)	8	34	—	—
TAT-1		1.588 (0.0625)		T	468.2 (67.9)	373.7 (54.2)	8	27	—	—
TAT-2		1.595 (0.0628)		T	458.5 (66.5)	368.2 (53.4)	8	33	75.8 (11.0)	0.328
AVG.					463.3 (67.2)	370.9 (53.8)	8	30	—	—
TAL-5	3.18 (0.125)	3.167 (0.1247)		L	466.8 (67.7)	384.7 (55.8)	10	33	—	—
TAL-6		3.190 (0.1256)		L	462.7 (67.1)	380.6 (55.2)	11	35	76.5 (11.1)	0.329
AVG.					464.7 (67.4)	382.6 (55.5)	10	34	—	—
TAT-5		3.180 (0.1252)		T	472.3 (68.5)	383.4 (55.6)	10	31	—	—
TAT-6		3.195 (0.1258)		T	469.5 (68.1)	382.7 (55.5)	9	28	81.4 (11.8)	0.338
AVG.					470.9 (68.3)	383.0 (55.5)	9	29	—	—
TAL-9	7.62 (0.300)	7.658 (0.3015)		L	478.5 (69.4)	402.7 (58.4)	12	28	—	—
TAL-10		7.666 (0.3018)		L	477.1 (69.2)	397.1 (57.6)	12	30	69.0 (10.0)	0.309
AVG.					477.8 (69.3)	399.9 (58.0)	12	29	—	—
TAT-9		7.640 (0.3008)		T	484.7 (70.3)	402.0 (58.3)	9	19	—	—
TAT-10		7.628 (0.3003)		T	484.7 (70.3)	399.2 (57.9)	9	17	73.8 (10.7)	0.312
AVG.					484.7 (70.3)	400.6 (58.1)	9	18	—	—

Table 7: LIQUID HYDROGEN TEMPERATURE TENSILE PROPERTIES OF 2219-T87 ALUMINUM ALLOY BASE METAL

SPECIMEN NUMBER	NOMINAL THICKNESS, mm (INCH)	MEASURED THICKNESS, mm (INCH)	TEST ATMOSHPERE	GRAIN DIRECTION L = LONGITUDINAL T = TRANSVERSE	ULTIMATE STRENGTH, MN/m^2 (KSI)	YIELD STRENGTH, MN/m^2 (KSI)	ELONGATION, % IN 50.8 mm (% IN 2.0 INCHES)	REDUCTION IN AREA, %	MODULUS OF ELASTICITY, $Ex10^3 MN/m^2$ ($Ex10^6$PSI)	POISSON'S RATIO
TAL-3	1.60 (0.063)	1.592 (0.0627)	LH_2 @ 20°K (-423°F)	L	664.7 (96.4)	475.7 (69.0)	15	23	80.7 (11.7)	—
TAL-4		1.575 (0.0620)		L	674.3 (97.8)	494.4 (71.7)	[1]	[1]	75.2 (10.9)	0.337
AVG.		—		—	669.5 (97.1)	484.7 (70.3)	—	—	77.9 (11.3)	—
TAT-3		1.585 (0.0624)		T	674.3 (97.8)	463.3 (67.2)	13	19	83.4 (12.1)	
TAT-4		1.582 (0.0623)		T	695.0 (100.8)	486.8 (70.6)	14	18	76.5 (11.1)	0.334
AVG.		—		—	684.7 (99.3)	475.1 (68.9)	13	18	80.0 (11.6)	—
TAL-7	3.18 (0.125)	3.170 (0.1248)		L	669.5 (97.1)	481.3 (69.8)	16	24	82.7 (12.0)	—
TAL-8		3.178 (0.1251)		L	662.6 (96.1)	474.4 (68.8)	15	18	72.2 (11.2)	0.375
AVG.		—		—	666.1 (96.6)	477.8 (69.3)	15	21	80.0 (11.6)	—
TAT-7		3.178 (0.1251)		T	698.5 (101.3)	490.9 (71.2)	16	20	81.4 (11.8)	—
TAT-8		3.183 (0.1253)		T	698.5 (101.3)	484.0 (70.2)	16	17	77.2 (11.2)	0.347
AVG.		—		—	698.5 (101.3)	487.5 (70.7)	16	18	79.3 (11.5)	—
TAL-11	7.62 (0.300)	7.668 (0.3019)		L	690.2 (100.1)	491.6 (71.3)	17	24	73.1 (10.6)	—
TAL-12		7.673 (0.3021)		L	692.9 (100.5)	497.1 (72.1)	17	22	76.5 (11.1)	0.341
AVG.		—		—	691.6 (100.3)	494.4 (71.7)	17	23	74.5 (10.8)	—
TAT-11		7.620 (0.3000)		T	701.9 (101.8)	502.0 (72.8)	14	17	75.8 (11.0)	—
TAT-12		7.648 (0.3011)		T	699.8 (101.5)	502.0 (72.8)	15	16	75.2 (10.9)	0.311
AVG.		—		—	700.5 (101.6)	502.0 (72.8)	14	16	75.2 (10.9)	—

[1] NOT AVAILABLE, SPECIMEN FAILED OUTSIDE OF MEASURED TEST SECTION

Table 8: ROOM TEMPERATURE TENSILE PROPERTIES OF 6Al-4V TITANIUM ALLOY BASE METAL, STA (COND. III, XBMS 7-174B)

SPECIMEN NUMBER	NOMINAL THICKNESS, mm (INCH)	MEASURED THICKNESS, mm (INCH)	TEST ATMOSPHERE	GRAIN DIRECTION L = LONGITUDINAL T = TRANSVERSE	ULTIMATE STRENGTH, MN/m^2 (KSI)	YIELD STRENGTH, MN/m^2 (KSI)	ELONGATION' % IN 50.8 mm (% IN 2.0 INCHES)	REDUCTION IN AREA, %	MODULUS OF ELASTICITY, $Ex10^3 MN/m^2$ ($Ex10^6$PSI)	POISSON'S RATIO
TTL-1	0.51 (0.020)	0.579 (0.0228)	AIR @ 295°K (72°F)	L	1125.3 (163.2)	1038.4 (150.6)	11	—	—	—
TTL-2		0.597 (0.0235)		L	1141.1 (165.5)	1057.0 (153.3)	13	—	104.1 (15.1)	0.332
AVG.					1132.8 (164.3)	1047.3 (151.9)	12	—	—	—
TTT-1		0.582 (0.0229)		T	1137.7 (165.0)	1048.7 (152.1)	8	—	—	—
TTT-2		0.538 (0.0212)		T	1170.1 (169.7)	1080.4 (156.7)	9	—	115.1 (16.7)	0.334
AVG.					1153.5 (167.3)	1064.6 (154.4)	8	—	—	—
TTL-5	2.03 (0.080)	1.961 (0.0772)		L	1156.3 (167.7)	1077.0 (156.2)	18	—	—	—
TTL-6		1.961 (0.0772)		L	1150.1 (166.8)	1079.8 (156.6)	16	—	117.2 (17.0)	0.333
AVG.					1152.8 (167.3)	1078.4 (156.4)	17	—	—	—
TTT-5		1.971 (0.0776)		T	1163.9 (168.8)	1079.8 (156.6)	16	—	—	—
TTT-6		1.971 (0.0776)		T	1167.3 (169.3)	1084.6 (157.3)	16	—	104.1 (15.1)	0.309
AVG.					1165.2 (169.0)	1081.8 (156.9)	16	—	—	—
TTL-9	6.35 (0.250)	6.421 (0.2528)		L	1124.6 (163.1)	1069.4 (155.1)	3	6	—	—
TTL-10		6.408 (0.2523)		L	1119.7 (162.4)	1021.8 (148.2)	3	4	107.6 (15.6)	0.329
AVG.					1121.8 (162.7)	1045.3 (151.6)	3	5	—	—
TTT-9		6.312 (0.2485)		T	1155.6 (167.6)	1055.6 (153.1)	3	5	—	—
TTT-10		6.467 (0.2546)		T	1129.4 (163.8)	1063.2 (154.2)	2	2	109.6 (15.9)	0.336
AVG.					1142.5 (165.7)	1059.1 (153.6)	2	3	—	—

Table 9: LIQUID HYDROGEN TEMPERATURE TENSILE PROPERTIES OF 6AI-4V TITANIUM ALLOY BASE METAL, STA (COND. III, XBMS 7-174B)

SPECIMEN NUMBER	NOMINAL THICKNESS, mm (INCH)	MEASURED THICKNESS, mm (INCH)	TEST ATMOSPHERE	GRAIN DIRECTION L = LONGITUDINAL T = TRANSVERSE	ULTIMATE STRENGTH, MN/m^2 (KSI)	YIELD STRENGTH, MN/m^2 (KSI)	ELONGATION, % IN 50.8 mm (% IN 2.0 INCHES)	REDUCTION IN AREA, %	MODULUS OF ELASTICITY, $Ex10^3 MN/m^2$ ($Ex10^6$PSI)	POISSON'S RATIO
TTL-3	0.51 (0.020)	0.541 (0.0213)	LH_2 @ 20°K (-423°F)	L	1920.3 (278.5)	1805.1 (261.8)	[1]	—	—	—
TTL-4		0.559 (0.0220)		L	1820.3 (264.0)	1820.3 (264.0)	[1]	—	114.5 (16.6)	0.352
AVG.					1870.6 (271.3)	1812.7 (262.9)	—	—	—	—
TTT-3		0.544 (0.0214)		T	1921.6 (278.7)	1803.7 (261.6)	[1]	—	—	—
TTT-4		0.579 (0.0228)		T	1863.7 (270.3)	1830.6 (265.5)	[1]	—	118.6 (17.2)	0.332
AVG.					1892.7 (274.5)	1816.8 (263.5)	—	—	—	—
TTL-7	2.03 (0.080)	1.956 (0.0770)		L	2003.0 (290.5)	1861.0 (269.9)	3.5	—	—	—
TTL-8		1.963 (0.0773)		L	2010.6 (291.6)	1869.2 (271.1)	3.5	—	122.7 (17.8)	0.368
AVG.					2006.4 (291.0)	1865.1 (270.5)	3.5	—	—	—
TTT-7		1.974 (0.0777)		T	2026.4 (293.9)	1877.5 (272.3)	3.5	—	—	—
TTT-8		1.961 (0.0772)		T	2005.8 (290.9)	1869.2 (271.1)	3.5	—	124.8 (18.1)	0.372
AVG.					2016.1 (292.4)	1873.4 (271.1)	3.5	—	—	—
TTL-11	6.35 (0.250)			L	[2]	—	—	—	—	—
TTL-12		6.403 (0.2521)		L	1398.3 (202.8)	—	[1]	—	120.0 (17.4)	0.291
AVG.					—	—	—	—	—	—
TTT-11				T	[3]	—	—	—	—	—
TTT-12		6.533 (0.2572)		T	1587.2 (230.2)	—	2.5	—	124.8 (18.1)	0.280
AVG.					—	—	—	—	—	—

[1] NOT AVAILABLE, SPECIMEN FAILED OUTSIDE MEASURED TEST SECTION

[2] SPECIMEN TTL-11 FAILED IN GRIPS AT TEST SECTION STRESS OF 1407 MN/m^2 (204 KSI)

[3] SPECIMEN TTT-11 FAILED IN GRIPS AT TEST SECTION STRESS OF 1531 MN/m^2 (222 KSI)

Table 10: ROOM TEMPERATURE TENSILE PROPERTIES OF 2219-T87 ALUMINUM WELDMENTS

SPECIMEN NUMBER	NOMINAL THICKNESS, mm (INCH)	MEASURED THICKNESS, mm (INCH)	TEST ATMOSPHERE	ULTIMATE STRENGTH, MN/m^2 (KSI)	INDICATED YIELD STRENGTH, 0.2% OFFSET IN 50.8 mm (2.0 INCHES) * MN/m^2 (KSI)	INDICATED YIELD STRENGTH, 0.2% OFFSET IN 3.18 mm (0.125 INCHES) ** MN/m^2 (KSI)	INDICATED ELONGATION % IN 50.8 mm (% IN 2.0 INCHES)
TAW-1	1.60 (0.063)	1.62 (0.0637)	AIR @ 295°K (72°F)	263.4 (38.2)	177.2 (25.7)	92.4 (13.4)	2.1
TAW-2		1.60 (0.0630)		257.9 (37.4)	172.4 (25.0)	104.8 (15.2)	2.8
AVG.	—	—		260.7 (37.8)	174.8 (25.3)	98.6 (14.3)	2.4
TAW-7	2.67 (0.105)	2.61 (0.1027)		266.1 (38.6)	183.4 (26.6)	102.7 (14.9)	2.7
TAW-8		2.55 (0.1004)		268.9 (39.0)	205.5 (29.8)	—	2.2
AVG.	—	—		267.5 (38.8)	194.5 (28.2)	—	2.4
TAW-13	7.62 (0.300)	7.66 (0.3016)		301.3 (43.7)	183.4 (26.6)	133.7 (19.4)	5.0
TAW-14		7.67 (0.3019)		299.9 (43.5)	177.4 (25.3)	124.1 (18.0)	6.0
AVG.	—	—		300.6 (43.6)	178.6 (25.9)	128.9 (18.7)	5.5

*0.2% OFFSET YIELD STRENGTH OBTAINED BY EXTENSOMETER ON 50.8 mm (2.0 INCHES) GAGE LENGTH

**0.2% OFFSET YIELD STRENGTH OBTAINED BY STRAIN GAGE ON 3.18 mm (0.125 INCH) GAGE LENGTH

Table 11: LIQUID NITROGEN TEMPERATURE TENSILE PROPERTIES OF 2219-T87 ALUMINUM WELDMENTS

SPECIMEN NUMBER	NOMINAL THICKNESS, mm (INCH)	MEASURED THICKNESS, mm (INCH)	TEST ATMOSPHERE	ULTIMATE STRENGTH, MN/m^2 (KSI)	INDICATED YIELD STRENGTH, 0.2% OFFSET IN 50.8 mm (2.0 INCHES) * MN/m^2 (KSI)	INDICATED YIELD STRENGTH, 0.2% OFFSET IN 3.18 mm (0.125 INCH) ** MN/m^2 (KSI)	INDICATED ELONGATION, % IN 50.8 mm (% IN 2.0 INCHES)
TAW-3	1.60 (0.063)	1.68 (0.0660)	LN_2 @ 78°K (-320°F)	379.9 (55.1)	223.4 (32.4)	144.1 (20.9)	3.8
TAW-4		1.65 (0.0651)		380.6 (55.2)	232.4 (33.7)	158.6 (23.0)	3.9
AVG.	—	—		380.2 (55.1)	227.9 (33.0)	151.3 (21.9)	3.8
TAW-9	2.67 (0.105)	2.60 (0.1022)		387.5 (56.2)	219.3 (31.8)	128.9 (18.7)	3.8
TAW-10		2.76 (0.1088)		360.6 (52.3)	200.0 (29.0)	118.6 (17.2)	3.8
AVG.	—	—		374.0 (54.2)	209.6 (30.4)	123.7 (17.9)	3.8
TAW-15	7.62 (0.300)	7.67 (0.3019)		416.5 (60.4)	224.8 (32.6)	168.2 (24.4)	6.5
TAW-16		7.67 (0.3018)		411.6 (59.7)	213.1 (30.9)	154.4 (22.4)	7.0
AVG.	—	—		413.7 (60.0)	218.6 (31.7)	161.3 (23.4)	6.7

*0.2% OFFSET YIELD STRENGTH OBTAINED BY EXTENSOMETER ON 50.8 mm (2.0 INCHES) GAGE LENGTH

**0.2% OFFSET YIELD STRENGTH OBTAINED BY STRAIN GAGE ON 3.18 mm (0.125 INCH) GAGE LENGTH

Table 12: LIQUID HYDROGEN TEMPERATURE TENSILE PROPERTIES OF 2219-T87 ALUMINUM WELDMENTS

SPECIMEN NUMBER	NOMINAL THICKNESS, mm (INCH)	MEASURED THICKNESS, mm (INCH)	TEST ATMOSPHERE	ULTIMATE STRENGTH, MN/m^2 (KSI)	INDICATED YIELD STRENGTH, 0.2% OFFSET IN 50.8 mm (2.0 INCHES) MN/m^2 (KSI) *	INDICATED YIELD STRENGTH, 0.2% OFFSET IN 3.18 mm (0.125 INCH) MN/m^2 (KSI) **	INDICATED ELONGATION, % IN 50.8 mm (% IN 2.0 INCHES)
TAW-5	1.60 (0.063)	1.65 (0.065)	LH_2 @ 20°K (-423°F)	513.0 (74.4)	348.9 (50.6)	289.6 (42.0)	3.5
TAW-6		1.60 (0.063)		519.9 (75.4)	299.9 (43.5)	186.9 (27.1)	3.5
AVG.	—	—		516.4 (74.9)	[1]	[1]	3.5
TAW-11	2.67 (0.105)	2.57 (0.101)		497.1 (72.1)	279.2 (40.5)	180.0 (26.1)	3.5
TAW-12		2.54 (0.100)		518.5 (75.2)	311.7 (45.2)	173.1 (25.1)	3.5
AVG.	—	—		507.5 (73.6)	295.1 (42.8)	176.5 (25.6)	3.5
TAW-17	7.62 (0.300)	7.67 (0.302)		490.2 (71.1)	269.6 (39.1)	210.3 (30.5)	4.0
TAW-18		7.67 (0.302)		468.2 (67.9)	266.8 (38.7)	192.4 (27.9)	4.0
AVG.	—	—		479.2 (69.5)	268.2 (38.9)	201.3 (29.2)	4.0

*0.2% OFFSET YIELD STRENGTH OBTAINED BY EXTENSOMETER ON 50.8 mm (2.0 INCHES) GAGE LENGTH

**0.2% OFFSET YIELD STRENGTH OBTAINED BY STRAIN GAGE ON 3.18 mm (0.125 INCH) GAGE LENGTH

[1] AVERAGE YIELD STRENGTH VALUES NOT COMPUTED BECAUSE YIELD STRENGTH VALUES FOR TAW-5 APPEAR UNUSUALLY HIGH

Table 13: ROOM TEMPERATURE TENSILE PROPERTIES OF TITANIUM 6AI-4V WELDMENTS

SPECIMEN NUMBER	NOMINAL THICKNESS, mm (INCH)	MEASURED THICKNESS, mm (INCH)	TEST ATMOSPHERE	ULTIMATE STRENGTH, MN/m^2 (KSI)	INDICATED YIELD STRENGTH, 0.2% OFFSET IN 50.8 mm (2.0 INCHES), MN/m^2 (KSI) *	INDICATED YIELD STRENGTH, 0.2% OFFSET IN 3.18 mm (0.125 INCH), MN/m^2 (KSI) **	INDICATED ELONGATION, % PER 50.8 mm (% PER 2.0 INCH)
TTW-1	0.51 (0.020)	0.52 (0.0205)	AIR @ 295°K (72°F)	1114.9 (161.7)	1101.1 (159.7)	1034.2 (150.0)	0.3
TTW-2		0.57 (0.0225)		1083.2 (157.1)	1053.6 (152.8)	1005.3 (145.8)	0.5
AVG		—		1099.1 (159.4)	1077.0 (156.2)	1019.8 (147.9)	0.4
TTW-5	1.78 (0.070)	1.81 (0.0711)		1125.3 (163.2)	1103.2 (160.0)	1034.2 (150.0)	0.6
TTW-6		1.85 (0.0729)		1113.5 (161.5)	1082.5 (157.0)	1035.6 (150.2)	1.4
AVG		—		1119.1 (162.3)	1092.9 (158.5)	1034.9 (150.1)	1.0
TTW-9	5.33 (0.210)	5.19 (0.2042)		1103.2 (160.0)	1030.8 (149.5)	969.4 (140.6)	—
TTW-10		5.37 (0.2115)		1087.3 (157.7)	1034.2 (150.0)	953.6 (138.3)	—
AVG		—		1094.9 (158.8)	1032.2 (149.7)	961.2 (139.4)	—

* 0.2% OFFSET YIELD STRENGTH OBTAINED BY EXTENSOMETER ON 50.8 mm (2.0 INCHES) GAGE LENGTH

** 0.2% OFFSET YIELD STRENGTH OBTAINED BY STRAIN GAGE ON 3.18 mm (0.125 INCH) GAGE LENGTH

Table 14: LIQUID HYDROGEN TEMPERATURE TENSILE PROPERTIES OF TITANIUM 6Al-4V WELDMENTS

SPECIMEN NUMBER	NOMINAL THICKNESS mm (INCH)	MEASURED THICKNESS, mm (INCH)	TEST ATMOSPHERE	ULTIMATE STRENGTH, MN/m^2 (KSI)	INDICATED YIELD STRENGTH 0.2% OFFSET IN 50.8 mm (2.0 INCHES) MN/m^2 (KSI)*	INDICATED YIELD STRENGTH, 0.2% OFFSET IN 3.18 mm (0.125 INCH) MN/m^2 (KSI)**	INDICATED ELONGATION, % PER 50.8 mm (% PER 2.0 INCH)
TTW-3	0.51 (0.020)	0.58 (0.0230)	LH_2 @ 20°K (-423°F)	1947.1 (282.4)	1947.1 (282.4)	1792.7 (260.0)	0.5
TTW-4		0.55 (0.0215)		1870.0 (271.2)	1870.0 (271.2)	1725.8 (250.3)	1.0
AVG		—		1908.5 (276.8)	1908.5 (276.8)	1758.9 (255.1)	0.7
TTW-7	1.78 (0.070)	1.82 (0.0716)		1976.1 (286.6)	1976.1 (286.6)	1825.8 (264.8)	1.5
TTW-8		1.83 (0.0720)		1927.2 (279.5)	1927.2 (279.5)	1783.7 (258.7)	1.5
AVG		—		1952.0 (283.1)	1952.0 (283.1)	1804.4 (261.7)	1.5
TTW-11	5.33 (0.210)	5.01 (0.1974)		1837.5 (266.5)	1837.5 (266.5)	1760.3 (255.3)	1.5
TTW-12		5.00 (0.1967)		1817.5 (263.6)	1817.5 (263.6)	1710.6 (248.1)	2.0
AVG		—		1827.2 (265.0)	1827.2 (265.0)	1735.5 (251.7)	1.7

* 0.2% OFFSET YIELD STRENGTH OBTAINED BY EXTENSOMETER ON 50.8 mm (2.0 INCHES) GAGE LENGTH

** 0.2% OFFSET YIELD STRENGTH OBTAINED BY STRAIN GAGE ON 3.18 mm (0.125 INCH) GAGE LENGTH

Table 15: STATIC FRACTURE TESTS – ROOM TEMPERATURE 2219-T87 BASE PLATE, WT FLAW ORIENTATION

SPECIMEN			TEST		FRACTURE DATA									
NUMBER	GAGE THICKNESS, t mm (INCH)	GAGE WIDTH, w mm (INCH)	DIMPLING GAGE LOCATION FROM CRACK TIP	ENVIRONMENT	FAILURE STRESS, σ_G MN/m^2 (KSI)	DIMPLING STRESS, σ_D MN/m^2 (KSI)	BREAKTHROUGH STRESS, σ_B MN/m^2 (KSI)	INITIAL FLAW DEPTH, a_i mm (INCH)	INITIAL FLAW LENGTH, $(2c)_i$ mm (INCH)	INITIAL FLAW DEPTH / GAGE THICKNESS, $(a/t)_i$	INITIAL FLAW DEPTH / INITIAL FLAW LENGTH, $(a/2c)_i$	σ_B/σ_Y [1]	σ_G/σ_Y [1]	IRWIN'S APPARENT K AT BREAKTHROUGH MN/m$^{3/2}$ (KSI$\sqrt{\text{IN}}$)
AB1-1	1.58 (0.0622)	88.96 (3.5022)	42°	ROOM AIR @ 295°K (72°F)	392.3 (56.9)	344.8 (50.0)	—	0.86 (0.034)	4.06 (0.160)	0.547	0.212	—	1.06	21.0 (19.1)
AB1-2	1.59 (0.0625)	89.05 (3.5060)	51°		357.9 (51.9)	229.6 (33.3)	—	1.19 (0.047)	7.49 (0.295)	0.752	0.159	—	0.96	23.8 (21.7)
AB2-1	3.16 (0.1244)	63.47 (2.4987)	6°		380.6 (55.2)	380.6 (55.2)	—	1.52 (0.060)	8.13 (0.320)	0.482	0.188	—	0.99	27.9 (25.4)
AB2-2	3.16 (0.1245)	63.50 (2.5000)	38°		339.9 (49.3)	259.9 (37.7)	—	2.16 (0.085)	14.48 (0.570)	0.683	0.149	—	0.89	30.3 (27.6)
AB3-1	7.63 (0.3004)	88.99 (3.5034)	51°		364.1 (52.8)	324.1 (47.0)	—	3.45 (0.136)	19.05 (0.750)	0.453	0.181	—	0.91	39.8 (36.2)
AB3-2	7.65 (0.3010)	89.02 (3.5048)	53°		379.2 (55.0)	354.4 (51.4)	—	2.87 (0.113)	18.80 (0.740)	0.375	0.153		0.95	39.2 (35.7)

[1] t = 1.60 mm (0.063 INCH), σ_Y = 371 MN/m^2 (53.8 KSI)
t = 3.18 mm (0.125 INCH), σ_Y = 383 MN/m^2 (55.5 KSI)
t = 7.62 mm (0.300 INCH), σ_Y = 401 MN/m^2 (58.1 KSI)

Table 16: STATIC FRACTURE TESTS — LIQUID HYDROGEN TEMPERATURE 2219-T87 BASE PLATE WT FLAW ORIENTATION

SPECIMEN			TEST		FRACTURE DATA									
NUMBER	GAGE THICKNESS, t mm (INCH)	GAGE WIDTH, w mm (INCH)	DIMPLING GAGE LOCATION FROM CRACK TIP	ENVIRONMENT	FAILURE STRESS, σ_G MN/m^2 (KSI)	DIMPLING STRESS, σ_D MN/m^2 (KSI)	BREAKTHROUGH STRESS, σ_B MN/m^2 (KSI)	INITIAL FLAW DEPTH, a_i mm (INCH)	INITIAL FLAW LENGTH, $(2c)_i$ mm (INCH)	$\frac{\text{INITIAL FLAW DEPTH}}{\text{GAGE THICKNESS}}$, (a/t)	$\frac{\text{INITIAL FLAW DEPTH}}{\text{INITIAL FLAW LENGTH}}$, $(a/2c)_i$	σ_B/σ_Y [1]	σ_G/σ_Y [1]	IRWIN'S APPARENT K AT BREAKTHROUGH MN/m$^{3/2}$ (KSI$\sqrt{\text{IN}}$)
AB1-3	1.57 (0.0620)	89.00 (3.5040)	55°	LH_2 @ 20°K (-423°F)	506.3 (73.43)	400.6 (58.10)	—	0.79 (0.031)	4.11 (0.162)	0.500	0.191	—	1.07	26.6 (24.2)
AB1-4	1.61 (0.0633)	89.06 (3.5064)	43°		470.5 (68.24)	—	465.9 (67.57)	1.19 (0.047)	7.44 (0.293)	0.742	0.160	0.98	0.99	31.1 (28.3)
AB2-3	3.17 (0.1248)	63.53 (2.5010)	49°		488.2 (70.81)	413.1 (59.92)	—	1.42 (0.056)	8.31 (0.327)	0.449	0.171	—	1.00	35.3 (32.1)
AB2-4	3.18 (0.1252)	63.56 (2.5024)	55°		419.9 (60.90)	264.5 (38.36)	411.1 (59.62)	2.21 (0.087)	14.86 (0.585)	0.695	0.149	0.84	0.86	36.8 (33.5)
AB3-3	7.70 (0.3030)	88.98 (3.5033)	56°		451.4 (65.47)	415.7 (60.29)	—	3.12 (0.123)	18.92 (0.745)	0.406	0.165	—	0.90	47.7 (43.4)
AB3-4	7.63 (0.3004)	88.98 (3.5030)	47°		455.4 (66.05)	424.6 (61.58)	—	2.84 (0.112)	18.80 (0.740)	0.373	0.151	—	0.91	46.7 (42.5)

[1] t = 1.60 mm (0.063 INCH), σ_Y = 475 MN/m^2 (68.9 KSI)
t = 3.18 mm (0.125 INCH), σ_Y = 488 MN/m^2 (70.7 KSI)
t = 7.62 mm (0.300 INCH), σ_Y = 502 MN/m^2 (72.8 KSI)

Table 17: STATIC FRACTURE TESTS — ROOM TEMPERATURE 6Al-4V TITANIUM (STA) BASE PLATE WT FLAW ORIENTATION

SPECIMEN			TEST		FRACTURE DATA									
NUMBER	GAGE THICKNESS, t mm (INCH)	GAGE WIDTH, w mm (INCH)	DIMPLING GAGE LOCATION FROM CRACK TIP	ENVIRONMENT	FAILURE STRESS, σ_G MN/m^2 (KSI)	DIMPLING STRESS, σ_D MN/m^2 (KSI)	BREAKTHROUGH STRESS, σ_B MN/m^2 (KSI)	INITIAL FLAW DEPTH, a_i mm (INCH)	INITIAL FLAW LENGTH, $(2c)_i$ mm (INCH)	$\frac{\text{INITIAL FLAW DEPTH}}{\text{GAGE THICKNESS}}$, (a/t)	$\frac{\text{INITIAL FLAW DEPTH}}{\text{INITIAL FLAW LENGTH}}$, $(a/2c)_i$	σ_B/σ_Y [1]	σ_G/σ_Y [1]	IRWIN'S APPARENT K AT BREAKTHROUGH MN/m$^{3/2}$ (KSI$\sqrt{\text{IN}}$)
TB1-1	0.51 (0.0200)	30.31 (1.1933)	68°	ROOM AIR @ 295°K (72°F)	1087.3 (157.7)	—	1077.0 (156.2)	0.20 (0.008)	1.45 (0.057)	0.400	0.211	1.01	1.02	30.8 (28.0)
TB1-2	0.53 (0.0210)	30.30 (1.1929)	82°		975.0 (141.4)	626.1 (90.8)	966.7 (140.2)	0.38 (0.015)	2.39 (0.094)	0.714	0.160	0.91	0.92	36.3 (33.0)
TB2-1	1.96 (0.0773)	30.50 (1.2007)	63°		969.4 (140.6)	—	—	0.81 (0.032)	5.51 (0.217)	0.414	0.147	—	0.90	53.2 (48.4)
TB2-2	1.96 (0.0771)	30.55 (1.2028)	71°		661.9 (96.0)	—	635.7 (92.2)	1.35 (0.053)	9.65 (0.380)	0.687	0.139	0.59	0.61	45.2 (41.1)
TB3-1	6.55 (0.2577)	76.29 (3.0037)	61°		698.5 (101.3)	—	686.1 (99.5)	4.19 (0.165)	17.78 (0.700)	0.640	0.236	0.64	0.66	76.5 (69.6)
TB3-2	6.55 (0.2580)	76.28 (3.0031)	41°		921.9 (133.7)	893.6 (129.6)	—	2.34 (0.092)	17.09 (0.673)	0.357	0.137	—	0.87	86.4 (78.6)

[1] t = 0.51mm (0.020 INCH), σ_Y = 1065 MN/m^2 (154.4 KSI)
t = 2.03mm (0.080 INCH), σ_Y = 1082 MN/m^2 (156.9 KSI)
t = 6.35mm (0.250 INCH), σ_Y = 1059 MN/m^2 (153.6 KSI)

Table 18: ***STATIC FRACTURE TESTS – LIQUID HYDROGEN TEMPERATURE 6Al-4V TITANIUM (STA) BASE PLATE WT FLAW ORIENTATION***

SPECIMEN			TEST		FRACTURE DATA									
NUMBER	GAGE THICKNESS, t mm (INCH)	GAGE WIDTH, w mm (INCH)	DIMPLING GAGE LOCATION FROM CRACK TIP	ENVIRONMENT	FAILURE STRESS, σ_G MN/m^2 (KSI)	DIMPLING STRESS, σ_D MN/m^2 (KSI)	BREAKTHROUGH STRESS, σ_B MN/m^2 (KSI)	INITIAL FLAW DEPTH, a_i mm (INCH)	INITIAL FLAW LENGTH, $(2c)_i$ mm (INCH)	$\frac{\text{INITIAL FLAW DEPTH}}{\text{GAGE THICKNESS}}$, $(a/t)_i$	$\frac{\text{INITIAL FLAW DEPTH}}{\text{INITIAL FLAW LENGTH}}$, $(a/2c)_i$	σ_B/σ_Y [1]	σ_G/σ_Y [1]	IRWIN'S APPARENT K AT BREAKTHROUGH MN/m$^{3/2}$ (KSI$\sqrt{\text{IN}}$)
TB1-3	0.51 (0.0200)	30.42 (1.1976)	54°	LH_2 @ 20°K (-423°F)	1408.0 (204.2)	1246.6 (180.8)	—	0.23 (0.009)	1.57 (0.062)	0.450	0.145	—	0.77	40.3 (36.7)
TB1-4	0.52 (0.0203)	30.35 (1.1948)	39°		1007.4 (146.1)	941.9 (136.6)	—	0.33 (0.013)	2.41 (0.095)	0.640	0.137	—	0.55	34.0 (30.9)
TB2-3	1.97 (0.0775)	30.47 (1.1998)	40°		711.6 (103.2)	—	—	0.86 (0.034)	5.53 (0.218)	0.439	0.156	—	0.38	37.5 (34.1)
TB2-4	1.97 (0.0776)	30.46 (1.1991)	36°		500.6 (72.6)	463.3 (67.2)	489.5 (71.0)	1.37 (0.054)	9.65 (0.380)	0.696	0.142	0.26	0.27	32.8 (29.8)
TB3-3	6.53 (0.2569)	76.33 (3.005)	—		—	—	—	2.54 (0.10)	17.02 (0.67)	—	—	—	—	— [2]
TB3-4	6.50 (0.2560)	44.70 (1.760)	44°		746.0 (108.2)	—	—	1.75 (0.069)	12.57 (0.495)	0.270	0.139	—	0.47	57.3 (52.1)

[1] t = 0.51mm (0.020 INCH), σ_Y = 1817 MN/m^2 (263.5 KSI)
t = 2.03mm (0.080 INCH), σ_Y = 1873 MN/m^2 (271.7 KSI)
t = 6.34mm (0.250 INCH), $\sigma_Y = \sigma_U$ = 1587 MN/m^2 (230.2 KSI)

[2] GRIP FAILURE

Table 19: STATIC FRACTURE TESTS ROOM TEMPERATURE 2219-T87 WELDMENT, t = 1.60mm (0.063 INCH)

SPECIMEN			TEST		FRACTURE DATA									
NUMBER	GAGE THICKNESS, t mm (INCH)	GAGE WIDTH, w mm (INCH)	DIMPLING GAGE LOCATION FROM CRACK TIP	ENVIRONMENT	FAILURE STRESS, σ_G MN/m^2 (KSI)	DIMPLING STRESS, σ_D MN/m^2 (KSI)	BREAKTHROUGH STRESS, σ_B MN/m^2 (KSI)	INITIAL FLAW DEPTH, a_i mm (INCH)	INITIAL FLAW LENGTH, $(2c)_i$ mm (INCH)	$\frac{\text{INITIAL FLAW DEPTH}}{\text{GAGE THICKNESS}}$, $(a/t)_i$	$\frac{\text{INITIAL FLAW DEPTH}}{\text{INITIAL FLAW LENGTH}}$, $(a/2c)_i$	σ_B/σ_Y [1]	σ_G/σ_Y [1]	IRWIN'S APPARENT K AT BREAKTHROUGH MN/m$^{3/2}$ (KSI$\sqrt{\text{IN}}$)
SAR 6-05-1	1.68 (0.0660)	89.0 (3.5032)	55°	AIR @ 295°K (72°F)	208.8 (30.28)	107.4 (15.57)	196.2 (28.46)	0.79 (0.031)	16.00 (0.630)	0.470	0.049	1.13	1.20	12.0 (10.9)
SAR 6-05-2	1.68 (0.0660)	127.0 (5.000)	46°		205.6 (29.82)	88.5 (12.84)	158.0 (22.91)	1.17 (0.046)	23.11 (0.910)	0.697	0.051	0.91	1.18	11.4 (10.4)
SAR 6-05-3	1.64 (0.0647)	152.1 (5.9900)	52°		197.9 (28.70)	69.4 (10.06)	130.8 (18.97)	1.32 (0.052)	27.56 (1.085)	0.804	0.048	0.75	1.13	9.8 (8.9)
SAR 6-1-1	1.50 (0.0592)	88.82 (3.4970)	54°		211.7 (30.7)	84.8 (12.3)	197.9 (28.7)	0.86 (0.034)	5.33 (0.210)	0.575	0.162	1.13	1.21	11.2 (10.2)
SAR 6-1-2	1.56 (0.0616)	89.07 (3.5067)	66°		220.0 (31.9)	133.1 (19.3)	191.0 (27.7)	1.17 (0.046)	7.37 (0.290)	0.747	0.159	1.09	1.26	12.6 (11.5)
SAR 6-1-3	1.60 (0.0629)	88.85 (3.4980)	81°		196.5 (28.5)	—	140.4 (20.36)	1.42 (0.056)	9.91 (0.390)	0.891	0.144	0.80	1.13	10.1 (9.2)
SAR 6-3-1	1.64 (0.0646)	89.06 (3.5062)	53°		221.3 (32.10)	142.2 (20.63)	219.2 (31.79)	0.79 (0.031)	2.44 (0.096)	0.480	0.323	1.26	1.27	9.8 (8.9)
SAR 6-3-2	1.60 (0.0629)	89.05 (3.5060)	55°		222.0 (32.20)	122.6 (17.78)	202.6 (29.39)	1.14 (0.045)	3.86 (0.152)	0.715	0.296	1.16	1.27	11.3 (10.3)
SAR 6-3-3	1.52 (0.0600)	88.96 (3.5022)	36°		229.7 (33.32)	102.4 (14.85)	175.5 (25.46)	1.35 (0.053)	4.88 (0.192)	0.883	0.276	1.01	1.32	10.9 (9.9)
SAR 6-3-4	1.62 (0.0639)	88.97 (3.5028)	25°		228.6 (33.15)	71.4 (10.35)	184.9 (26.81)	1.35 (0.053)	4.83 (0.190)	0.829	0.279	1.06	1.31	11.4 (10.4)
SAR 6-3-5	1.63 (0.0642)	88.83 (3.4974)	45°		231.3 (33.54)	89.1 (12.92)	187.3 (27.17)	1.27 (0.050)	4.95 (0.195)	0.779	0.256	1.07	1.33	11.5 (10.5)

[1] σ_Y = 174.4 MN/m^2 (25.3 KSI)

Table 20: STATIC FRACTURE TESTS – ROOM TEMPERATURE 2219-T87 WELDMENT, t = 2.67mm (0.105 INCH)

SPECIMEN			TEST		FRACTURE DATA									
NUMBER	GAGE THICKNESS, t mm (INCH)	GAGE WIDTH, w mm (INCH)	DIMPLING GAGE LOCATION FROM CRACK TIP	ENVIRONMENT	FAILURE STRESS, σ_G MN/m^2 (KSI)	DIMPLING STRESS, σ_D MN/m^2 (KSI)	BREAKTHROUGH STRESS, σ_B MN/m^2 (KSI)	INITIAL FLAW DEPTH, a_i mm (INCH)	INITIAL FLAW LENGTH, $(2c)_i$ mm (INCH)	$\frac{\text{INITIAL FLAW DEPTH}}{\text{GAGE THICKNESS}}$, $(a/t)_i$	$\frac{\text{INITIAL FLAW DEPTH}}{\text{INITIAL FLAW LENGTH}}$, $(a/2c)_i$	σ_B/σ_Y [1]	σ_G/σ_Y [1]	IRWIN'S APPARENT K AT BREAKTHROUGH MN/m$^{3/2}$ (KSI$\sqrt{\text{IN}}$)
SAR 1-05-1	2.75 (0.1083)	152.4 (5.9988)	57°	AIR @ 295°K (72°F)	216.5 (31.40)	121.0 (17.55)	207.3 (30.06)	1.32 (0.052)	29.21 (1.150)	0.480	0.045	1.07	1.11	16.4 (14.9)
SAR 1-05-2	2.56 (0.1008)	228.7 (9.005)	56°		195.1 (28.29)	57.7 (8.37)	107.1 (15.53)	2.24 (0.088)	44.20 (1.740)	0.873	0.051	0.55	1.00	10.1 (9.2)
SAR 1-05-3	2.63 (0.1035)	241.4 (9.504)	33°		199.8 (28.98)	77.1 (11.18)	126.2 (18.30)	2.16 (0.085)	49.02 (1.930)	0.821	0.044	0.65	1.03	11.9 (10.8)
SAR 1-05-4	2.76 (0.1085)	228.6 (9.000)	38°		201.3 (29.19)	55.8 (8.09)	153.2 (22.22)	1.85 (0.073)	40.13 (1.580)	0.673	0.046	0.79	1.04	13.6 (12.4)
SAR 1-1-1	2.68 (0.1058)	127.1 (5.0040)	38°		253.9 (36.83)	117.8 (17.09)	240.2 (35.70)	1.40 (0.055)	9.14 (0.360)	0.520	0.153	1.27	1.31	18.0 (16.4)
SAR 1-1-2	2.67 (0.1050)	127.1 (5.0038)	43°		234.5 (34.01)	96.8 (14.04)	208.2 (30.19)	1.83 (0.072)	12.45 (0.490)	0.686	0.147	1.07	1.21	17.5 (15.9)
SAR 1-1-3	2.73 (0.1075)	127.1 (5.0040)	67°		214.0 (31.04)	—	98.7 (14.31)	2.57 (0.101)	16.38 (0.645)	0.940	0.167	0.51	1.10	9.0 (8.2)
SAR 1-1-4	2.71 (0.1065)	127.1 (5.0040)	32°		221.3 (32.09)	107.4 (15.58)	201.8 (29.27)	1.88 (0.074)	14.73 (0.580)	0.695	0.128	1.04	1.14	17.6 (16.0)
SAR 1-1-5	2.68 (0.1056)	127.1 (5.0050)	5°		219.2 (31.79)	89.4 (12.96)	170.9 (24.79)	2.03 (0.080)	13.97 (0.550)	0.758	0.145	0.88	1.13	14.8 (13.5)
SAR 1-3-4	2.72 (0.1071)	127.1 (5.0056)	60°		239.3 (34.70)	141.5 (20.52)	199.3 (28.91)	2.13 (0.084)	6.99 (0.275)	0.784	0.305	1.03	1.23	14.9 (13.6)
SAR 1-3-5	2.78 (0.1095)	127.1 (5.0045)	12°		238.2 (34.54)	137.1 (19.89)	222.7 (32.30)	1.83 (0.072)	7.29 (0.287)	0.658	0.251	1.15	1.22	16.6 (15.1)
SAR 1-3-6	2.72 (0.1070)	127.2 (5.0061)	7°		233.2 (33.82)	95.2 (13.81)	189.2 (27.44)	2.08 (0.082)	7.87 (0.310)	0.766	0.265	0.97	1.20	14.7 (13.4)

[1] σ_Y = 194.4 MN/m^2 (28.2 KSI)

Table 21: STATIC FRACTURE TESTS – ROOM TEMPERATURE 2219-T87 WELDMENT, t = 7.62mm (0.30 INCH)

SPECIMEN			TEST		FRACTURE DATA									
NUMBER	GAGE THICKNESS, t mm (INCH)	GAGE WIDTH, w mm (INCH)	DIMPLING GAGE LOCATION FROM CRACK TIP	ENVIRONMENT	FAILURE STRESS, σ_G MN/m^2 (KSI)	DIMPLING STRESS, σ_D MN/m^2 (KSI)	BREAKTHROUGH STRESS, σ_B MN/m^2 (KSI)	INITIAL FLAW DEPTH, a_i mm (INCH)	INITIAL FLAW LENGTH, $(2c)_i$ mm (INCH)	$\frac{\text{INITIAL FLAW DEPTH}}{\text{GAGE THICKNESS}}$, $(a/t)_i$	$\frac{\text{INITIAL FLAW DEPTH}}{\text{INITIAL FLAW LENGTH}}$, $(a/2c)_i$	σ_B/σ_Y [1]	σ_G/σ_Y [1]	IRWIN'S APPARENT K AT BREAKTHROUGH MN/m$^{3/2}$ (KSI$\sqrt{\text{IN}}$)
SAR 3-1-1	7.64 (0.3010)	228.6 (9.000)	47°	AIR @ 295°K (72°F)	217.6 (31.56)	102.3 (14.84)	208.7 (30.27)	3.43 (0.135)	24.38 (0.96)	0.449	0.141	1.17	1.22	24.2 (22.0)
SAR 3-1-2	7.71 (0.3035)	229.1 (9.020)	54°		209.3 (30.35)	105.8 (15.34)	193.4 (28.05)	4.95 (0.195)	34.80 (1.37)	0.643	0.142	1.08	1.17	26.9 (24.5)
SAR 3-1-3	7.63 (0.3003)	193.8 (9.0721)	42°		204.1 (29.60)	80.2 (11.63)	162.9 (23.63)	6.22 (0.245)	42.67 (1.68)	0.816	0.146	0.91	1.14	24.8 (22.6)
SAR 3-1-4	7.59 (0.2990)	228.6 (9.000)	43°		191.4 (27.76)	83.0 (12.04)	134.5 (19.51)	6.78 (0.267)	45.97 (1.81)	0.893	0.148	0.75	1.07	20.9 (19.0)
SAR 3-3-1	7.57 (0.2980)	127.1 (5.0042)	47°		225.2 (32.66)	106.5 (15.45)	—	3.63 (0.143)	12.45 (0.490)	0.480	0.292	—	1.26	22.4 (20.4)
SAR 3-3-2	7.65 (0.3010)	127.1 (5.0050)	51°		213.7 (31.00)	97.8 (14.18)	203.2 (29.47)	5.08 (0.200)	17.40 (0.685)	0.664	0.292	1.14	1.20	24.0 (21.8)
SAR 3-3-3	7.68 (0.3025)	127.1 (5.0034)	56°		198.6 (28.81)	108.6 (15.75)	173.1 (25.11)	6.22 (0.245)	22.73 (0.895)	0.810	0.274	0.97	1.11	23.0 (20.9)
SAR 3-5-1	7.65 (0.3010)	88.89 (3.4998)	47°		223.9 (32.47)	132.2 (19.18)	—	3.56 (0.140)	7.75 (0.305)	0.465	0.459	—	1.25	18.1 (16.5)
SAR 3-5-2	7.65 (0.3011)	88.97 (3.5028)	44°		222.3 (32.24)	107.8 (15.63)	—	4.83 (0.190)	10.85 (0.427)	0.631	0.445	—	1.24	21.3 (19.4)
SAR 3-5-3	7.73 (0.3042)	88.93 (3.5010)	31°		205.3 (29.77)	115.9 (16.81)	192.9 (27.98)	6.10 (0.240)	13.59 (0.535)	0.790	0.449	1.08	1.15	20.8 (18.9)
SAR 3-5-4	7.65 (0.3010)	88.94 (3.5017)	20°		185.1 (26.85)	87.9 (12.75)	151.8 (22.01)	6.60 (0.260)	14.73 (0.580)	0.864	0.448	0.85	1.04	16.7 (15.2)
SAR 3-5-5	7.58 (0.2986)	88.94 (3.5014)	9°		195.9 (28.41)	104.2 (15.11)	153.0 (22.19)	6.78 (0.267)	15.11 (0.595)	0.894	0.449	0.86	1.10	17.1 (15.6)

[1] σ_Y = 178.6 MN/m^2 (25.9 KSI)

Table 22: *STATIC FRACTURE TESTS* *LIQUID NITROGEN TEMPERATURE 2219-T87 WELDMENT, t = 1.60mm (0.063 INCH)*

SPECIMEN			TEST		FRACTURE DATA									
NUMBER	GAGE THICKNESS, t mm (INCH)	GAGE WIDTH, w mm (INCH)	DIMPLING GAGE LOCATION FROM CRACK TIP	ENVIRONMENT	FAILURE STRESS, σ_G MN/m^2 (KSI)	DIMPLING STRESS, σ_D MN/m^2 (KSI)	BREAKTHROUGH STRESS, σ_B MN/m^2 (KSI)	INITIAL FLAW DEPTH, a_i mm (INCH)	INITIAL FLAW LENGTH, $(2c)_i$ mm (INCH)	$\frac{\text{INITIAL FLAW DEPTH}}{\text{GAGE THICKNESS}}$, (a/t)	$\frac{\text{INITIAL FLAW DEPTH}}{\text{INITIAL FLAW LENGTH}}$, $(a/2c)_i$	σ_B/σ_Y [1]	σ_G/σ_Y [1]	IRWIN'S APPARENT K AT BREAKTHROUGH MN/m$^{3/2}$ (KSI$\sqrt{\text{IN}}$)
SAN 6-05-1	1.62 (0.0638)	88.9 (3.5000)	57°	LN_2 @ 78°K (-320°F)	249.5 (36.18)	119.8 (17.38)	210.9 (30.45)	1.02 (0.040)	16.12 (0.635)	0.627	0.063	0.92	1.10	14.1 (12.8)
SAN 6-05-2	1.65 (0.0650)	127.0 (5.0010)	32°		257.1 (37.29)	114.6 (16.62)	182.4 (26.46)	1.17 (0.046)	22.35 (0.880)	0.708	0.052	0.80	1.13	12.9 (11.7)
SAN 6-05-3	1.63 (0.0640)	152.3 (5.9972)	62°		269.5 (39.08)	98.5 (14.28)	181.5 (26.32)	1.32 (0.052)	25.91 (1.020)	0.813	0.051	0.80	1.18	13.6 (12.4)
SAN 6-05-4	1.65 (0.0650)	152.5 (6.0030)	40°		271.4 (39.36)	87.5 (12.69)	171.4 (24.86)	1.35 (0.053)	25.65 (1.010)	0.815	0.052	0.75	1.19	12.9 (11.7)
SAN 6-1-1	1.64 (0.0644)	88.98 (3.5030)	39°		305.7 (44.33)	135.2 (19.61)	273.2 (39.63)	0.74 (0.029)	5.33 (0.210)	0.450	0.138	1.20	1.34	14.7 (13.4)
SAN 6-1-2	1.58 (0.0621)	89.02 (3.5050)	68°		275.5 (39.96)	166.3 (24.12)	227.5 (33.00)	1.19 (0.047)	7.37 (0.290)	0.757	0.162	1.00	1.21	15.2 (13.8)
SAN 6-1-3	1.57 (0.0618)	89.08 (3.5070)	86°		269.6 (39.09)	—	136.5 (19.84)	1.50 (0.059)	9.78 (0.385)	0.955	0.153	0.60	1.18	9.7 (8.8)
SAN 6-1-4	1.67 (0.0658)	88.97 (3.5027)	29°		293.7 (42.60)	87.5 (12.69)	206.4 (29.93)	1.35 (0.053)	9.14 (0.360)	0.805	0.147	0.91	1.29	14.6 (13.3)
SAN 6-3-1	1.58 (0.0624)	89.05 (3.5058)	43°		284.9 (41.32)	187.5 (27.19)	263.7 (38.25)	0.76 (0.030)	2.62 (0.103)	0.481	0.291	1.16	1.25	12.2 (11.1)
SAN 6-3-2	1.60 (0.0630)	89.09 (3.5075)	48°		297.9 (43.21)	168.7 (24.47)	279.5 (40.54)	0.94 (0.037)	3.68 (0.145)	0.587	0.255	1.23	1.31	14.8 (13.5)
SAN 6-3-3	1.61 (0.0635)	89.12 (3.5085)	53°		281.6 (40.84)	138.2 (20.05)	227.7 (33.03)	1.32 (0.052)	4.65 (0.183)	0.819	0.284	1.00	1.24	13.8 (12.6)
SAN 6-3-4	1.61 (0.0633)	88.93 (3.5012)	20°		304.3 (44.13)	112.0 (16.25)	225.0 (32.63)	1.32 (0.052)	4.70 (0.185)	0.822	0.281	0.99	1.34	13.7 (12.5)
SAN 6-3-5	1.58 (0.0624)	88.83 (3.4972)	—		327.0 (47.43)	[2]	253.1 (36.71)	1.40 (0.055)	5.00 (0.197)	0.881	0.279	1.11	1.44	15.9 (14.5)

[1] σ_Y = 227.5 MN/m^2 (33.0 KSI)

[2] DIMPLING COULD NOT BE DETERMINED BECAUSE OF STRAIN GAGE FAILURE.

Table 23: STATIC FRACTURE TESTS — LIQUID NITROGEN TEMPERATURE 2219-T87 WELDMENT , t = 2.67 mm (0.105 INCH)

SPECIMEN			TEST		FRACTURE DATA									
NUMBER	GAGE THICKNESS, t mm (INCH)	GAGE WIDTH, w mm (INCH)	DIMPLING GAGE LOCATION FROM CRACK TIP	ENVIRONMENT	FAILURE STRESS, σ_G MN/m^2 (KSI)	DIMPLING STRESS, σ_D MN/m^2 (KSI)	BREAKTHROUGH STRESS, σ_B MN/m^2 (KSI)	INITIAL FLAW DEPTH, a_i mm (INCH)	INITIAL FLAW LENGTH, $(2c)_i$ mm (INCH)	INITIAL FLAW DEPTH / GAGE THICKNESS, $(a/t)_i$	INITIAL FLAW DEPTH / INITIAL FLAW LENGTH, $(a/2c)_i$	σ_B/σ_Y [1]	σ_G/σ_Y [1]	IRWIN'S APPARENT K AT BREAKTHROUGH MN/m$^{3/2}$ (KSI$\sqrt{IN}$)
SAN 1-05-1	2.69 (0.1058)	152.2 (5.9940)	46°	LN_2 @ 78°K (-320°F)	255.5 (37.05)	138.1 (20.03)	239.2 (34.69)	1.35 (0.053)	29.97 (1.180)	0.501	0.045	1.14	1.22	19.0 (17.3)
SAN 1-05-2	2.75 (0.1081)	228.7 (9.004)	54°		236.8 (34.34)	45.4 (6.58)	134.6 (19.52)	2.29 (0.090)	44.45 (1.750)	0.833	0.051	0.59	1.13	13.0 (11.8)
SAN 1-05-3	2.66 (0.1048)	241.4 (9.505)	35°		228.4 (33.13)	67.2 (9.74)	141.9 (20.58)	2.26 (0.089)	48.26 (1.900)	0.849	0.047	0.62	1.09	13.7 (12.5)
SAN 1-05-4	2.74 (0.1080)	228.7 (9.002)	35°		274.5 (39.81)	107.1 (15.53)	188.0 (27.26)	1.83 (0.072)	36.83 (1.450)	0.667	0.050	0.83	1.31	16.9 (15.4)
SAN 1-1-1	2.72 (0.1069)	127.1 (5.0030)	56°		300.4 (43.57)	156.0 (22.63)	265.5 (38.51)	1.37 (0.054)	9.02 (0.355)	0.505	0.152	1.27	1.43	19.2 (17.5)
SAN 1-1-2	2.69 (0.1060)	127.1 (5.0043)	48°		295.1 (42.80)	120.9 (17.53)	232.0 (33.65)	1.85 (0.073)	12.57 (0.495)	0.689	0.147	1.11	1.41	19.7 (17.9)
SAN 1-1-3	2.78 (0.1093)	127.1 (5.0042)	42°		280.8 (40.73)	86.3 (12.52)	189.1 (27.42)	2.21 (0.087)	15.75 (0.620)	0.796	0.140	0.90	1.34	17.3 (15.7)
SAN 1-1-4	2.78 (0.1096)	127.1 (5.0052)	42°		280.9 (40.74)	68.5 (9.93)	198.0 (28.71)	2.06 (0.081)	13.72 (0.540)	0.739	0.150	0.94	1.34	17.4 (15.8)
SAN 1-1-5	2.73 (0.1075)	127.2 (5.0065)	47°		280.6 (40.69)	103.1 (14.96)	202.4 (29.36)	2.13 (0.084)	14.22 (0.560)	0.781	0.150	0.97	1.34	18.2 (16.6)
SAN 1-3-1	2.43 (0.0955)	89.10 (3.5080)	35°		296.4 (42.99)	159.5 (23.13)	277.9 (40.30)	1.35 (0.053)	4.70 (0.185)	0.555	0.286	1.33	1.41	17.0 (15.5)
SAN 1-3-2	2.45 (0.0965)	89.04 (3.5055)	47°		277.2 (40.20)	131.1 (19.01)	244.6 (35.47)	1.63 (0.064)	5.97 (0.235)	0.663	0.272	1.17	1.32	16.7 (15.2)
SAN 1-3-3	2.50 (0.0985)	89.09 (3.5075)	73°		273.4 (39.65)	—	167.6(EST) (24.31)	2.24 (0.088)	8.13 (0.320)	0.893	0.275	0 30	1.30	13.0 (11.8)
SAN 1-3-4	2.63 (0.1052)	125.1 (5.0050)	43°		297.9 (43.21)	116.5 (16.90)	216.1 (31.34)	2.10 (0.084)	7.25 (0.290)	0.798	0.290	1.03	1.42	16.6 (15.1)
SAN 1-3-5	2.69 (0.1075)	125.2 (5.0061)	42°		315.2 (45.71)	119.8 (17.37)	243.4 (35.30)	2.13 (0.085)	7.48 (0.299)	0.791	0.284	1.16	1.50	18.9 (17.2)
SAN 1-3-6	2.65 (0.1043)	127.2 (5.0072)	17°		316.8 (45.95)	149.2 (21.64)	204.6 (29.68)	2.16 (0.085)	7.92 (0.312)	0.815	0.272	0.98	1.51	16.0 (14.6)

[1] σ_Y = 209.6 MN/m^2 (30.4 KSI)

Table 24: STATIC FRACTURE TESTS – LIQUID NITROGEN TEMPERATURE 2219-T87 WELDMENT, t = 7.62 mm (0.30 In.)

SPECIMEN			TEST		FRACTURE DATA										
NUMBER	GAGE THICKNESS, t mm (INCH)	GAGE WIDTH, w mm (INCH)	DIMPLING GAGE LOCATION FROM CRACK TIP	ENVIRONMENT	FAILURE STRESS, σ_G MN/m^2 (KSI)	DIMPLING STRESS, σ_D MN/m^2 (KSI)	BREAKTHROUGH STRESS, σ_B MN/m^2 (KSI)	INITIAL FLAW DEPTH, a_i mm (INCH)	INITIAL FLAW LENGTH, $(2c)_i$ mm (INCH)	$\frac{\text{INITIAL FLAW DEPTH}}{\text{GAGE THICKNESS}}$, (a/t)	$\frac{\text{INITIAL FLAW DEPTH}}{\text{INITIAL FLAW LENGTH}}$, $(a/2c)_i$	σ_B/σ_Y [1]	σ_G/σ_Y [1]	IRWIN'S APPARENT K AT BREAKTHROUGH MN/m$^{3/2}$ (KSI$\sqrt{\text{IN}}$)
SAN 3-1-1	7.57 (0.2980)	228.9 (9.010)	48°	LN_2 @ 78°K (-320°F)	214.4 (31.10)	96.3 (13.97)	—	3.81 (0.150)	24.38 (0.960)	0.503	0.156	—	0.98	25.7 (23.4)
SAN 3-1-2	7.63 (0.3002)	228.7 (9.005)	54°		196.4 (28.49)	83.2 (12.06)	181.1 (26.27)	5.59 (0.220)	34.80 (1.37)	0.733	0.161	0.79	0.90	25.4 (23.1)
SAN 3-1-3	7.66 (0.3015)	228.7 (9.005)	49°		186.6 (27.07)	57.6 (8.36)	152.4 (22.10)	6.60 (0.260)	42.67 (1.68)	0.862	0.155	0.65	0.85	23.0 (20.9)
SAN 3-1-4	7.62 (0.3000)	228.6 (9.000)	62°		216.4 (31.39)	138.6 (20.11)	203.0 (29.44)	5.36 (0.211)	36.96 (1.455)	0.703	0.145	0.93	0.99	28.9 (26.3)
SAN 3-1-5	7.62 (0.3000)	228.7 (9.004)	24°		247.3 (35.87)	212.9 (30.88)	—	3.73 (0.147)	25.27 (0.995)	0.490	0.148	—	1.13	29.7 (27.0)
SAN 3-2-1	7.70 (0.3033)	127.1 (5.0045)	49°		224.0 (32.49)	122.2 (17.72)	214.0 (31.03)	5.03 (0.198)	22.61 (0.890)	0.653	0.222	0.98	1.02	27.3 (24.8)
SAN 3-2-2	8.97 (0.3530)	127.1 (5.0047)	35°		213.1 (30.91)	120.6 (17.49)	199.1 (28.87)	6.10 (0.240)	26.92 (1.060)	0.680	0.226	0.91	0.98	27.5 (25.0)
SAN 3-3-1	7.62 (0.3000)	127.0 (5.0016)	46°		247.7 (35.92)	142.2 (20.63)	—	3.81 (0.150)	12.70 (0.500)	0.500	0.300	—	1.13	25.1 (22.8)
SAN 3-3-2	7.75 (0.3053)	127.1 (5.0021)	44°		231.6 (33.59)	112.0 (16.24)	—	5.08 (0.200)	17.40 (0.685)	0.655	0.292	—	1.06	27.4 (24.9)
SAN 3-3-3	7.54 (0.2968)	127.1 (5.0030)	26°		213.1 (30.91)	114.4 (16.59)	182.9 (26.53)	6.48 (0.255)	22.73 (0.895)	0.859	0.285	0.84	0.98	24.1 (21.9)
SAN 3-3-4	7.69 (0.3026)	127.1 (5.0041)	44°		228.4 (33.13)	111.6 (16.18)	209.5 (30.38)	5.84 (0.230)	20.57 (0.810)	0.760	0.284	0.96	1.05	26.6 (24.2)
SAN 3-5-1	7.65 (0.3010)	88.87 (3.4990)	47°		262.5 (38.07)	161.7 (23.45)	—	3.63 (0.143)	8.00 (0.315)	0.475	0.454	—	1.20	21.7 (19.7)
SAN 3-5-2	7.66 (0.3017)	88.89 (3.4996)	48°		244.2 (35.42)	131.6 (19.09)	—	4.95 (0.195)	10.97 (0.432)	0.646	0.451	—	1.12	23.5 (21.4)
SAN 3-5-3	7.64 (0.3008)	88.96 (3.5022)	23°		226.4 (32.84)	139.4 (20.22)	216.0 (31.32)	6.35 (0.250)	14.35 (0.565)	0.831	0.442	0.99	1.04	23.8 (21.7)
SAN 3-5-4	7.61 (0.2995)	88.96 (3.5025)	15°		212.4 (30.81)	122.5 (17.77)	189.3 (27.45)	6.68 (0.263)	14.73 (0.580)	0.878	0.453	0.87	0.97	20.9 (19.0)

[1] σ_Y = 218.6 MN/m^2 (31.7 KSI)

Table 25: *STATIC FRACTURE TESTS — LIQUID NITROGEN TEMPERATURE 2219-T87 WELDMENT , t = 1.60 mm (0.063 In.)*

SPECIMEN			TEST		FRACTURE DATA									
NUMBER	GAGE THICKNESS, t mm (INCH)	GAGE WIDTH, w mm (INCH)	DIMPLING GAGE LOCATION FROM CRACK TIP	ENVIRONMENT	FAILURE STRESS, σ_G MN/m^2 (KSI)	DIMPLING STRESS, σ_D MN/m^2 (KSI)	BREAKTHROUGH STRESS, σ_B MN/m^2 (KSI)	INITIAL FLAW DEPTH, a_i mm (INCH)	INITIAL FLAW LENGTH, $(2c)_i$ mm (INCH)	$\frac{\text{INITIAL FLAW DEPTH}}{\text{GAGE THICKNESS}}$, $(a/t)_i$	$\frac{\text{INITIAL FLAW DEPTH}}{\text{INITIAL FLAW LENGTH}}$, $(a/2c)_i$	σ_B/σ_Y [1]	σ_G/σ_Y [1]	IRWIN'S APPARENT K AT BREAKTHROUGH MN/m$^{3/2}$ (KSI$\sqrt{\text{IN}}$)
SAH 6-05-1	1.65 (0.0649)	88.88 (3.4992)	46°	LH_2 @ 20°K (−423°F)	267.9 (38.86)	177.6 (25.76)	264.1 (38.31)	0.89 (0.035)	15.75 (0.620)	0.539	0.056	0.88	0.89	16.5 (15.0)
SAH 6-05-2	1.57 (0.0620)	127.0 (4.9982)	48°		256.4 (37.19)	141.3 (20.49)	209.1 (30.33)	1.09 (0.043)	22.61 (0.890)	0.694	0.048	0.70	0.85	14.1 (12.8)
SAH 6-05-3	1.65 (0.0650)	152.1 (5.9890)	77°		257.7 (37.37)	—	168.2 (29.40)	1.32 (0.052)	26.16 (1.030)	0.800	0.050	0.56	0.86	12.2 (11.1)
SAH 6-05-4	1.64 (0.0645)	88.88 (3.4992)	13°		295.6 (42.87)	201.6 (29.24)	—	0.38 (0.015)	10.16 (0.400)	0.233	0.038	—	0.99	12.5 (11.4)
SAH 6-1-1	1.61 (0.0634)	88.79 (3.4958)	54°		273.0 (39.60)	160.9 (23.33)	253.6 (36.78)	0.79 (0.031)	5.46 (0.215)	0.489	0.144	0.85	0.91	13.6 (12.4)
SAH 6-1-2	1.54 (0.0608)	89.07 (3.5068)	77°		284.6 (41.28)	—	189.2 (27.44)	1.50 (0.059)	7.49 (0.295)	0.970	0.200	0.63	0.95	12.9 (11.7)
SAH 6-1-3	1.56 (0.0614)	89.05 (3.5060)	85°		263.4 (38.20)	—	185.6 (26.94)	1.37 (0.054)	9.65 (0.380)	0.879	0.142	0.62	0.88	12.7 (11.6)
SAH 6-1-4	1.61 (0.0632)	88.91 (3.5002)	31°		275.9 (40.01)	166.8 (24.19)	224.4 (32.55)	1.14 (0.045)	7.11 (0.280)	0.712	0.161	0.75	0.92	14.1 (12.8)
SAH 6-3-1	1.59 (0.0626)	89.03 (3.5050)	47°		319.0 (46.26)	179.1 (25.98)	308.0 (44.67)	0.71 (0.028)	2.67 (0.105)	0.447	0.267	1.03	1.06	14.1 (12.8)
SAH 6-3-2	1.60 (0.0630)	89.06 (3.5063)	45°		263.4 (38.93)	193.5 (28.07)	252.8 (36.67)	1.07 (0.042)	3.76 (0.148)	0.667	0.284	0.84	0.89	13.5 (12.3)
SAH 6-3-3	1.57 (0.0620)	89.00 (3.5040)	68°		250.0 (36.26)	128.6 (18.65)	201.6(EST) (29.24)	1.47 (0.058)	4.88 (0.192)	0.935	0.302	0.67	0.83	12.2 (11.1)

[1] σ_Y = 299.9 MN/m^2 (43.5 KSI)

Table 26: STATIC FRACTURE TESTS — LIQUID NITROGEN TEMPERATURE 2219-T87 WELDMENT , t = 2.67 mm (0.105 In.)

SPECIMEN			TEST		FRACTURE DATA									
NUMBER	GAGE THICKNESS, t mm (INCH)	GAGE WIDTH, w mm (INCH)	DIMPLING GAGE LOCATION FROM CRACK TIP	ENVIRONMENT	FAILURE STRESS, σ_G MN/m^2 (KSI)	DIMPLING STRESS, σ_D MN/m^2 (KSI)	BREAKTHROUGH STRESS, σ_B MN/m^2 (KSI)	INITIAL FLAW DEPTH, a_i mm (INCH)	INITIAL FLAW LENGTH, $(2c)_i$ mm (INCH)	$\frac{\text{INITIAL FLAW DEPTH}}{\text{GAGE THICKNESS}}$, $(a/t)_i$	$\frac{\text{INITIAL FLAW DEPTH}}{\text{INITIAL FLAW LENGTH}}$, $(a/2c)_i$	σ_B/σ_Y [1]	σ_G/σ_Y [1]	IRWIN'S APPARENT K AT BREAKTHROUGH MN/m$^{3/2}$ (KSI$\sqrt{\text{IN}}$)
SAH 1-05-1	2.66 (0.1048)	152.3 (5.9965)	31°	LH_2 @ 20°K (−423°F)	250.7 (36.36)	193.7 (28.09)	221.7 (32.15)	1.52 (0.060)	28.70 (1.130)	0.573	0.053	0.75	0.85	17.7 (16.1)
SAH 1-05-2	2.65 (0.1044)	228.7 (9.005)	15°		234.0 (33.94)	—	216.4 (31.38)	1.70 (0.067)	37.85 (1.490)	0.642	0.045	0.73	0.79	18.2 (16.6)
SAH 1-05-3	2.62 (0.1030)	241.4 (9.505)	62°		231.3 (33.55)	102.5 (14.86)	172.6 (25.03)	2.13 (0.084)	46.99 (1.850)	0.816	0.045	0.58	0.78	15.9 (14.5)
SAH 1-05-4	2.74 (0.1079)	127.1 (5.0047)	52°		261.7 (37.96)	186.4 (27.04)	255.4 (37.04)	1.17 (0.046)	22.35 (0.880)	0.426	0.052	0.87	0.89	18.2 (16.6)
SAH 1-1-1	2.69 (0.1058)	127.1 (5.0040)	43°		312.6 (45.33)	173.2 (25.12)	295.7 (42.88)	1.40 (0.055)	9.32 (0.367)	0.520	0.150	1.00	1.06	21.7 (19.7)
SAH 1-1-2	2.63 (0.1035)	127.1 (5.0044)	41°		280.8 (40.73)	153.1 (22.20)	250.2 (36.29)	1.85 (0.073)	12.57 (0.495)	0.705	0.147	0.85	0.95	20.6 (18.7)
SAH 1-1-3	2.57 (0.1010)	127.1 (5.0020)	63°		270.9 (39.29)	117.4 (17.02)	188.4 (27.32)	2.29 (0.090)	16.13 (0.635)	0.891	0.142	0.64	0.92	16.8 (15.3)
SAH 1-1-4	2.79 (0.1098)	127.0 (4.9994)	48°		283.9 (41.17)	161.4 (23.41)	245.0 (35.53)	1.60 (0.063)	10.54 (0.415)	0.574	0.152	0.83	0.96	18.6 (16.9)
SAH 1-3-1	2.51 (0.0990)	89.00 (3.5040)	62°		295.2 (42.81)	199.1 (28.88)	287.2 (41.65)	1.45 (0.057)	4.83 (0.190)	0.576	0.300	0.97	1.00	17.8 (16.2)
SAH 1-3-2	2.55 (0.1005)	89.08 (3.5072)	60°		255.3 (37.02)	151.6 (21.99)	240.6 (34.89)	1.75 (0.069)	6.12 (0.241)	0.687	0.286	0.82	0.86	16.4 (14.9)
SAH 1-3-3	2.62 (0.1030)	89.05 (3.5058)	82°		282.6 (40.99)	161.3 (23.40)	236.8 (34.34)	2.18 (0.086)	7.87 (0.310)	0.835	0.277	0.80	0.96	18.1 (16.5)
SAH 1-3-4	2.62 (0.1033)	127.1 (5.0041)	50°		324.1 (47.01)	126.7 (18.38)	300.1 (43.53)	1.75 (0.069)	5.84 (0.230)	0.668	0.300	1.02	1.10	20.6 (18.7) [2]
SAH 1-3-5	2.80 (0.1102)	127.1 (5.0050)	28°		273.7 (39.70)	123.1 (17.86)	230.0 (33.36)	2.18 (0.086)	7.67 (0.302)	0.780	0.285	0.78	0.93	17.5 (15.9)

[1] σ_Y = 295.1 MN/m^2 (42.8 KSI)

[2] LOADS ESTIMATED, CRYOSTAT INTERFERED WITH LOADING

Table 27: ***STATIC FRACTURE TESTS — LIQUID HYDROGEN TEMPERATURE 2219-T87 WELDMENT, t = 7.62 mm (0.30 In.)***

SPECIMEN			TEST		FRACTURE DATA									
NUMBER	GAGE THICKNESS, t mm (INCH)	GAGE WIDTH, w mm (INCH)	DIMPLING GAGE LOCATION FROM CRACK TIP	ENVIRONMENT	FAILURE STRESS, σ_G MN/m^2 (KSI)	DIMPLING STRESS, σ_D MN/m^2 (KSI)	BREAKTHROUGH STRESS, σ_B MN/m^2 (KSI)	INITIAL FLAW DEPTH, a_i mm (INCH)	INITIAL FLAW LENGTH, $(2c)_i$ mm (INCH)	$\frac{\text{INITIAL FLAW DEPTH}}{\text{GAGE THICKNESS}}$, $(a/t)_i$	$\frac{\text{INITIAL FLAW DEPTH}}{\text{INITIAL FLAW LENGTH}}$, $(a/2c)_i$	σ_B/σ_Y [1]	σ_G/σ_Y [1]	IRWIN'S APPARENT K AT BREAKTHROUGH MN/m$^{3/2}$ (KSI$\sqrt{\text{IN}}$)
SAH 3-1-1	7.58 (0.2985)	228.7 (9.005)	46°	LH_2 @ 20°K (-423°F)	250.8 (36.37)	166.0 (24.07)	248.8 (36.09)	3.63 (0.143)	24.89 (0.980)	0.479	0.146	0.93	0.93	29.1 (26.5)
SAH 3-1-2	7.66 (0.3015)	228.7 (9.004)	43°		214.0 (31.03)	117.1 (16.99)	207.2 (30.05)	5.33 (0.210)	34.54 (1.360)	0.697	0.154	0.77	0.80	28.4 (25.8)
SAH 3-1-3	7.66 (0.3015)	228.7 (9.005)	48°		189.2 (27.44)	82.3 (11.93)	142.2 (20.63)	6.68 (0.263)	42.93 (1.690)	0.872	0.156	0.53	0.71	21.1 (19.2)
SAH 3-3-2	7.64 (0.3008)	127.1 (5.0036)	34°		271.5 (39.37)	180.9 (26.24)	—	2.59 (0.102)	12.95 (0.510)	0.339	0.200	—	1.01	25.6 (23.3)
SAH 3-3-1	7.61 (0.2998)	127.1 (5.0020)	47°		257.5 (37.34)	174.7 (25.34)	252.9 (36.68)	3.68 (0.145)	12.70 (0.500)	0.484	0.290	0.94	0.96	25.3 (23.0)
SAH 3-3-3	7.57 (0.2982)	127.1 (5.0039)	36°		209.3 (30.35)	127.1 (18.43)	205.6 (29.82)	6.43 (0.253)	22.48 (0.885)	0.848	0.286	0.77	0.78	26.6 (24.2)
SAH 3-3-4	7.59 (0.2990)	89.0 (3.5023)	49°		220.6 (31.99)	185.7 (26.93)	217.3 (31.51)	5.08 (0.200)	17.40 (0.685)	0.669	0.292	0.81	0.82	24.9 (22.7)
SAH 3-3-5	7.64 (0.3008)	88.9 (3.5022)	45°		238.9 (34.65)	160.4 (23.26)	—	4.06 (0.160)	14.61 (0.575)	0.532	0.278	—	0.89	25.2 (22.9)
SAH 3-5-1	7.63 (0.3003)	88.92 (3.5008)	42°		272.1 (39.47)	205.3 (29.77)	—	3.56 (0.140)	7.82 (0.308)	0.466	0.455	—	1.02	22.2 (20.2)
SAH 3-5-2	7.63 (0.3004)	88.91 (3.5002)	48°		245.9 (35.66)	169.2 (24.54)	242.6 (35.19)	4.70 (0.185)	10.92 (0.430)	0.616	0.430	0.90	0.92	23.1 (21.0)
SAH 3-5-3	7.67 (0.3020)	88.90 (3.5000)	30°		221.8 (32.17)	155.3 (22.52)	208.7 (30.27)	6.43 (0.253)	14.22 (0.560)	0.838	0.452	0.78	0.83	22.4 (20.4)

[1] σ_Y = 268.2 MN/m^2 (38.9 KSI)

Table 28: *STATIC FRACTURE TESTS — ROOM TEMPERATURE 6Al-4V TITANIUM WELDMENT, t = 0.51 mm (0.020 In.)*

SPECIMEN			TEST		FRACTURE DATA											
NUMBER	GAGE THICKNESS, t mm (INCH)	GAGE WIDTH, w mm (INCH)	DIMPLING GAGE LOCATION FROM CRACK TIP	ENVIRONMENT	FAILURE STRESS, σ_G MN/m^2 (KSI)	DIMPLING STRESS, σ_D MN/m^2 (KSI)	BREAKTHROUGH STRESS, σ_B MN/m^2 (KSI)	INITIAL FLAW DEPTH, a_i mm (INCH)	INITIAL FLAW LENGTH, $(2c)_i$ mm (INCH)	$\frac{\text{INITIAL FLAW DEPTH}}{\text{GAGE THICKNESS}}$, (a/t)	$\frac{\text{INITIAL FLAW DEPTH}}{\text{INITIAL FLAW LENGTH}}$, $(a/2c)_i$	σ_B/σ_Y [1]	σ_G/σ_Y [1]	IRWIN'S APPARENT K AT BREAKTHROUGH MN/m$^{3/2}$ (KSI$\sqrt{\text{IN}}$)	K_{CN} AT FINAL FAILURE MN/m$^{3/2}$ (KSI$\sqrt{\text{IN}}$)
STR 2-05-1	0.55 (0.0215)	30.54 (1.2025)	55°	AIR @ 295°K (72°F)	985.3 (142.9)	630.9 (91.5)	—	0.28 (0.011)	4.06 (0.160)	0.512	0.069	—	0.97	34.8 (31.7)	—
STR 2-05-2	0.55 (0.0217)	30.46 (1.1992)	—		912.2 (132.3)	[2]	801.2 (116.2)	0.41 (0.016)	5.84 (0.230)	0.696	0.070	0.79	0.90	32.9 (29.9)	—
STR 2-05-3	0.54 (0.0213)	30.50 (1.2008)	35°		764.7 (110.9)	368.9 (53.5)	600.6 (87.1)	0.43 (0.017)	7.37 (0.290)	0.798	0.059	0.59	0.75	24.8 (22.6)	—
STR 2-1-1	0.54 (0.0212)	30.47 (1.1998)	60°		1012.9 (146.9)	716.4 (103.9)	993.6 (144.1)	0.33 (0.013)	1.70 (0.067)	0.613	0.194	0.97	0.99	33.5 (30.5)	—
STR 2-1-2	0.52 (0.0204)	30.47 (1.1998)	70°		1012.9 (146.9)	—	900.5 (130.6)	0.41 (0.016)	2.34 (0.092)	0.784	0.174	0.88	0.99	33.8 (30.8)	—
STR 2-1-3	0.49 (0.0192)	30.46 (1.1996)	5°		944.6 (137.0)	—	877.7 (127.3)	0.41 (0.016)	3.05 (0.120)	0.833	0.133	0.86	0.93	34.4 (31.3)	—
STR 2-3-1	0.49 (0.0192)	30.51 (1.2013)	24°		1074.2 (155.8)	886.7 (128.6)	—	0.20 (0.008)	0.76 (0.030)	0.417	0.267	—	1.05	26.2 (23.8)	—
STR 2-3-2	0.53 (0.0208)	30.44 (1.1985)	0°		1006.7 (146.0)	840.5 (121.9)	966.7 (140.2)	0.33 (0.013)	1.22 (0.048)	0.625	0.271	0.95	0.99	29.6 (26.9)	—
STR 2-3-3	0.56 (0.0219)	30.58 (1.2038)	83°		1057.7 (153.4)	—	1031.5 (149.6)	0.48 (0.019)	1.40 (0.055)	0.868	0.345	1.01	1.04	35.2 (32.0)	—
STR 2-3-4	0.56 (0.0222)	30.42 (1.1978)	—		977.0 (141.7)	[2]	937.7 (136.0)	0.46 (0.018)	1.37 (0.054)	0.811	0.333	0.92	0.96	31.2 (28.4)	—
STR 2-5-1	0.55 (0.0215)	30.52 (1.2015)	41°		1117.0 (162.0)	974.3 (141.3)	—	0.25 (0.010)	0.58 (0.023)	0.465	0.435	—	1.10	24.8 (22.6)	—
STR 2-5-2	0.50 (0.0198)	30.48 (1.2000)	70°		1115.6 (161.8)	932.9 (135.3)	1089.4 (158.0)	0.38 (0.015)	0.81 (0.032)	0.757	0.469	1.07	1.09	28.6 (26.0)	—
STR 2-5-3	0.55 (0.0215)	30.48 (1.2001)	78°		1035.6 (150.2)	915.7 (132.8)	—	0.43 (0.017)	0.99 (0.039)	0.791	0.436	—	1.02	30.0 (27.3)	—

[1] σ_Y = 1020 MN/m^2 (147.9 KSI)

[2] NOT INSTRUMENTED FOR DIMPLING

Table 29: STATIC FRACTURE TESTS – ROOM TEMPERATURE 6Al-4V TITANIUM WELDMENT, t = 1.78mm (0.070 INCH)

SPECIMEN			TEST		FRACTURE DATA										
NUMBER	GAGE THICKNESS, t mm (INCH)	GAGE WIDTH, w mm (INCH)	DIMPLING GAGE LOCATION FROM CRACK TIP	ENVIRONMENT	FAILURE STRESS, σ_G MN/m^2 (KSI)	DIMPLING STRESS, σ_D MN/m^2 (KSI)	BREAKTHROUGH STRESS, σ_B MN/m^2 (KSI)	INITIAL FLAW DEPTH, a_i mm (INCH)	INITIAL FLAW LENGTH, $(2c)_i$ mm (INCH)	$\frac{\text{INITIAL FLAW DEPTH}}{\text{GAGE THICKNESS}}$, (a/t)	$\frac{\text{INITIAL FLAW DEPTH}}{\text{INITIAL FLAW LENGTH}}$, $(a/2c)_i$	σ_B/σ_Y [1]	σ_G/σ_Y [1]	IRWIN'S APPARENT K AT BREAKTHROUGH MN/m$^{3/2}$ (KSI$\sqrt{\text{IN}}$)	K_{CN} AT FINAL FAILURE MN/m$^{3/2}$ (KSI$\sqrt{\text{IN}}$)
STR 8-1-1	1.81 (0.0712)	63.41 (2.4965)	37°	AIR @ 295°K (72°F)	991.5 (143.8)	785.3 (113.9)	—	0.84 (0.033)	5.92 (0.233)	0.463	0.142	—	0.96	56.4 (51.3)	—
STR 8-1-2	1.84 (0.0725)	44.63 (1.7570)	43°		795.7 (115.4)	503.3 (73.0)	773.6 (112.2)	1.32 (0.052)	8.38 (0.330)	0.717	0.158	0.75	0.77	52.3 (47.6)	—
STR 8-1-3	1.74 (0.0686)	44.67 (1.7588)	48°		737.1 (106.9)	319.9 (46.4)	599.9 (87.0)	1.45 (0.057)	10.54 (0.415)	0.831	0.137	0.58	0.71	42.4 (38.6)	—
STR 8-1-4	1.70 (0.0670)	44.44 (1.7496)	27°		829.5 (120.3)	639.9 (92.8)	—	1.09 (0.043)	7.75 (0.305)	0.642	0.141	—	0.80	52.3 (47.6)	—
STR 8-3-1	1.79 (0.0705)	31.72 (1.2490)	54°		1037.7 (150.5)	940.5 (136.4)	—	0.84 (0.033)	2.84 (0.112)	0.468	0.295	—	1.00	49.6 (45.1)	—
STR 8-3-2	1.84 (0.0723)	31.67 (1.2468)	49°		991.5 (143.8)	741.9 (107.6)	—	1.17 (0.046)	3.94 (0.155)	0.636	0.297	—	0.96	55.4 (50.4)	—
STR 8-3-3	1.78 (0.0702)	31.65 (1.2462)	37°		892.9 (129.5)	567.5 (82.3)	827.4 (120.0)	1.45 (0.057)	4.83 (0.190)	0.812	0.300	0.80	0.86	50.2 (45.7)	—
STR 8-3-4	1.70 (0.0668)	31.95 (1.2577)	—		886.7 (128.6)	[2]	746.7 (108.3)	1.45 (0.057)	5.21 (0.205)	0.853	0.278	0.72	0.86	46.2 (42.0)	—
STR 8-5-1	1.78 (0.0700)	20.17 (0.7940)	51°		1096.3 (159.0)	738.5 (107.1)	—	0.81 (0.032)	1.70 (0.067)	0.457	0.478	—	1.06	41.7 (37.9)	—
STR 8-5-2	1.78 (0.0702)	20.41 (0.8034)	58°		1045.3 (151.6)	926.0 (134.3)	1036.3 (150.3)	1.14 (0.045)	2.46 (0.097)	0.641	0.464	1.00	1.01	47.4 (43.1)	—
STR 8-5-3	1.80 (0.0708)	20.31 (0.7997)	56°		969.4 (140.6)	614.3 (89.1)	957.7 (138.9)	1.52 (0.060)	3.23 (0.127)	0.847	0.472	0.93	0.94	49.7 (45.2)	—
STR 8-5-4	1.81 (0.0712)	31.94 (1.2573)	—		900.5 (130.6)	[2]	834.3 (121.0)	1.55 (0.061)	3.68 (0.145)	0.857	0.421	0.81	0.87	45.7 (41.6)	—

[1] σ_Y = 1035 MN/m^2 (150.1 KSI)

[2] NOT INSTRUMENTED FOR DIMPLING

Table 30: STATIC FRACTURE TESTS ROOM TEMPERATURE 6Al-4V TITANIUM WELDMENT, t = 5.33 mm (0.21 INCH)

SPECIMEN			TEST		FRACTURE DATA											
NUMBER	GAGE THICKNESS, t mm (INCH)	GAGE WIDTH, w mm (INCH)	DIMPLING GAGE LOCATION FROM CRACK TIP	ENVIRONMENT	FAILURE STRESS, σ_G MN/m^2 (KSi)	DIMPLING STRESS, σ_D MN/m^2 (KSI)	BREAKTHROUGH STRESS, σ_B MN/m^2 (KSI)	INITIAL FLAW DEPTH, a_i mm (INCH)	INITIAL FLAW LENGTH, $(2c)_i$ mm (INCH)	$\frac{\text{INITIAL FLAW DEPTH}}{\text{GAGE THICKNESS}}$, $(a/t)_i$	$\frac{\text{INITIAL FLAW DEPTH}}{\text{INITIAL FLAW LENGTH}}$, $(a/2c)_i$	σ_B/σ_Y [1]	σ_G/σ_Y [1]	IRWIN'S APPARENT K AT BREAKTHROUGH MN/m$^{3/2}$ (KSI$\sqrt{\text{IN}}$)	K_{CN} AT FINAL FAILURE MN/m$^{3/2}$ (KSI$\sqrt{\text{IN}}$)
STR 21-1-1	5.25 (0.2068)	76.35 (3.0061)	52°	AIR @ 295°K (72°F)	863.2 (125.2)	[2]	—	2.62 (0.103)	18.54 (0.730)	0.498	0.141	—	0.90	85.7 (78.0)	—
STR 21-1-2	5.30 (0.2086)	153.17 (6.0302)	47°		731.6 (106.1)	501.3 (72.7)	715.7 (103.8)	3.56 (0.140)	24.77 (0.975)	0.671	0.144	0.74	0.76	80.6 (73.3)	146.7 (133.5)
STR 21-1-3	5.31 (0.2091)	152.37 (5.9990)	44°		623.3 (90.4)	241.3 (35.0)	477.1 (69.2)	4.70 (0.185)	29.59 (1.165)	0.885	0.159	0.50	0.65	59.0 (53.7)	137.6 (125.2)
STR 21-1-4	5.37 (0.2115)	76.36 (3.0063)	47°		981.2 (142.3)	877.0 (127.2)	—	1.75 (0.069)	11.56 (0.455)	0.326	0.152	—	1.02	80.4 (73.2)	—
STR 21-3-1	5.13 (0.2020)	45.57 (1.7942)	53°		901.9 (130.8)	779.8 (113.1)	—	2.72 (0.107)	9.19 (0.362)	0.530	0.296	—	0.94	76.7 (69.8)	—
STR 21-3-2	5.53 (0.2178)	76.48 (3.0111)	41°		867.4 (125.8)	630.9 (91.5)	—	3.68 (0.145)	12.83 (0.515)	0.666	0.282	—	0.90	86.9 (79.1)	—
STR 21-3-3	5.67 (0.2232)	76.35 (3.0058)	40°		770.9 (111.8)	—	—	4.62 (0.182)	16.59 (0.653)	0.815	0.279	—	0.80	85.7 (78.0)	—
STR 21-3-4	5.51 (0.2170)	76.26 (3.0025)	46°		948.1 (137.5)	793.6 (115.1)	—	2.64 (0.104)	9.25 (0.364)	0.479	0.286	—	0.99	81.1 (73.8)	—
STR 21-3-5	5.23 (0.2060)	152.74 (6.0132)	43°		870.1 (126.2)	623.3 (90.4)	—	3.73 (0.147)	13.34 (0.525)	0.714	0.280	—	0.91	88.0 (80.1)	—
STR 21-3-6	5.30 (0.2086)	152.86 (6.0180)	27°		757.8 (109.9)	315.8 (45.8)	609.5 (88.4)	4.70 (0.185)	16.43 (0.647)	0.887	0.286	0.63	0.79	66.6 (60.6)	—

[1] σ_Y = 961.2 MN/m^2 (139.4 KSI)

[2] DIMPLING STRESS NOT OBTAINED BECAUSE OF STRAIN GAGE MALFUNCTION

Table 30: (Continued)

SPECIMEN			TEST		FRACTURE DATA											
NUMBER	GAGE THICKNESS, t mm (INCH)	GAGE WIDTH, w mm (INCH)	DIMPLING GAGE LOCATION FROM CRACK TIP	ENVIRONMENT	FAILURE STRESS, σ_G MN/m^2 (KSI)	DIMPLING STRESS, σ_D MN/m^2 (KSI)	BREAKTHROUGH STRESS, σ_B MN/m^2 (KSI)	INITIAL FLAW DEPTH, a_i mm (INCH)	INITIAL FLAW LENGTH, $(2c)_i$ mm (INCH)	$\frac{\text{INITIAL FLAW DEPTH}}{\text{GAGE THICKNESS}}$, (a/t)	$\frac{\text{INITIAL FLAW DEPTH}}{\text{INITIAL FLAW LENGTH}}$, $(a/2c)_i$	σ_B/σ_Y [1]	σ_G/σ_Y [1]	IRWIN'S APPARENT K AT BREAKTHROUGH MN/m$^{3/2}$ (KSI$\sqrt{\text{IN}}$)	K_{CN} AT FINAL FAILURE MN/m$^{3/2}$ (KSI$\sqrt{\text{IN}}$)
STR 21-5-2	4.88 (0.1922)	38.12 (1.5006)	51°	AIR @ 295°K (72°F)	853.6 (123.8)	568.8 (82.5)	—	3.61 (0.142)	7.75 (0.305)	0.739	0.466	—	0.89	68.5 (62.3)	—
STR 21-5-3	5.28 (0.2079)	45.82 (1.8040)	44°		755.3 (108.1)	503.3 (73.0)	739.8 (107.3)	4.50 (0.177)	9.55 (0.376)	0.851	0.471	0.77	0.78	65.2 (59.3)	—
STR 21-5-4	5.02 (0.1977)	38.36 (1.5102)	53°		939.0 (136.2)	895.0 (129.8)	—	2.62 (0.103)	5.61 (0.221)	0.521	0.466	—	0.98	64.6 (58.8)	—
STR 21-5-5	5.35 (0.2105)	76.26 (3.0025)	42°		981.8 (142.4)	849.5 (123.2)	—	2.62 (0.103)	5.69 (0.224)	0.489	0.460	—	1.02	68.2 (62.1)	—
STR 21-5-6	5.36 (0.2110)	76.25 (3.002)	40°		919.1 (133.3)	701.9 (101.8)	—	3.71 (0.146)	7.95 (0.313)	0.692	0.466	—	0.96	75.1 (68.3)	—
STR 21-5-7	5.64 (0.2220)	76.38 (3.0072)	36°		857.0 (124.3)	568.8 (82.5)	847.4 (122.9)	4.65 (0.183)	9.88 (0.389)	0.824	0.470	0.88	0.89	76.7 (69.8)	—

[1] σ_Y = 961.2 MN/m^2 (139.4 KSI)

Table 31: STATIC FRACTURE TESTS — LIQUID HYDROGEN TEMPERATURE 6Al-4V TITANIUM WELDMENT, t = 0.51mm (0.020 INCH)

SPECIMEN			TEST		FRACTURE DATA											
NUMBER	GAGE THICKNESS, t mm (INCH)	GAGE WIDTH, w mm (INCH)	DIMPLING GAGE LOCATION FROM CRACK TIP	ENVIRONMENT	FAILURE STRESS, σ_G MN/m^2 (KSI)	DIMPLING STRESS, σ_D MN/m^2 (KSI)	BREAKTHROUGH STRESS, σ_B MN/m^2 (KSI)	INITIAL FLAW DEPTH, a_i mm (INCH)	INITIAL FLAW LENGTH, $(2c)_i$ mm (INCH)	$\frac{\text{INITIAL FLAW DEPTH}}{\text{GAGE THICKNESS}}$, (a/t)	$\frac{\text{INITIAL FLAW DEPTH}}{\text{INITIAL FLAW LENGTH}}$, $(a/2c)_i$	σ_B/σ_Y [1]	σ_G/σ_Y [1]	IRWIN'S APPARENT K AT BREAKTHROUGH MN/m$^{3/2}$ (KSI$\sqrt{\text{IN}}$)	K_{CN} AT FINAL FAILURE MN/m$^{3/2}$ (KSI$\sqrt{\text{IN}}$)
STH 2-05-1	0.51 (0.0201)	30.49 (1.2002)	49°	LH_2 @ 20°K (-423°F)	1473.5 (213.7)	1259.0 (182.6)	1401.8 (203.3)	0.18 (0.007)	2.16 (0.085)	0.348	0.082	0.80	0.84	37.8 (34.4)	—
STH 2-05-2	0.56 (0.0219)	30.47 (1.1996)	—		1186.6 (172.1)	[2]	1061.8 (154.0)	0.23 (0.009)	3.05 (0.120)	0.411	0.075	0.60	0.67	31.7 (28.8)	82.6 (75.2)
STH 2-05-3	0.57 (0.0223)	30.44 (1.1985)	67°		948.8 (137.6)	—	877.7 (127.3)	0.33 (0.013)	4.95 (0.195)	0.583	0.067	0.50	0.54	31.2 (28.4)	85.1 (77.4)
STH 2-05-4	0.56 (0.0222)	30.43 (1.1979)	—		1231.4 (178.6)	[2]	1010.8 (146.6)	0.23 (0.009)	3.40 (0.134)	0.405	0.067	0.57	0.70	30.2 (27.5)	90.8 (82.6)
STH 2-1-1	0.55 (0.0216)	30.42 (1.1978)	40°		1377.6 (199.8)	1022.5 (148.3)	1288.7 (186.9)	0.30 (0.012)	1.68 (0.066)	0.556	0.182	0.73	0.78	40.7 (37.0)	—
STH 2-1-2	0.52 (0.0203)	30.45 (1.1988)	62°		1234.2 (179.0)	755.0 (109.5)	1001.8 (145.3)	0.38 (0.015)	2.39 (0.094)	0.739	0.160	0.57	0.70	35.5 (32.3)	75.8 (69.0)
STH 2-1-3	0.53 (0.0208)	30.41 (1.1971)	28°		997.0 (144.6)	628.8 (91.2)	839.1 (121.7)	0.43 (0.017)	3.05 (0.120)	0.817	0.142	0.48	0.57	32.0 (29.1)	69.5 (63.2)
STH 2-1-4	0.52 (0.0203)	30.45 (1.1988)	—		1510.7 (219.1)	[2]	—	0.18 (0.007)	1.19 (0.047)	0.345	0.149	—	0.86	38.5 (35.0)	—
STH 2-1-5	0.54 (0.0212)	30.50 (1.2008)	—		1419.7 (205.9)	[2]	[3]	0.30 (0.012)	1.78 (0.070)	0.566	0.171	—	0.81	45.8 (41.7)	—
STH 2-1-6	0.54 (0.0211)	30.54 (1.2023)	60°		NA [4]	1148.0 (166.5)	1303.2 (189.0)	0.30 (0.012)	1.70 (0.067)	(0.569)	0.179	0.74	—	41.3 (37.6)	—

[1] σ_Y = 1759 MN/m^2 (255.1 KSI)
[2] NOT INSTRUMENTED FOR DIMPLING
[3] NO BREAKTHROUGH INDICATION, MAY HAVE BEEN MALFUNCTION IN PRESSURE CUPS
[4] SPECIMEN WAS LOAD/UNLOAD TESTED, THEN MARKED BEFORE FINAL FAILURE

Table 31: ***(Continued)***

SPECIMEN			TEST		FRACTURE DATA											
NUMBER	GAGE THICKNESS, t mm (INCH)	GAGE WIDTH, w mm (INCH)	DIMPLING GAGE LOCATION FROM CRACK TIP	ENVIRONMENT	FAILURE STRESS, σ_G MN/m^2 (KSI)	DIMPLING STRESS, σ_D MN/m^2 (KSI)	BREAKTHROUGH STRESS, σ_B MN/m^2 (KSI)	INITIAL FLAW DEPTH, a_i mm (INCH)	INITIAL FLAW LENGTH, $(2c)_i$ mm (INCH)	$\frac{\text{INITIAL FLAW DEPTH}}{\text{GAGE THICKNESS}}$, $(a/t)_i$	$\frac{\text{INITIAL FLAW DEPTH}}{\text{INITIAL FLAW LENGTH}}$, $(a/2c)_i$	σ_B/σ_Y [1]	σ_G/σ_Y [1]	IRWIN'S APPARENT K AT BREAKTHROUGH $MN/m^{3/2}$ (KSI$\sqrt{IN}$)	K_{CN} AT FINAL FAILURE $MN/m^{3/2}$ (KSI$\sqrt{IN}$)
STH 2-3-1	0.49 (0.0192)	30.51 (1.2011)	55°	LH_2 @ 20°K (-423°F)	1716.2 (248.9)	1531.4 (222.1)	—	0.20 (0.008)	0.79 (0.031)	0.417	0.258	—	0.98	42.0 (38.2)	—
STH 2-3-2	0.54 (0.0211)	30.49 (1.2002)	57°		1458.3 (211.5)	—	1390.0 (201.6)	0.33 (0.013)	1.17 (0.046)	0.616	0.283	0.79	0.83	41.1 (37.4)	—
STH 2-3-3	0.51 (0.0201)	30.54 (1.2024)	85°		1197.0 (173.6)	—	1119.7 (162.4)	0.46 (0.018)	1.40 (0.055)	0.896	0.327	0.64	0.68	36.5 (33.2)	56.2 (51.1)
STH 2-5-1	0.51 (0.0200)	30.52 (1.2015)	63°		1687.9 (244.8)	—	1652.0 (239.6)	0.25 (0.010)	0.58 (0.023)	0.500	0.435	0.94	0.96	35.2 (32.0)	—
STH 2-5-2	0.51 (0.0199)	30.51 (1.2012)	55°		1586.5 (230.1)	—	1471.4 (213.4)	0.38 (0.015)	0.86 (0.034)	0.754	0.441	0.84	0.90	39.2 (35.7)	—
STH 2-5-3	0.53 (0.0207)	30.45 (1.1990)	73°		1425.2 (206.7)	—	1390.0 (201.6)	0.43 (0.017)	1.07 (0.042)	0.821	0.405	0.79	0.81	40.9 (37.2)	—
STH 2-5-4	0.54 (0.0211)	30.51 (1.2011)	18°		1450.7 (210.4)	1210.1 (175.5)	1390.0 (201.6)	0.46 (0.018)	0.94 (0.037)	0.853	0.486	0.79	0.82	38.5 (35.0)	—

[1] σ_Y = 1759 MN/m^2 (255.1 KSI)

Table 32: STATIC FRACTURE TESTS — LIQUID HYDROGEN TEMPERATURE 6Al-4V TITANIUM WELDMENT, t = 1.78 mm (0.070 INCH)

SPECIMEN			TEST		FRACTURE DATA											
NUMBER	GAGE THICKNESS, t mm (INCH)	GAGE WIDTH, w mm (INCH)	DIMPLING GAGE LOCATION FROM CRACK TIP	ENVIRONMENT	FAILURE STRESS, σ_G MN/m^2 (KSI)	DIMPLING STRESS, σ_D MN/m^2 (KSI)	BREAKTHROUGH STRESS, σ_B MN/m^2 (KSI)	INITIAL FLAW DEPTH, a_i mm (INCH)	INITIAL FLAW LENGTH, $(2c)_i$ mm (INCH)	$\frac{\text{INITIAL FLAW DEPTH}}{\text{GAGE THICKNESS}}$, $(a/t)_i$	$\frac{\text{INITIAL FLAW DEPTH}}{\text{INITIAL FLAW LENGTH}}$, $(a/2c)_i$	σ_B/σ_Y [1]	σ_G/σ_Y [1]	IRWIN'S APPARENT K AT BREAKTHROUGH MN/m$^{3/2}$ (KSI$\sqrt{\text{IN}}$)	K_{CN} AT FINAL FAILURE MN/m$^{3/2}$ (KSI$\sqrt{\text{IN}}$)
STH 8-1-1	1.72 (0.0678)	44.78 (1.7630)	50°	LH_2 @ 20°K (-423°F)	833.6 (120.9)	718.5 (104.2)	825.3 (119.7)	0.89 (0.035)	6.10 (0.240)	0.516	0.146	0.46	0.46	44.8 (40.8)	82.5 (75.1)
STH 8-1-2	1.76 (0.0693)	44.58 (1.755)	59°		694.3 (100.7)	652.3 (94.6)	—	1.22 (0.048)	8.38 (0.330)	0.693	0.145	—	0.38	44.0) (40.0)	—
STH 8-1-3	1.82 (0.0718)	44.68 (1.759)	53°		567.5 (82.3)	423.4 (61.4)	557.1 (80.8)	1.47 (0.058)	10.41) (0.410)	0.808	0.141	0.31	0.31	38.7 (35.2)	75.1 (68.3)
STH 8-1-4	1.76 (0.0691)	31.62 (1.2450)	—		1654.8 (240.0)	[2]	—	0.38 (0.015)	1.75 (0.069)	0.217	0.217	—	0.92	57.7 (52.5)	—
STH 8-1-5	1.73 (0.0681)	32.02 (1.2605)	44°		1361.8 (197.5)	—	—	0.51 (0.020)	3.43 (0.135)	0.294	0.148	—	0.75	57.7 (52.5)	—
STH 8-3-1	1.83 (0.0719)	31.91 (1.2564)	—		1316.9 (191.0)	[2]	—	0.71 (0.028)	2.49 (0.098)	0.389	0.286	—	0.73	56.6 (51.5)	—
STH 8-3-2	1.74 (0.0687)	31.88 (1.255)	37°		1001.8 (145.3)	815.7 (118.3)	943.9 (136.9)	1.14 (0.045)	3.94 (0.155)	0.655	0.290	0.52	0.56	50.2 (45.7)	79.6 (72.4)
STH 8-3-3	1.73 (0.0683)	31.75 (1.250)	47°		772.9 (112.1)	557.1 (80.8)	702.6 (101.9)	1.42 (0.056)	5.21 (0.205)	0.820	0.273	0.39	0.43	42.1 (38.3)	71.1 (64.7)
STH 8-3-4	1.74 (0.0686)	31.91 (1.2562)	—		1503.8 (218.1)	[2]	—	0.56 (0.022)	1.63 (0.064)	0.321	0.344	—	0.83	54.2 (49.3)	—
STH 8-5-1	1.78 (0.0701)	20.41 (0.8037)	42°		1419.7 (205.9)	1389.3 (201.5)	—	0.81 (0.032)	1.73 (0.068)	0.456	0.471	—	0.79	53.3 (48.5)	—
STH 8-5-2	1.78 (0.0702)	20.41 (0.8034)	38°		1094.2 (158.7)	969.4 (140.6)	1075.6 (156.0)	1.14 (0.045)	2.39 (0.094)	0.641	0.479	0.60	0.61	46.9 (42.7)	67.6 (61.5)
STH 8-5-3	1.78 (0.0700)	20.37 (0.8020)	0°		917.7 (133.1)	786.0 (114.0)	906.0 (131.4)	1.50 (0.059)	3.20 (0.126)	0.843	0.468	0.50	0.51	45.5 (41.4)	66.0 (60.1)
STH 8-5-4	1.68 (0.0663)	31.93 (1.2570)	—		1514.8 (219.7)	[2]	—	0.69 (0.027)	1.42 (0.056)	0.407	0.482	—	0.84	51.8 (47.1)	—

[1] σ_Y = 1804 MN/m^2 (261.7 KSI)

[2] NOT INSTRUMENTED FOR DIMPLING

Table 33: STATIC FRACTURE TESTS — LIQUID HYDROGEN TEMPERATURE 6AI-4V TITANIUM WELDMENT, t = 5.33 mm (0.21 INCH)

SPECIMEN			TEST		FRACTURE DATA											
NUMBER	GAGE THICKNESS, t mm (INCH)	GAGE WIDTH, w mm (INCH)	DIMPLING GAGE LOCATION FROM CRACK TIP	ENVIRONMENT	FAILURE STRESS, σ_G MN/m^2 (KSI)	DIMPLING STRESS, σ_D MN/m^2 (KSI)	BREAKTHROUGH STRESS, σ_B MN/m^2 (KSI)	INITIAL FLAW DEPTH, a_i mm (INCH)	INITIAL FLAW LENGTH, $(2c)_i$ mm (INCH)	$\frac{\text{INITIAL FLAW DEPTH}}{\text{GAGE THICKNESS}}$, (a/t)	$\frac{\text{INITIAL FLAW DEPTH}}{\text{INITIAL FLAW LENGTH}}$, $(a/2c)_i$	σ_B/σ_Y [1]	σ_G/σ_Y [1]	IRWIN'S APPARENT K AT BREAKTHROUGH MN/m$^{3/2}$ (KSI$\sqrt{\text{IN}}$)	K_{CN} AT FINAL FAILURE MN/m$^{3/2}$ (KSI$\sqrt{\text{IN}}$)
STH 21-1-1	4.95 (0.1950)	76.42 (3.0086)	52°	LH_2 @ 20°K (-423°F)	564.0 (81.8)	—	—	2.62 (0.103)	18.59 (0.732)	0.528	0.141	—	0.32	52.3 (47.6)	—
STH 21-1-2	5.30 (0.2086)	153.17 (6.0302)	49°		378.5 (54.9)	373.0 (54.1)	—	3.63 (0.143)	25.27 (0.995)	0.686	0.144	—	0.22	41.0 (37.3)	—
STH 21-1-3	5.31 (0.2091)	152.37 (5.9990)	48°		384.7 (55.8)	302.0 (43.8)	368.2 (53.4)	4.52 (0.178)	29.34 (1.155)	0.851	0.154	0.21	0.22	44.1 (40.1)	84.5 (76.9)
STH 21-3-1	5.31 (0.2092)	45.73 (1.8005)	52°		608.8 (88.3)	—	—	2.64 (0.104)	9.09 (0.358)	0.497	0.291	—	0.35	48.7 (44.3)	—
STH 21-3-2	5.61 (0.2210)	76.25 (3.0018)	35°		605.4 (87.8)	557.8 (80.9)	—	3.63 (0.143)	13.08 (0.515)	0.647	0.278	—	0.35	57.6 (52.4)	—
STH 21-3-3	5.62 (0.2212)	76.45 (3.0100)	39°		473.7 (68.7)	424.7 (61.6)	—	4.67 (0.184)	16.84 (0.663)	0.832	0.278	—	0.27	50.9 (46.3)	—
STH 21-5-1	5.07 (0.1998)	38.01 (1.4964)	52°		881.2 (127.8)	—	—	2.54 (0.100)	5.54 (0.218)	0.501	0.459	—	0.51	58.2 (53.0)	—
STH 21-5-2	4.99 (0.1966)	38.19 (1.5035)	53°		661.2 (95.9)	—	—	3.56 (0.140)	7.54 (0.297)	0.712	0.471	—	0.38	50.8 (46.2)	—
STH 21-5-3	5.00 (0.1967)	45.79 (1.8027)	53°		553.7 (80.3)	—	—	4.45 (0.175)	9.45 (0.372)	0.890	0.470	—	0.32	47.5 (43.2)	—

[1] σ_Y = 1735 MN/m^2 (251.7 KSI)

Table 34: CYCLIC TESTS OF 1.60 mm (0.063 INCH) 2219 ALUMINUM WELDS PASSING σ_Y PROOF AND CYCLED AT 0.85 σ_Y IN ROOM TEMPERATURE AIR (SPECIMENS PROOFED BEFORE CYCLED)

SPECIMEN NUMBER	THICKNESS t mm (INCH)	WIDTH, W mm (INCH)	DIMPLING GAGE LOCATION FROM CRACK TIP	LOADING SEQUENCE	FLAW DEPTH, a mm (INCH)	FLAW LENGTH, 2c mm (INCH)	STRESS, σ MN/m^2 (KSI)	σ/σ_Y [1]	a/2c	a/t	STRESS INTENSITY, $K_{I_{MAX}}$ $MN/m^{3/2}$ (KSI$\sqrt{IN}$)	REMARKS
PA6-Y-85-1	1.60 (0.0629)	127.2 (5.0072)	45°	START PROOF	1.14 (0.045)	20.57 (0.810)	174.4 (25.3)	1.00	0.056	0.715	19.1 (17.4)	DIMPLED AT 82.1 MN/m^2 (11.90 KSI)
				END PROOF	1.27 (0.050)	20.57 (0.810)	174.4 (25.3)	1.00	0.062	0.795	21.7 (19.7)	
				START CYCLES	1.27 (0.050)	20.57 (0.810)	148.2 (21.5)	0.85	0.062	0.795	17.8 (16.2)	
				END CYCLES	1.60 (0.0629)	20.57 (0.810)	148.2 (21.5)	0.85	0.078	1.000	21.8 (19.8)	BT AT 75 ~
				FRACTURE	1.60 (0.0629)	20.57 (0.810)	220.6 (32.0)	1.26	0.078	1.000	—	
PA6-Y-85-2	1.55 (0.0612)	89.0 (3.5050)	53°	START PROOF	1.42 (0.056)	10.67 (0.420)	140.0 (20.3)	0.80	0.133	0.915	16.5 (15.0)	DIMPLED AT 71.0 MN/m^2 (10.30 KSI)
				END PROOF	1.55 (0.0612)	10.67 (0.420)	140.0 (20.3)	0.80	0.146	1.000	17.3 (15.7)	
				FRACTURE	1.55 (0.0612)	10.67 (0.420)	218.9 (31.75)	1.25	0.146	1.000	—	
PA6-Y-85-3	1.62 (0.0638)	88.9 (3.5050)	65°	START PROOF	1.24 (0.049)	4.32 (0.170)	174.4 (25.3)	1.00	0.288	0.768	12.9 (11.7)	DIMPLED AT 109.4 MN/m^2 (15.86 KSI)
				END PROOF	1.24 (0.049)	4.32 (0.170)	174.4 (25.3)	1.00	0.288	0.768	12.9 (11.7)	
				START CYCLES	1.24 (0.049)	4.32 (0.170)	148.2 (21.5)	0.85	0.288	0.768	10.7 (9.7)	
				END CYCLES	1.62 (0.0638)	4.95 (0.195)	148.2 (21.5)	0.85	0.327	1.000	12.3 (11.2)	BT AT 1392~
				FRACTURE	1.62 (0.0638)	5.16 (0.203)	185.3 (26.88)	1.06	0.314	1.000	—	
PA6-Y-85-4	1.54 (0.0607)	89.0 (3.5045)	66°	START PROOF	1.07 (0.042)	9.91 (0.390)	174.4 (25.3)	1.00	0.108	0.692	16.5 (15.0)	DIMPLED AT 112.5 MN/m^2 (16.31 KSI)
				END PROOF	1.17 (0.046)	9.91 (0.390)	174.4 (25.3)	1.00	0.118	0.758	17.9 (16.3)	
				START CYCLES	1.17 (0.046)	9.91 (0.390)	148.2 (21.5)	0.85	0.118	0.758	14.8 (13.5)	
				END CYCLES	1.54 (0.0607)	9.91 (0.390)	148.2 (21.5)	0.85	0.156	1.000	18.1 (16.5)	BT AT 213~
				FRACTURE	1.54 (0.0607)	9.91 (0.390)	215.5 (31.26)	1.24	0.156	1.000	—	
PA6-Y-85-5	1.60 (0.0629)	127.2 (5.0080)	63°	START PROOF	1.12 (0.044)	22.86 (0.900)	173.8 (25.2)	1.00	0.049	0.700	18.7 (17.0)	DIMPLED AT 109.4 MN/m^2 (15.87 KSI)
				END PROOF	1.27 (0.050)	22.86 (0.900)	173.8 (25.2)	1.00	0.056	0.795	21.8 (19.8)	
				START CYCLES	1.27 (0.050)	22.86 (0.900)	146.2 (21.2)	0.84	0.056	0.795	17.7 (16.1)	
				END CYCLES	1.60 (0.0629)	22.86 (0.900)	146.2 (21.2)	0.84	0.070	1.000	21.8 (19.8)	BT AT 75~
				FRACTURE	1.60 (0.0629)	22.86 (0.900)	212.1 (30.76)	1.22	0.070	1.000	—	

[1] σ_Y = 174.4 MN/m^2 (25.3 KSI) BT = BREAKTHROUGH

Table 35: CYCLIC TESTS OF 1.60 mm (0.063 INCH) 2219 ALUMINUM WELDS CAPABLE OF PASSING σ_y PROOF AND CYCLED AT 0.85 σ_y IN ROOM TEMPERATURE AIR (SPECIMENS NOT PROOFED)

SPECIMEN NUMBER	THICKNESS t mm (INCH)	WIDTH, W mm (INCH)	DIMPLING GAGE LOCATION FROM CRACK TIP	LOADING SEQUENCE	FLAW DEPTH, a mm (INCH)	FLAW LENGTH, 2c mm (INCH)	STRESS, σ MN/m^2 (KSI)	σ/σ_Y [1]	a/2c	a/t	STRESS INTENSITY, $K_{I_{MAX}}$ $MN/m^{3/2}$ ($KSI\sqrt{IN}$)	REMARKS
A6-Y-85-1	1.62 (0.0638)	127.1 (5.0029)	STRAIN GAGE BROKE ON LOADING	START CYCLES	1.19 (0.047)	20.83 (0.820)	148.2 (21.5)	0.85	0.057	0.737	16.4 (14.9)	
				END CYCLES	1.62 (0.0638)	20.83 (0.820)	148.2 (21.5)	0.85	0.078	1.000	22.1 (20.1)	BT AT 104~
				FRACTURE	1.62 (0.0638)	20.83 (0.820)	210.6 (30.55)	1.21	0.078	1.000	—	
A6-Y-85-2	1.56 (0.0616)	89.0 (3.5049)	21°	START CYCLES	1.30 (0.051)	10.54 (0.415)	148.2 (21.5)	0.85	0.123	0.828	16.4 (14.9)	DIMPLED AT 100.9 MN/m^2 (14.64 KSI)
				END CYCLES	1.56 (0.0616)	10.54 (0.415)	148.2 (21.5)	0.85	0.148	1.000	18.5 (16.8)	
				FRACTURE	1.56 (0.0616)	10.54 (0.415)	229.9 (33.35)	1.32	0.148	1.000	—	BT AT 64~
A6-Y-85-3	1.59 (0.0625)	88.9 (3.4985)	13°	START CYCLES	1.30 (0.051)	4.32 (0.170)	148.2 (21.5)	0.85	0.300	0.816	10.9 (9.9)	DIMPLING LOAD N.A.
				END CYCLES	1.59 (0.0625)	4.83 (0.190)	148.2 (21.5)	0.85	0.329	1.000	12.1 (11.0)	
				FRACTURE	1.59 (0.0625)	4.95 (0.195)	189.1 (27.43)	1.08	0.321	1.000	—	BT AT 873~

[1] σ_Y = 174.4 MN/m^2 (25.3 KSI)

BT = BREAKTHROUGH

Table 36: CYCLIC TESTS OF 1.60 mm (0.063 INCH) 2219 ALUMINUM WELDS PASSING σ_Y PROOF AND CYCLED AT 0.70 σ_Y IN ROOM TEMPERATURE AIR (SPECIMENS PROOFED BEFORE CYCLED)

SPECIMEN NUMBER	THICKNESS, t mm (INCH)	WIDTH, W mm (INCH)	DIMPLING GAGE LOCATION FROM CRACK TIP	LOADING SEQUENCE	FLAW DEPTH, a mm (INCH)	FLAW LENGTH, 2c mm (INCH)	STRESS, σ MN/m^2 (KSI)	σ/σ_Y [1]	a/2c	a/t	STRESS INTENSITY, $K_{I_{MAX}}$ $MN/m^{3/2}$ (KSI$\sqrt{IN}$)	REMARKS
PA6-Y-70-1	1.53 (0.0604)	127.2 (5.0061)	57°	START PROOF	1.22 (0.048)	20.83 (0.820)	130.0 (18.85)	0.75	0.059	0.795	15.1 (13.7)	DIMPLED AT 97.5 MN/m^2 (14.14 KSI) [2]
				END PROOF	1.53 (0.0604)	20.83 (0.820)	130.0 (18.85)	0.75	0.074	1.000	18.2 (16.6)	
				FRACTURE	1.53 (0.0604)	20.83 (0.820)	218.9 (31.75)	1.25	0.074	1.000	—	
PA6-Y-70-2	1.65 (0.0648)	89.0 (3.5044)	21°	START PROOF	1.32 (0.052)	10.67 (0.420)	174.4 (25.3)	1.00	0.124	0.802	19.7 (17.9)	DIMPLED AT 84.3 MN/m^2 (12.22 KSI) BT AT PROOF LOAD
				END PROOF	1.65 (0.0648)	10.67 (0.420)	174.4 (25.3)	1.00	0.154	1.000	22.6 (20.6)	
				FRACTURE	1.65 (0.0648)	10.67 (0.420)	217.1 (31.48)	1.24	0.154	1.000	—	
PA6-Y-70-3	1.61 (0.0635)	88.9 (3.4992)	0°	START PROOF	1.27 (0.050)	4.39 (0.173)	174.4 (25.3)	1.00	0.289	0.787	13.1 (11.9)	DIMPLED AT 120.4 MN/m^2 (17.46 KSI)
				END PROOF	1.32 (0.052)	4.39 (0.173)	174.4 (25.3)	1.00	0.301	0.819	13.2 (12.0)	
				START CYCLES	1.32 (0.052)	4.39 (0.173)	122.0 (17.7)	0.70	0.301	0.819	8.9 (8.1)	
				END CYCLES	1.61 (0.0635)	5.26 (0.207)	122.0 (17.7)	0.70	0.307	1.000	10.2 (9.3)	BT AT 8095~
				FRACTURE	1.61 (0.0635)	5.26 (0.207)	249.8 (36.23)	1.43	0.307	1.000	—	
PA6-Y-70-4	1.60 (0.0629)	127.1 (5.0069)	54°	START PROOF	1.09 (0.043)	22.48 (0.885)	174.4 (25.3)	1.00	0.049	0.684	18.2 (16.6)	DIMPLED AT 122.5 MN/m^2 (17.77 KSI)
				END PROOF	1.14 (0.045)	22.48 (0.885)	174.4 (25.3)	1.00	0.051	0.715	19.2 (17.5)	
				START CYCLES	1.14 (0.045)	22.48 (0.885)	122.0 (17.7)	0.70	0.051	0.715	12.6 (11.5)	
				END CYCLES	1.60 (0.0629)	22.48 (0.885)	122.0 (17.7)	0.70	0.071	1.000	17.7 (16.1)	BT AT 539~
				FRACTURE	1.60 (0.0629)	22.48 (0.885)	198.2 (28.74)	1.14	0.071	1.000	—	

[1] σ_Y = 174.4 MN/m^2 (25.3 KSI)

[2] BT AT 130.0 MN/m^2 (18.85 KSI), MAX. LOAD REACHED WAS 157.3 MN/m^2 (22.81 KSI)

BT = BREAKTHROUGH

Table 36: (Continued)

SPECIMEN NUMBER	THICKNESS, t mm (INCH)	WIDTH, W mm (INCH)	DIMPLING GAGE LOCATION FROM CRACK TIP	LOADING SEQUENCE	FLAW DEPTH, a mm (INCH)	FLAW LENGTH, 2c mm (INCH)	STRESS, σ MN/m^2 (KSI)	σ/σ_Y [1]	a/2c	a/t	STRESS INTENSITY, $K_{I_{MAX}}$ $MN/m^{3/2}$ (KSI$\sqrt{IN}$)	REMARKS
PA6-Y-70-5	1.64 (0.0645)	89.0 (3.5035)	51°	START PROOF	1.12 (0.044)	9.98 (0.393)	174.4 (25.3)	1.00	0.112	0.682	16.6 (15.1)	DIMPLED AT 92.1 MN/m^2 (13.36 KSI)
				END PROOF	1.19 (0.047)	9.98 (0.393)	174.4 (25.3)	1.00	0.120	0.729	17.6 (16.0)	
				START CYCLES	1.19 (0.047)	9.98 (0.393)	122.0 (17.7)	0.70	0.120	0.729	11.6 (10.6)	
				END CYCLES	1.64 (0.0645)	9.98 (0.393)	122.0 (17.7)	0.70	0.164	1.000	14.7 (13.4)	BT AT 1597~
				FRACTURE	1.64 (0.0645)	9.98 (0.393)	204.4 (29.65)	1.17	0.164	1.000	—	
PA6-Y-70-6	1.65 (0.0649)	152.5 (6.0058)	55°	START PROOF	1.04 (0.041)	22.61 (0.890)	171.0 (24.8)	0.98	0.046	0.632	16.5 (15.0)	DIMPLED AT 75.1 MN/m^2 (10.89 KSI)
				END PROOF	1.24 (0.049)	22.61 (0.890)	171.0 (24.8)	0.98	0.055	0.755	20.3 (18.5)	
				START CYCLES	1.24 (0.049)	22.61 (0.890)	122.0 (17.7)	0.70	0.055	0.755	13.6 (12.4)	
				END CYCLES	1.65 (0.0649)	22.61 (0.890)	122.0 (17.7)	0.70	0.073	1.000	17.9 (16.3)	BT AT 476~
				FRACTURE	1.65 (0.0649)	22.61 (0.890)	217.5 (31.55)	1.25	0.073	1.000	—	

[1] σ_Y = 174.4 MN/m^2 (25.3 KSI)

Table 37. *CYCLIC TESTS OF 1.60 mm (0.063 INCH) 2219 ALUMINUM WELDS CAPABLE OF PASSING σ_Y PROOF AND CYCLED AT 0.70 σ_Y IN ROOM TEMPERATURE AIR (SPECIMENS NOT PROOFED)*

SPECIMEN NUMBER	THICKNESS, t mm (INCH)	WIDTH, W mm (INCH)	DIMPLING GAGE LOCATION FROM CRACK TIP	LOADING SEQUENCE	FLAW DEPTH, a mm (INCH)	FLAW LENGTH, 2c mm (INCH)	STRESS, σ MN/m^2 (KSI)	σ/σ_Y [1]	a/2c	a/t	STRESS INTENSITY, $K_{I_{MAX}}$ $MN/m^{3/2}$ (KSI$\sqrt{IN}$)	REMARKS
A6-Y-70-1	1.60 (0.0628)	127.2 (5.0074)	30°	START CYCLES	1.37 (0.054)	21.59 (0.850)	122.0 (17.7)	0.70	0.064	0.860	15.6 (14.2)	DIMPLING LOAD N.A.
				END CYCLES	1.60 (0.0628)	21.59 (0.850)	122.0 (17.7)	0.70	0.074	1.000	17.6 (16.0)	BT AT 75~
				FRACTURE	1.60 (0.0628)	21.59 (0.850)	210.4 (30.52)	1.21	0.074	1.000	—	
A6-Y-70-2	1.63 (0.0643)	89.0 (3.5052)	56°	START CYCLES	1.35 (0.053)	10.54 (0.415)	122.0 (17.7)	0.70	0.128	0.824	13.3 (12.1)	DIMPLED AT 85.4 MN/m^2 (12.38 KSI)
				END CYCLES	1.63 (0.0643)	10.54 (0.415)	122.0 (17.7)	0.70	0.155	1.000	15.1 (13.7)	BT AT 464~
				FRACTURE	1.63 (0.0643)	10.54 (0.415)	221.2 (32.08)	1.27	0.155	1.000	—	
A6-Y-70-3	1.61 (0.0635)	88.8 (3.4975)	24°	START CYCLES	1.22 (0.048)	4.32 (0.170)	122.0 (17.7)	0.70	0.282	0.756	8.6 (7.8)	DIMPLED AT 4363~
				END CYCLES	1.61 (0.0635)	5.21 (0.205)	122.0 (17.7)	0.70	0.310	1.000	10.2 (9.3)	BT AT 6507~
				FRACTURE	1.61 (0.0635)	5.21 (0.205)	238.4 (34.58)	1.37	0.310	1.000	—	
A6-Y-70-4	1.60 (0.0630)	127.2 (5.0063)	53°	START CYCLES	0.99 (0.039)	2.24 (0.880)	122.0 (17.7)	0.70	0.044	0.619	10.8 (9.8)	DIMPLED AT 110.4 MN/m^2 (16.01 KSI)
				END CYCLES	1.60 (0.0630)	2.24 (0.880)	122.0 (17.7)	0.70	0.072	1.000	17.7 (16.1)	BT AT 602~
				FRACTURE	1.60 (0.0630)	2.24 (0.880)	204.6 (29.68)	1.17	0.072	1.000	—	

[1] σ_Y = 174.4 MN/m^2 (25.3 KSI)

BT = BREAKTHROUGH

Table 38: *CYCLIC TESTS OF 1.60 mm (0.063 INCH) 2219 ALUMINUM WELDS PASSING 0.91 σ_Y PROOF AND CYCLED AT 0.70 σ_Y IN ROOM TEMPERATURE AIR (SPECIMENS PROOFED BEFORE CYCLING)*

SPECIMEN NUMBER	THICKNESS t mm (INCH)	WIDTH, W mm (INCH)	DIMPLING GAGE LOCATION FROM CRACK TIP	LOADING SEQUENCE	FLAW DEPTH, a mm (INCH)	FLAW LENGTH, 2c mm (INCH)	STRESS, σ MN/m^2 (KSI)	σ/σ_Y [1]	a/2c	a/t	STRESS INTENSITY, $K_{I_{MAX}}$ $MN/m^{3/2}$ (KSI$\sqrt{IN}$)	REMARKS
PA6-9-70-1	1.70 (0.0671)	152.5 (6.0036)	60°	START PROOF	1.22 (0.048)	23.11 (0.910)	146.3 (21.22)	0.84	0.053	0.715	16.0 (14.6)	DIMPLED AT 95.5 MN/m^2 (13.85 KSI) [2]
				END PROOF	1.70 (0.0671)	23.11 (0.910)	146.3 (21.22)	0.84	0.074	1.000	22.1 (20.1)	
				FRACTURE	1.70 (0.0671)	23.11 (0.910)	164.3 (23.83)	0.94	0.074	1.000	—	
PA6-9-70-2	1.59 (0.0625)	89.0 (3.5046)	34°	START PROOF	1.40 (0.055)	11.86 (0.467)	146.1 (21.19)	0.84	0.118	0.880	17.5 (15.9)	DIMPLED AT 81.8 MN/m^2 (11.87 KSI) [3]
				END PROOF	1.59 (0.0625)	11.86 (0.467)	146.1 (21.19)	0.84	0.134	1.000	18.9 (17.2)	
				FRACTURE	1.59 (0.0625)	11.86 (0.467)	214.1 (31.05)	1.23	0.134	1.000	—	
PA6-9-70-3	1.63 (0.0642)	88.9 (3.4987)	44°	START PROOF	1.37 (0.054)	7.62 (0.300)	158.6 (23.0)	0.91	0.180	0.841	16.3 (14.8)	DIMPLED AT 99.0 MN/m^2 (14.36 KSI)
				END PROOF	1.40 (0.055)	7.62 (0.300)	158.6 (23.0)	0.91	0.183	0.857	16.5 (15.0)	
				START CYCLES	1.40 (0.055)	7.62 (0.300)	122.0 (17.7)	0.70	0.183	0.857	12.3 (11.2)	
				END CYCLES	1.63 (0.0642)	7.87 (0.310)	122.0 (17.7)	0.70	0.207	1.000	13.3 (12.1)	BT AT 679~
				FRACTURE	1.63 (0.0642)	7.87 (0.310)	230.2 (33.39)	1.32	0.207	1.000	—	
PA6-9-70-5	1.62 (0.0637)	127.2 (5.0082)	50°	START PROOF	1.14 (0.045)	12.62 (0.497)	140.7 (20.41)	0.81	0.091	0.706	13.0 (12.6)	DIMPLED AT 75.2 MN/m^2 (10.91 KSI)
				END PROOF	1.17 (0.046)	12.62 (0.497)	140.7 (20.41)	0.81	0.093	0.722	14.2 (12.9)	
				START CYCLES	1.17 (0.046)	12.62 (0.497)	122.0 (17.7)	0.70	0.093	0.722	12.1 (11.0)	
				END CYCLES	1.62 (0.0637)	12.62 (0.497)	122.0 (17.7)	0.70	0.128	1.000	15.9 (14.5)	BT AT 750~
				FRACTURE	1.62 (0.0637)	12.62 (0.497)	210.4 (30.52)	1.21	0.128	1.000	—	

[1] σ_Y = 174.4 MN/m^2 (25.3 KSI)

[2] BT AT 146.3 MN/m^2 (21.22 KSI), MAX LOAD REACHED WAS 158.6 MN/m^2 (23.0 KSI)

[3] BT AT 146.1 MN/m^2 (21.19 KSI), MAX LOAD REACHED WAS 158.6 MN/m^2 (23.0 KSI)

BT = BREAKTHROUGH

Table 39: *CYCLIC TESTS OF 1.60 mm (0.063 INCH) 2219 ALUMINUM WELDS CAPABLE OF PASSING 0.91 σ_y PROOF AND CYCLED AT 0.70 σ_y IN ROOM TEMPERATURE AIR (SPECIMENS NOT PROOFED)*

SPECIMEN NUMBER	THICKNESS t mm (INCH)	WIDTH, W mm (INCH)	DIMPLING GAGE LOCATION FROM CRACK TIP	LOADING SEQUENCE	FLAW DEPTH, a mm (INCH)	FLAW LENGTH, 2c mm (INCH)	STRESS, σ MN/m^2 (KSI)	σ/σ_Y [1]	a/2c	a/t	STRESS INTENSITY, $K_{I_{MAX}}$ $MN/m^{3/2}$ ($KSI\sqrt{IN}$)	REMARKS
A6-9-70-1	1.62 (0.0639)	127.2 (5.0074)	63°	START CYCLES	1.30 (0.051)	23.37 (0.920)	122.0 (17.7)	0.70	0.055	0.798	14.5 (13.2)	DIMPLED AT 69.2 MN/m^2 (10.03 KSI)
				END CYCLES	1.62 (0.0639)	23.37 (0.920)	122.0 (17.7)	0.70	0.069	1.000	17.9 (16.3)	BT AT 87~
				FRACTURE	1.62 (0.0639)	23.37 (0.920)	209.1 (30.33)	1.20	0.069	1.000	—	
A6-9-70-2	1.61 (0.0635)	89.0 (3.5046)	NA	START CYCLES	1.35 (0.053)	11.68 (0.460)	122.0 (17.7)	0.70	0.115	0.835	13.7 (12.5)	DIMPLING LOAD NA
				END CYCLES	1.61 (0.0635)	11.68 (0.460)	122.0 (17.7)	0.70	0.138	1.000	15.5 (14.1)	BT AT 334~
				FRACTURE	1.61 (0.0635)	11.68 (0.460)	213.8 (31.01)	1.23	0.138	1.000	—	
A6-9-70-3	1.61 (0.0634)	89.0 (3.5037)	26°	START CYCLES	1.35 (0.053)	7.70 (0.303)	122.0 (17.7)	0.70	0.175	0.836	12.1 (11.0)	DIMPLED AT 119.5 MN/m^2 (17.33 KSI)
				END CYCLES	1.61 (0.0634)	7.87 (0.310)	122.0 (17.7)	0.70	0.205	1.000	13.2 (12.1)	BT AT 809~
				FRACTURE	1.61 (0.0634)	7.87 (0.310)	221.7 (32.15)	1.27	0.205	1.000	—	
A6-9-70-4	1.62 (0.0636)	152.6 (6.0060)	60°	START CYCLES	1.12 (0.044)	22.48 (0.885)	122.0 (17.7)	0.70	0.050	0.692	12.2 (11.1)	DIMPLED AT 92.0 MN/m^2 (13.35 KSI)
				END CYCLES	1.62 (0.0636)	22.48 (0.885)	122.0 (17.7)	0.70	0.072	1.000	17.8 (16.2)	BT AT 268~
				FRACTURE	1.62 (0.0636)	22.48 (0.885)	216.1 (31.34)	1.24	0.072	1.000	—	

[1] σ_Y = 174.4 MN/m^2 (25.3 KSI)

BT = BREAKTHROUGH

Table 40: *CYCLIC TESTS OF 2.67 mm (0.105 INCH) 2219 ALUMINUM WELDS PASSING σ_Y PROOF AND CYCLED AT 0.85 σ_Y IN ROOM TEMPERATURE AIR (SPECIMENS PROOFED BEFORE CYCLED)*

SPECIMEN NUMBER	THICKNESS t mm (INCH)	WIDTH, W mm (INCH)	DIMPLING GAGE LOCATION FROM CRACK TIP	LOADING SEQUENCE	FLAW DEPTH, a mm (INCH)	FLAW LENGTH, 2c mm (INCH)	STRESS, σ MN/m^2 (KSI)	σ/σ_Y ▷1	a/2c	a/t	STRESS INTENSITY, $K_{I_{MAX}}$ $MN/m^{3/2}$ ($KSI\sqrt{IN}$)	REMARKS
PA1-Y-85-3	2.66 (0.1048)	126.9 (4.9968)	39°	START PROOF	2.03 (0.080)	7.03 (0.277)	194.4 (28.2)	1.00	0.289	0.763	18.2 (16.6)	DIMPLED AT 121.8 MN/m^2 (17.66 KSI)
				END PROOF	2.03 (0.080)	7.03 (0.277)	194.4 (28.2)	1.00	0.289	0.763	18.2 (16.6)	
				START CYCLES	2.03 (0.080)	7.03 (0.277)	165.5 (24.0)	0.85	0.289	0.763	15.2 (13.8)	
				END CYCLES	2.66 (0.1048)	8.13 (0.320)	165.5 (24.0)	0.85	0.327	1.000	17.6 (16.0)	BT AT 650~
				FRACTURE	2.66 (0.1048)	8.13 (0.320)	240.9 (34.94)	1.24	0.327	1.000	—	
PA1-Y-85-4	2.63 (0.1035)	127.2 (5.0085)	NA	START PROOF	1.52 (0.060)	16.56 (0.652)	188.9 (27.4)	0.97	0.097	0.609	20.6 (17.9)	DIMPLED AT 99.8 MN/m^2 (14.47 KSI)
				END PROOF	1.60 (0.063)	16.56 (0.652)	188.9 (27.4)	0.97	0.097	0.609	20.6 (18.7)	
				START CYCLES	1.60 (0.063)	16.56 (0.652)	165.5 (24.0)	0.85	0.097	0.609	17.5 (15.9)	
				END CYCLES	2.63 (0.1035)	16.56 (0.652)	165.5 (24.0)	0.85	0.159	1.000	26.2 (23.8)	BT AT 404~
				FRACTURE	2.63 (0.1035)	16.56 (0.652)	212.3 (30.79)	1.09	0.159	1.000	—	
PA1-Y-85-5	2.59 (0.1021)	88.8 (3.4946)	66°	START PROOF	2.13 (0.084)	4.85 (0.191)	194.4 (28.2)	1.00	0.440	0.823	13.7 (12.5)	DIMPLED AT 98.5 MN/m^2 (14.29 KSI)
				END PROOF	2.36 (0.093)	5.08 (0.200)	194.4 (28.2)	1.00	0.465	0.911	14.4 (13.1)	
				START CYCLES	2.36 (0.093)	5.08 (0.200)	165.5 (24.0)	0.85	0.465	0.911	12.1 (11.0)	
				END CYCLES	2.59 (0.1021)	5.46 (0.215)	165.5 (24.0)	0.85	0.475	1.000	12.7 (11.6)	BT AT 322~
				FRACTURE	2.59 (0.1021)	5.46 (0.215)	228.4 (33.13)	1.18	0.475	1.000	—	
PA1-Y-85-6	2.58 (0.1016)	152.6 (6.0070)	49°	START PROOF	1.37 (0.054)	29.97 (1.180)	191.0 (27.7)	0.98	0.046	0.531	19.1 (17.4)	DIMPLED AT 97.2 MN/m^2 (14.09 KSI)
				END PROOF	1.57 (0.062)	29.97 (1.180)	191.0 (27.7)	0.98	0.053	0.610	22.1 (20.1)	
				START CYCLES	1.57 (0.062)	29.97 (1.180)	165.5 (24.0)	0.85	0.053	0.610	18.6 (16.9)	
				END CYCLES	2.58 (0.1016)	29.97 (1.180)	165.5 (24.0)	0.85	0.086	1.000	30.4 (27.7)	BT AT 127~
				FRACTURE	2.58 (0.1016)	29.97 (1.180)	204.0 (29.59)	1.05	0.086	1.000	—	

▷1 σ_Y = 194.4 MN/m^2 (28.2 KSI)

BT = BREAKTHROUGH

Table 41: CYCLIC TESTS OF 2.67 mm (0.105 INCH) 2219 ALUMINUM WELDS CAPABLE OF PASSING σ_y PROOF AND CYCLED AT 0.85 σ_y IN ROOM TEMPERATURE AIR (SPECIMENS NOT PROOFED)

SPECIMEN NUMBER	THICKNESS t mm (INCH)	WIDTH, W mm (INCH)	DIMPLING GAGE LOCATION FROM CRACK TIP	LOADING SEQUENCE	FLAW DEPTH, a mm (INCH)	FLAW LENGTH, 2c mm (INCH)	STRESS, σ MN/m^2 (KSI)	σ/σ_Y ▷1◁	a/2c	a/t	STRESS INTENSITY, $K_{I_{MAX}}$ $MN/m^{3/2}$ ($KSI\sqrt{IN}$)	REMARKS
A1-Y-85-1	2.58 (0.1016)	152.5 (6.0049)	47°	START CYCLES	1.60 (0.063)	29.85 (1.175)	165.5 (24.0)	0.85	0.054	0.620	18.9 (17.2)	DIMPLED AT 79.7 MN/m^2 (11.56 KSI) BT AT 67~
				END CYCLES	2.58 (0.1016)	29.85 (1.175)	165.5 (24.0)	0.85	0.086	1.000	30.4 (27.7)	
				FRACTURE	2.58 (0.1016)	29.85 (1.175)	197.7 (28.67)	1.02	0.086	1.000	—	
A1-Y-85-2	2.70 (0.1063)	127.2 (5.0081)	57°	START CYCLES	2.21 (0.087)	16.13 (0.635)	165.5 (24.0)	0.85	0.137	0.818	23.1 (21.0)	DIMPLED AT 86.3 MN/m^2 (12.51 KSI) BT AT 73~
				END CYCLES	2.70 (0.1063)	16.13 (0.635)	165.5 (24.0)	0.85	0.167	1.000	26.0 (23.7)	
				FRACTURE	2.70 (0.1063)	16.13 (0.635)	213.7 (30.99)	1.10	0.167	1.000	—	
A1-Y-85-3	2.63 (0.1036)	126.9 (4.9973)	34°	START CYCLES	1.96 (0.077)	6.99 (0.275)	165.5 (24.0)	0.85	0.280	0.743	15.1 (13.7)	DIMPLED AT 165.5 MN/m^2 (24.0 KSI) BT AT 564~
				END CYCLES	2.63 (0.1036)	8.38 (0.330)	165.5 (24.0)	0.85	0.314	1.000	17.9 (16.3)	
				FRACTURE	2.63 (0.1036)	8.38 (0.330)	212.2 (30.77)	1.09	0.314	1.000	—	
A1-Y-85-4	2.67 (0.1052)	127.2 (5.0082)	49°	START CYCLES	1.60 (0.063)	16.64 (0.655)	165.5 (24.0)	0.85	0.096	0.599	17.4 (15.8)	DIMPLED AT 99.2 MN/m^2 (14.38 KSI) BT AT 372~
				END CYCLES	2.67 (0.1052)	16.76 (0.660)	165.5 (24.0)	0.85	0.159	1.000	26.4 (24.0)	
				FRACTURE	2.67 (0.1052)	16.76 (0.660)	226.6 (32.86)	1.17	0.159	1.000	—	
A1-Y-85-5	2.62 (0.1031)	88.8 (3.4960)	64°	START CYCLES	2.08 (0.082)	5.16 (0.203)	165.5 (24.0)	0.85	0.404	0.795	12.1 (11.0)	DIMPLED AT 94.9 MN/m^2 (13.77 KSI) BT AT 688~
				END CYCLES	2.62 (0.1031)	6.35 (0.250)	165.5 (24.0)	0.85	0.412	1.000	15.1 (13.7)	
				FRACTURE	2.62 (0.1031)	6.35 (0.250)	224.4 (32.55)	1.05	0.412	1.000	—	

▷1◁ σ_Y = 194.4 MN/m^2 (28.2 KSI)

BT = BREAKTHROUGH

Table 42: CYCLIC TESTS OF 2.67 mm (0.105 INCH) 2219 ALUMINUM WELDS PASSING σ_Y PROOF AND CYCLED AT 0.70 σ_Y IN ROOM TEMPERATURE AIR (SPECIMENS PROOFED BEFORE CYCLED)

SPECIMEN NUMBER	THICKNESS t mm (INCH)	WIDTH, W mm (INCH)	DIMPLING GAGE LOCATION FROM CRACK TIP	LOADING SEQUENCE	FLAW DEPTH, a mm (INCH)	FLAW LENGTH, 2c mm (INCH)	STRESS, σ MN/m^2 (KSI)	σ/σ_Y ①	a/2c	a/t	STRESS INTENSITY, $K_{I_{MAX}}$ $MN/m^{3/2}$ ($KSI\sqrt{IN}$)	REMARKS
PA1-Y-70-2	2.65 (0.1042)	126.9 (4.9967)	51°	START PROOF	1.83 (0.072)	16.00 (0.630)	194.4 (28.2)	1.00	0.114	0.691	23.7 (21.6)	DIMPLED AT 111.2 MN/m^2 (16.13 KSI)
				END PROOF	2.16 (0.085)	16.00 (0.630)	194.4 (28.2)	1.00	0.135	0.816	27.7 (25.2)	
				START CYCLES	2.16 (0.085)	16.00 (0.630)	135.8 (19.7)	0.70	0.135	0.816	18.4 (16.7)	
				END CYCLES	2.65 (0.1042)	16.00 (0.630)	135.8 (19.7)	0.70	0.165	1.000	20.8 (18.9)	BT AT 130~
				FRACTURE	2.65 (0.1042)	16.00 (0.630)	214.5 (31.11)	1.10	0.165	1.000	—	
PA1-Y-70-3	2.66 (0.1047)	127.0 (4.9995)	38°	START PROOF	1.83 (0.072)	6.86 (0.270)	194.4 (28.2)	1.00	0.267	0.688	17.4 (15.8)	DIMPLED AT 126.5 MN/m^2 (18.34 KSI)
				END PROOF	1.93 (0.076)	6.99 (0.275)	194.4 (28.2)	1.00	0.276	0.726	17.9 (16.3)	
				START CYCLES	1.93 (0.076)	6.99 (0.275)	135.8 (19.7)	0.70	0.276	0.726	12.0 (10.9)	
				END CYCLES	2.66 (0.1047)	8.89 (0.350)	135.8 (19.7)	0.70	0.299	1.000	14.8 (13.5)	BT AT 4719~
				FRACTURE	2.66 (0.1047)	8.89 (0.350)	243.5 (35.31)	1.25	0.299	1.000	—	
PA1-Y-70-4	2.56 (0.1008)	152.6 (6.0083)	59°	START PROOF	1.40 (0.055)	29.21 (1.150)	194.4 (28.2)	1.00	0.048	0.546	20.1 (18.3)	DIMPLED AT 108.2 MN/m^2 (15.69 KSI)
				END PROOF	1.57 (0.062)	29.21 (1.150)	194.4 (28.2)	1.00	0.054	0.615	22.6 (20.6)	
				START CYCLES	1.57 (0.062)	29.21 (1.150)	135.8 (19.7)	0.70	0.054	0.615	14.8 (13.5)	
				END CYCLES	2.56 (0.1008)	29.21 (1.150)	135.8 (19.7)	0.70	0.088	1.000	24.2 (22.0)	BT AT 531~
				FRACTURE	2.56 (0.1008)	29.21 (1.150)	194.7 (28.24)	1.00	0.088	1.000	—	

① σ_Y = 194.4 MN/m^2 (28.2 KSI)

BT = BREAKTHROUGH

Table 43: CYCLIC TESTS OF 2.67 mm (0.105 INCH) 2219 ALUMINUM WELDS CAPABLE OF PASSING σ_y PROOF AND CYCLED AT 0.70 σ_y IN ROOM TEMPERATURE AIR (SPECIMENS NOT PROOFED)

SPECIMEN NUMBER	THICKNESS t mm (INCH)	WIDTH, W mm (INCH)	DIMPLING GAGE LOCATION FROM CRACK TIP	LOADING SEQUENCE	FLAW DEPTH, a mm (INCH)	FLAW LENGTH, 2c mm (INCH)	STRESS, σ MN/m^2 (KSI)	σ/σ_Y [1]	a/2c	a/t	STRESS INTENSITY, K_{1MAX} $MN/m^{3/2}$ ($KSI\sqrt{IN}$)	REMARKS
A1-Y-70-1	2.55 (0.1002)	152.6 (6.0065)	52°	START CYCLES	1.68 (0.066)	29.72 (1.170)	135.8 (19.7)	0.70	0.056	0.659	15.9 (14.5)	DID NOT DIMPLE
				END CYCLES	2.55 (0.1002)	29.72 (1.170)	135.8 (19.7)	0.70	0.086	1.000	24.2 (22.0)	BT AT 210~
				FRACTURE	2.55 (0.1002)	29.72 (1.170)	206.9 (30.01)	1.06	0.086	1.000	—	
A1-Y-70-2	2.69 (0.1059)	127.2 (5.0080)	45°	START CYCLES	1.88 (0.074)	16.00 (0.630)	135.8 (19.7)	0.70	0.117	0.699	15.9 (14.5)	DIMPLED AT 87.8 MN/m^2 (12.73 KSI) BT AT 375~
				END CYCLES	2.69 (0.1059)	16.00 (0.630)	135.8 (19.7)	0.70	0.168	1.000	20.8 (18.9)	
				FRACTURE	2.69 (0.1059)	16.00 (0.630)	218.4 (31.68)	1.12	0.168	1.000	—	
A1-Y-70-3	2.67 (0.1051)	126.9 (4.9978)	32°	START CYCLES	2.06 (0.081)	7.11 (0.280)	135.8 (19.7)	0.70	0.289	0.771	12.4 (11.3)	DIMPLING LOAD NA
				END CYCLES	2.67 (0.1051)	8.13 (0.320)	135.8 (19.7)	0.70	0.328	1.000	14.2 (12.9)	BT AT 1336~
				FRACTURE	2.67 (0.1051)	8.13 (0.320)	240.2 (34.84)	1.24	0.328	1.000	—	

[1] σ_Y = 194.4 MN/m^2 (28.2 KSI)

BT = BREAKTHROUGH

Table 44: *CYCLIC TESTS OF 2.67 mm (0.105 INCH) 2219 ALUMINUM WELDS PASSING 0.91 σ_Y PROOF AND CYCLED AT 0.70 σ_Y IN ROOM TEMPERATURE AIR (SPECIMENS PROOFED BEFORE CYCLED)*

SPECIMEN NUMBER	THICKNESS, t mm (INCH)	WIDTH, W mm (INCH)	DIMPLING GAGE LOCATION FROM CRACK TIP	LOADING SEQUENCE	FLAW DEPTH, a mm (INCH)	FLAW LENGTH, 2c mm (INCH)	STRESS, σ MN/m^2 (KSI)	σ/σ_Y [1]	a/2c	a/t	STRESS INTENSITY, $K_{I_{MAX}}$ $MN/m^{3/2}$ ($KSI\sqrt{IN}$)	REMARKS
PA1-9-70-1	2.74 (0.1079)	228.6 (9.0010)	52°	START PROOF	1.88 (0.074)	33.53 (1.320)	177.2 (25.7)	0.91	0.056	0.686	23.6 (21.5)	DIMPLED AT 111.9 MN/m^2 (16.23 KSI)
				END PROOF	2.11 (0.083)	33.53 (1.320)	177.2 (25.7)	0.91	0.063	0.769	26.9 (24.5)	
				START CYCLES	2.11 (0.083)	33.53 (1.320)	135.8 (19.7)	0.70	0.063	0.769	19.9 (18.1)	
				END CYCLES	2.74 (0.1079)	33.53 (1.320)	135.8 (19.7)	0.70	0.082	1.000	25.3 (23.0)	BT AT 193~
				FRACTURE	2.74 (0.1079)	33.53 (1.320)	217.7 (31.57)	1.12	0.082	1.000	—	
PA1-9-70-2	2.69 (0.1059)	127.2 (5.0081)	63°	START PROOF	2.36 (0.093)	16.76 (0.660)	128.7 (18.67)	0.66	0.141	0.878	18.6 (16.9)	DIMPLED AT 91.1 MN/m^2 (13.21 KSI) [2]
				END PROOF	2.69 (0.1059)	16.76 (0.660)	128.7 (18.67)	0.66	0.160	1.000	20.2 (18.4)	
				FRACTURE	2.69 (0.1059)	16.76 (0.660)	219.2 (31.79)	1.13	0.160	1.000	—	
PA1-9-70-3	2.69 (0.1060)	127.2 (5.0082)	46°	START PROOF	2.08 (0.082)	7.29 (0.287)	177.2 (25.7)	0.91	0.286	0.774	16.8 (15.3)	DIMPLED AT 115.5 MN/m^2 (16.75 KSI)
				END PROOF	2.08 (0.082)	7.29 (0.287)	177.2 (25.7)	0.91	0.286	0.774	16.8 (15.3)	
				START CYCLES	2.08 (0.082)	7.29 (0.287)	135.8 (19.7)	0.70	0.286	0.774	12.5 (11.4)	
				END CYCLES	2.69 (0.1060)	8.26 (0.325)	135.8 (19.7)	0.70	0.326	1.000	14.3 (13.0)	BT AT 3140~
				FRACTURE	2.69 (0.1060)	8.26 (0.325)	233.7 (33.90)	1.20	0.326	1.000	—	
PA1-9-70-4	2.65 (0.1045)	127.2 (5.0073)	51°	START PROOF	1.78 (0.070)	16.64 (0.655)	177.2 (25.7)	0.91	0.107	0.670	20.8 (18.9)	DIMPLED AT 85.0 MN/m^2 (12.33 KSI)
				END PROOF	1.88 (0.074)	16.64 (0.655)	177.2 (25.7)	0.91	0.113	0.708	21.9 (19.9)	
				START CYCLES	1.88 (0.074)	16.64 (0.655)	135.8 (19.7)	0.70	0.113	0.708	16.2 (14.7)	
				END CYCLES	2.65 (0.1045)	16.64 (0.655)	135.8 (19.7)	0.70	0.160	1.000	21.1 (19.2)	BT AT 667~
				FRACTURE	2.65 (0.1045)	16.64 (0.655)	231.6 (33.59)	1.19	0.160	1.000	—	

[1] σ_Y = 194.4 MN/m^2 (28.2 KSI)

[2] BT AT 128.7 MN/m^2 (18.67 KSI), MAX. LOAD REACHED WAS 159.5 MN/m^2 (23.13 KSI)

BT = BREAKTHROUGH

Table 44 : (CONTINUED)

SPECIMEN NUMBER	THICKNESS t mm (INCH)	WIDTH, W mm (INCH)	DIMPLING GAGE LOCATION FROM CRACK TIP	LOADING SEQUENCE	FLAW DEPTH, a mm (INCH)	FLAW LENGTH, 2c mm (INCH)	STRESS, σ MN/m^2 (KSI)	σ/σ_Y [1]	a/2c	a/t	STRESS INTENSITY, $K_{I_{MAX}}$ $MN/m^{3/2}$ (KSI$\sqrt{IN}$)	REMARKS
PA1-Y-85-1	2.60 (0.1024)	152.5 (6.0052)	46°	START PROOF	1.65 (0.065)	29.72 (1.170)	171.7 (24.9)	0.88	0.056	0.635	20.2 (18.4)	DIMPLED AT 76.3 MN/m^2 (11.06 KSI)
				END PROOF	1.91 (0.075)	29.72 (1.170)	171.7 (24.9)	0.88	0.064	0.732	23.7 (21.6)	
				START CYCLES	1.91 (0.075)	29.72 (1.170)	135.8 (19.7)	0.70	0.064	0.732	18.1 (16.5)	
				END CYCLES	2.60 (0.1024)	29.72 (1.170)	135.8 (19.7)	0.70	0.088	1.000	24.4 (22.2)	BT AT 172 ~
				FRACTURE	2.60 (0.1024)	29.72 (1.170)	205.2 (29.76)	1.06	0.088	1.000	—	
PA1-Y-85-2	2.69 (0.1061)	127.2 (5.0066)	63°	START PROOF	2.21 (0.087)	16.13 (0.635)	163.4 (23.7)	0.85	0.137	0.820	22.7 (20.7)	DIMPLED AT 110.3 MN/m^2 (16.00 KSI)
				END PROOF	2.29 (0.090)	16.13 (0.635)	163.4 (23.7)	0.85	0.142	0.848	23.4 (21.3)	
				START CYCLES	2.29 (0.090)	16.13 (0.635)	135.8 (19.7)	0.70	0.142	0.848	19.0 (17.3)	
				END CYCLES	2.69 (0.1061)	16.13 (0.635)	135.8 (19.7)	0.70	0.167	1.000	20.9 (19.0)	BT AT 163 ~
				FRACTURE	2.69 (0.1061)	16.13 (0.635)	225.9 (32.76)	1.16	0.167	1.000	—	
PA1-Y-70-1	2.59 (0.1021)	162.6 (6.0064)	49°	START PROOF	1.65 (0.065)	29.97 (1.180)	177.2 (25.7)	0.91	0.055	0.637	21.1 (19.2)	DIMPLED AT 85.4 MN/m^2 (12.39 KSI)
				END PROOF	1.91 (0.075)	29.97 (1.180)	177.2 (25.7)	0.91	0.064	0.735	24.7 (22.5)	
				START CYCLES	1.91 (0.075)	29.97 (1.180)	135.8 (19.7)	0.70	0.064	0.735	18.2 (16.6)	
				END CYCLES	2.59 (0.1021)	29.97 (1.180)	135.8 (19.7)	0.70	0.087	1.000	24.4 (22.2)	BT AT 190 ~
				FRACTURE	2.59 (0.1021)	29.97 (1.180)	(NA)	—	0.087	1.000	—	

[1] σ_Y = 194.4 MN/m^2 (28.2 KSI)

BT = BREAKTHROUGH

Table 45: CYCLIC TESTS OF 2.67 mm (0.105 INCH) 2219 ALUMINUM WELDS CAPABLE OF PASSING 0.91 σ_Y PROOF AND CYCLED AT 0.70 σ_Y IN ROOM TEMPERATURE AIR (SPECIMENS NOT PROOFED)

SPECIMEN NUMBER	THICKNESS t mm (INCH)	WIDTH, W mm (INCH)	DIMPLING GAGE LOCATION FROM CRACK TIP	LOADING SEQUENCE	FLAW DEPTH, a mm (INCH)	FLAW LENGTH, 2c mm (INCH)	STRESS, σ MN/m^2 (KSI)	σ/σ_Y ▷1	a/2c	a/t	STRESS INTENSITY, $K_{I_{MAX}}$ $MN/m^{3/2}$ (KSI$\sqrt{IN}$)	REMARKS
A1-9-70-1	2.75 (0.1081)	228.7 (9.0050)	28°	START CYCLES	1.78 (0.070)	33.78 (1.330)	135.8 (19.7)	0.70	0.053	0.648	16.4 (14.9)	DIMPLING LOAD N.A.
				END CYCLES	2.75 (0.1081)	33.78 (1.330)	135.8 (19.7)	0.70	0.081	1.000	25.4 (23.1)	BT AT 155~
				FRACTURE	2.75 (0.1081)	33.78 (1.330)	213.3 (30.94)	1.10	0.081	1.000	—	
A1-9-70-2	2.68 (0.1057)	127.2 (5.0090)	59°	START CYCLES	2.16 (0.085)	16.64 (0.655)	135.8 (19.7)	0.70	0.130	0.804	18.4 (16.7)	DIMPLED AT 85.4 MN/m^2 (12.38 KSI)
				END CYCLES	2.68 (0.1057)	16.64 (0.655)	135.8 (19.7)	0.70	0.161	1.000	21.1 (19.2)	BT AT 156~
				FRACTURE	2.68 (0.1057)	16.64 (0.655)	205.5 (29.80)	1.06	0.161	1.000	—	
A1-9-70-3	2.70 (0.1063)	127.2 (5.0074)	6°	START CYCLES	1.91 (0.075)	7.24 (0.285)	135.8 (19.7)	0.70	0.263	0.706	12.1 (11.0)	DIMPLED AT 1160~
				END CYCLES	2.70 (0.1063)	8.38 (0.330)	135.8 (19.7)	0.70	0.322	1.000	14.4 (13.1)	BT AT 2170~
				FRACTURE	2.70 (0.1063)	8.38 (0.330)	240.9 (34.94)	1.24	0.322	1.000	—	
A1-9-70-4	2.68 (0.1057)	127.2 (5.0078)	64°	START CYCLES	1.80 (0.071)	16.64 (0.655)	135.8 (19.7)	0.70	0.108	0.672	15.5 (14.1)	DIMPLED AT 122.7 MN/m^2 (17.80 KSI)
				END CYCLES	2.68 (0.1057)	16.64 (0.655)	135.8 (19.7)	0.70	0.161	1.000	21.1 (19.2)	BT AT 571~
				FRACTURE	2.68 (0.1057)	17.45 (0.687)	195.4 (28.34)	1.01	0.154	1.000	—	

▷1 σ_Y = 194.4 MN/m^2 (28.2 KSI)

BT = BREAKTHROUGH

Table 46: CYCLIC TESTS OF 7.62 mm (0.300 INCH) 2219 ALUMINUM WELDS PASSING σ_Y PROOF AND CYCLED AT 0.85 σ_Y IN ROOM TEMPERATURE AIR (SPECIMENS PROOFED BEFORE CYCLED)

SPECIMEN NUMBER	THICKNESS t mm (INCH)	WIDTH, W mm (INCH)	DIMPLING GAGE LOCATION FROM CRACK TIP	LOADING SEQUENCE	FLAW DEPTH, a mm (INCH)	FLAW LENGTH, 2c mm (INCH)	STRESS, σ MN/m^2 (KSI)	σ/σ_Y [1]	a/2c	a/t	STRESS INTENSITY, $K_{I_{MAX}}$ $MN/m^{3/2}$ (KSI$\sqrt{IN}$)	REMARKS
PA3-Y-85-1	7.61 (0.2998)	228.5 (8.9980)	48°	START PROOF	5.54 (0.218)	38.35 (1.510)	172.4 (25.0)	0.97	0.144	0.727	35.4 (32.2)	DIMPLED AT 81.3 MN/m^2 (11.79 KSI)
				END PROOF	6.22 (0.245)	38.74 (1.525)	172.4 (25.0)	0.97	0.161	0.817	39.0 (35.5)	
				START CYCLES	6.22 (0.245)	38.74 (1.525)	151.7 (22.0)	0.70	0.161	0.817	33.6 (30.6)	
				END CYCLES	7.61 (0.2998)	40.89 (1.610)	151.7 (22.0)	0.70	0.186	1.000	38.2 (34.8)	BT AT 70~
				FRACTURE	7.61 (0.2998)	40.89 (1.610)	199.3 (28.91)	1.12	0.186	1.000	—	
PA3-Y-85-2	7.63 (0.3005)	127.1 (5.0002)	37°	START PROOF	5.64 (0.222)	21.08 (0.830)	176.5 (25.6)	0.99	0.267	0.739	28.5 (25.9)	DIMPLED AT 97.3 MN/m^2 (14.11 KSI)
				END PROOF	6.22 (0.245)	21.08 (0.830)	176.5 (25.6)	0.99	0.295	0.815	29.2 (26.6)	
				START CYCLES	6.22 (0.245)	21.08 (0.830)	151.7 (22.0)	0.70	0.295	0.815	24.7 (22.5)	
				END CYCLES	7.63 (0.3005)	23.62 (0.930)	151.7 (22.0)	0.70	0.323	1.000	27.5 (25.0)	BT AT 216~
				FRACTURE	7.63 (0.3005)	23.62 (0.930)	193.1 (28.00)	1.08	0.323	1.000	—	
PA3-Y-85-3	7.62 (0.3000)	88.9 (3.5012)	38°	START PROOF	5.84 (0.230)	14.78 (0.582)	173.5 (25.16)	0.97	0.395	0.767	21.7 (19.7)	DIMPLED AT 109.3 MN/m^2 (15.85 KSI)
				END PROOF	5.97 (0.235)	15.49 (0.610)	173.5 (25.16)	0.97	0.385	0.783	22.5 (20.5)	
				START CYCLES	5.97 (0.235)	15.49 (0.610)	151.7 (22.0)	0.70	0.385	0.783	19.5 (17.7)	
				END CYCLES	7.62 (0.3000)	20.96 (0.825)	151.7 (22.0)	0.70	0.364	1.000	25.7 (23.4)	BT AT 369~
				FRACTURE	7.62 (0.3000)	20.96 (0.825)	174.1 (25.25)	0.97	0.364	1.000	—	

[1] σ_Y = 178.6 MN/m^2 (25.9 KSI)

BT = BREAKTHROUGH

Table 47: CYCLIC TESTS OF 7.62 mm (0.300 INCH) 2219 ALUMINUM WELDS CAPABLE OF PASSING σ_y PROOF AND CYCLED AT 0.85 σ_y IN ROOM TEMPERATURE AIR (SPECIMENS NOT PROOFED)

SPECIMEN NUMBER	THICKNESS t mm (INCH)	WIDTH, W mm (INCH)	DIMPLING GAGE LOCATION FROM CRACK TIP	LOADING SEQUENCE	FLAW DEPTH, a mm (INCH)	FLAW LENGTH, 2c mm (INCH)	STRESS, σ MN/m^2 (KSI)	σ/σ_Y [1]	a/2c	a/t	STRESS INTENSITY, $K_{I_{MAX}}$ $MN/m^{3/2}$ ($KSI\sqrt{IN}$)	REMARKS
A3-Y-85-1	7.64 (0.3006)	228.5 (8.9980)	51°	START CYCLES	5.66 (0.223)	37.92 (1.493)	151.7 (22.0)	0.85	0.149	0.742	30.9 (28.1)	DIMPLING LOAD N.A.
				END CYCLES	7.64 (0.3006)	37.92 (1.493)	151.7 (22.0)	0.85	0.201	1.000	36.9 (33.6)	BT AT 63~
				FRACTURE	7.64 (0.3006)	37.92 (1.493)	203.1 (29.45)	1.14	0.201	1.000	—	
A3-Y-85-2	7.57 (0.2979)	127.3 (5.0011)	51°	START CYCLES	5.64 (0.222)	21.08 (0.830)	151.7 (22.0)	0.85	0.267	0.745	24.1 (21.9)	DIMPLED AT 92.8 MN/m^2 (13.46 KSI)
				END CYCLES	7.57 (0.2979)	24.38 (0.960)	151.7 (22.0)	0.85	0.310	1.000	27.9 (25.4)	BT AT 275~
				FRACTURE	7.57 (0.2979)	24.38 (0.960)	187.8 (27.23)	1.05	0.310	1.000	—	
A3-Y-85-3	7.76 (0.3056)	88.9 (3.4997)	33°	START CYCLES	5.87 (0.231)	14.61 (0.575)	151.7 (22.0)	0.85	0.402	0.756	18.4 (16.7)	DIMPLED AT 108.9 MN/m^2 (15.80 KSI)
				END CYCLES	7.76 (0.3056)	21.21 (0.835)	151.7 (22.0)	0.85	0.366	1.000	25.8 (23.5)	BT AT 455~
				FRACTURE	7.76 (0.3056)	21.21 (0.835)	179.1 (25.97)	1.00	0.366	1.000	—	

[1] σ_Y = 178.6 MN/m^2 (25.9 KSI)

BT = BREAKTHROUGH

Table 48: *CYCLIC TESTS OF 7.62 mm (0.300 INCH) 2219 ALUMINUM WELDS PASSING σ_Y PROOF AND CYCLED AT 0.70 σ_Y IN ROOM TEMPERATURE AIR (SPECIMENS PROOFED BEFORE CYCLED)*

SPECIMEN NUMBER	THICKNESS t mm (INCH)	WIDTH, W mm (INCH)	DIMPLING GAGE LOCATION FROM CRACK TIP	LOADING SEQUENCE	FLAW DEPTH, a mm (INCH)	FLAW LENGTH, 2c mm (INCH)	STRESS, σ MN/m^2 (KSI)	σ/σ_Y [1]	a/2c	a/t	STRESS INTENSITY, $K_{f_{MAX}}$ $MN/m^{3/2}$ ($KSI\sqrt{IN}$)	REMARKS
PA3-Y-70-1	7.62 (0.3001)	228.5 (8.9970)	45°	START PROOF	5.59 (0.220)	38.10 (1.500)	175.1 (25.4)	0.98	0.147	0.733	36.3 (33.0)	DIMPLED AT 81.2 MN/m^2 (11.78 KSI)
				END PROOF	6.43 (0.253)	38.35 (1.510)	175.1 (25.4)	0.98	0.168	0.843	40.6 (36.9)	
				START CYCLES	6.43 (0.253)	38.35 (1.510)	124.8 (18.1)	0.70	0.168	0.843	27.6 (25.1)	
				END CYCLES	7.62 (0.3001)	39.75 (1.565)	124.8 (18.1)	0.70	0.192	1.000	30.4 (27.7)	BT AT 265~
				FRACTURE	7.62 (0.3001)	39.75 (1.565)	196.5 (28.50)	1.10	0.192	1.000	—	
PA3-Y-70-2	7.63 (0.3002)	127.0 (5.0004)	53°	START PROOF	5.59 (0.220)	20.96 (0.825)	171.4 (24.86)	0.96	0.267	0.733	27.4 (24.9)	DIMPLED AT 102.9 MN/m^2 (14.92 KSI)
				END PROOF	6.10 (0.240)	21.34 (0.840)	171.4 (24.86)	0.96	0.286	0.799	28.5 (25.9)	
				START CYCLES	6.10 (0.240)	21.34 (0.840)	124.8 (18.1)	0.70	0.286	0.799	20.0 (18.2)	
				END CYCLES	7.63 (0.3002)	25.15 (0.990)	124.8 (18.1)	0.70	0.303	1.000	23.0 (20.9)	BT AT 975~
				FRACTURE	7.63 (0.3002)	25.15 (0.990)	134.8 (19.55)	0.75	0.303	1.000	—	
PA3-Y-70-3	7.62 (0.3000)	88.9 (3.5017)	35°	START PROOF	5.97 (0.235)	15.11 (0.595)	166.2 (24.1)	0.93	0.395	0.783	21.0 (19.1)	DIMPLED AT 100.7 MN/m^2 (14.61 KSI)
				END PROOF	6.48 (0.255)	15.93 (0.627)	166.2 (24.1)	0.93	0.407	0.850	22.1 (20.1)	
				START CYCLES	6.48 (0.255)	15.93 (0.627)	124.8 (18.1)	0.70	0.407	0.850	16.3 (14.8)	
				END CYCLES	7.62 (0.3000)	19.43 (0.765)	124.8 (18.1)	0.70	0.392	1.000	19.9 (18.1)	BT AT 1002~
				FRACTURE	7.62 (0.3000)	19.43 (0.765)	187.1 (27.13)	1.05	0.392	1.000	—	

[1] σ_Y = 178.6 MN/m^2 (25.9 KSI)

BT = BREAKTHROUGH

Table 49: CYCLIC TESTS OF 7.62 mm (0.300 INCH) 2219 ALUMINUM WELDS CAPABLE OF PASSING σ_y PROOF AND CYCLED AT 0.70 σ_y IN ROOM TEMPERATURE AIR (SPECIMENS NOT PROOFED)

SPECIMEN NUMBER	THICKNESS, t mm (INCH)	WIDTH, W mm (INCH)	DIMPLING GAGE LOCATION FROM CRACK TIP	LOADING SEQUENCE	FLAW DEPTH, a mm (INCH)	FLAW LENGTH, 2c mm (INCH)	STRESS, σ MN/m^2 (KSI)	σ/σ_Y [1]	a/2c	a/t	STRESS INTENSITY, $K_{I_{MAX}}$ $MN/m^{3/2}$ (KSI$\sqrt{IN}$)	REMARKS
A3-Y-70-1	7.63 (0.3002)	228.5 (8.9980)	44°	START CYCLES	5.46 (0.215)	37.47 (1.475)	124.8 (18.1)	0.70	0.146	0.716	24.1 (21.9)	DIMPLED AT 91.2 MN/m^2 (13.22 KSI)
				END CYCLES	7.63 (0.3002)	38.61 (1.520)	124.8 (18.1)	0.70	0.198	1.000	30.0 (27.3)	BT AT 353~
				FRACTURE	7.63 (0.3002)	38.61 (1.520)	194.5 (28.21)	1.09	0.198	1.000	—	
A3-Y-70-2	7.62 (0.2999)	127.0 (5.0010)	42°	START CYCLES	5.61 (0.221)	21.08 (0.830)	124.8 (18.1)	0.70	0.266	0.737	19.3 (17.6)	DIMPLED AT 106.7 MN/m^2 (15.47 KSI)
				END CYCLES	7.62 (0.2999)	25.27 (0.995)	124.8 (18.1)	0.70	0.301	1.000	23.0 (20.9)	BT AT 938~
				FRACTURE	7.62 (0.2999)	25.27 (0.995)	NA	—	0.301	1.000	—	
A3-Y-70-3	7.62 (0.3001)	88.9 (3.4984)	22°	START CYCLES	4.90 (0.193)	13.97 (0.550)	124.8 (18.1)	0.70	0.351	0.643	14.5 (13.2)	DIMPLING LOAD N.A.
				END CYCLES	7.62 (0.3001)	20.70 (0.815)	124.8 (18.1)	0.70	0.368	1.000	20.7 (18.8)	BT AT 2000~
				FRACTURE	7.62 (0.3001)	20.70 (0.815)	182.2 (26.43)	1.02	0.368	1.000	—	
A3-Y-70-4	7.59 (0.2988)	88.8 (3.4970)	45°	START CYCLES	5.59 (0.220)	15.11 (0.595)	124.8 (18.1)	0.70	0.370	0.736	15.5 (14.1)	DIMPLED AT 99.6 MN/m^2 (14.45 KSI)
				END CYCLES	7.59 (0.2988)	19.56 (0.770)	124.8 (18.1)	0.70	0.388	1.000	20.0 (18.2)	BT AT 1309~
				FRACTURE	7.59 (0.2988)	19.56 (0.770)	178.2 (25.84)	1.00	0.388	1.000	—	

[1] σ_Y = 178.6 MN/m^2 (25.9 KSI)

BT = BREAKTHROUGH

Table 50: CYCLIC TESTS OF 7.62 mm (0.300 INCH) 2219 ALUMINUM WELDS PASSING 0.91 σ_Y PROOF AND CYCLED AT 0.70 σ_Y IN ROOM TEMPERATURE AIR (SPECIMENS PROOFED BEFORE CYCLED)

SPECIMEN NUMBER	THICKNESS, t mm (INCH)	WIDTH, W mm (INCH)	DIMPLING GAGE LOCATION FROM CRACK TIP	LOADING SEQUENCE	FLAW DEPTH, a mm (INCH)	FLAW LENGTH, 2c mm (INCH)	STRESS, σ MN/m^2 (KSI)	σ/σ_Y [1]	a/2c	a/t	STRESS INTENSITY, $K_{I_{MAX}}$ $MN/m^{3/2}$ ($KSI\sqrt{IN}$)	REMARKS
PA3-9-70-1	7.56 (0.2975)	228.6 (9.0010)	43°	START PROOF	6.35 (0.250)	41.02 (1.615)	162.7 (23.6)	0.91	0.155	0.840	38.0 (34.6)	DIMPLED AT 74.3 MN/m^2 (10.78 KSI)
				END PROOF	7.56 (0.2975)	41.02 (1.615)	162.7 (23.6)	0.91	0.184	1.000	41.2 (37.5)	BT AT PROOF LOAD
				FRACTURE	7.56 (0.2975)	41.02 (1.615)	194.3 (28.18)	1.09	0.184	1.000	—	
PA3-9-70-2	7.69 (0.3027)	127.1 (5.0040)	54°	START PROOF	6.35 (0.250)	23.95 (0.943)	162.7 (23.6)	0.91	0.265	0.826	29.1 (26.5)	DIMPLED AT 95.6 MN/m^2 (13.86 KSI)
				END PROOF	6.83 (0.269)	24.64 (0.970)	162.7 (23.6)	0.91	0.277	0.889	30.1 (27.4)	
				START CYCLES	6.83 (0.269)	24.64 (0.970)	124.8 (18.1)	0.70	0.277	0.889	22.5 (20.5)	
				END CYCLES	7.69 (0.3027)	25.91 (1.020)	124.8 (18.1)	0.70	0.297	1.000	23.4 (21.3)	BT AT 251~
				FRACTURE	7.69 (0.3027)	25.91 (1.020)	191.2 (27.73)	1.07	0.297	1.000	—	
PA3-9-70-3	7.66 (0.3016)	89.0 (3.5040)	40°	START PROOF	6.20 (0.244)	14.94 (0.588)	162.7 (23.6)	0.91	0.415	0.809	20.3 (18.5)	DIMPLED AT 101.1 MN/m^2 (14.67KSI)
				END PROOF	6.68 (0.263)	15.62 (0.615)	162.7 (23.6)	0.91	0.428	0.872	21.2 (19.3)	
				START CYCLES	6.68 (0.263)	15.62 (0.615)	124.8 (18.1)	0.70	0.428	0.872	16.0 (14.6)	
				END CYCLES	7.66 (0.3016)	18.03 (0.710)	124.8 (18.1)	0.70	0.425	1.000	18.6 (16.9)	BT AT 760~
				FRACTURE	7.66 (0.3016)	18.03 (0.710)	188.3 (27.31)	1.05	0.425	1.000	—	
PA3-9-70-4	7.63 (0.3002)	228.7 (9.0040	48°	START PROOF	5.84 (0.230)	41.28 (1.625)	168.2 (24.39)	0.94	0.142	0.766	26.7 (33.4)	DIMPLED AT 91.4 MN/m^2 (13.26 KSI)
				END PROOF	6.12 (0.241)	41.28 (1.625)	168.2 (24.39)	0.94	0.148	0.803	38.2 (34.8)	
				START CYCLES	6.12 (0.241)	41.28 (1.625)	124.8 (18.1)	0.70	0.148	0.803	27.3 (24.8)	
				END CYCLES	7.63 (0.3002)	41.28 (1.625)	124.8 (18.1)	0.70	0.185	1.000	31.0 (28.2)	BT AT 245~
				FRACTURE	7.63 (0.3002)	41.28 (1.625)	198.2 (28.75)	1.11	0.185	1.000	—	

[1] σ_Y = 178.6 MN/m^2 (25.9 KSI)

BT = BREAKTHROUGH

Table 51: CYCLIC TESTS OF 7.62 mm (0.300 INCH) 2219 ALUMINUM WELDS CAPABLE OF PASSING 0.91 σ_Y PROOF AND CYCLED AT 0.70 σ_Y IN ROOM TEMPERATURE AIR (SPECIMENS NOT PROOFED)

SPECIMEN NUMBER	THICKNESS t mm (INCH)	WIDTH, W mm (INCH)	DIMPLING GAGE LOCATION FROM CRACK TIP	LOADING SEQUENCE	FLAW DEPTH, a mm (INCH)	FLAW LENGTH, 2c mm (INCH)	STRESS, σ MN/m^2 (KSI)	σ/σ_Y [1]	a/2c	a/t	STRESS INTENSITY, $K_{I_{MAX}}$ $MN/m^{3/2}$ ($KSI\sqrt{IN}$)	REMARKS
A3-9-70-1	7.85 (0.3090)	228.6 (9.0010)	34°	START CYCLES	5.99 (0.236)	41.02 (1.615)	124.8 (18.1)	0.70	0.146	0.764	26.2 (23.8)	DIMPLING LOAD N.A.
				END CYCLES	7.85 (0.3090)	42.42 (1.670)	124.8 (18.1)	0.70	0.185	1.000	31.4 (28.6)	BT AT 193~
				FRACTURE	7.85 (0.3090)	42.42 (1.670)	NA	—	0.185	1.000	—	
A3-9-70-2	7.67 (0.3020)	127.0 (5.0012)	45°	START CYCLES	6.22 (0.245)	24.13 (0.950)	124.8 (18.1)	0.70	0.258	0.811	21.8 (19.8)	DIMPLING LOAD N.A.
				END CYCLES	7.67 (0.3020)	25.65 (1.010)	124.8 (18.1)	0.70	0.299	1.000	23.2 (21.1)	BT AT 324~
				FRACTURE	7.67 (0.3020)	25.65 (1.010)	191.7 (27.81)	1.07	0.299	1.000	—	
A3-9-70-3	7.63 (0.3002)	89.0 (3.5027)	27°	START CYCLES	6.10 (0.240)	15.04 (0.592)	124.8 (18.1)	0.70	0.405	0.799	15.4 (14.0)	DIMPLED AT 114.7 MN/m^2 (16.64 KSI)
				END CYCLES	7.63 (0.3002)	19.56 (0.770)	124.8 (18.1)	0.70	0.390	1.000	20.0 (18.2)	BT AT 883~
				FRACTURE	7.63 (0.3002)	19.56 (0.770)	172.7 (25.05)	0.97	0.390	1.000	—	

[1] σ_Y = 178.6 MN/m^2 (25.9 KSI)

BT = BREAKTHROUGH

Table 52: CYCLIC TESTS OF 0.51 mm (0.020 INCH) 6Al-4V STA TITANIUM WELDS PASSING σ_Y PROOF AND CYCLED AT 0.85 σ_Y, R = 0 IN ROOM TEMPERATURE AIR (SPECIMENS PROOFED BEFORE CYCLED)

SPECIMEN NUMBER	THICKNESS, t mm (INCH)	WIDTH, W mm (INCH)	DIMPLING GAGE LOCATION FROM CRACK TIP	LOADING SEQUENCE	FLAW DEPTH, a mm (INCH)	FLAW LENGTH, 2c mm (INCH)	STRESS, σ MN/m^2 (KSI)	σ/σ_Y [1]	a/2c	a/t	STRESS INTENSITY, $K_{I_{MAX}}$ $MN/m^{3/2}$ ($KSI\sqrt{IN}$)	REMARKS
PT-02-Y 85-1	0.53 (0.0208)	30.51 (1.2011)	22°	START PROOF	0.28 (0.011)	3.12 (0.123)	952 (138.0)	0.93	0.089	0.529	40.3 (36.7)	DIMPLED AT 78.3 MN/m^2 (113.6 KSI) FAILED IN PROOF
				END PROOF	—	—	952 (138.0)	0.93	—	—	—	
PT 02-Y-85-2	0.56 (0.0219)	30.46 (1.1991)	55°	START PROOF	0.25 (0.010)	1.68 (0.066)	1020 (147.9)	1.00	0.152	0.457	36.2 (32.9)	
				END PROOF	0.25 (0.010)	1.68 (0.066)	1020 (147.9)	1.00	0.152	0.457	36.2 (32.9)	
				START CYCLES	0.25 (0.010)	1.68 (0.066)	867 (125.7)	0.85	0.152	0.457	30.0 (27.3)	DIMPLED AT 285~
				END CYCLES	0.56 (0.0219)	1.80 (0.071)	867 (125.7)	0.85	0.309	1.000	43.4 (39.5)	BT AT 319~
				FRACTURE	0.56 (0.0219)	1.80 (0.071)	1040 (150.8)	1.02	0.309	1.000	—	
PT 02-Y-85-3	0.53 (0.0210)	30.47 (1.1997)	24°	START PROOF	0.30 (0.012)	1.02 (0.040)	1020 (147.9)	1.00	0.300	0.571	32.5 (29.6)	DIMPLED AT 851 MN/m^2 (123.4 KSI)
				END PROOF	0.30 (0.012)	1.02 (0.040)	1020 (147.9)	1.00	0.300	0.571	32.5 (29.6)	
				START CYCLES	0.30 (0.012)	1.02 (0.040)	867 (125.7)	0.85	0.300	0.571	27.1 (24.7)	
				END CYCLES	0.53 (0.0210)	1.91 (0.075)	867 (125.7)	0.85	0.280	1.000	45.5 (41.4)	BT AT 414~
				FRACTURE	0.53 (0.0210)	1.91 (0.075)	1047 (151.8)	1.03	0.280	1.000	—	
PT 02-Y-85-4	0.50 (0.0198)	30.40 (1.1970)	70°	START PROOF	0.30 (0.012)	3.12 (0.123)	954 (138.4)	0.94	0.098	0.606	44.6 (40.6)	DIMPLED AT 881 MN/m^2 (127.8 KSI)
				END PROOF	—	—	954 (138.4)	0.94	—	—	—	FAILED IN PROOF
PT 02-Y-85-5	0.54 (0.0212)	30.65 (1.2065)	32°	START PROOF	0.25 (0.010)	3.30 (0.130)	1007 (146.1)	0.99	0.077	0.472	40.0 (36.4)	DIMPLED AT 674 MN/m^2 (97.7 KSI)
				END PROOF	—	—	1007 (146.1)	0.99	—	—	—	FAILED IN PROOF
PT 02-Y-85-6	0.54 (0.0213)	30.59 (1.2045)	48°	START PROOF	0.25 (0.010)	3.18 (0.125)	1011 (146.7)	0.99	0.080	0.469	40.0 (36.4)	DIMPLED AT 698 MN/m^2 (101.2 KSI)
				END PROOF	—	—	1011 (146.7)	0.99	—	—	—	FAILED IN PROOF
PT 02-Y-85-7	0.54 (0.0213)	30.40 (1.1967)	55°	START PROOF	0.15 (0.006)	2.95 (0.116)	1020 (147.9)	1.00	0.052	0.282	30.9 (28.1)	DIMPLED AT 761 MN/m^2 (110.4 KSI)
				END PROOF	0.15 (0.006)	2.95 (0.116)	1020 (147.9)	1.00	0.052	0.282	43.2 (39.3)	
				START CYCLES	0.15 (0.006)	2.95 (0.116)	867 (125.7)	0.85	0.052	0.282	24.0 (21.8)	
				END CYCLES	0.54 (0.0213)	2.95 (0.116)	867 (125.7)	0.85	0.184	1.000	58.7 (53.4)	BT AT 512~
				FRACTURE	0.54 (0.0213)	2.95 (0.116)	1022 (148.2)	1.00	0.184	1.000	—	

[1] σ_Y = 1020 MN/m^2 (147.9 KSI)

BT = BREAKTHROUGH

Table 53: CYCLIC TESTS OF 0.51 mm (0.020 INCH) 6AI-4V STA TITANIUM WELDS CAPABLE OF PASSING σ_Y PROOF AND CYCLED AT 0.85 σ_Y, R = 0 IN ROOM TEMPERATURE AIR (SPECIMENS NOT PROOFED)

SPECIMEN NUMBER	THICKNESS, t mm (INCH)	WIDTH, W mm (INCH)	DIMPLING GAGE LOCATION FROM CRACK TIP	LOADING SEQUENCE	FLAW DEPTH, a mm (INCH)	FLAW LENGTH, 2c mm (INCH)	STRESS, σ MN/m^2 (KSI)	σ/σ_Y [1]	a/2c	a/t	STRESS INTENSITY, $K_{I_{MAX}}$ $MN/m^{3/2}$ ($KSI\sqrt{IN}$)	REMARKS
T 02- Y-85-1	0.53 (0.0209)	30.56 (1.2030)	10°	START CYCLES	0.25 (0.010)	3.05 (0.120)	867 (125.7)	0.85	0.083	0.478	33.2 (30.2)	DIMPLED AT 107~
				END CYCLES	0.53 (0.0209)	3.05 (0.120)	867 (125.7)	0.85	0.174	1.000	59.3 (54.0)	BT AT 170~
				FRACTURE	0.53 (0.0209)	3.05 (0.120)	NA	—	0.174	1.000	—	
T 02-Y-85-2	0.54 (0.0211)	30.51 (1.2012)	45°	START CYCLES	0.20 (0.008)	1.57 (0.062)	867 (125.7)	0.85	0.129	0.379	26.4 (24.0)	DIMPLED AT 19~
				END CYCLES	0.54 (0.0211)	1.73 (0.068)	867 (125.7)	0.85	0.310	1.000	42.4 (38.6)	BT AT 375~
				FRACTURE	0.54 (0.0211)	1.73 (0.068)	1019 (147.8)	1.00	0.310	1.000	—	
T 02-Y-85-3	0.54 (0.0212)	30.54 (1.2023)	11°	START CYCLES	0.28 (0.011)	1.02 (0.040)	867 (125.7)	0.85	0.275	0.519	26.5 (24.1)	DIMPLED AT 867 MN/m^2 (125.7 KSI)
				END CYCLES	0.54 (0.0212)	1.27 (0.050)	867 (125.7)	0.85	0.424	1.000	34.7 (31.6)	BT AT 318~
				FRACTURE	0.54 (0.0212)	1.27 (0.050)	1082 (156.9)	1.06	0.424	1.000	—	

[1] σ_Y = 1020 MN/m^2 (147.9 KSI)

BT = BREAKTHROUGH

Table 54: *CYCLIC TESTS OF 0.51 mm (0.020 INCH) 6Al-4V STA TITANIUM WELDS PASSING σ_Y PROOF AND CYCLED AT 0.70 σ_Y, R = 0 IN ROOM TEMPERATURE AIR (SPECIMENS PROOFED BEFORE CYCLED)*

SPECIMEN NUMBER	THICKNESS, t mm (INCH)	WIDTH, W mm (INCH)	DIMPLING GAGE LOCATION FROM CRACK TIP	LOADING SEQUENCE	FLAW DEPTH, a mm (INCH)	FLAW LENGTH, 2c mm (INCH)	STRESS, σ MN/m^2 (KSI)	σ/σ_Y [1]	a/2c	a/t	STRESS INTENSITY, $K_{I_{MAX}}$ $MN/m^{3/2}$ (KSI$\sqrt{IN}$)	REMARKS
PT 02-Y 70-1	0.54 (0.0213)	30.44 (1.1984)	35°	START PROOF	0.18 (0.007)	2.29 (0.090)	1005 (145.7)	0.99	0.078	0.329	43.2 (39.3)	DIMPLED AT 841 MN/m^2 (122.0 KSI)
				END PROOF	0.30 (0.012)	2.29 (0.090)	1005 (145.7)	0.99	0.133	0.563	43.2 (39.3)	
				START CYCLES	0.30 (0.012)	2.29 (0.090)	714 (103.5)	0.70	0.133	0.563	29.2 (26.6)	
				END CYCLES	0.54 (0.0213)	2.29 (0.090)	714 (103.5)	0.70	0.237	1.000	41.4 (37.7)	BT AT 445~
				FRACTURE	0.54 (0.0213)	2.29 (0.090)	980 (142.2)	0.96	0.237	1.000	—	
PT 02-Y-70-2	0.53 (0.0209)	30.46 (1.1993)	47°	START PROOF	0.18 (0.007)	1.63 (0.064)	1020 (147.9)	1.00	0.109	0.335	30.3 (27.6)	DIMPLED AT 847 MN/m^2 (122.9 KSI)
				END PROOF	0.18 (0.007)	1.63 (0.064)	1020 (147.9)	1.00	0.109	0.335	30.3 (27.6)	
				START CYCLES	0.180 (0.007)	1.63 (0.064)	714 (103.5)	0.70	0.109	0.335	20.1 (18.3)	
				END CYCLES	0.53 (0.0209)	1.80 (0.071)	714 (103.5)	0.70	0.294	1.000	35.4 (32.2)	BT AT 1090~
				FRACTURE	0.53 (0.0209)	1.80 (0.071)	986 (143.0)	0.97	0.294	1.000	—	
PT 02-Y-70-3	0.54 (0.0212)	30.48 (1.2000)	36°	START PROOF	0.23 (0.009)	1.07 (0.042)	1020 (147.9)	1.00	0.214	0.425	30.6 (27.8)	DIMPLED AT 939 MN/m^2 (136.2 KSI)
				END PROOF	0.23 (0.009)	1.07 (0.042)	1020 (147.9)	1.00	0.214	0.425	30.6 (27.8)	
				START CYCLES	0.23 (0.009)	1.07 (0.042)	714 (103.5)	0.70	0.214	0.425	20.4 (18.6)	
				END CYCLES	0.54 (0.0212)	1.70 (0.067)	714 (103.5)	0.70	0.316	1.000	34.2 (31.1)	BT AT 1918~
				FRACTURE	0.54 (0.0212)	1.70 (0.067)	1015 (147.2)	1.00	0.316	1.000	—	

[1] σ_Y = 1020 MN6m^2 (147.9 KSI)

BT = BREAKTHROUGH

Table 55: CYCLIC TESTS OF 0.51 mm (0.020 INCH) 6AI-4V STA TITANIUM WELDS CAPABLE OF PASSING σ_Y PROOF AND CYCLED AT 0.70 σ_Y, R = 0 IN ROOM TEMPERATURE AIR (SPECIMENS NOT PROOFED)

SPECIMEN NUMBER	THICKNESS t mm (INCH)	WIDTH, W mm (INCH)	DIMPLING GAGE LOCATION FROM CRACK TIP	LOADING SEQUENCE	FLAW DEPTH, a mm (INCH)	FLAW LENGTH, 2c mm (INCH)	STRESS, σ MN/m^2 (KSI)	σ/σ_Y [1]	a/2c	a/t	STRESS INTENSITY, $K_{I_{MAX}}$ $MN/m^{3/2}$ ($KSI\sqrt{IN}$)	REMARKS
T 02-Y-70-1	0.54 (0.0214)	30.45 (1.1990)	43°	START CYCLES	0.13 (0.005)	2.34 (0.092)	714 (103.5)	0.70	0.054	0.234	17.0 (15.5)	DIMPLED AT 675~
				END CYCLES	0.54 (0.0214)	2.39 (0.094)	714 (103.5)	0.70	0.228	1.000	42.5 (38.7)	BT AT 714~
				FRACTURE	0.54 (0.0214)	2.39 (0.094)	980 (142.2)	0.96	0.228	1.000	—	
T 02-Y-70-2	0.53 (0.0208)	30.48 (1.2000)	44°	START CYCLES	0.13 (0.005)	1.60 (0.063)	714 (103.5)	0.70	0.079	0.240	16.8 (15.3)	DIMPLED AT 935~
				END CYCLES	0.53 (0.0208)	1.73 (0.068)	714 (103.5)	0.70	0.306	1.000	34.4 (31.3)	BT AT 1127~
				FRACTURE	0.53 (0.0208)	1.73 (0.068)	1031 (149.6)	1.01	0.306	1.000	—	
T 02-Y-70-3	0.54 (0.0211)	30.48 (1.2001)	40°	START CYCLES	0.23 (0.009)	0.91 (0.036)	714 (103.5)	0.70	0.250	0.427	19.5 (17.7)	DIMPLED AT 665~
				END CYCLES	0.54 (0.0211)	1.52 (0.060)	714 (103.5)	0.70	0.352	1.000	32.2 (29.3)	BT AT 1175~
				FRACTURE	0.54 (0.0211)	1.52 (0.060)	1049 (152.2)	1.03	0.352	1.000	—	

[1] σ_Y = 1020 MN/m^2 (147.9 KSI)

BT = BREAKTHROUGH

Table 56: *CYCLIC TESTS OF 0.51 mm (0.020 INCH) 6AI-4V STA TITANIUM WELDS PASSING 0.91 σ_Y PROOF AND CYCLED AT 0.70 σ_Y, R = 0 IN ROOM TEMPERATURE AIR (SPECIMENS PROOFED BEFORE CYCLED)*

SPECIMEN NUMBER	THICKNESS, t mm (INCH)	WIDTH, W mm (INCH)	DIMPLING GAGE LOCATION FROM CRACK TIP	LOADING SEQUENCE	FLAW DEPTH, a mm (INCH)	FLAW LENGTH, 2c mm (INCH)	STRESS, σ MN/m^2 (KSI)	σ/σ_Y [1]	a/2c	a/t	STRESS INTENSITY, $K_{I_{MAX}}$ $MN/m^{3/2}$ ($KSI\sqrt{IN}$)	REMARKS
PT 02-9-70-1	0.50 (0.0197)	30.47 (1.1998)	39°	START PROOF	0.28 (0.011)	4.57 (0.180)	891 (129.2)	0.87	0.061	0.558	39.8 (36.2)	DIMPLED AT 742 MN/m^2 (107.6 KSI)
				END PROOF	0.50 (0.0197)	(NA)	891 (129.2)	0.87	NA	1.000	—	[2]
				FRACTURE	0.50 (0.0197)	(NA)	918 (133.1)	0.90	NA	1.000	—	
PT 02-9-70-2	0.54 (0.0214)	30.46 (1.1991)	30°	START PROOF	0.28 (0.011)	2.26 (0.089)	928 (134.6)	0.91	0.124	0.514	36.6 (33.3)	DIMPLED AT 885 MN/m^2 (128.4 KSI)
				END PROOF	0.30 (0.012)	2.26 (0.089)	928 (134.6)	0.91	0.135	0.561	39.1 (35.6)	
				START CYCLES	0.30 (0.012)	2.26 (0.089)	714 (103.5)	0.70	0.135	0.561	29.1 (26.5)	
				END CYCLES	0.54 (0.0214)	2.26 (0.089)	714 (103.5)	0.70	0.240	1.000	41.2 (37.5)	BT AT 435~
				FRACTURE	0.54 (0.0214)	2.26 (0.089)	945 (137.0)	0.93	0.240	1.000	—	
PT 02-9-70-3	0.51 (0.0202)	30.52 (1.2016)	72°	START PROOF	0.43 (0.017)	1.78 (0.070)	918 (133.1)	0.90	0.243	0.842	45.6 (41.5)	DIMPLED AT 704 MN/m^2 (102.1 KSI)
				END PROOF	0.46 (0.018)	1.78 (0.070)	918 (133.1)	0.90	0.257	0.891	46.2 (42.0)	
				START CYCLES	0.46 (0.018)	1.78 (0.070)	714 (103.5)	0.70	0.257	0.891	35.1 (31.9)	
				END CYCLES	0.51 (0.0202)	1.80 (0.071)	714 (103.5)	0.70	0.285	1.000	35.7 (32.5)	BT AT 57~
				FRACTURE	0.51 (0.0202)	1.80 (0.071)	979 (142.0)	0.96	0.285	1.000	—	
PT 02-9-70-4	0.51 (0.0200)	30.78 (1.2120)	45°	START PROOF	0.25 (0.010)	4.95 (0.195)	898 (130.2)	0.88	0.051	0.500	36.7 (33.4)	DIMPLED AT 774 MN/m^2 (112.2 KSI)
				END PROOF	0.33 (0.013)	4.95 (0.195)	898 (130.2)	0.88	0.067	0.650	47.4 (43.1)	
				START CYCLES	0.33 (0.013)	4.95 (0.195)	714 (103.5)	0.70	0.067	0.650	36.4 (33.1)	
				END CYCLES	0.51 (0.0200)	5.21 (0.205)	714 (103.5)	0.70	0.098	1.000	55.5 (50.5)	BT AT 161~
				FRACTURE	0.51 (0.0200)	5.21 (0.205)	932 (135.1)	0.91	0.098	1.000	—	

[1] σ_Y 1020 MN/m^2 (147.9 KSI)

[2] BT AT 891 MN/m^2 (129.2 KSI) MAX LOAD REACHED WAS 928 MN/m^2 (134.6 KSI)

BT = BREAKTHROUGH

Table 57: CYCLIC TESTS OF 0.51 mm (0.020 INCH) 6AI-4V STA TITANIUM WELDS CAPABLE OF PASSING 0.91 σ_y PROOF AND CYCLED AT 0.70 σ_y, R = 0 IN ROOM TEMPERATURE AIR (SPECIMENS NOT PROOFED)

SPECIMEN NUMBER	THICKNESS, t mm (INCH)	WIDTH, W mm (INCH)	DIMPLING GAGE LOCATION FROM CRACK TIP	LOADING SEQUENCE	FLAW DEPTH, a mm (INCH)	FLAW LENGTH, 2c mm (INCH)	STRESS, σ MN/m^2 (KSI)	σ/σ_Y [1]	a/2c	a/t	STRESS INTENSITY, $K_{I_{MAX}}$ $MN/m^{3/2}$ ($KSI\sqrt{IN}$)	REMARKS
T 02-9-70-1	0.51 (0.0202)	30.45 (1.1990)	44°	START CYCLES	0.30 (0.012)	4.95 (0.195)	714 (103.5)	0.70	0.062	0.594	33.3 (30.3)	DIMPLED AT 714 MN/m^2 (103.5 KSI)
				END CYCLES	0.51 (0.0202)	4.95 (0.195)	714 (103.5)	0.70	0.104	1.000	55.2 (50.2)	BT AT 68~
				FRACTURE	0.51 (0.0202)	4.95 (0.195)	855 (124.0)	0.84	0.104	1.00	—	
T 02-9-70-2	0.55 (0.0216)	30.53 (1.2018)	GAGE FAILED	START CYCLES	0.25 (0.010)	2.26 (0.089)	714 (103.5)	0.70	0.112	0.463	25.4 (23.1)	
				END CYCLES	0.55 (0.0216)	2.39 (0.094)	714 (103.5)	0.70	0.230	1.000	42.5 (38.7)	BT AT 478~
				FRACTURE	0.55 (0.0216)	2.39 (0.094)	1008 (146.2)	0.99	0.230	1.000	—	
T 02-9-70-3	0.56 (0.0220)	30.50 (1.2007)	NA	START CYCLES	0.38 (0.015)	1.78 (0.070)	714 (103.5)	0.70	0.214	0.682	30.9 (28.1)	DIMPLED AT 714 MN/m^2 (103.5 KSI)
				END CYCLES	0.56 (0.0220)	1.83 (0.072)	714 (103.5)	0.70	0.306	1.000	35.4 (32.2)	BT AT 174~
				FRACTURE	0.56 (0.0220)	1.83 (0.072)	982 (142.4)	0.96	0.306	1.000	—	

[1] σ_Y = 1020 MN/m^2 (147.9 KSI)

BT = BREAKTHROUGH

Table 58: *CYCLIC TESTS OF 1.78 mm (0.070 INCH) 6AI-4V STA TITANIUM WELDS PASSING σ_Y PROOF AND CYCLED AT 0.85 σ_Y, R = 0 IN ROOM TEMPERATURE AIR (SPECIMENS PROOFED BEFORE CYCLED)*

SPECIMEN NUMBER	THICKNESS t mm (INCH)	WIDTH, W mm (INCH)	DIMPLING GAGE LOCATION FROM CRACK TIP	LOADING SEQUENCE	FLAW DEPTH, a mm (INCH)	FLAW LENGTH, 2c mm (INCH)	STRESS, σ MN/m^2 (KSI)	σ/σ_Y [1]	a/2c	a/t	STRESS INTENSITY, $K_{I_{MAX}}$ $MN/m^{3/2}$ ($KSI\sqrt{IN}$)	REMARKS
PT 7-Y-85-1	1.79 (0.0705)	44.31 (1.7446)	9°	START PROOF	0.66 (0.026)	4.95 (0.195)	1000 (145.1)	0.97	0.133	0.369	55.7 (50.7)	DIMPLED AT 889 MN/m^2 (128.9 KSI)
				END PROOF	0.89 (0.035)	4.95 (0.195)	1000 (145.1)	0.97	0.179	0.496	64.5 (58.7)	
				START CYCLES	0.89 (0.035)	4.95 (0.195)	880 (127.6)	0.85	0.179	0.496	55.6 (50.6)	
				END CYCLES	1.79 (0.0705)	5.21 (0.205)	880 (127.6)	0.85	0.344	1.000	74.6 (67.9)	BT AT 53~
				FRACTURE	1.79 (0.0705)	5.21 (0.205)	925 (134.1)	0.89	0.344	1.000	—	
PT 7-Y-85-2	1.75 (0.0689)	31.68 (1.2472)	54°	START PROOF	0.74 (0.029)	2.97 (0.117)	1010 (146.5)	0.98	0.248	0.421	51.2 (46.6)	DIMPLED AT 879 MN/m^2 (127.5 KSI)
				END PROOF	0.76 (0.030)	2.97 (0.117)	1010 (146.5)	0.98	0.256	0.435	51.8 (47.1)	
				START CYCLES	0.76 (0.030)	2.97 (0.117)	880 (127.6)	0.85	0.256	0.435	44.2 (40.2)	
				END CYCLES	1.75 (0.0689)	3.68 (0.145)	880 (127.6)	0.85	0.475	1.000	55.8 (50.8)	BT AT 389~
				FRACTURE	1.75 (0.0689)	3.68 (0.145)	889 (128.9)	0.86	0.475	1.000	—	
PT 7-Y-85-3	1.67 (0.0656)	31.65 (1.2461)	43°	START PROOF	0.94 (0.037)	2.21 (0.087)	1017 (147.5)	0.98	0.425	0.564	45.4 (41.3)	DIMPLED AT 878 MN/m^2 (127.3 KSI)
				END PROOF	1.04 (0.041)	2.21 (0.087)	1017 (147.5)	0.98	0.471	0.625	45.1 (41.0)	
				START CYCLES	1.04 (0.041)	2.21 (0.087)	880 (127.6)	0.85	0.471	0.625	38.5 (35.0)	
				END CYCLES	1.67 (0.0656)	3.56 (0.140)	880 (127.6)	0.85	0.469	1.000	55.4 (50.4)	BT AT 110~
				FRACTURE	1.67 (0.0656)	3.56 (0.140)	987 (143.2)	0.95	0.469	1.000		
PT 7-Y-85-4	1.77 (0.0698)	31.20 (1.2282)	45°	START PROOF	1.19 (0.047)	3.25 (0.128)	965 (140.0)	0.93	0.367	0.673	55.3 (50.3)	DIMPLED AT 700 MN/m^2 (101.5 KSI)
				END PROOF	—	—	—	—	—	—	—	FAILED IN PROOF
PT 7-Y-85-5	1.82 (0.0718)	44.39 (1.7478)	45°	START PROOF	1.27 (0.050)	2.54 (0.100)	995 (144.3)	0.96	0.500	0.696	46.8 (42.6)	DIMPLED AT 736 MN/m^2 (106.8 KSI)
				END PROOF	1.27 (0.050)	2.54 (0.100)	995 (144.3)	0.96	0.500	0.696	46.8 (42.6)	
				START CYCLES	1.27 (0.050)	2.54 (0.100)	880 (127.6)	0.85	0.500	0.696	41.0 (37.3)	
				END CYCLES	1.82 (0.0718)	3.30 (0.130)	880 (127.6)	0.85	0.453	1.000	51.0 (46.4)	BT AT 78~
				FRACTURE	1.82 (0.0718)	3.30 (0.130)	961 (139.4)	0.93	0.453	1.000	—	

[1] σ_Y = 1035 MN/m^2 (150.1 KSI)

BT = BREAKTHROUGH

Table 59: CYCLIC TESTS OF 1.78 mm (0.070 INCH) 6AI-4V STA TITANIUM WELDS CAPABLE OF PASSING σ_Y PROOF AND CYCLED AT 0.85 σ_Y, R = 0 IN ROOM TEMPERATURE AIR (SPECIMENS NOT PROOFED)

SPECIMEN NUMBER	THICKNESS t mm (INCH)	WIDTH, W mm (INCH)	DIMPLING GAGE LOCATION FROM CRACK TIP	LOADING SEQUENCE	FLAW DEPTH, a mm (INCH)	FLAW LENGTH, 2c mm (INCH)	STRESS, σ MN/m^2 (KSI)	σ/σ_Y [1]	a/2c	a/t	STRESS INTENSITY, $K_{I_{MAX}}$ $MN/m^{3/2}$ ($KSI\sqrt{IN}$)	REMARKS
T 7-Y-85-1	1.73 (0.0682)	44.49 (1.7516)	38°	START CYCLES	0.61 (0.024)	5.08 (0.200)	880 (127.6)	0.85	0.120	0.352	46.6 (42.4)	DIMPLED AT 843 MN/m^2 (122.2 KSI)
				END CYCLES	1.73 (0.0682)	6.10 (0.240)	880 (127.6)	0.85	0.284	1.000	82.3 (74.9)	BT AT 154~
				FRACTURE	1.73 (0.0682)	6.10 (0.240)	880 (127.6)	0.85	0.284	1.000	—	
T 7-Y-85-2	1.79 (0.0703)	31.73 (1.2493)	54°	START CYCLES	0.76 (0.030)	2.95 (0.116)	880 (127.6)	0.85	0.259	0.427	44.0 (40.0)	DIMPLED AT 100~
				END CYCLES	1.79 (0.0703)	3.43 (0.135)	880 (127.6)	0.85	0.480	1.000	51.9 (47.2)	BT AT 289~
				FRACTURE	1.79 (0.0703)	3.43 (0.135)	895 (129.8)	0.86	0.480	1.000	—	
T 7-Y-85-3	1.78 (0.0700)	31.73 (1.2492)	43°	START CYCLES	0.91 (0.036)	2.36 (0.093)	880 (127.6)	0.85	0.387	0.514	40.2 (36.6)	DIMPLED AT 880 MN/m^2 (127.6 KSI)
				END CYCLES	1.78 (0.0700)	3.81 (0.150)	880 (127.6)	0.85	0.467	1.000	57.5 (52.3)	BT AT 288~
				FRACTURE	1.78 (0.0700)	3.81 (0.150)	947 (137.3)	0.91	0.467	1.000	—	
T 7-Y-85-4	1.81 (0.0712)	31.30 (1.2322)	48°	START CYCLES	1.19 (0.047)	2.87 (0.113)	880 (127.6)	0.85	0.416	0.660	45.3 (41.2)	DIMPLED AT 762 MN/m^2 (110.5 KSI)
				END CYCLES	1.81 (0.0712)	5.33 (0.210)	880 (127.6)	0.85	0.339	1.000	75.7 (68.7)	BT AT 101~
				FRACTURE	1.81 (0.0712)	5.33 (0.210)	967 (140.3)	0.93	0.339	1.000	—	
T 7-Y-85-5	1.78 (0.0700)	44.51 (1.7525)	59°	START CYCLES	1.22 (0.048)	2.90 (0.114)	880 (127.6)	0.85	0.421	0.686	45.7 (41.6)	DIMPLED AT 821 MN/m^2 (119.0 KSI)
				END CYCLES	1.78 (0.0700)	3.66 (0.144)	880 (127.6)	0.85	0.486	1.000	54.7 (49.8)	BT AT 117~
				FRACTURE	1.78 (0.0700)	3.66 (0.144)	958 (138.9)	0.93	0.486	1.000	—	

[1] σ_Y = 1035 MN/m^2 (150.1 KSI)

BT = BREAKTHROUGH

Table 60: *CYCLIC TESTS OF 1.78 mm (0.070 INCH) 6Al-4V STA TITANIUM WELDS PASSING σ_Y PROOF AND CYCLED AT 0.70 σ_Y, R = 0 IN ROOM TEMPERATURE AIR (SPECIMENS PROOFED BEFORE CYCLED)*

SPECIMEN NUMBER	THICKNESS, t mm (INCH)	WIDTH, W mm (INCH)	DIMPLING GAGE LOCATION FROM CRACK TIP	LOADING SEQUENCE	FLAW DEPTH, a mm (INCH)	FLAW LENGTH, 2c mm (INCH)	STRESS, σ MN/m^2 (KSI)	σ/σ_Y [1]	a/2c	a/t	STRESS INTENSITY, $K_{I_{MAX}}$ $MN/m^{3/2}$ ($KSI\sqrt{IN}$)	REMARKS
PT 7-Y-70-1	1.83 (0.0720)	31.74 (1.2496)	46°	START PROOF	0.61 (0.024)	4.45 (0.175)	991 (143.7)	0.96	0.137	0.333	52.2 (47.5)	DIMPLED AT 869 MN/m^2 (126.1 KSI)
				END PROOF	0.66 (0.026)	4.45 (0.175)	991 (143.7)	0.96	0.149	0.361	53.9 (49.0)	
				START CYCLES	0.66 (0.026)	4.45 (0.175)	725 (105.1)	0.70	0.149	0.361	37.7 (34.3)	
				END CYCLES	1.83 (0.0720)	6.22 (0.245)	725 (105.1)	0.70	0.294	1.000	66.7 (60.7)	BT AT 1027~
				FRACTURE	1.83 (0.0720)	6.22 (0.245)	855 (124.0)	0.83	0. 294	1.000	—	
PT 7-Y-70-2	1.73 (0.0681)	31.72 (1.2488)	54°	START PROOF	0.74 (0.029)	2.87 (0.113)	1012 (146.8)	0.98	0.257	0.426	50.8 (46.2)	DIMPLED AT 888 MN/m^2 (128.8 KSI)
				END PROOF	0.84 (0.033)	2.87 (0.113)	1012 (146.8)	0.98	0.292	0.485	52.2 (47.5)	
				START CYCLES	0.84 (0.033)	2.87 (0.113)	725 (105.1)	0.70	0.292	0.485	36.0 (32.8)	
				END CYCLES	1.73 (0.0681)	5.08 (0.200)	725 (105.1)	0.70	0.340	1.000	59.8 (54.4)	BT AT 779~
				FRACTURE	1.73 (0.0681)	5.08 (0.200)	869 (126.0)	0.84	0.340	1.000	—	
PT 7-Y-70-3	1.80 (0.0707)	31.25 (1.2305)	32°	START PROOF	0.94 (0.037)	2.31 (0.091)	1035 (150.1)	1.00	0.407	0.523	47.3 (43.0)	DIMPLED AT 998 MN/m^2 (144.8 KSI)
				END PROOF	1.04 (0.041)	2.31 (0.091)	1035 (150.1)	1.00	0.451	0.580	47.0 (42.8)	
				START CYCLES	1.04 (0.041)	2.31 (0.091)	725 (105.1)	0.70	0.451	0.580	32.1 (29.2)	[2]
				END CYCLES	1.80 (0.0707)	4.06 (0.160)	725 (105.1)	0.70	0.442	1.000	50.1 (45.6)	BT AT 991~
				FRACTURE	1.80 (0.0707)	(NA)	725 (105.1)	0.70	—	—	—	

[1] σ_Y = 1035 MN/m^2 (150.1 KSI)

[2] 2c AT BT IS ESTIMATED

BT = BREAKTHROUGH

Table 61: CYCLIC TESTS OF 1.78 mm (0.070 INCH) 6Al-4V STA TITANIUM WELDS CAPABLE OF PASSING σ_Y PROOF AND CYCLED AT 0.70 σ_Y, R = 0 IN ROOM TEMPERATURE AIR (SPECIMENS NOT PROOFED)

SPECIMEN NUMBER	THICKNESS t mm (INCH)	WIDTH, W mm (INCH)	DIMPLING GAGE LOCATION FROM CRACK TIP	LOADING SEQUENCE	FLAW DEPTH, a mm (INCH)	FLAW LENGTH, 2c mm (INCH)	STRESS, σ MN/m^2 (KSI)	σ/σ_Y [1]	a/2c	a/t	STRESS INTENSITY, $K_{1_{MAX}}$ $MN/m^{3/2}$ ($KSI\sqrt{IN}$)	REMARKS
T 7-Y-70-1	1.81 (0.0711)	31.70 (1.2480)	52°	START CYCLES	0.56 (0.022)	4.42 (0.174)	725 (105.1)	0.70	0.126	0.309	35.2 (32.0)	DIMPLED AT 180~
				END CYCLES	1.81 (0.0711)	5.84 (0.230)	725 (105.1)	0.70	0.309	1.000	64.3 (58.5)	BT AT 1118~
				FRACTURE	1.81 (0.0711)	5.84 (0.230)	874 (126.8)	0.84	0.309	1.000	—	
T 7-Y-70-2	1.82 (0.0715)	31.74 (1.2498)	51°	START CYCLES	0.74 (0.029)	2.87 (0.113)	725 (105.1)	0.70	0.257	0.406	34.7 (31.6)	DID NOT DIMPLE
				END CYCLES	1.82 (0.0715)	4.57 (0.180)	725 (105.1)	0.70	0.397	1.000	56.0 (51.0)	BT AT 1114~
				FRACTURE	1.82 (0.0715)	4.57 (0.180)	905 (131.2)	0.87	0.397	1.000	—	
T 7-Y-70-3	1.81 (0.0712)	31.20 (1.2283)	48°	START CYCLES	0.89 (0.035)	2.24 (0.088)	725 (105.1)	0.70	0.398	0.492	31.5 (28.7)	DIMPLED AT 623~
				END CYCLES	1.81 (0.0712)	4.83 (0.190)	725 (105.1)	0.70	0.375	1.000	58.0 (52.8)	BT AT 1070~
				FRACTURE	1.81 (0.0712)	4.83 (0.190)	910 (132.0)	0.88	0.375	1.000	—	

[1] σ_Y = 1035 MN/m^2 (150.1 KSI)

BT = BREAKTHROUGH

Table 62: *CYCLIC TESTS OF 1.78 mm (0.070 INCH) 6Al-4V STA TITANIUM WELDS PASSING 0.91 σ_Y PROOF AND CYCLED AT 0.70 σ_Y, R = 0 IN ROOM TEMPERATURE AIR (SPECIMENS PROOFED BEFORE CYCLED)*

SPECIMEN NUMBER	THICKNESS t mm (INCH)	WIDTH, W mm (INCH)	DIMPLING GAGE LOCATION FROM CRACK TIP	LOADING SEQUENCE	FLAW DEPTH, a mm (INCH)	FLAW LENGTH, 2c mm (INCH)	STRESS, σ MN/m^2 (KSI)	σ/σ_Y [1]	a/2c	a/t	STRESS INTENSITY, $K_{I_{MAX}}$ $MN/m^{3/2}$ ($KSI\sqrt{IN}$)	REMARKS
PT 7-9-70-1	1.78 (0.0700)	44.38 (1.7473)	48°	START PROOF	0.89 (0.035)	6.73 (0.265)	942 (136.6)	0.91	0.132	0.500	64.7 (58.9)	DIMPLED AT 727 MN/m^2 (105.5 KSI)
				END PROOF	1.07 (0.042)	6.73 (0.265)	942 (136.6)	0.91	0.158	0.600	73.5 (66.9)	
				START CYCLES	1.07 (0.042)	6.73 (0.265)	725 (105.1)	0.70	0.158	0.600	54.7 (49.8)	
				END CYCLES	1.78 (0.0700)	6.73 (0.265)	725 (105.1)	0.70	0.264	1.000	71.1 (64.7)	BT AT 169~
				FRACTURE	1.78 (0.0700)	6.73 (0.265)	837 (121.4)	0.81	0.264	1.000	—	
PT 7-9-70-2	1.85 (0.0728)	31.61 (1.2444)	45°	START PROOF	0.99 (0.039)	3.94 (0.155)	942 (136.6)	0.91	0.252	0.536	57.5 (52.3)	DIMPLED AT 780 MN/m^2 (113.1 KSI)
				END PROOF	1.09 (0.043)	3.94 (0.155)	942 (136.6)	0.91	0.277	0.591	59.2 (53.9)	
				START CYCLES	1.09 (0.043)	3.94 (0.155)	725 (105.1)	0.70	0.277	0.591	44.4 (40.4)	
				END CYCLES	1.85 (0.0728)	5.08 (0.200)	725 (105.1)	0.70	0.364	1.000	59.6 (54.2)	BT AT 557~
				FRACTURE	1.85 (0.0728)	5.08 (0.200)	886 (128.5)	0.86	0.364	1.000	—	
PT 7-9-70-3	1.77 (0.0697)	31.65 (1.2461)	11°	START PROOF	1.24 (0.049)	3.23 (0.127)	933 (135.3)	0.90	0.386	0.703	52.9 (48.1)	DIMPLED AT 933 MN/m^2 (135.3 KSI)
				END PROOF	1.32 (0.052)	3.23 (0.127)	933 (135.3)	0.90	0.409	0.746	52.9 (48.1)	
				START CYCLES	1.32 (0.052)	3.23 (0.127)	725 (105.1)	0.70	0.409	0.746	40.3 (36.7)	
				END CYCLES	1.77 (0.0697)	4.83 (0.190)	725 (105.1)	0.70	0.367	1.000	58.1 (52.9)	BT AT 324~
				FRACTURE	1.77 (0.0697)	4.83 (0.190)	912 (132.2)	0.88	0.367	1.000	—	

[1] σ_Y = 1035 MN/m^2 (150.1 KSI)

BT = BREAKTHROUGH

Table 63: CYCLIC TESTS OF 1.78 mm (0.070 INCH) 6AI-4V STA TITANIUM WELDS CAPABLE OF PASSING 0.91 σ_Y PROOF AND CYCLED AT 0.70 σ_Y, R = 0 IN ROOM TEMPERATURE AIR (SPECIMENS NOT PROOFED)

SPECIMEN NUMBER	THICKNESS, t mm (INCH)	WIDTH, W mm (INCH)	DIMPLING GAGE LOCATION FROM CRACK TIP	LOADING SEQUENCE	FLAW DEPTH, a mm (INCH)	FLAW LENGTH, 2c mm (INCH)	STRESS, σ MN/m^2 (KSI)	σ/σ_Y [1]	a/2c	a/t	STRESS INTENSITY, $K_{I_{MAX}}$ $MN/m^{3/2}$ (KSI$\sqrt{IN}$)	REMARKS
T 7-9-70-1	1.75 (0.0690)	44.43 (1.7494)	27°	START CYCLES	0.94 (0.037)	6.86 (0.270)	725 (105.1)	0.70	0.137	0.536	50.6 (46.0)	DIMPLED AT 697 MN/m^2 (101.1 KSI)
				END CYCLES	1.75 (0.0690)	7.06 (0.278)	725 (105.1)	0.70	0.248	1.000	73.6 (67.0)	BT AT 146~
				FRACTURE	1.75 (0.0690)	7.06 (0.278)	874 (126.8)	0.84	0.248	1.000		
T 7-9-70-2	1.74 (0.0684)	31.63 (0.1452)	42°	START CYCLES	1.02 (0.040)	3.91 (0.154)	725 (105.1)	0.70	0.266	0.585	44.2 (40.2)	DIMPLED AT 725 MN/m^2 (105.1 KSI)
				END CYCLES	1.74 (0.0684)	5.21 (0.205)	72.5 (105.1)	0.70	0.334	1.000	60.7 (55.2)	BT AT 360~
				FRACTURE	1.74 (0.0684)	5.21 (0.205)	876 (127.1)	0.85	0.334	1.000		
T7-9-70-3	1.75 (0.0690)	31.62 (1.2450)	19°	START CYCLES	1.24 (0.049)	3.12 (0.123)	725 (105.1)	0.70	0.398	0.710	39.3 (35.8)	DIMPLED AT 249~
				END CYCLES	1.75 (0.0690)	4.14 (0.163)	725 (105.1)	0.70	0.423	1.000	51.8 (47.1)	BT AT 421~
				FRACTURE	1.75 (0.0690)	4.14 (0.163)	1060 (153.7)	1.02	0.423	1.000		

[1] σ_Y = 1035 MN/m^2 (150.1 KSI)

BT = BREAKTHROUGH

Table 64: *CYCLIC TESTS OF 5.33 mm (0.210 INCH) 6AI-4V STA TITANIUM WELDS PASSING σ_Y PROOF AND CYCLED AT 0.85 σ_Y, R = 0 IN ROOM TEMPERATURE AIR (SPECIMENS PROOFED BEFORE CYCLED)*

SPECIMEN NUMBER	THICKNESS t mm (INCH)	WIDTH, W mm (INCH)	DIMPLING GAGE LOCATION FROM CRACK TIP	LOADING SEQUENCE	FLAW DEPTH, a mm (INCH)	FLAW LENGTH, 2c mm (INCH)	STRESS, σ MN/m^2 (KSI)	σ/σ_Y ①	a/2c	a/t	STRESS INTENSITY, $K_{I_{MAX}}$ $MN/m^{3/2}$ ($KSI\sqrt{IN}$)	REMARKS
PT 21-Y-85-1	5.44 (0.2140)	76.38 (3.0072)	45°	START PROOF	1.70 (0.067)	11.68 (0.460)	948 (137.5)	0.99	0.146	0.313	82.5 (75.1)	DIMPLED AT 829 MN/m^2 (120.3 KSI)
				END PROOF	2.16 (0.085)	11.68 (0.460)	948 (137.5)	0.99	0.185	0.397	89.9 (81.8)	
				START CYCLES	2.16 (0.085)	11.68 (0.460)	817 (118.5)	0.85	0.185	0.397	75.6 (68.8)	
				END CYCLES	5.44 (0.2140)	16.51 (0.650)	817 (118.5)	0.85	0.329	1.000	123.6 (112.5)	FAILED AT 160 ~
PT 21-Y-85-2	5.37 (0.2113)	76.32 (3.0048)	47°	START PROOF	2.13 (0.084)	7.44 (0.293)	961 (139.4)	1.00	0.287	0.398	77.9 (70.7)	DIMPLED AT 855 MN/m^2 (124.0 KSI)
				END PROOF	2.34 (0.092)	7.44 (0.293)	961 (139.4)	1.00	0.314	0.435	78.8 (71.7)	
				START CYCLES	2.34 (0.092)	7.44 (0.293)	817 (118.5)	0.85	0.314	0.435	65.7 (59.8)	
				END CYCLES	5.37 (0.2113)	11.56 (0.455)	817 (118.5)	0.85	0.464	1.000	93.3 (84.9)	BT AT 247 ~
				FRACTURE	5.37 (0.2113)	11.56 (0.455)	883 (128.1)	0.92	0.464	1.000	—	
PT 21-Y-85-3	5.37 (0.2115)	76.53 (3.0129)	49°	START PROOF	2.59 (0.102)	6.12 (0.241)	951 (137.9)	0.99	0.423	0.482	69.9 (63.6)	DIMPLED AT 812 MN/m^2 (117.7 KSI)
				END PROOF	2.79 (0.110)	7.75 (0.305)	951 (137.9)	0.99	0.361	0.520	80.8 (73.5)	
				START CYCLES	2.79 (0.110)	7.75 (0.305)	817 (118.5)	0.85	0.361	0.520	68.2 (62.1)	
				END CYCLES	5.37 (0.2115)	12.32 (0.485)	817 (118.5)	0.85	0.436	1.000	100.3 (91.3)	BT AT 148 ~
				FRACTURE	5.37 (0.2115)	12.32 (0.485)	848 (123.0)	0.88	0.436	1.000	—	

① σ_Y = 961 MN/m^2 (139.4 KSI)

BT = BREAKTHROUGH

Table 65: CYCLIC TESTS OF 5.33 mm (0.210 INCH) 6AI-4V STA TITANIUM WELDS CAPABLE OF PASSING σ_y PROOF AND CYCLED AT 0.85 σ_y, R = 0 IN ROOM TEMPERATURE AIR (SPECIMENS NOT PROOFED)

SPECIMEN NUMBER	THICKNESS, t mm (INCH)	WIDTH, W mm (INCH)	DIMPLING GAGE LOCATION FROM CRACK TIP	LOADING SEQUENCE	FLAW DEPTH, a mm (INCH)	FLAW LENGTH, 2c mm (INCH)	STRESS, σ MN/m^2 (KSI)	σ/σ_Y [1]	a/2c	a/t	STRESS INTENSITY, $K_{I_{MAX}}$ $MN/m^{3/2}$ (KSI$\sqrt{IN}$)	REMARKS
T 21-Y-85-1	5.12 (0.2015	76.23 (3.0011)	50°	START CYCLES	1.75 (0.069)	11.48 (0.452)	817 (118.5)	0.85	0.153	0.342	70.2 (63.9)	DIMPLED AT 7~
				END CYCLES	5.12 (0.2015)	14.48 (0.570)	817 (118.5)	0.85	0.354	1.000	115.4 (105.0)	FAILED AT 144~
T 21-Y-85-2	5.24 (0.2064)	76.14 (2.9978)	55°	START CYCLES	2.11 (0.083)	7.37 (0.290)	817 (118.5)	0.85	0.286	0.402	64.4 (58.6)	DIMPLED AT 78~
				END CYCLES	5.24 (0.2064)	12.70 (0.500)	817 (118.5)	0.85	0.413	1.000	105.0 (95.5)	BT AT 292~
				FRACTURE	5.24 (0.2064)	12.70 (0.500)	873 (126.6)	0.91	0.413	1.000	—	
T 21-Y-85-3	5.31 (0.2091)	76.14 (2.9978)	48°	START CYCLES	2.49 (0.098)	5.97 (0.235)	817 (118.5)	0.85	0.417	0.469	58.5 (53.2)	DIMPLED AT 19~
				END CYCLES	5.31 (0.2091)	11.18 (0.440)	817 (118.5)	0.85	0.475	1.000	90.3 (82.2)	BT AT 307~
				FRACTURE	5.31 (0.2091)	11.18 (0.44)	814 (118.0)	0.85	0.475	1.000	—	

[1] σ_y = 961 MN/m^2 (139.4 KSI)

BT = BREAKTHROUGH

Table 66: *CYCLIC TESTS OF 5.33 mm (0.210 INCH) 6AI-4V STA TITANIUM WELDS PASSING σ_Y PROOF AND CYCLED AT 0.70 σ_Y, R = 0 IN ROOM TEMPERATURE AIR (SPECIMENS PROOFED BEFORE CYCLED)*

SPECIMEN NUMBER	THICKNESS t mm (INCH)	WIDTH, W mm (INCH)	DIMPLING GAGE LOCATION FROM CRACK TIP	LOADING SEQUENCE	FLAW DEPTH, a mm (INCH)	FLAW LENGTH, 2c mm (INCH)	STRESS, σ MN/m^2 (KSI)	σ/σ_Y [1]	a/2c	a/t	STRESS INTENSITY, K_{1MAX} $MN/m^{3/2}$ ($KSI\sqrt{IN}$)	REMARKS
PT 21-Y-70-1	5.38 (0.2120)	75.96 (2.9905)	51°	START PROOF	1.70 (0.067)	11.48 (0.452)	956 (138.6)	0.99	0.148	0.316	83.2 (75.7)	DIMPLED AT 821 MN/m^2 (119.0 KSI)
				END PROOF	2.24 (0.088)	11.48 (0.452)	956 (138.6)	0.99	0.195	0.415	91.9 (83.6)	
				START CYCLES	2.24 (0.088)	11.48 0.452)	673 (97.6)	0.70	0.195	0.415	61.8 (56.2)	
				END CYCLES	5.38 (0.2120)	14.99 (0.590)	673 (97.6)	0.70	0.359	1.000	95.2 (86.6)	BT AT 666 ~
				FRACTURE	5.38 (0.2120)	14.99 (0.590)	791 (114.7)	0.82	0.359	1.000		
PT 21-Y-70-2	5.34 (0.2103)	76.36 (3.0062)	48°	START PROOF	2.16 (0.085)	7.49 (0.295)	949 (137.6)	0.99	0.288	0.404	76.9 (70.0)	DIMPLED AT 823 MN/m^2 (119.3 KSI)
				END PROOF	2.54 (0.100)	7.49 (0.295)	949 (137.6)	0.99	0.339	0.476	78.7 (71.6)	
				START CYCLES	2.54 (0.100)	7.49 (0.295)	673 (97.6)	0.70	0.339	0.476	54.1 (49.2)	
				END CYCLES	5.34 (0.2103)	12.45 (0.490)	673 (97.6)	0.70	0.429	1.000	82.8 (75.3)	BT AT 765 ~
				FRACTURE	5.34 (0.2103)	12.45 (0.490)	821 (119.1)	0.85	0.429	1.000		
PT 21-Y-70-3	5.36 (0.2110)	76.24 (3.0017)	46°	START PROOF	2.59 (0.102)	6.10 (0.240)	961 (139.4)	1.00	0.425	0.483	70.6 (64.2)	DIMPLED AT 833 MN/m^2 (120.8 KSI)
				END PROOF	2.79 (0.110)	6.99 (0.275)	961 (139.4)	1.00	0.400	0.521	76.4 (69.5)	
				START CYCLES	2.79 (0.110)	6.99 (0.275)	673 (97.6)	0.70	0.400	0.521	52.0 (47.3)	
				END CYCLES	5.36 (0.2110)	12.57 (0.495)	673 (97.6)	0.70	0.426	1.000	83.5 (76.0)	BT AT 891 ~
				FRACTURE	5.36 (0.2110)	12.57 (0.495)	825 (119.6)	0.86	0.426	1.000		

[1] σ_Y = 961 MN/m^2 (139.4 KSI)

BT = BREAKTHROUGH

Table 67: CYCLIC TESTS OF 5.33 mm (0.210 INCH) 6AI-4V STA TITANIUM WELDS CAPABLE OF PASSING σ_y PROOF AND CYCLED AT 0.70 σ_y, R = 0 IN ROOM TEMPERATURE AIR (SPECIMENS NOT PROOFED)

SPECIMEN NUMBER	THICKNESS t mm (INCH)	WIDTH, W mm (INCH)	DIMPLING GAGE LOCATION FROM CRACK TIP	LOADING SEQUENCE	FLAW DEPTH, a mm (INCH)	FLAW LENGTH, 2c mm (INCH)	STRESS, σ MN/m^2 (KSI)	σ / σ_y [1]	a/2c	a/t	STRESS INTENSITY, $K_{I_{MAX}}$ $MN/m^{3/2}$ ($KSI\sqrt{IN}$)	REMARKS
T 21-Y-70-1	5.13 (0.2018)	75.96 (2.9904)	49°	START CYCLES	1.68 (0.066)	11.56 (0.455)	673 (97.6)	0.70	0.145	0.327	55.6 (50.6)	DID NOT DIMPLE
				END CYCLES	5.13 (0.2018)	14.35 (0.565)	673 (97.6)	0.70	0.357	1.000	93.2 (84.8)	BT AT 605~
				FRACTURE	5.13 (0.2018)	14.35 (0.565)	780 (113.1)	0.81	0.357	1.000	—	
T 21-Y-70-2	5.30 (0.2088)	76.28 (3.0033)	50°	START CYCLE	2.16 (0.085)	7.47 (0.294)	673 (97.6)	0.70	0.289	0.407	52.6 (47.9)	DIMPLED AT 312~
				END CYCLES	5.30 (0.2088)	11.05 (0.435)	673 (97.6)	0.70	0.480	1.000	72.6 (66.1)	BT AT 864~
				FRACTURE	5.30 (0.2088)	11.05 (0.435)	836 (121.3)	0.87	0.480	1.000	—	
T 21-Y-70-3	5.38 (0.2117)	76.18 (2.9993)	45°	START CYCLES	2.67 (0.105)	6.43 (0.253)	673 (97.6)	0.70	0.415	0.496	49.5 (45.0)	DID NOT DIMPLE
				END CYCLES	5.38 (0.2117)	11.56 (0.455)	673 (97.6)	0.70	0.465	1.000	75.9 (69.1)	BT AT 906~
				FRACTURE	5.38 (0.2117)	11.56 (0.455)	867 (125.7)	0.90	0.465	1.000	—	

[1] σ_y = 961 MN/m^2 (139.4 KSI)

BT = BREAKTHROUGH

Table 68: *CYCLIC TESTS OF 5.33 mm (0.210 INCH) 6AI-4V STA TITANIUM WELDS PASSING 0.91 σ_Y PROOF AND CYCLED AT 0.70 σ_Y, R = 0 IN ROOM TEMPERATURE AIR (SPECIMENS PROOFED BEFORE CYCLED)*

SPECIMEN NUMBER	THICKNESS t mm (INCH)	WIDTH, W mm (INCH)	DIMPLING GAGE LOCATION FROM CRACK TIP	LOADING SEQUENCE	FLAW DEPTH, a mm (INCH)	FLAW LENGTH, 2c mm (INCH)	STRESS, σ MN/m^2 (KSI)	σ/σ_Y [1]	a/2c	a/t	STRESS INTENSITY, $K_{I_{MAX}}$ $MN/m^{3/2}$ ($KSI\sqrt{IN}$)	REMARKS
PT 21-9-70-1	5.72 (0.2250)	152.82 (6.0165)	45°	START PROOF	2.21 (0.087)	15.37 (0.605)	860 (124.8)	0.90	0.144	0.387	85.6 (77.9)	DIMPLED AT 827 MN/m^2 (120 KSI)
				END PROOF	2.36 (0.093)	15.37 (0.605)	860 (124.8)	0.90	0.154	0.413	88.4 (80.4)	
		88.95 (3.5021) [2]		START CYCLES	2.36 (0.093)	15.37 (0.605)	673 (97.6)	0.70	0.154	0.413	67.0 (61.0)	
				END CYCLES	5.72 (0.2250)	17.27 (0.680)	673 (97.6)	0.70	0.331	1.000	102.5 (93.3)	BT AT 540~
				FRACTURE	5.72 (0.2250)	17.27 (0.680)	712 (103.2)	0.74	0.331	1.000	—	
PT 21-9-70-2	5.41 (0.2128)	75.92 (2.9890)	46°	START PROOF	2.97 (0.117)	11.56 (0.455)	875 (126.9)	0.91	0.257	0.550	92.3 (84.0)	DIMPLED AT 732 MN/m^2 (106.1 KSI)
				END PROOF	3.23 (0.127)	11.76 (0.463)	875 (126.9)	0.91	0.274	0.597	95.4 (86.8)	
				START CYCLES	3.23 (0.127)	11.76 (0.463)	673 (97.6)	0.70	0.274	0.597	71.5 (65.1)	
				END CYCLES	5.41 (0.2128)	14.86 (0.585)	673 (97.6)	0.70	0.364	1.000	94.7 (86.2)	BT AT 318~
				FRACTURE	5.41 (0.2128)	14.86 (0.585)	796 (115.5)	0.83	0.364	1.000	—	
PT 21-9-70-3	5.40 (0.2127)	76.31 (3.0042)	31°	START PROOF	3.73 (0.147)	9.09 (0.358)	869 (126.1)	0.90	0.411	0.691	80.9 (73.6)	DIMPLED AT 652 MN/m^2 (94.6 KSI)
				END PROOF	4.04 (0.159)	9.91 (0.390)	869 (126.1)	0.90	0.408	0.748	86.5 (78.7)	
				START CYCLES	4.04 (0.159)	9.91 (0.390)	673 (97.6)	0.70	0.408	0.748	65.7 (59.8)	
				END CYCLES	5.40 (0.2127)	13.21 (0.520)	673 (97.6)	0.70	0.409	1.000	87.5 (79.6)	BT AT 311~
				FRACTURE	5.40 (0.2127)	13.21 (0.520)	794 (115.1)	0.83	0.409	1.000	—	

[1] σ_Y = 961 MN/m^2 (139.4 KSI)

[2] GRIPS FAILED IN PROOF TEST, SPECIMEN REMACHINED FOR CYCLIC TEST

BT = BREAKTHROUGH

Table 69: CYCLIC TESTS OF 5.33 mm (0.210 INCH) 6AI-4V STA TITANIUM WELDS CAPABLE OF PASSING 0.91 σ_y PROOF AND CYCLED AT 0.70 σ_y, R = 0 IN ROOM TEMPERATURE AIR (SPECIMENS NOT PROOFED)

SPECIMEN NUMBER	THICKNESS, t mm (INCH)	WIDTH, W mm (INCH)	DIMPLING GAGE LOCATION FROM CRACK TIP	LOADING SEQUENCE	FLAW DEPTH, a mm (INCH)	FLAW LENGTH, 2c mm (INCH)	STRESS, σ MN/m^2 (KSI)	σ/σ_Y [1]	a/2c	a/t	STRESS INTENSITY, $K_{I_{MAX}}$ $MN/m^{3/2}$ (KSI$\sqrt{IN}$)	REMARKS
T 21-9-70-1	5.19 (0.2045)	152.44 (6.0015)	50°	START CYCLES	2.21 (0.087)	15.49 (0.610)	673 (97.6)	0.70	0.143	0.425	66.3 (60.3)	DID NOT DIMPLE
				END CYCLES	5.19 (0.2045)	16.26 (0.640)	673 (97.6)	0.70	0.320	1.000	99.6 (90.6)	BT AT 220~
				FRACTURE	5.19 (0.2045)	16.26 (0.640)	NA	—	—	—	—	
T 20-9-70-2	5.39 (0.2121)	76.38 (3.0072)	47°	START CYCLE	3.00 (0.118)	11.61 (0.457)	673 (97.6)	0.70	0.258	0.556	69.6 (63.3)	DIMPLED AT 78~
				END CYCLES	5.39 (0.2121)	13.72 (0.540)	673 (97.6)	0.70	0.393	1.000	90.3 (82.2)	BT AT 264~
				FRACTURE	5.39 (0.2121)	13.72 (0.540)	778 (112.9)	0.81	0.393	1.000		
T 21-9-70-3	5.40 (0.2125)	76.31 (3.0045)	42°	START CYCLES	3.76 (0.148)	8.89 (0.350)	673 (97.6)	0.70	0.423	0.696	60.6 (55.1)	DIMPLED AT 6~
				END CYCLES	5.40 (0.2125)	11.05 (0.435)	673 (97.6)	0.70	0.489	1.000	71.8 (65.3)	BT AT 268~
				FRACTURE	5.40 (0.2125)	11.05 (0.435)	838 (121.5)	0.87	0.489	1.000		

[1] σ_y = 961 MN/m^2 (139.4 KSI)

BT = BREAKTHROUGH